



climate

Urban Climate and Adaptation Tools

Edited by

Teodoro Georgiadis and Letizia Cremonini

Printed Edition of the Special Issue Published in *Climate*

Urban Climate and Adaptation Tools

Urban Climate and Adaptation Tools

Editors

Teodoro Georgiadis

Letizia Cremonini

MDPI • Basel • Beijing • Wuhan • Barcelona • Belgrade • Manchester • Tokyo • Cluj • Tianjin



Editors

Teodoro Georgiadis
National Research Council of Italy
Italy

Letizia Cremonini
National Research Council of Italy
Italy

Editorial Office

MDPI
St. Alban-Anlage 66
4052 Basel, Switzerland

This is a reprint of articles from the Special Issue published online in the open access journal *Climate* (ISSN 2225-1154) (available at: https://www.mdpi.com/journal/climate/special_issues/Urban.Climate.Adaptation).

For citation purposes, cite each article independently as indicated on the article page online and as indicated below:

LastName, A.A.; LastName, B.B.; LastName, C.C. Article Title. *Journal Name* **Year**, *Volume Number*, Page Range.

ISBN 978-3-0365-0144-4 (Hbk)

ISBN 978-3-0365-0145-1 (PDF)

© 2021 by the authors. Articles in this book are Open Access and distributed under the Creative Commons Attribution (CC BY) license, which allows users to download, copy and build upon published articles, as long as the author and publisher are properly credited, which ensures maximum dissemination and a wider impact of our publications.

The book as a whole is distributed by MDPI under the terms and conditions of the Creative Commons license CC BY-NC-ND.

Contents

About the Editors	vii
Preface to “Urban Climate and Adaptation Tools”	ix
Dirk Lauwaet, Bino Maiheu, Koen De Ridder, Wesley Boënné, Hans Hooyberghs, Matthias Demuzere and Marie-Leen Verdonck A New Method to Assess Fine-Scale Outdoor Thermal Comfort for Urban Agglomerations Reprinted from: <i>Climate</i> 2020, 8, 6, doi:10.3390/cli8010006	1
Giulia Villani, Stefania Nanni, Fausto Tomei, Stefania Pasetti, Rita Mangiaracina, Alberto Agnetti, Paolo Leoni, Marco Folegani, Gianluca Mazzini, Lucio Botarelli and Sergio Castellari The RainBO Platform for Enhancing Urban Resilience to Floods: An Efficient Tool for Planning and Emergency Phases Reprinted from: <i>Climate</i> 2019, 7, 145, doi:10.3390/cli7120145	15
Marianna Nardino and Nicola Laruccia Land Use Changes in a Peri-Urban Area and Consequences on the Urban Heat Island Reprinted from: <i>Climate</i> 2019, 7, 133, doi:10.3390/cli7110133	47
Alejandro Salcido, Susana Carreón-Sierra and Ana-Teresa Celada-Murillo Air Pollution Flow Patterns in the Mexico City Region Reprinted from: <i>Climate</i> 2019, 7, 128, doi:10.3390/cli7110128	59
Luisa Sturiale and Alessandro Scuderi The Role of Green Infrastructures in Urban Planning for Climate Change Adaptation Reprinted from: <i>Climate</i> 2019, 7, 119, doi:10.3390/cli7100119	87
Jonatan A. Lassa Negotiating Institutional Pathways for Sustaining Climate Change Resilience and Risk Governance in Indonesia Reprinted from: <i>Climate</i> 2019, 7, 95, doi:10.3390/cli7080095	111
Sorin Cheval, Dana Micu, Alexandru Dumitrescu, Anișoara Irimescu, Maria Frighenciu, Cristian Iojă, Nicu Constantin Tudose, Șerban Davidescu and Bogdan Antonescu Meteorological and Ancillary Data Resources for Climate Research in Urban Areas Reprinted from: <i>Climate</i> 2020, 8, 37, doi:10.3390/cli8030037	133
Andre Santos Nouri and Andreas Matzarakis The Maturing Interdisciplinary Relationship between Human Biometeorological Aspects and Local Adaptation Processes: An Encompassing Overview Reprinted from: <i>Climate</i> 2019, 7, 134, doi:10.3390/cli7120134	157
Eleanor Tonks and Sean Lockie Urban Transformation: From Single-Point Solutions to Systems Innovation Reprinted from: <i>Climate</i> 2020, 8, 17, doi:10.3390/cli8010017	189

About the Editors

Teodoro Georgiadis Graduated in Physics, in Astronomy, and in Environmental and Civil Engineering, Master's Degree in Territorial Planning. Senior Scientist at the Institute for the BioEconomy (former Institute of Biometeorology) of the CNR of Bologna. He deals with surface energy balances in the urban environment and with the mitigation of the effects of interactions between the atmosphere and the built environment. Member of the Capacity Building Committee of IAMAS-IUGG. Invited Scientist in the Commission of Agrometeorology of WMO.

Letizia Cremonini Postdoc at the IBE-CNR Institute of BioEconomy and freelance architect with Ph.D. in Town and Landscape Planning. Her Ph.D. thesis was entitled "The Role of Landscape in New Urban Neighborhoods in Europe". She develops projects related to the planning and ecological planning at the urban scale, maintenance of urban plant biodiversity, and studies of the relationship between vegetation and built environments and their influence on climate parameters.

Preface to “Urban Climate and Adaptation Tools”

In 1925, Le Corbusier, in his book *Urbanisme*, wondered if cities are still capable of preserving the dignity of human beings. That question today appears even more motivated by two phenomena that have become increasingly evident over time: urbanization and climate change.

Urbanization has led the human community to find itself, today, within the geographical perimeter of cities with growth rates that in a few decades into the future, will ensure that all men can be defined as citizens; but citizenship has a much deeper meaning than living in one place. Citizenship means being able to provide the human being with all those elements of life and well-being that reconcile all aspects of one’s nature: opportunities for one’s expectations, physiological well-being, social well-being, protection of one’s own safety. That ability to live fully, being able to bring out all their physical and intellectual abilities. Well-being understood as the overall state of being human. Almost a century after that question, the answer cannot be positive. Although it is not possible for cities to define a precise development model, what we have seen was an urbanization that has profoundly undermined the sustainable livelihoods of places and, therefore, of the human being.

The climate–environmental problem has therefore caused all the contradictions of the modern era to explode, placing humankind in danger. Pollution, rising temperatures, intense precipitation phenomena endanger life but, above all, the well-being of citizens, with health understood as a primary good. It is the task of politics to find solutions, and the task of science and technology to find the tools to support politics in the search for solutions.

The time is actually ripe for a transition—for a transition to a more sustainable world where the human being is at the center of the system, the replacement of gross domestic product with gross domestic well-being. We already own our toolbox, which can also be improved and implemented, and this collection of works allows us to understand that the passage to the answer to that fundamental question is within reach. In reading, it will be clear that, today, we have tools to respond, we have risk reduction methodologies, we have policies based on scientific assumptions, we have the possibility of transforming a danger into new growth opportunities. The overview offered is vast, and this can only lead us to be optimistic. The real knot is not given by science or the will of politics: the real knot is given by the citizen’s ability to make this hope their own, to transform it into daily awareness of what can be done in an exercise of democracy in understanding that there exists diversity that must be protected and that special actions are necessary for these; protections that are then transformed into greater resources to be redistributed for the benefit of all. The environment and climate today can represent an opportunity; by building more resilient cities, we not only protect the weakest groups but, in fact, we free up resources represented by health costs which in healthier environments are reduced, allowing access to a full life to all citizens.

The recent pandemic, with all the grief and suffering, has opened our eyes to the future and to the meaning of being a community. It has also shown us how the contradictions of modern living can explode in a very short time for us, used to talking about what the world will be like in 2050, and we understand that we don’t know what tomorrow itself will be like. But we have the tools to change, and you have them in your hands right now, and now is the time to apply them.

Teodoro Georgiadis, Letizia Cremonini

Editors

Article

A New Method to Assess Fine-Scale Outdoor Thermal Comfort for Urban Agglomerations

Dirk Lauwaet ^{1,*}, Bino Maiheu ¹, Koen De Ridder ¹, Wesley Boëne ¹, Hans Hooyberghs ¹,
Matthias Demuzere ^{2,3} and Marie-Leen Verdonck ⁴

¹ Vlaamse Instelling voor Technologisch Onderzoek (VITO), 2400 Mol, Belgium; bino.maiheu@vito.be (B.M.); koen.deridder@vito.be (K.D.R.); wesley.boenne@vito.be (W.B.); hans.hooyberghs@vito.be (H.H.)

² Department of Geography, Ruhr-University Bochum, 44801 Bochum, Germany; matthias.demuzere@rub.de

³ Department of Environment, Laboratory of Hydrology and Water Management, Ghent University, 9000 Ghent, Belgium

⁴ Antea Group, 2000 Antwerpen, Belgium; marie-leen.verdonck@anteargroup.com

* Correspondence: dirk.lauwaet@vito.be

Received: 6 November 2019; Accepted: 4 January 2020; Published: 6 January 2020

Abstract: In urban areas, high air temperatures and heat stress levels greatly affect human thermal comfort and public health, with climate change further increasing the mortality risks. This study presents a high resolution (100 m) modelling method, including detailed offline radiation calculations, that is able to efficiently calculate outdoor heat stress for entire urban agglomerations for a time period spanning several months. A dedicated measurement campaign was set up to evaluate model performance, yielding satisfactory results. As an example, the modelling tool was used to assess the effectiveness of green areas and water surfaces to cool air temperatures and wet bulb globe temperatures during a typical hot day in the city of Ghent (Belgium), since the use of vegetation and water bodies are shown to be promising in mitigating the adverse effects of urban heat islands and improving thermal comfort. The results show that air temperature reduction is most profound over water surfaces during the afternoon, while open rural areas are coolest during the night. Radiation shading from trees, and to a lesser extent, from buildings, is found to be most effective in reducing wet bulb globe temperatures and improving thermal comfort during the warmest moments of the day.

Keywords: thermal comfort; urban greening; urban heat island; UrbClim model; water bodies

1. Introduction

Rapid urban growth coupled with high population density increases the vulnerability of cities to extreme weather [1]. In cities, heat extremes are among the most important weather-related health hazards. Moreover, the effects of extreme heat are exacerbated by the presence of the urban heat island (UHI) [2]. This UHI is caused by a combination of the increased heat capacity of cities, anthropogenic heat sources, and the imperviousness of urban surfaces, which inhibit evaporative cooling [3–5]. Due to the UHI increment, cities are particularly vulnerable to heat waves, causing higher heat-related excess mortalities [6–8]. The risks of morbidity and mortality in urban areas are further increased by climate change, due to the increasing frequency of weather extremes [9,10].

In this context, integrating mitigation and adaptation measures can help avoid locking a city into counterproductive infrastructure and policies. Urban greenery has been proposed as an effective measure to mitigate the UHI and improve the urban microclimate [11–13]. Green areas are generally cooler than their surrounding built up areas, which is demonstrated by observational studies reporting instantaneous air temperature differences of 1 °C up to 7 °C [14,15]. Vegetation cools cities via shading, evapotranspiration, and alteration of the wind pattern [16]. The cooling intensity of, for example, city parks, is often largest in the evenings and during the night (like the UHI) and tends to increase

with park size [17]. During the afternoon, parks with extensive tree coverage tend to be cooler due to shading effects, while at night more open parks are cooler due to greater long-wave radiative cooling [18].

Similar to parks, water features have the potential to alleviate high urban temperatures through enhanced evaporation and reduced sensible heat fluxes [19]. A number of observational studies have shown that temperatures adjacent or downwind of water bodies are reduced by around 1–2 °C compared to surrounding areas [20,21]. On specific days during the afternoon, Murakawa et al. [22] observed 3–5 °C cooler temperatures near a wide river in Hiroshima, Japan. In contrast to urban parks where the cooling effect is most pronounced during the evening and the night, these studies suggest that open water effects are most pronounced during the day, because water bodies can maintain warmer temperatures at night due to the high heat capacity and thermal inertia of water [23].

However, air temperatures are only part of the story when assessing outdoor human comfort, as humidity, wind, and radiation also play a role [24,25]. During the day in summertime, radiation is even the single most important meteorological factor influencing the human energy balance [26]. Hence, by blocking solar radiation, trees can substantially improve thermal comfort, even if air temperature reductions are small. The relationship between urban greening and outdoor thermal comfort has been the subject of many modelling studies (e.g., [12,27,28]). At the same time, new urban modelling tools have been developed that focus on the introduction of green in urban design [29,30]. Most of these studies have been performed with high resolution models (e.g., ENVI-met) that can only perform simulations for limited areas in a city and for limited time periods.

In this study, we present an offline GIS-based post processing method, coupled to the urban boundary layer climate model UrbClim [31], that is able to calculate outdoor thermal comfort for an entire urban agglomeration and for time periods of several months to years. As a heat stress indicator, we applied the wet bulb globe temperature (WBGT), the ISO standard to quantify human thermal comfort [32]. The modelling method can easily be validated, which is done by performing an extensive measurement campaign in the city of Ghent, Belgium. As an example, the model is used to assess the effectiveness of urban vegetation and open water areas in reducing air temperatures and heat stress for the city of Ghent during a particularly warm summer day.

2. Materials and Methods

2.1. The UrbClim Model

The urban boundary layer climate model UrbClim [31] is designed to cover agglomeration-scale domains at a high spatial resolution, taken as 100 m for this study. The model consists of a land surface scheme, including simplified urban physics, which is coupled to a 3-D atmospheric boundary layer model. To ensure that the synoptic forcing is properly taken into account, the boundary layer model is tied to synoptic-scale meteorological fields through the lateral and top boundary conditions. The land surface scheme used in UrbClim is based on the soil–vegetation–atmosphere transfer scheme of De Ridder and Schayes [33], extended to account for urban surface physics. This urbanization is implemented by representing the urban surface as a rough impermeable slab, with appropriate values for the albedo, emissivity, thermal conductivity, and volumetric heat capacity. The main feature of the urbanization scheme is the inclusion of a parameterization of the inverse Stanton number, which is known to be much higher in urban areas [34,35]. A full description of the UrbClim model can be found in De Ridder et al. [31].

The spatial distribution of land cover types, needed for the specification of required land surface parameters, is taken from the reference land use map for Flanders, described in White et al. [36]. The percentage of urban land cover is attributed by applying the urban soil sealing raster data files that are distributed by the European environment agency. From the normalized difference vegetation index (NDVI) acquired by the MODIS instrument on-board the TERRA satellite platform, maps of vegetation cover fraction were obtained. This fraction is specified as a function of the NDVI using a

linear relationship proposed by Gutman and Ignatov [37], and then interpolated to the model grid. Model grid cells are divided into vegetation and bare soil (the complementary fraction) if they do not feature urban land use types. Where grid cells contain urban land use, the urban fraction, as derived from the soil sealing data, takes precedence over the fractional vegetation cover data, in case both sum to over 100%. In case they sum to less than that, the remaining fraction is assigned to bare soil. Terrain elevation data are taken from the GMTED2010 Dataset [38].

The UrbClim model has previously been validated regarding its energy fluxes, 2 m wind speeds, air temperatures, and urban–rural temperature differences for the cities of Antwerp, Brussels, and Ghent in Belgium, Toulouse in France, and Barcelona in Spain [31,39–41]. Also, the land surface temperatures in the UrbClim land surface scheme have already been validated with satellite data for the city of London [42]. In De Ridder [43], the urban parameterization was tested for the city of Paris, and the simulated land surface temperature compared favorably to observed values obtained from thermal infrared satellite imagery.

2.2. Outdoor WBGT Calculation

The UrbClim model has already been coupled offline to a building energy simulation model to calculate indoor heat stress, based on the WBGT [44]. Here, we present a method to calculate outdoor WBGT values from the UrbClim model results. Therefore, we follow the method of Liljegren et al. [45] to calculate the WBGT from standard meteorological variables, which is recommended for outdoor WBGT calculations in a review paper by Lemke and Kjellstrom [46]. The (outdoor) WBGT is the weighted sum of the natural wet bulb temperature T_w , the globe temperature T_g , and the dry bulb (ambient) temperature T_a :

$$\text{WBGT} = 0.7T_w + 0.2T_g + 0.1T_a \quad (1)$$

Separate calculation models for the natural wet bulb temperature and the globe temperature are used by Liljegren et al. [45], where all details on the calculations and required input parameters can be found.

In our modelling approach, hourly 2 m air temperatures, specific humidity, and wind speeds were taken from the UrbClim output data as input for the WBGT calculations. Downward solar radiation and surface pressure are also needed, and were taken from the ERA-interim re-analysis of the European centre for medium-range weather forecasting (ECMWF). Both these variables also serve as input data for the UrbClim model. To calculate the detailed amount of shade (either from buildings or trees) in a grid cell, shape files with building height and tree height were obtained from the city administration of Ghent. These files were converted to 1 m resolution raster files, and subsequently, for every hour of the period under study (see Section 2.3), the incoming solar radiation for the different solar zenith angles was calculated with the potential incoming solar radiation module of the system for automated geoscientific analyses (SAGA), an open-source geographic information system [47]. The results of these calculations were resampled to the UrbClim model grid, yielding fractional coverages of building shadow and tree shadow in every grid cell for every hour of the day. Finally, the fraction of the grid cells occupied by buildings was defined by resampling the building footprint raster to the model grid. We excluded this fraction from the calculations since we assume people do not stand regularly on their roof.

In the end, there were three types of locations in every grid cell: open, in the shadow of buildings, or in the shadow of trees. The open locations received the full amount of incoming solar radiation (both direct and diffuse, which are separately needed for the WBGT calculation), while for locations in the shadow of buildings, the direct fraction is set to 0 and only the diffuse fraction remains. In the shade of trees, the amount of direct and diffuse solar radiation was calculated according to the radiation transfer through the tree canopy scheme of De Ridder [48]. The overall WBGT value in a grid cell was taken as the weighted average of the respective WBGT values from these fractions.

Based on the approach outlined above, it is possible to obtain, in a fairly simple manner, outdoor heat stress values from general climate models, taking into account the detailed radiative shading effects of buildings and trees.

2.3. Experiment Setup

In order to evaluate the performance of the UrbClim model and the WBGT calculation, while also assessing the effectiveness of green and blue infrastructure in reducing outdoor heat stress, a dedicated measurement campaign was set up during the summer of 2015 in the city of Ghent. A measurement station was installed in the middle of a square of a public nature museum (Wereld van Kina, <http://www.dewereldvankina.be/>) in the city center during the months of July and August 2015. The station featured a WBGT sensor measuring 2 m (dry bulb) air temperatures, wet bulb and black globe temperatures, and relative humidity. The dry bulb temperature was measured using a highly accurate 43347 RTD temperature probe housed inside a fan-aspirated radiation shield, yielding a reported measurement uncertainty of only 0.1 °K. The relative humidity sensor has a reported measurement uncertainty of up to 5%.

During a particularly warm and sunny day (the 3rd of July 2015), two bikes were equipped with autonomous Onset HOBO U23-002 (<http://www.onsetcomp.com/products/data-loggers/u23-002>) temperature/humidity loggers at 2 m height and driven around the city center, through urban parks and to nearby rural areas, during the afternoon (12–16 h Local Time). The sensor tips were mounted in the same fan-aspirated radiation shields as the reference measurement station, using battery packs to power the fans during the trips. These measurements have a temporal resolution of 1 s. Furthermore, a floating fixed platform [49] was equipped with an automatic ventilated air temperature sensor (HOBO U23-002) at 2 m height to measure the cooling effect of a small lake near the city center, during the same time period as the bike measurements. Figure 1 shows the location and trajectories of all measurement devices.

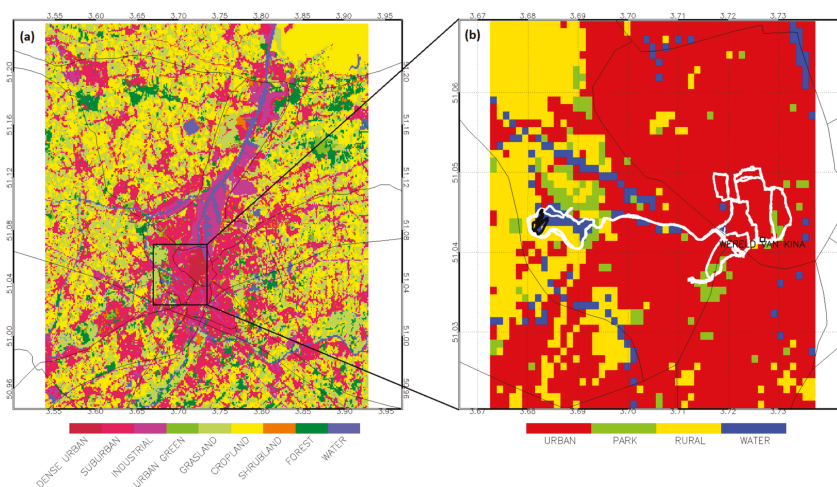


Figure 1. Extent and land use classification of the UrbClim model domain (a) and the focus area of this study around the measurement locations (b). The location of the observational station and the trajectories of the cycling (white) and boating (black) measurements are shown in the panel on the right.

Afterwards, the UrbClim model and the offline WBGT calculation were used to simulate the summer of 2015 for the wider agglomeration of Ghent, directly driven with meteorological data from the ERA-Interim re-analysis of the ECMWF, as was the setup in previous validation experiments [31,39–41]. The model domain is configured with 301×301 grid cells in the horizontal direction, using a spatial

resolution of 100 m. Figure 1 shows the extent of the UrbClim model domain and the land use in the domain. In the vertical direction, 20 levels are specified, with the first level 10 m above the displacement height, the resolution smoothly decreasing upward to 250 m at the model top located at 3 km height. This vertical discretization closely matches that of the ECMWF host model. The simulation is initialized on 1 May at 0000 LT, resulting in a two-month spin-up before the start of the analysis on 1 July, in order to ensure model equilibrium between external forcing and internal dynamics, especially in terms of soil variables. Initial soil temperature and soil moisture data are taken from the ERA-Interim re-analysis.

3. Results

3.1. Model Evaluation

Figure 2 shows the time series and error statistics of the measured and modelled 2 m air temperatures, dew point temperatures, and wet bulb globe temperatures at the observational station for the months of July and August 2015. There is a good correspondence between the measured and simulated air temperatures, with almost no bias, root mean square errors well below 2 °C, and a correlation coefficient over 0.9. These statistics are in line with previous validation results of the UrbClim model [31,39,41]. There is more variability in the comparison of the dew point temperatures, which is to some extent due to the larger uncertainty in the measurements. The measured dew point temperature is estimated from the air temperature and the relative humidity, of which the combined measurement errors can lead to an uncertainty well of over 0.5 °C. With this in mind, the error statistics are certainly reasonable. For the wet bulb globe temperatures, there is again a very good correspondence between measured and simulated temperatures, with a small positive bias, a root mean square error just above 1 °C, and a correlation coefficient of 0.95. There are a few days (e.g., 2 July) where the simulations deviate significantly from the observations, due to some observed cloudiness that is not picked up by the ERA-Interim re-analysis.

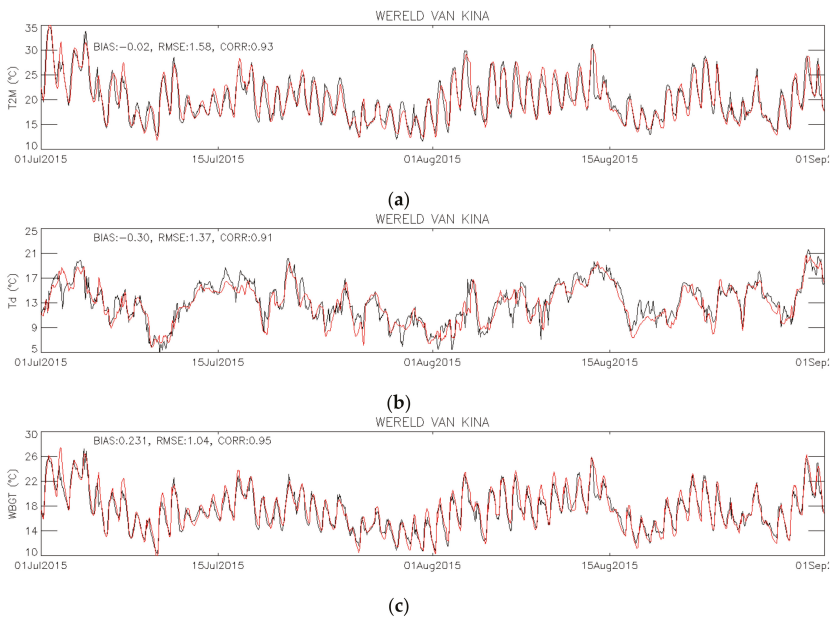


Figure 2. Time series of 2 m air temperatures (a), 2 m dew point temperatures (b), and wet bulb globe temperatures (c) for July and August 2015. Observations are in black, model results in red. The quantities given are the bias, root mean square error (RMSE), and correlation coefficient (CORR).

It is not straightforward to compare the simulated air temperatures to the mobile measurements. First of all, there is some local variability in land use that cannot be captured by the 100 m model resolution. Moreover, the model results have an hourly temporal resolution, whereas the observations have a temporal resolution of 1 s. To overcome these issues, we have grouped the measurements in four relevant land use classes (urban, park, rural, and water) and calculated the average value and standard deviation during a specific two hour period (14–16 h LT) of the afternoon of 3 July 2015. These values are compared to the modelled air temperatures for the same hours, taken from all grid cells of the focus area (Figure 1) for the respective land use classes. Table 1 shows the results of this comparison.

Table 1. Overview per land use class of the mean modelled and measured 2 m air temperatures, and their standard deviations (SD), for the afternoon (14–16 h Local Time) of 3 July 2015.

Land Use	Model		Measurements	
	Mean [°C]	SD [°C]	Mean [°C]	SD [°C]
Urban	30.2	0.26	30.0	0.45
Park	30.0	0.28	29.9	0.85
Rural	30.1	0.29	29.0	0.36
Water	28.4	0.43	28.4	0.32

The average model results are very close to the observed values for all land use classes, except for the rural class. The simulated rural air temperatures in the afternoon are almost as high as the urban ones, but the measured rural air temperatures are 1 °C lower than the urban air temperatures, so the model seems to underestimate, to some extent, the cooling effect of the rural locations during the afternoon. The differences between the other land use classes are well captured by the model, with the air temperatures over water being almost 2 °C lower than the urban and park air temperatures. The standard deviations of the measurements are significantly larger than these of the model results, demonstrating the large local variability within each land use class, which is difficult to capture for a 100 m resolution model.

Overall, the model performs satisfactorily compared to the measurements.

3.2. Effect of Green and Blue Areas on Air Temperatures

On the 3rd of July 2015, the air temperatures in the city of Ghent rose quickly during the day due to sunny and calm conditions, reaching over 30 °C during the day and only cooling down slightly during the evening and the night. In Figure 3 the daily cycle of modelled 2 m air temperatures for the different land use classes is presented. The results show that during these types of days, air temperature is highest in the urban areas, while urban parks show limited or no cooling effect on air temperatures during midday hours. The measurements presented in Table 1 suggested that the rural areas just outside the city are around 1 °C cooler than the city center during these warm hours, while the model estimates this effect to be a lot smaller. Both the measurements and the model show that the lowest temperatures during the afternoon are clearly found over water surfaces, being around 2 °C cooler during the warmest moment of the day.

It is important to also investigate the differences in night time temperatures, since this is the moment that the UHI is the strongest and has the biggest potential impact on human health, because the warmer urban night-time temperatures limit the recuperation of city inhabitants from heat stress during daytime [50,51]. During the night, the urban air temperatures are warmest, with the air temperatures in parks and over water being around 0.5 °C cooler. The lowest air temperatures during the night are found in the rural areas, which are around 2 °C cooler due to the greater long-wave radiative cooling in the open fields and grasslands.

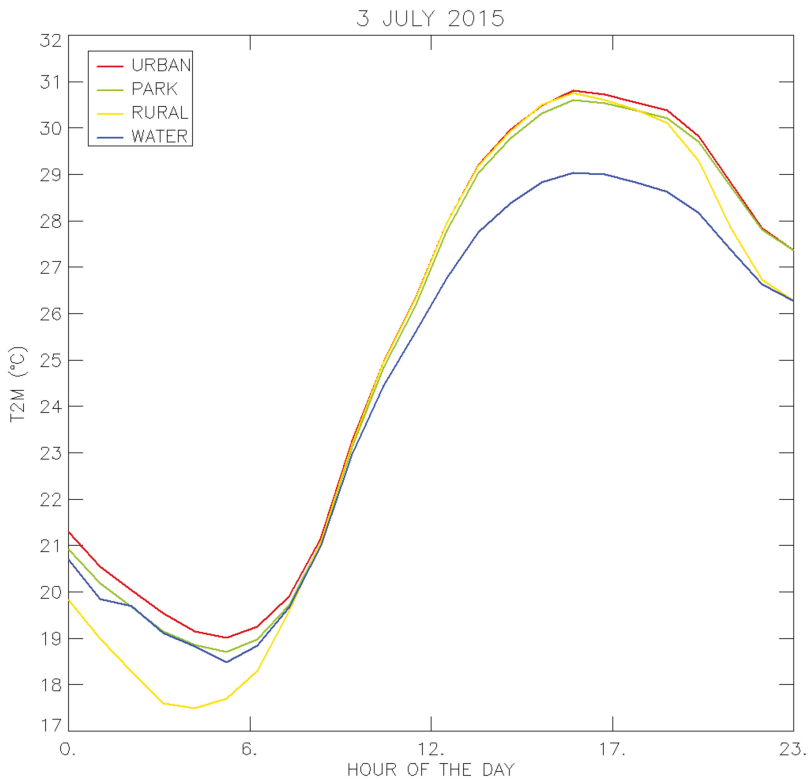


Figure 3. Daily cycle of modelled 2 m air temperatures with an hourly time resolution, averaged per land use class for the focus area.

3.3. Effect of Green and Blue Areas on Thermal Comfort

As explained in the introduction, it is important to also include humidity, wind speed, and radiation when assessing outdoor thermal comfort. Here, we apply the WBGT as a heat stress indicator, which is the ISO standard for human thermal comfort and takes these variables into account. In Figure 4, the daily cycle of the WBGT for the different land use classes is presented, differentiating between open and shaded locations.

Shading clearly plays a very important role regarding thermal comfort during the afternoon, when the differences in WBGT between all open locations are small (<1 °C), regardless of the land use. Even the water areas, where the air temperatures are several degrees cooler, have a WBGT value comparable to urban areas in the afternoon, due to the higher humidity, which offsets the cooler air temperatures. In urban areas, building shade provides a substantial cooling effect of 2 °C on the WBGT. The shade of trees in urban parks and rural areas has an even bigger cooling effect of around 3 °C. These are certainly the best places to avoid outdoor heat stress during a typical hot day in Ghent.

During the night, when there is no solar radiation, the WBGT values are in line with the air temperature results. Urban areas are warmest, with WBGT values in parks and over water being around 0.5 °C cooler. The coolest locations are the open rural areas, where minimal WBGT values are around 2 °C cooler than in urban areas due to the lower air temperatures there.

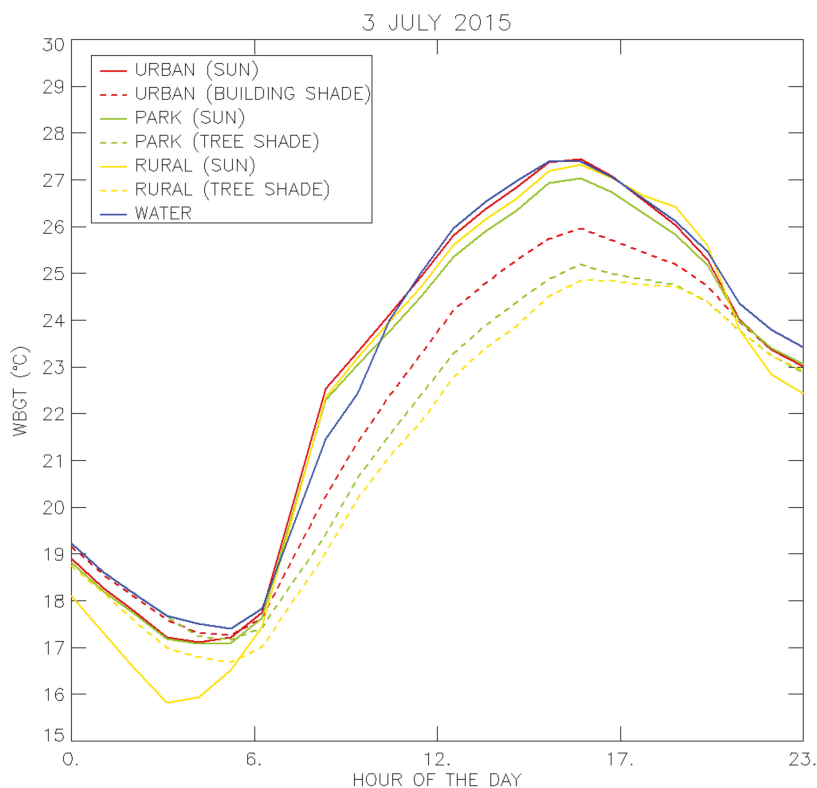


Figure 4. Daily cycle of modelled wet bulb globe temperatures with an hourly time resolution, averaged per land use class for the focus area. A distinction is made between unshaded (full lines) and fully shaded (dashed lines) areas.

4. Discussion and Conclusions

In this paper, we have presented an offline GIS-based post processing method, coupled to the urban climate model UrbClim, that can be used to calculate outdoor thermal comfort. The main advantage of our methodology is that we are able to calculate outdoor thermal comfort with a relatively high horizontal resolution for entire urban agglomerations and for long time periods (months to years), which is not possible with state of the art microclimate models. Moreover, the model can be easily validated with measurements, as we have demonstrated for the city of Ghent in Belgium, yielding satisfactorily results. As an example of the potential use of the model, the effectiveness of urban vegetation and open water areas in reducing air temperatures and heat stress for the city of Ghent during a particular warm summer day was assessed.

The modelling results regarding the effect of vegetation and water surfaces on air temperatures are in line with previous observational and modelling studies [20,21], with cooling effects of water surfaces up to 2 °C during daytime, and much smaller effects for night time temperatures when the water bodies maintain high water temperatures due to their high heat capacity. The cooling effect of park areas that is found in this study is small in comparison to reported observed values [12,13], which is probably due to the very small size of the city parks in Ghent, which, on top of that, feature a considerable amount of sealed surfaces. Related research studies on the effect of trees and water on outdoor heat stress have found similar results to the impact numbers reported here [27,28], with trees providing a substantial improvement to human thermal comfort by blocking solar radiation, even if air

temperature reductions are negligible. These types of scenario studies for urban areas (e.g., [52]) are performed with limited-area microclimate models such as ENVI-met that can only model a small part of a city for a few selected days.

Our methodology allows us to map outdoor thermal comfort for an entire city. As an example, Figures 5 and 6 show the daily maximum and minimum WBGT values on the 3rd of July for the city of Ghent, respectively. The results are limited to the city administrative area, since we only have the detailed building and tree height data for this area. The figures provide further evidence for the results discussed above, as the highest maximum WBGT values are found over open water and open urban areas, whereas the lowest maximum WBGT values are found in forested areas. The minimum WBGT map reflects the UHI situation for the city of Ghent with the warmest locations found in the city center and the urbanized areas around the city, and the coolest locations being the open rural areas outside the city.

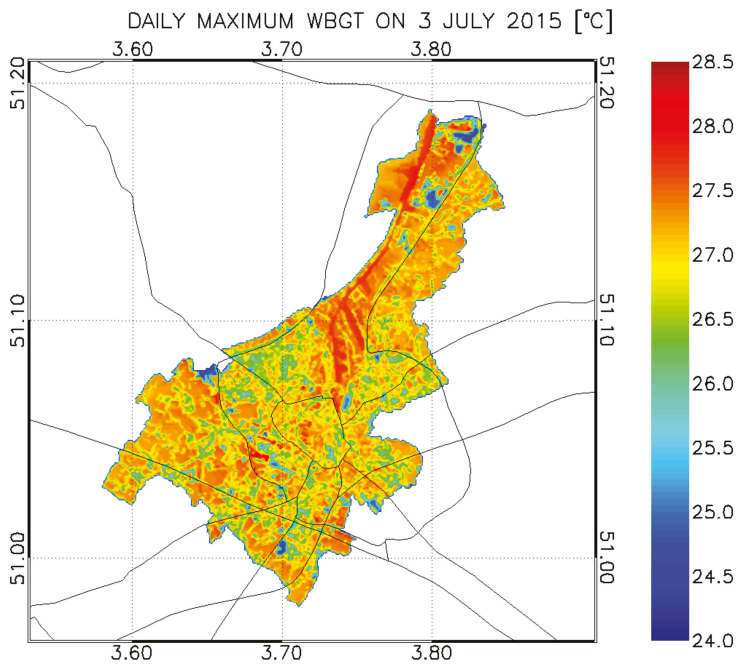


Figure 5. Map of the daily maximal wet bulb globe temperature for the city of Ghent.

Note that our analysis here focuses on a single hot day with calm and clear sky conditions. The reported cooling effects for the different land use types will differ and are lower when winds are stronger or more clouds are present. Also, in reality, the shading effect of trees will be dependent on the specific tree species and the health of the trees, which can be problematic in urban areas. Given these limitations and uncertainties, the results presented here are not suited for local risk assessment but should rather provide a coherent picture of potential outdoor heat stress benefits from water surfaces and green areas.

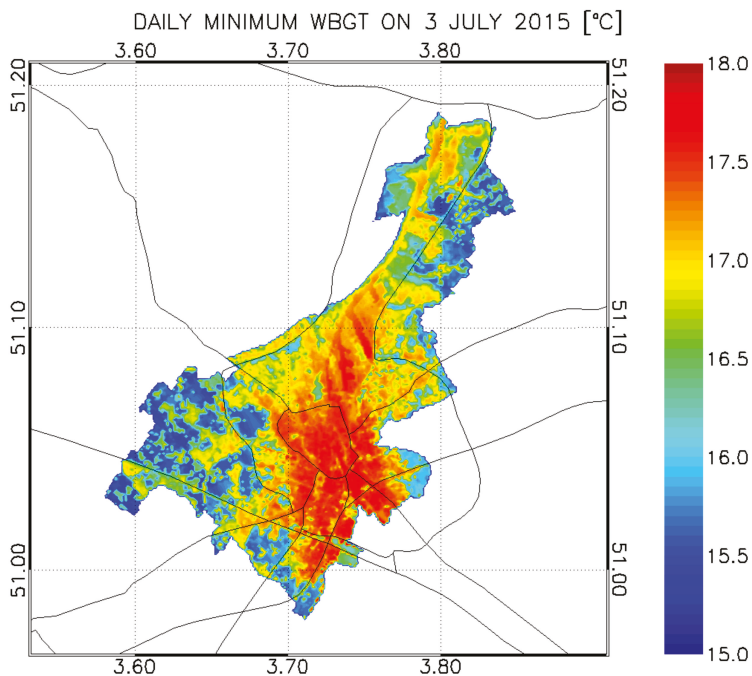


Figure 6. Map of the daily minimal wet bulb globe temperature for the city of Ghent.

Author Contributions: All authors contributed extensively to the work presented in this paper. K.D.R. supervised the project and is the creator of the UrbClim model. B.M. supervised the measurement campaign to which also K.D.R., W.B., M.D., and M.-L.V. contributed. H.H. was involved in the model creation and scripting. D.L. performed the model simulations, data analysis, wrote the manuscript, and drafted the figures. All authors discussed the results and implications and commented on the manuscript at all stages. All authors have read and agreed to the published version of the manuscript.

Funding: This research has been performed in the framework of the CORDEX.be project, funded by the Belgian Science Policy Office (BELSPO) under contract number BR/143/A2. Furthermore, the work described in this paper has received funding from the European Community’s 7th Framework Programme under Grant Agreements Nos. 308497 (RAMSES) and 308299 (NACLIM) and from the European Union’s H2020 Research and Innovation Programme under Grant Agreement No. 73004 (PUCS/Climate-fit.city). Marie-Leen Verdonck was funded by the Belgian Federal Science Policy Office, as part of the UrbanEARS project. Matthias Demuzere was funded by the FWO (Fund for Scientific Research) of the Flemish regional government.

Conflicts of Interest: The authors declare no conflict of interest.

References

1. Rosenzweig, C.C.; Solecki, W.W.; Romero-Lankao, P.P.; Mehrotra, S.; Dhakal, S.S.; Bowman, T.T.; Ali Ibrahim, S. *ARC3.2 Summary for City Leaders. Urban Climate Change Research Network*; Columbia University: New York, NY, USA, 2015.
2. Lemonsu, A.A.; Vigiú, V.V.; Daniel, M.M.; Masson, V.V. Vulnerability to heat waves: Impact of urban expansion scenarios on urban heat island and heat stress in Paris (France). *Urban Clim.* **2015**, *14*, 586–605. [\[CrossRef\]](#)
3. Oke, T.R.R.; Johnson, G.T.T.; Steyn, D.G.G.; Watson, I.D. Simulation of surface urban heat islands under “ideal” conditions at night. Part 2: Diagnosis of causation. *Bound. Layer Meteorol.* **1991**, *56*, 339–358. [\[CrossRef\]](#)
4. Masson, V. Urban surface modeling and the meso-scale impact of cities. *Theor. Appl. Climatol.* **2006**, *84*, 35–45. [\[CrossRef\]](#)

5. Lynn, B.H.H.; Carlson, T.N.N.; Rosenzweig, C.; Goldberg, R.; Druyan, L.; Cox, J.; Gaffin, S.; Parshall, L.; Civerolo, K. A modification to the NOAA LSM to simulate heat mitigation strategies in the New York City Metropolitan Area. *J. Appl. Meteorol. Climatol.* **2009**, *48*, 199–216. [[CrossRef](#)]
6. Gabriel, K.M.A.A.; Endlicher, W.R. Urban and rural mortality rates during heat waves in Berlin and Brandenburg, Germany. *Environ. Pollut.* **2011**, *159*, 2044–2050. [[CrossRef](#)]
7. Dousset, B.B.; Gourmelon, F.F.; Laaidi, K.K.; Zeghnoun, A.A.; Giraudet, E.E.; Bretin, P.P.; Maurid, E.E.; Vandentorren, S. Satellite monitoring of summer heat waves in the Paris metropolitan area. *Int. J. Climatol.* **2010**, *31*, 313–323. [[CrossRef](#)]
8. Sherwood, S.C.C.; Huber, M. An adaptability limit to climate change due to heat stress. *Proc. Natl. Acad. Sci. USA* **2010**, *107*. [[CrossRef](#)]
9. Martinez, G.S.S.; Baccini, M.M.; De Ridder, K.K.; Hooyberghs, H.H.; Lefebvre, W.W.; Kendrovski, V.V.; Scott, K.K.; Spasenovska, M. Projected heat-related mortality under climate change in the metropolitan area of Skopje. *BMC Public Health* **2016**, *16*, 407. [[CrossRef](#)]
10. Wouters, H.; De Ridder, K.K.; Willems, P.P.; Poelmans, L.; Hosseinzadehtalaei, P.P.; Tabari, H.H.; Brouwers, J.J.; Vanden Broucke, S.S.; van Lipzig, N.P.M.M.; Demuzere, M. Heat stress increase towards the mid-21st century is twice as large for cities compared to rural areas. *Geophys. Res. Lett.* **2017**, *44*, 8997–9007. [[CrossRef](#)]
11. Demuzere, M.M.; Orru, K.K.; Heidrich, O.O.; Olazabal, E.E.; Geneletti, D.D.; Orru, H.H.; Faehnle, M. Mitigating and adapting to climate change: Multi-functional and multi-scale assessment of green urban infrastructure. *J. Environ. Manag.* **2014**, *146*, 107–115. [[CrossRef](#)]
12. Tan, Z.Z.; Ka-Lun Lau, K.K.; Ng, E. Urban tree design approaches for mitigating daytime urban heat island effects in a high-density urban environment. *Energy Build.* **2016**, *114*, 265–274. [[CrossRef](#)]
13. Kong, L.L.; Lau, K.K.K.; Yuan, C.C.; Chen, Y.Y.; Xu, Y.Y.; Ren, C. Regulation of outdoor thermal comfort by trees in Hong Kong. *Sustain. Cities Soc.* **2017**, *31*, 12–25. [[CrossRef](#)]
14. Bowler, D.E.E.; Buyung-Ali, L.L.; Knight, T.M.M.; Pullin, A.S. Urban greening to cool towns and cities: A systematic review of the empirical evidence. *Landsc. Urban Plan.* **2010**, *97*, 147–155. [[CrossRef](#)]
15. Armson, D.D.; Stringer, P.P.; Ennos, A.R. The effect of tree shade and grass on surface and globe temperatures in an urban area. *Urban For. Urban Green.* **2012**, *11*, 245–255. [[CrossRef](#)]
16. Jamei, E.E.; Rajagopalan, P.P.; Seyedmahmoudian, M.M.; Jamei, Y. Review on the impact of urban geometry and pedestrian level greening on outdoor thermal comfort. *Renew. Sustain. Energy Rev.* **2016**, *54*, 1002–1017. [[CrossRef](#)]
17. Upmanis, H.H.; Chen, D. Influence of geographical factors and meteorological variables on nocturnal urban-park temperature differences—A case study of summer 1995 in Göteborg, Sweden. *Clim. Res.* **1999**, *13*, 125–139. [[CrossRef](#)]
18. Chang, C.R.R.; Li, M.H.H.; Chang, S.D. A preliminary study on the local cool-island intensity of Taipei city parks. *Landsc. Urban Plan.* **2007**, *80*, 386–395. [[CrossRef](#)]
19. Coutts, A.M.M.; Tapper, N.J.J.; Beringer, J.J.; Loughnan, M.M.; Demuzere, M. Watering our cities: The capacity for Water Sensitive Urban Design to support urban cooling and improve human thermal comfort in the Australian context. *Prog. Phys. Geogr.* **2012**, *37*, 2–28. [[CrossRef](#)]
20. Chen, Z.Z.; Zhao, L.L.; Meng, Q. Field measurements on microclimate in residential community in Guangzhou, China. *Front. Archit. Civ. Eng. China* **2009**, *3*, 462–468. [[CrossRef](#)]
21. Saaroni, H.H.; Ziv, B. The impact of a small lake on heat stress in a Mediterranean urban park: The case of Tel Aviv, Israel. *Int. J. Biometeorol.* **2003**, *47*, 156–165. [[CrossRef](#)]
22. Murakawa, S.S.; Sekine, T.T.; Narita, K.I.I.; Nishina, D. Study of the effects of a river on the thermal environment in an urban area. *Energy Build.* **1991**, *16*, 993–1001. [[CrossRef](#)]
23. Steeneveld, G.J.J.; Koopmans, S.S.; Heusinkveld, B.G.G.; Theeuwes, N.E. Refreshing the role of open water surfaces on mitigating the maximum urban heat island effect. *Landsc. Urban Plan.* **2014**, *121*, 92–96. [[CrossRef](#)]
24. Höpfe, P. The physiological equivalent temperature—A universal index for the biometeorological assessment of the thermal environment. *Int. J. Biometeorol.* **1999**, *43*, 71–75. [[CrossRef](#)] [[PubMed](#)]
25. Buzan, J.R.R.; Oleson, K.K.; Huber, M. Implementation and comparison of a suite of heat stress metrics within the Community Land Model version 4.5. *Geosci. Model Dev.* **2015**, *8*, 151–170. [[CrossRef](#)]
26. Matzarakis, A.A.; Rutz, F.F.; Mayer, H. Modelling radiation fluxes in simple and complex environments—Application of the RayMan model. *Int. J. Biometeorol.* **2007**, *51*, 323–334. [[CrossRef](#)] [[PubMed](#)]

27. Ng, E.E.; Chen, L.L.; Wang, Y.Y.; Yuan, C. A study on the cooling effects of greening in a high-density city: An experience from Hong Kong. *Build. Environ.* **2012**, *47*, 256–271. [[CrossRef](#)]
28. Shashua-Bar, L.L.; Pearlmutter, D.D.; Erell, E. The influence of trees and grass on outdoor thermal comfort in a hot-arid environment. *Int. J. Climatol.* **2010**, *31*, 1498–1506. [[CrossRef](#)]
29. Coccolo, S.S.; Pearlmutter, D.D.; Kämpf, J.J.; Scartezzini, J.-L. Thermal Comfort Maps to estimate the impact of urban greening on the outdoor human comfort. *Urban For. Urban Green.* **2018**, *35*. [[CrossRef](#)]
30. Reinhart, C.C.; Dogan, T.T.; Jakubiec, J.J.; Rakha, T.T.; Sang, A. UMI—An urban simulation environment for building energy use, daylighting and walkability. In Proceedings of the BS 2013: 13th Conference of the International Building Performance Simulation Association, Chambéry, France, 26–28 August 2013; Available online: http://www.ibpsa.org/proceedings/BS2013/p_1404.pdf (accessed on 5 January 2020).
31. De Ridder, K.K.; Lauwaet, D.D.; Maiheu, B. UrbClim—A fast urban boundary layer climate model. *Urban Clim.* **2015**, *12*, 21–48. [[CrossRef](#)]
32. ISO. *Hot Environments—Estimation of the Heat Stress on Working Man, Based on the WBGT-Index (Wet Bulb Globe Temperature)*; ISO Standard 7243; International Standards Organization: Geneva, Switzerland, 1989.
33. De Ridder, K.K.; Schayes, G. The IAGL Land Surface Model. *J. Appl. Meteorol.* **1997**, *36*, 167–182. [[CrossRef](#)]
34. Kanda, M.M.; Kanega, M.M.; Kawai, T.T.; Moriwaki, R.R.; Sugawara, H. Roughness lengths for momentum and heat derived from outdoor urban-scale models. *J. Appl. Meteorol. Climatol.* **2007**, *46*, 1067–1079. [[CrossRef](#)]
35. De Ridder, K.K.; Bertrand, C.C.; Casanova, G.G.; Lefebvre, W. Exploring a new method for the retrieval of urban thermophysical properties using thermal infrared remote sensing and deterministic modelling. *J. Geophys. Res.* **2012**, *117*. [[CrossRef](#)]
36. White, R.R.; Engelen, G.G.; Uljee, I. *Modeling Cities and Regions as Complex Systems*; The MIT Press: Cambridge, MA, USA, 2015; p. 330.
37. Gutman, G.G.; Ignatov, A. Derivation of green vegetation fraction from NOAA/AVHRR for use in weather prediction models. *Int. J. Remote Sens.* **1998**, *19*, 1533–1543. [[CrossRef](#)]
38. Danielson, J.J.J.; Gesch, D.B. *Global Multi-Resolution Terrain Elevation Data 2010 (GMTED2010)*; 2011–1073; U.S. Geological Survey: Reston, WV, USA, 2011; p. 26.
39. García-Díez, M.M.; Lauwaet, D.D.; Hooyberghs, H.H.; Ballester, J.J.; De Ridder, K.K.; Rodó, X. Advantages of using a fast urban boundary layer model as compared to a full mesoscale model to simulate the urban heat island of Barcelona. *Geosci. Model Dev.* **2016**, *9*, 4439–4450. [[CrossRef](#)]
40. Lauwaet, D.D.; Hooyberghs, H.H.; Maiheu, B.B.; Lefebvre, W.W.; Driesen, G.G.; Van Looy, S.S.; De Ridder, K. Detailed Urban Heat Island projections for cities worldwide: Dynamical downscaling CMIP5 global climate models. *Climate* **2015**, *3*, 391–415. [[CrossRef](#)]
41. Lauwaet, D.D.; De Ridder, K.; Saeed, S.; Brisson, E.; Chatterjee, F.; van Lipzig, N.P.M.; Maiheu, B.; Hooyberghs, H. Assessing the current and future urban heat island of Brussels. *Urban Clim.* **2016**, *15*, 1–15. [[CrossRef](#)]
42. Zhou, B.; Lauwaet, D.; Hooyberghs, H.; De Ridder, K.; Kropp, J.P.; Rybski, D. Assessing seasonality in the surface urban heat island of London. *J. Appl. Meteorol. Climatol.* **2016**, *55*, 493–505. [[CrossRef](#)]
43. De Ridder, K. Testing Brutsaert’s temperature roughness parameterization for representing urban surfaces in atmospheric models. *Geophys. Res. Lett.* **2006**, *33*. [[CrossRef](#)]
44. Hooyberghs, H.; Verbeke, S.; Lauwaet, D.; Costa, H.; Floater, G.; De Ridder, K. Influence of climate change on summer cooling costs and heat stress in urban office buildings. *Clim. Change* **2017**, *144*, 721–735. [[CrossRef](#)]
45. Liljegren, J.C.; Carhart, R.A.; Lawday, P.; Tschopp, S.; Sharp, R. Modeling the Wet Bulb Globe Temperature Using Standard Meteorological Measurements. *J. Occup. Environ. Hyg.* **2008**, *5*, 645–655. [[CrossRef](#)]
46. Lemke, B.; Kjellstrom, T. Calculating Workplace WBGT from Meteorological Data: A Tool for Climate Change Assessment. *Ind. Health* **2012**, *50*, 267–278. [[CrossRef](#)] [[PubMed](#)]
47. Conrad, O.; Bechtel, B.; Bock, M.; Dietrich, H.; Fischer, E.; Gerlitz, L.; Wehberg, J.; Wichmann, V.; Boehner, J. System for Automated Geoscientific Analyses (SAGA) v. 2.1.4. *Geosci. Model Dev.* **2015**, *8*, 1991–2007. [[CrossRef](#)]
48. De Ridder, K. Radiative transfer in the IAGL land surface model. *J. Appl. Meteorol.* **1997**, *36*, 12–21. [[CrossRef](#)]
49. Boëne, W.; Desmet, N.; Van Looy, S.; Seuntjens, P. Use of online water quality monitoring for assessing the effects of WWTP overflows in rivers. *Environ. Sci. Process. Impacts* **2014**, *16*, 1510. [[CrossRef](#)] [[PubMed](#)]

50. Changnon, S.A.; Kunkel, K.E.; Reinke, B.C. Impacts and responses to the 1995 heat wave: A call to action. *Bull. Am. Meteorol. Soc.* **1996**, *77*, 1497–1506. [[CrossRef](#)]
51. Loughnan, M.; Nicholls, N.; Tapper, N.J. Mapping Heat Health Risks in Urban Areas. *Int. J. Popul. Res.* **2012**, e518687. [[CrossRef](#)]
52. Yang, F.; Lau, S.S.; Qian, F. Thermal comfort effects of urban design strategies in high-rise urban environments in a sub-tropical climate. *Archit. Sci. Rev.* **2011**, *54*, 285–304. [[CrossRef](#)]



© 2020 by the authors. Licensee MDPI, Basel, Switzerland. This article is an open access article distributed under the terms and conditions of the Creative Commons Attribution (CC BY) license (<http://creativecommons.org/licenses/by/4.0/>).

Article

The RainBO Platform for Enhancing Urban Resilience to Floods: An Efficient Tool for Planning and Emergency Phases

Giulia Villani ^{1,*}, Stefania Nanni ², Fausto Tomei ¹, Stefania Pasetti ³, Rita Mangiaracina ⁴, Alberto Agnetti ¹, Paolo Leoni ¹, Marco Folegani ³, Gianluca Mazzini ², Lucio Botarelli ¹ and Sergio Castellari ^{5,6}

¹ Arpaè SIMC—Regional Agency for Prevention, Environment and Energy of Emilia-Romagna, HydroMeteoClimate Service, 40122 Bologna, Italy; ftomei@arpae.it (F.T.); aagnetti@arpae.it (A.A.); pleoni@arpae.it (P.L.); lbotarelli@arpae.it (L.B.)

² LepidaScpA, Research and Prototype Area, 40128 Bologna, Italy; stefania.nanni@lepida.it (S.N.); g.mazzini@ieee.org (G.M.)

³ MEE0 srl, 44123 Ferrara, Italy; pasetti@meeo.it (S.P.); folegani@meeo.it (M.F.)

⁴ NIER Ingegneria spa, 40013 Castel Maggiore (Bologna), Italy; r.mangiaracina@niering.it

⁵ EEA—European Environment Agency, 1050 Copenhagen, Denmark; sergio.castellari@eea.europa.eu

⁶ INGV—Istituto Nazionale di Geofisica e Vulcanologia, Sezione di Bologna, 40128 Bologna, Italy

* Correspondence: gvillani@arpae.it; Tel.: +39-051-649-7562

Received: 31 October 2019; Accepted: 11 December 2019; Published: 17 December 2019

Abstract: Many urban areas face an increasing flood risk, which includes the risk of flash floods. Increasing extreme precipitation events will likely lead to greater human and economic losses unless reliable and efficient early warning systems (EWS) along with other adaptation actions are put in place in urban areas. The challenge is in the integration and analysis in time and space of the environmental, meteorological, and territorial data from multiple sources needed to build up EWS able to provide efficient contribution to increase the resilience of vulnerable and exposed urban communities to flooding. Efficient EWS contribute to the preparedness phase of the disaster cycle but could also be relevant in the planning of the emergency phase. The RainBO Life project addressed this matter, focusing on the improvement of knowledge, methods, and tools for the monitoring and forecast of extreme precipitation events and the assessment of the associated flood risk for small and medium watercourses in urban areas. To put this into practice, RainBO developed a webGIS platform, which contributes to the “planning” of the management of river flood events through the use of detailed data and flood risk/vulnerability maps, and the “event management” with real-time monitoring/forecast of the events through the collection of observed data from real sensors, estimated/forecasted data from hydrologic models as well as qualitative data collected through a crowdsourcing app.

Keywords: web-based platform; early warning system; vulnerability simulations; flood risk maps; rainfall estimates; microwave links; CML; crowdsourcing; sensible targets

1. Introduction

Climate change affects the water cycle by intensifying it and this can change the magnitude, frequency, and timing of river floods in areas of the planet [1] such as some parts of Europe [2]. In particular, Blöschl et al. [3,4] by analyzing a pan-European database over the past five decades found clear patterns of change in flood timing in Europe due to changes in climate. However, the increasing trend of disasters due to floods in Europe is due also to non-climatic drivers, such as continued socio-economic growth, which induces population growth, economic wealth, and unplanned urbanization. Furthermore, the projected change in frequency of discharge extremes in Europe is likely

to have a large impact on the flood hazard, e.g., current 100-year flood peaks are projected to double in frequency within three decades [5].

The Floods Directive 2007/60/EC [6] published by the European Commission (EC), driven from the rising of human and economic losses of natural hazards, such as floods in Europe, aims to enhance the prevention, preparedness, protection, and response to flooding events and to increase the awareness of risk prevention measures within society. The early warning systems (EWS) are mentioned in this Directive as a relevant part of this disaster risk management cycle to support effective preparedness towards floods. Hence, it is fundamental for the European Member States to better identify the risk and occurrence of river floods and to better monitor the vulnerability of the society in order to establish effective early warning systems.

The usage of EWS as a useful tool to prevent damage, enhance the resilience of a society from natural hazards has been highlighted in the recent global policy treaties for climate change and disaster risk reduction in the last decade (e.g., the Paris Agreement in Articles 7 and 8 and the Sendai Framework for Disaster Risk Reduction in Priority 3 and 4). Furthermore, several success stories have shown that major EWS developments have been carried out due to technological advances (e.g., better forecasts made possible from radar nowcasting, ensemble weather models, high-resolution satellite data, more effective communication and sharing of information) [7–11]. Early warning systems can have a significant positive cost/benefit ratio in both disaster risk reduction and climate change adaptation [8,11–13]. In addition, the 2030 Agenda for Sustainable Development [14] has endorsed early warning systems as an essential action to be financed for protecting lives and property, thus contributing to sustainable development [15].

Early warning systems are defined by the United Nation Office for Disaster Risk Reduction (UNDRR) as “integrated system of hazard monitoring, forecasting and prediction, disaster risk assessment, communication and preparedness activities systems and processes that enables individuals, communities, governments, businesses and others to take timely action to reduce disaster risks in advance of hazardous events.” All these activities need to be coordinated in specific areas under interest and across multiple levels of governance to work effectively and to provide input in short times.

The challenge is to develop and implement early warning systems for any kind of scale of river catchments and especially for small catchments with a drainage area of a few hundred square kilometers that can be subjected to flash floods causing large amounts of damage in the urban context.

General review studies have discussed advances in river flood and river flash flood monitoring/forecasting and confirm the great hydrological challenge in developing and implementing an efficient early warning system despite the reliability of forecasts having increased due to the efficient integration of meteorological and hydrological modeling capabilities in the last years, especially in the developed countries [16,17].

Alfieri et al. [7] reviewed the current European operational warning systems for water-related hazards (e.g., river floods and coastal floods, flash floods, debris flows, mudflows, rainfall-induced landslides) due to severe weather conditions. This study identified those EWS including a weather prediction component to detect extreme events with considerable lead time, which can support early preparedness and effective disaster risk reduction. Further work is needed to better exploit the benefits provided by such systems [7].

Acosta-Coll et al. [18] conducted a systematic review to define the adequate structure of EWS for pluvial flash floods in urban areas. They identified the need for people-centered EWS with fail-safe systems able to guarantee the dissemination and communication of timely alerts during rainfall events. For doing so, the amount of rain and the water level need to be monitored and processed in real-time through the ultrasonic or radar sensors, which are more suitable for these applications. Finally, Acosta-Coll et al. [18] divided the EWS into four structures: “Disaster Risk Knowledge,” “Forecasting,” “Dissemination and Communication of Information,” and “Preparedness and Response.”

The presence of large complicated areas with barriers blocking, stormwater flow, insufficient drainage capacity, or the vicinity of a river, along with population growth and climate change impacts

makes the urban areas highly vulnerable to flash floods. Reliable EWS for flash flood forecasting in urban watersheds are challenging and need special attention to the overall control of all components to reduce potential severe losses and as well are key for more effective and coherent implementation of existing European Union (EU) policies on disaster risk reduction and climate change adaptation [19,20].

Finally, recent European projects started to find new solutions for adapting to intense river floods in urban areas by addressing the different aspects of monitoring and forecasting. The EU Interreg project URBAN-PREX (monitoring, forecasting, and development of online public early warning systems for extreme precipitation and pluvial floods in urban areas in the Hungarian–Serbian cross-border region) [21] supported, as components of online public early warning systems for citizens and public authorities, the implementation of monitoring precipitation networks through rain gauges in urban areas in the Hungarian–Serbian cross-border region. On the other hand, the EU Interreg project RAINGAIN [22] used radar technology to provide high-resolution estimates of rainfall in cities to forecast pluvial floods in test urban sites in the UK, Netherlands, Belgium, and France. The EU FP7 project STAR-FLOOD (STrengthening And Redesigning European FLOOD risk practices: Towards appropriate and resilient flood risk governance arrangements) [23] aimed to improve the implementation of flood risk strategies in urban areas which are vulnerable to pluvial floods in different European countries (UK, Sweden, Poland, Netherlands, Belgium and France) by designing policies for an appropriate and resilient flood risk governance. Among its different outcomes, this project highlighted the need for further improving systems for forecasting, warning and emergency responses for urban floods that are proactive, risk-based and use collaborative approaches, for instance by optimizing the use of ICT (apps).

The need to improve the EWS and emergency communications related to flood risk in urban areas has been addressed from the EU Horizon 2020 project FLOOD-serv (Public FLOOD Emergency and Awareness SERVICE) [24]. This project aimed to develop a collaborative platform that links citizens, public authorities, and other stakeholders and to enable the public to be warned in due time to reduce the adverse effects of floods.

Taking into consideration past studies and experience, the project RainBO focuses on the improvement of knowledge, methods and tools for the monitoring and forecast of extreme precipitation events and the assessment of the associated flood risk for small and medium watercourses in urban areas.

RainBO, funded by the EU Life Program, is a follow-up of the BLUEAP (Bologna Local Urban Environment Adaptation Plan for a Resilient City) LIFE project and T-Rain, a Climate-KIC (Knowledge and Innovation Community) project, in terms of implementing a reliable service based on big data coming from cellular networks.

The partners within the RainBO project, under the coordination of Lepida scpa (the in-house company of the Emilia-Romagna Region in charge of planning and implementing telecommunication infrastructures and IT services), comprise Arpae SIMC (the HydroMeteoClimate Service of the Regional Agency for Prevention, Environment and Energy of Emilia-Romagna is involved), the municipality of Bologna, MEEO (a small and medium enterprise with expertise in remote sensing and Commercial microwave links technology) and NIER (a consulting company with expertise on environmental analysis and risk evaluation).

The present article aims to describe the RainBO project and its main outcome: a webGIS (Geographic Information System) modular platform addressed local administrations to provide information from observed data, forecasts, and models before and during extreme events of precipitation in vulnerable river basins. On the platform, weather data are collected from traditional and innovative monitoring systems, weather forecasts are gathered from existing meteorological models whereas hydrological forecasts are provided by operational and newly developed models. The platform has been tested on two Italian urban areas, as detailed in the following.

The structure of the article is as follows: Section 2 describes an examination of existing data and useful models for the purposes of the RainBO platform, and afterward, the innovative methodologies developed within the project are explained. In Section 3, the platform and the main results achieved

during the project are then presented, with a description of its main structure, databases, and modules. Finally, remarks for further developments are described.

2. Materials and Methods

2.1. Study Areas

The application of the RainBO platform is performed on two test areas, the cities of Bologna and Parma, located in the Emilia-Romagna region, Italy. The climatic features referred to 1991–2015 period for these two cities are shown in Table 1 [25].

Table 1. Annual climatic features of Bologna and Parma (reference climate: 1991–2015).

Variable	Bologna	Parma
Minimum temperatures (unit: °C)	9.88	8.76
Maximum temperatures (unit: °C)	19.27	19.14
Mean temperatures (unit: °C)	14.59	13.95
Precipitation (unit: mm)	775.7	795.3

Both these urban areas are crossed by watercourses: the Ravone creek flows through Bologna, the Parma river flows through Parma (Figure 1).

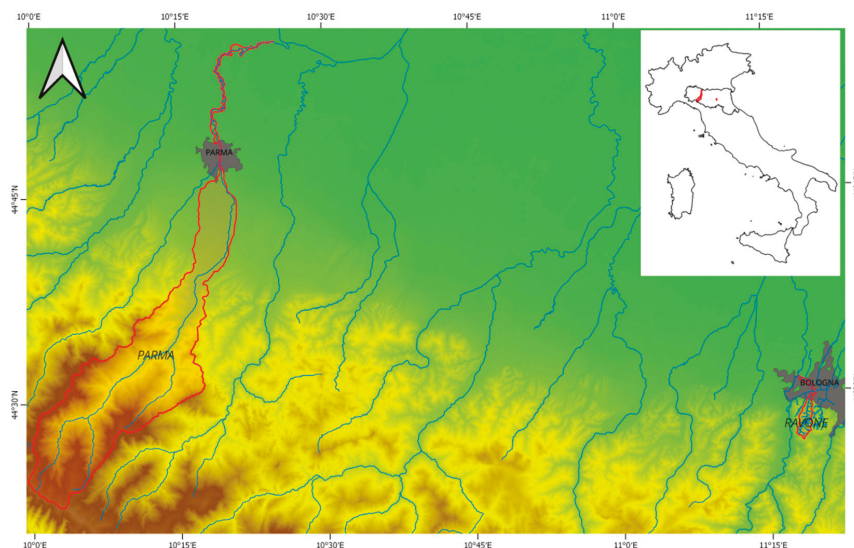


Figure 1. Study areas of the RainBO project.

As shown in the figure, the catchment of the Ravone creek is small, whereas the catchment of the Parma river is medium-large. The different sizes of the catchments are reflected in two different modeling approaches of the hydrologic forecasts, as explained below.

It is worthy to mention that each hydraulic section of the Emilia-Romagna catchments has three specific thresholds/levels of alarm: yellow threshold/warning, orange threshold/pre-alarm and red threshold/alarm. These thresholds are site-specific and defined according to Civil Protection purposes for public safety, taking into account the geometry of the hydraulic section of the watercourse and the statistical distribution of historical recordings.

2.1.1. Ravone Catchment

The Ravone catchment, together with the Aposa catchment, is the largest river basins at SW of Bologna. They flow from the hills directly across the central part of the city. The upper part of the Ravone catchment is characterized by hills and steep slopes, with a prevalent vegetation coverage (grass, shrubs, and forest) and partial urbanization in the stream valley. In contrast, the lower portion is flat and densely urbanized, the drainage network is mainly artificial, and the watercourse is connected with the main urban drainage system in a critical spillway crosspoint, flowing in a culvert underneath the city's urban area before joining the Reno river. The length of the natural reach of the Ravone is approximately 4 km covering an area of 6 km².

The Ravone catchment has been chosen as a study area of RainBO because, as recorded in historical data, the response of the catchment to extreme rainfall past events caused significant damages. For instance, during a flood that occurred on July 22nd, 1932, a victim and severe damages to streets and houses in the Southern part of the city were recorded [26].

The catchment is equipped by an existing monitoring network (Figure 2), including a weather station 500 m far from the Ravone catchment equipped with a rain gauge on S. Luca hill where data have been collected since the early 1930s. To integrate the available dataset and to better monitor the Ravone catchment, in 2014 a second rain gauge was installed at the catchment upstream end of mount Paderno and a water level gauge was installed at the culvert entry of the Ravone creek (Figure 3).

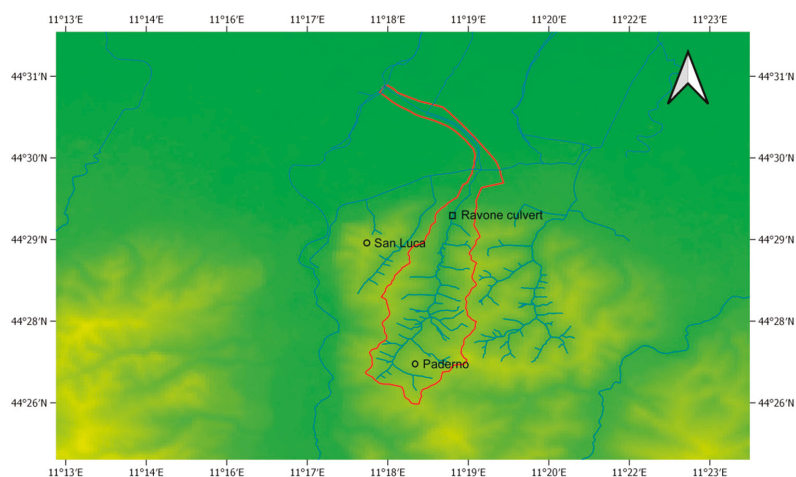


Figure 2. Map of existing monitoring network on the Ravone area. The circles are the rain gauges, the square is the water level gauge.



Figure 3. The entry of the culvert of the Ravone creek where the water level gauge is installed and the alarm thresholds are highlighted.

2.1.2. Parma Catchment

Parma river is the main river flowing through a homonymous city in Emilia-Romagna; it starts from Mount Marmagna at 1842 m.a.s.l. and flows in an N-NE direction joining the River Po near the city of Colorno as the right tributary. Usually, the hydrological responses for these basins are characterized by high discharges in the spring and autumn and low discharges in the summer.

The small catchment area and the steep part of the valley give high hydrological response during severe storms, generating, under particular conditions, flash flood events. Its major tributary is the Baganza River which has a very similar course and joins the main river on its left in the city of Parma (Figure 4).



Figure 4. Baganza river in Parma after the October 2014 event.

The available monitoring network for the Parma basin is composed of 15 rain gauges, 11 thermometers, and 6 water level gauges, these sensors are sufficient for the application of the RF Model, hence, no other installation was required (Figure 5).

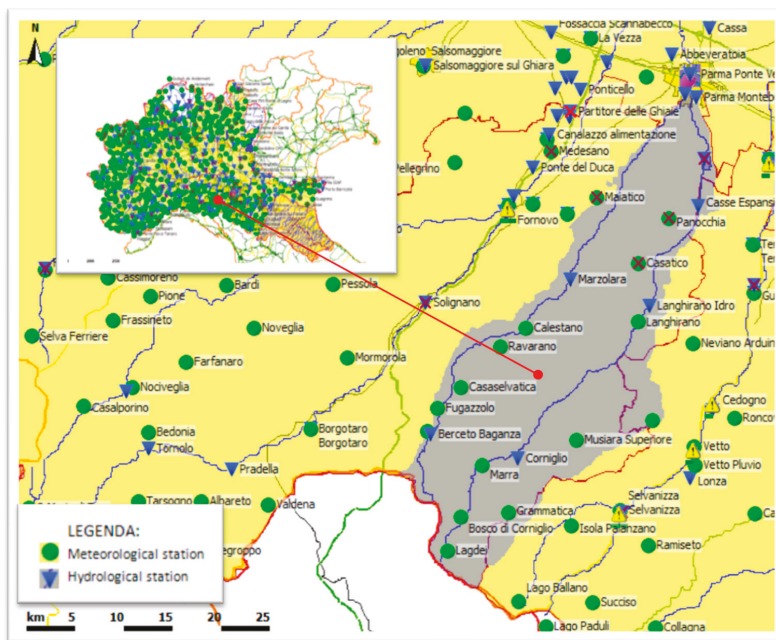


Figure 5. Parma-Baganza basin and monitoring network.

2.2. Background of the RainBO Project

The existing data and models at the beginning of the project identified as necessary for the development of the RainBO platform are described.

2.2.1. Territorial Data

According to the existing national and regional guidelines for the planning of Civil Protection, the following maps on the Emilia-Romagna region are available:

- Regional technical cartography (CTR) 1:5000 updated in 2013 with the topographic database (TIFF format)
- Ortho-photo Agea2014 (TIFF format) resolution 50 m
- Digital Surface Model Agea2008 (TIFF format) resolution 5 m × 5 m
- Digital Terrain Model Agea2008 (TIFF format) resolution 5 m × 5 m
- River catchments from numerical data 1:10.000 (shapefile format)
- Toponymy (shapefile format) 1:5000

These data are projected in the WGS84 UTM32N reference system.

2.2.2. Hazard, Vulnerability, and Risk Maps

To set up a tool for the management of flood risk in the Member States of the European Union, the main legislative reference is the Floods Directive [6]. In the directive, the hydraulic risk is the product of the hazard and potential damage at a specific event:

$$R = P \times E \times V = P \times D_p, \tag{1}$$

where:

- P (Hazard): it is the probability of occurrence, within a certain area and in a certain time interval, of a natural phenomenon of assigned intensity
- E (Exposure): it represents people and/or assets (structures, infrastructures, etc.) and/or activities (economic, social, etc.) exposed to a natural event
- V (vulnerability): the degree of capacity (or incapacity) of a system/element to resist at the natural event
- D_p (potential damage): it is considered as the degree of foreseeable loss following a natural phenomenon of a given intensity, the function of both value and vulnerability of the exposure
- R (risk): expected number of victims, injured persons, damage to property, cultural assets and environmental, destruction or interruption of economic activities, as a result of a natural phenomenon of assigned intensity

Emilia-Romagna Region has developed the Flood Risk Management Plan (FRMP), to be compliant with the Floods Directive [6] and Legislative Decree 49/2010, which requires these flood risk management plans to include measures to reduce the probability of flooding and its potential consequences and to address all phases of the flood risk management cycle but in particular the prevention, the protection, and the preparedness. As the causes and consequences of floods are different in the different member states of the Community, the Management Plans take into account the specific characteristics of the territories and propose specific objectives and measures tailored to the needs and priorities.

The FRMP of the Emilia-Romagna Region is represented by three projects, one for each hydrographic district (Po River, Northern Apennines, and Central Apennines).

Existing hazard maps represent the potential extent of flooding caused by watercourses (natural and artificial) with reference to three scenarios (rare floods, infrequent, and frequent) colored with three different shades intensity of blue, depending on the frequency of flooding as follows:

- rare floods of extreme intensity: return time up to 500 years from the event (low probability)
- infrequent floods: return time between 100 and 200 years (average probability)
- frequent floods: return time between 20 and 50 years (high probability)

The hazard maps from the Floods Directive are available on the whole Italian territory. They constitute the reference hazard maps for the computation of hydraulic risk and, for the purpose of the RainBO project, they have been selected on the study areas of Bologna and Parma.

Moreover, for the Bologna study case, in addition to the reference hazard map where the Ravone and other small streams are not included, a specific map for the Ravone creek is available [27]. This has been obtained through scenarios of flood analysis [28].

The existing vulnerability maps from the Floods Directive have been clipped on the study areas of Bologna and Parma. It should be noted that these reference maps do not consider in detail population distribution issues, as well as risk maps, as a consequence. In particular, to define the expected damages of a flood, the Directive suggests including the following main items:

- urban areas and urban expansion areas
- industrial and technological areas
- environmental heritage and cultural assets of significant interest
- presence of critical infrastructures such as transport, communication, utility networks
- presence of public and private services: sports plant, recreational facilities, accommodation facilities

The risk maps indicate the presence of potentially exposed elements (population involved, services, infrastructure, economic activities, etc.) which fall within floodable areas by means of a classification in 4 risk categories, represented by a color scale: yellow (moderate or no risk), orange (medium risk), red (high risk), purple (very high risk).

Existing risk maps from Floods Directive, created by the integration of hazard maps and vulnerability ones, identify static situations and do not take into account urban territory resilience peculiarity. In this case, risk maps have also been selected for the study areas of Bologna and Parma.

2.2.3. Historical Events

A catalog of historical events from 1981 is available for the Parma and Reno, including the Ravone catchment. A historical event is defined as the exceedance of at least one pre-alarm threshold. For each event, the involved catchment, the exceeded thresholds of water level gauge, as well as the description of the flooded area are recorded.

Moreover, where available, for each event further information (i.e., the number of people evacuated, dead or wounded people, emergency state—if requested, the possible assessment of economic damages) were collected. Moreover, the reports for all the events that occurred in Emilia-Romagna are available [29].

2.2.4. Observed Meteorological Data

A complex infrastructure for environmental monitoring and for an early-warning system is based on the integration of different data from many sources. The hydro-pluviometric network of Arpae collects data from rain gauges, thermometers, and water level gauges on the Emilia-Romagna region (Figure 6).

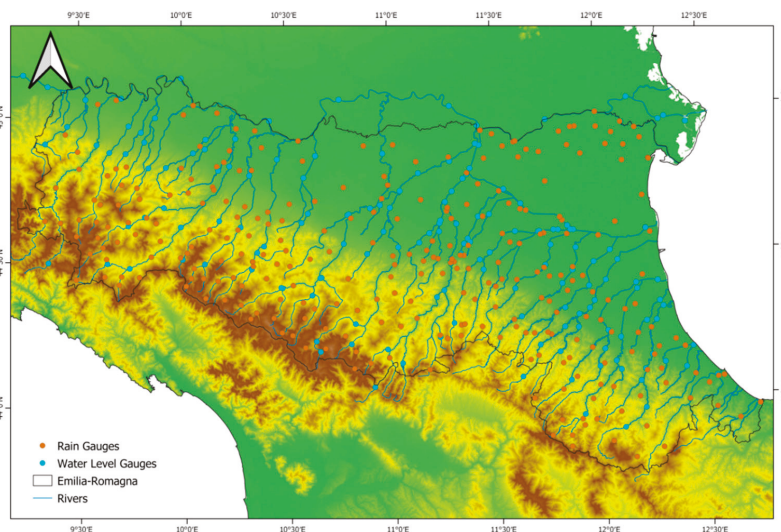


Figure 6. The hydro-pluviometric network of Emilia-Romagna.

For the RainBO purposes, the key variables are water level gauges (242 sensors) and rain gauges (282 sensors). Data coming from the hydro-pluviometric monitoring system are available on the Arpae ftp server. These data are acquired from the network every 15 min, the units are millimeters (mm) for precipitation and meters (m) for water level. In general terms, the series starts from 2003, the historical series for some sensors start from 1980.

These data are integrated into the Sensornet platform through a web service. Sensornet is the Internet of Things Platform of the Emilia-Romagna Region, that collects data and information from thousands of sensors distributed on the territory and builds a digital map over time [30].

The development of the RainBO platform implied also the empowerment of the monitoring network in critical areas not properly covered by sensors such as the Ravone catchment. For this reason, new monitoring sensors were installed in the Ravone area:

- a new real-time water level gauge has been installed in the upper part of the river basin
- a new weighing rain gauge has been located in a public property on the right side of the valley

These new monitoring sensors installed in the Ravone area are aimed at measuring environmental variables to be collected in the RainBO platform and at monitoring the Ravone creek with a high degree of accuracy.

2.2.5. Forecast Meteorological Data

The COSMO-LAMI forecasts provided by Arpaè-SIMC are available on an open data platform as GRIB files over Emilia-Romagna [31].

Meteorological COSMO-LAMI forecasts are based on the operative non-hydrostatic limited-area atmospheric COSMO (Consortium for Small-scale Modelling) model, nested on the ECMWF (European Centre for Medium-Range Weather Forecasts) operational global forecast. This system is developed and maintained by the homonymous European consortium, and managed by Arpaè-SIMC on the basis of the LAMI (Limited Area Model Italia) agreement. The forecast is issued twice a day (00 and 12 UTC) with a time range of 72 h on a regular 5×5 km grid covering the Mediterranean area.

2.2.6. Estimated Data

Commercial microwave links and radar data are estimated data, essential for the purposes of RainBO in order to monitor precipitation events.

The microwave links based on the rainfall monitoring system is an innovative but already tested technology, exploiting the microwave links used in commercial cellular communication networks (so-called commercial microwave links, CML).

Conventional rain gauges are not so effective during intense precipitation as their operating principle is based on mechanical tilting parts, which makes their measurements unreliable during this type of phenomenon. Rain gauges provide point-like measurements of the amount of rain fallen within the instrument sampling area, cumulated on time intervals, usually ranging from one minute to one day, with well known instrumental [32] and representativeness [33] limitations.

A relatively new and independent approach to the estimates of precipitation at the ground became available in the last decades with the broad diffusion of CMLs for cellular communication: integral precipitation content along a line path between two antennas can be estimated by measuring the attenuation of the microwave signal along the same path [34].

Heavy rain causes electromagnetic signal attenuation (from the transmitting antenna to the receiving one) and, subsequently, path-averaged rainfall intensity can be retrieved from the signal's attenuation between transmitter and receiver by applying, almost in real-time, a rainfall retrieval algorithm.

A distributed monitoring system can be developed by using received signal level data from the massive number of CMLs used worldwide in commercial cellular communication networks.

The first studies on this technology were concentrated on algorithms for spatial-temporal interpolation [35] from the joint analysis of multiple CMLs. The great potential of CMLs for ungauged regions was demonstrated by the Burkina Faso application [36]. In 2012, Overeem [37] demonstrated that processing algorithms are capable of providing real-time rainfall maps for an entire country, in this case, the Netherlands.

With regard to radar data, an existing dataset on Emilia-Romagna is based on hourly precipitation estimates obtained from the merger of the regional radar network managed by Arpaè-SIMC. This network is composed of two C-Band systems, one located at San Pietro Capofiume (Bologna) and the other in Gattatico (Reggio Emilia). Every 5 min during precipitation events, the radars provide reflectivity data that are processed by several algorithms. The reflectivity value is correlated to the precipitation intensity. Reflectivity data are provided by Arpaè-SIMC in open data [38].

For the RainBO project, an ad hoc stream was triggered for the automatic and periodic distribution of both reflectivity maps and hourly precipitation maps on the ftp server provided by Lepida, according to the RainBO project goals. Sent images are a merge of the two systems (reflectivity radar maps and accumulated hourly precipitation). Every new capture of the reflectivity (the frequency of observations is related to the weather conditions at the time) generates a merged image, which is then sent to the Lepida ftp server.

2.2.7. Crowdsourcing

A platform addressed to provide information for planning and management of extreme events and flash floods in urban areas should comprise also observations and contributions from citizens. These types of data, usually collected by means of applications, are a source of additional information during ongoing events but they are also conceived in order to engage and raise awareness of citizens. In this regard, the system Rmap [39] is a participatory monitoring and exchange system promoted by Arpa-SIMC, based on open hardware and software infrastructures, to collect and share meteorological data gathered by citizens between public and private institutions.

The Rmap application is mainly addressed to users and citizens with meteorological domain expertise and collects automatically the weather data in a WMO (World Meteorological Organization) binary data software (Binary Universal Form for the Representation of meteorological data—BUFR) through dedicated devices based on open hardware and free software. The weather information data can also be uploaded manually by expert users by using an on-line application, but the graphical user interface is not conceived as a smart tool for the general public.

It defines a set of standards for meteorological data sensing (security, reliability, elaboration) and for the transmission data system (transmission protocols, data formats, metadata formats, etc.).

The Rmap project has been promoted by Arpa-SIMC for some years, as it is an interesting project with the objective of defining methods, protocols, and formats to collect and share environmental data. The project is also promoted by Arpa Veneto, Cineca and the Computer Science Department of the University of Bologna and the RaspiBO network.

The Rmap system was taken into consideration because of this robust partnership and the relevant effort spent in its standardization.

The Rmap project adopts indeed a scientific approach based on standards defined by the WMO, in particular using their elaboration and classification process.

2.2.8. Models

The models used for the development of the RainBO services are:

- CRITERIA-1D
- CRITERIA-3D
- RANDOM FOREST

CRITERIA-1D [40,41] is a one-dimensional model developed by Arpae simulating the soil water balance, nitrogen balance, and crop development. The model is usually applied to agricultural case studies, nonetheless one of its main outputs (i.e., soil moisture) is a crucial variable for hydrological purposes. The CRITERIA-1D model simulates soil water movement by using a simplified model (tipping bucket) or a numerical model. It requires as an input at least daily data of temperature and precipitation, soil features, and crop information.

CRITERIA-3D [42] is a physically-based model developed by Arpae that works at the catchment-scale and solves equations of surface and subsurface water flow in a three-dimensional domain. The hydrologic component is a dynamic link library integrated into the other Arpae software, implemented within a comprehensive model that simulates the physical processes occurring in the catchment: surface energy, radiation budget, snow accumulation and melt, potential evapotranspiration, plant development, and plant water uptake.

The two models are under development and they are available as open-source code [43].

After the flooding of the Parma and Baganza rivers in Parma on October 2014, caused by heavy rains, the Civil Protection Agency of the Emilia-Romagna region required Arpae to develop a hydrological simulation model capable of promptly evaluating in advance the probability of overcoming the alert thresholds, especially for rapid or flash flood events. The RANDOM FOREST (RF) algorithm, applied in a hydrological context, provides the probability of overcoming the alert thresholds of some observation points for basins at small and medium scales in the oncoming next 6–8 h.

The RF model was added beside the existent hydrological-hydraulic model applied in real-time into the Flood Early Warning System Emilia-Romagna (FEWS-EMR) to provide a fast and preliminary response during flash flood or extreme rainfall events in the Emilia-Romagna basins.

The model is an ensemble learning method that operates by constructing a multitude of decision trees at training time and outputting the mode of the classes (classification) or mean prediction (regression) of the individual trees. Each tree classifies the dataset using a subset of variables. The number of trees in the forest and the number of variables in the subset are hyper-parameters and, for this reason, they have to be chosen a priori.

The number of trees is in the order of hundreds, while the subset of variables is quite small, if compared to the total number of variables, in Figure 7. the final Random Forests tree generated for Parma River at Ponte Verdi is shown, all paths end with terminal node that contains the probability of exceedance for each H.T.A. (hydrometric thresholds alert).

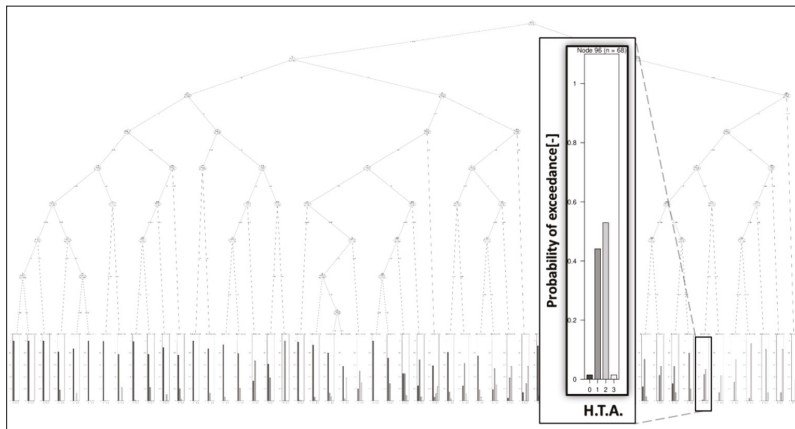


Figure 7. Random Forest tree generated for the main Parma River section (Ponte Verdi).

RF also provides a natural way to assess the importance of input variables (predictors). This is achieved by removing a variable at a time and assessing whether the out-of-bag error changes or not. If the out-of-bag error changes, the variable is important for the decision [44].

Model parameterization was performed using historical data (2003–2016), while recent data (2017–2019) are used for validation. Model parameterization was accomplished primarily by extracting historical events for each river section, hence defining the reference response time of the basin. This value was then used in the RF model, defining the maximum aggregation time for rainfall (Figure 8). For the RainBO project, the model was implemented using as input the same observed date used for the other Hydrological-Hydraulic model: observed mean hourly rainfall and discharge data.

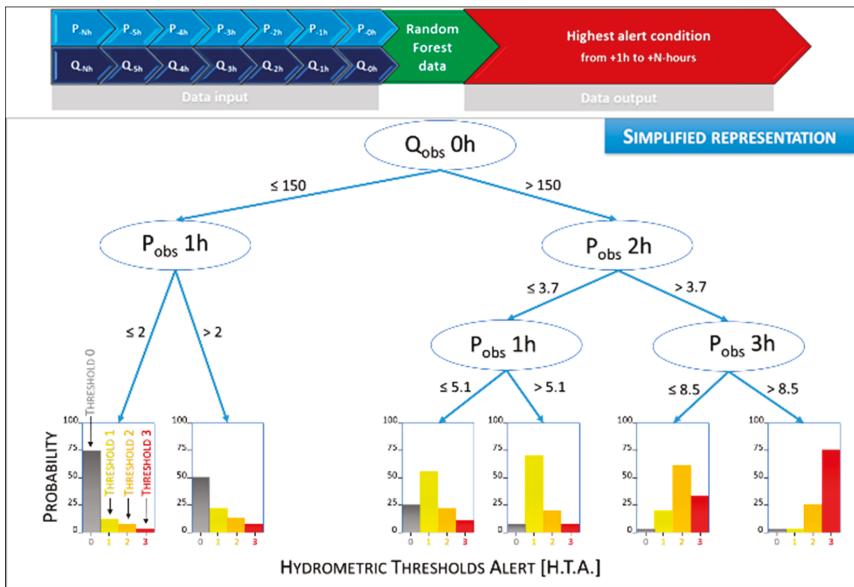


Figure 8. Random Forest model schematization. P_{obs} = observed mean hourly rainfall (unit: mm), Q = discharge (unit: m^3/s).

2.3. Foreground of RainBO Project: Innovation and Development

The development of the RainBO infrastructure started from existing data and models, then it focused on the application of new models specifically developed and new technologies, such as CML to enhance the monitoring systems during extreme events.

The project includes the development of a crowdsourcing web application for collecting and sharing information on the observed weather and its possible local effects/impact.

2.3.1. Commercial Microwave Links

The rainfall monitoring system proposed in the RainBO project exploits the Commercial Microwave links (CML or simply Microwave links—MWL) used worldwide in commercial cellular communication networks. Rain-induced attenuation and, as a consequence, path-averaged rainfall intensity can be retrieved from the signal’s attenuation by applying, almost in real-time, a rainfall retrieval algorithm. The algorithm chosen for this purpose is the RAINLINK retrieval algorithm [37]. The code is an open-source R package available for free download on GitHub [45].

The implementation of the algorithm for the specific needs of the Italian test areas, as well as code debugging and improving, was carried out within the RainBO project.

To validate the algorithm, a dataset was provided by Vodafone Italia on Bologna and Parma urban areas from February 2016 to June 2016. Other (not commercial) microwave link data were supplied by Lepida to cover the Apennines area, from March 2016 up to date, providing near-real-time data.

During the project, the CML data validation on the Bologna area was performed by comparing the quantitative precipitation estimates (QPE) from CML, radar, and rain gauges.

Radar and rain gauges data were chosen for the validation because they are currently validated, used, and published by ARPAE in their operative meteorological services. It resulted that the coherence between CML and the other estimates is quite promising even if it requires a tuning activity to integrate the dataset with existing technologies (like rain gauges or radar).

Excellent results are achieved mainly in a convective event as shown in Figure 9. On 11 May 2016 precipitation occurred with a well-defined gradient in the West–East direction and some local maxima in the North–West and South–West part of the province. Microwave accumulation slightly underestimated the rainfall field while an overestimation is recorded in the non-adjusted radar. The adjustment procedure well calibrates radar data as displayed in the top right panel of Figure 9. Fine-scale structure of the daily amount is well detected in both remote sensing maps.

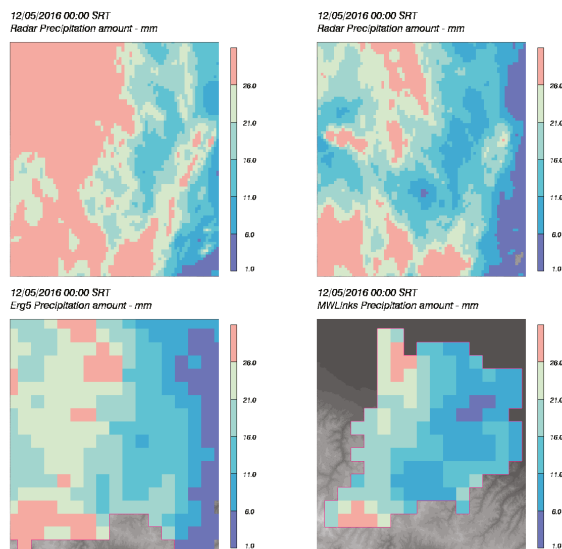


Figure 9. Quantitative precipitation estimates accumulated from 11/05/2016 00 UTC to 12/05/2016 00 UTC. (top left) Radar quantitative precipitation estimates (QPE), (top right) radar adjusted QPE; (bottom left) ERG5; (bottom right) microwave links QPE.

A qualitative analysis showed that the performance of the CLM estimate seems to increase in the second half of the analyzed period (May and June), mainly characterized by convective storms, even embedded in frontal patterns, where showers and heavy rain play an important role. As the microwave estimate is based on the attenuation that occurred in the link path, it is strongly related to rainfall intensity and the signal is, normally, stronger in the convective season. This behavior was confirmed by the quantitative analysis done by using statistical indicators that confirm a good rainfall estimation by CML data during summer and spring seasons. The validation has pointed out that CML estimation slightly underestimates precipitation occurrence both in spatial coverage and point amount, while radar adjusted has a complementary feature.

The precipitation monitoring infrastructure implemented during the RainBO project, based on the CML data, was called Rainlink4EMR (as the RAINLINK algorithm was applied to the Emilia-Romagna region) and a near-real-time module was implemented, which downloads the power attenuation raw data (CML data) from the Lepida telecommunication infrastructure and provides rainfall estimates on the midpoint of the links with a delay of a few minutes.

The validation study allowed us to achieve a first operational version of the related service, providing satisfactory reliability in monitoring convective events.

2.3.2. Crowdsourcing App

A crowdsourcing web application was implemented in RainBO to collect and display information regarding the observed current weather from expert users, as well as from people without any technical

skills. This webApp was created by means of a networking activity with the Rmap project [39] and, thus, it was called Rmap4RainBO.

The Rmap application is mainly addressed to users with meteorological domain expertise and collects automatically data coming from standard hardware devices and weather observation manually uploaded. The RainBO crowdsourcing application, called Rmap4RainBO, develops and improves the Rmap functionalities for the uploading and visualization of the observed weather and it keeps the WMO standard in the weather code. The RainBO crowdsourcing component, differently from the Rmap one, aims to address people without any technical skills so, as a consequence, it was developed as an intuitive and smart application that can be accessed through the RainBO project homepage [46].

The Rmap4RainBO application can benefit from the Rmap data and vice versa as the crowdsourcing information uploaded by citizens through Rmap4RainBO feeds the Rmap database.

Differently from the Rmap, the RainBO crowdsourcing webApp records the impacts, meant as effects of weather on the territory (damaged roads, fallen trees, ice on the road, etc.). The codes used to label the impacts were defined internally at the RainBO consortium as any official code was found on WMO standards; it represents a further innovative contribution by the RainBO project.

2.3.3. RainBO Vulnerability Model

The vulnerability module calculates the degree of vulnerability of exposed items over flood events.

The vulnerability reference maps do not consider in detail population distribution issues, whereas the vulnerability model developed for RainBO includes the presence of sensible targets in the territory (e.g., schools, nurseries, hospitals) and critical targets that can worsen a scenario reducing resilience, such as the fire brigade building.

To take into account in a realistic way the distribution of people on a territory, the developed algorithm considers different time frames: for example, the distribution of the population is supposed to be different in night hours (mainly in houses) with respect to working hours (mainly in workplaces). In a similar way, during morning time, students and teachers are supposed to be in schools, while during the afternoon school users decrease, and during the night no one is supposed to occupy these target buildings.

Vulnerability maps calculated by the vulnerability module are based on territorial data collected on the platform. Moreover, the maps, in summary, are calculated as a function of:

- time frame
- resident population distribution (based on land use—Copernicus, Urban Atlas 2012)
- employees distribution of industrial, commercial and agricultural sectors (based on land use—Copernicus, Urban Atlas 2012)
- users of sensible targets
- presence of critical targets as institutional site and first aid structures that could reduce the resilience of a territory, if they are involved by emergency events
- presence of critical targets such as industrial areas and utility networks, which could produce a domino effect if they are involved by emergency events

The platform provides 32 vulnerability maps (20×20 m grids in raster format), corresponding to 32 reference time frames.

This information is useful not only to compute more realistic vulnerability maps but also because it can be used by the early warning module. Through these data, the priority of targets to be warned during an ongoing emergency can be identified.

2.3.4. Hydrologic Forecast for Small Catchments

One of the main activities of the project has been the development of a model of the hydrological forecast for small basins, by using Ravone as a test case.

Within the available dataset (from 2014 to 2018) of observed water level at the culvert entry there are not events that exceed the alarm threshold. For this reason, CRITERIA-3D model has been used to simulate scenarios in order to assess the effects of severe rainfall events potentially able to exceed the alarm threshold (Figure 10), starting from initial conditions of soil moisture corresponding to the most remarkable event within the dataset (recorded on March 25th, 2015). The scenarios include three possible precipitation sum (70, 85, and 100 mm per event) with two possible event lengths (9 or 14 h) and two possible precipitation hyetographs (triangular and trapezoidal). These choices correspond to a discretization of the precipitation intensities recorded during the most remarkable past events (including the event recorded in 1932) when water level gauges were not installed. Thus, 12 possible precipitation scenarios on the Ravone catchment have been simulated with the CRITERIA-3D model. This discretization is a compromise between the need to simulate as many cases as possible and to run simulations within an acceptable computational time.

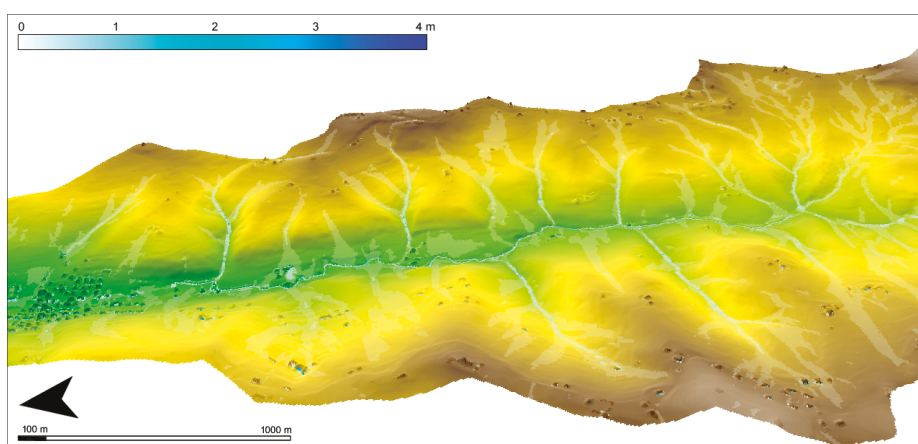


Figure 10. CRITERIA-3D simulation of the surface water flow on the Ravone catchment during a rainfall event. The color scale represents the surface water level (unit: m).

The water levels simulated by CRITERIA-3D have been integrated with observed data. On the resulting dataset, a statistical analysis has been performed, taking into account water levels, precipitation and soil moisture (defined as water holding capacity, see below for further details). As a result, a significant logistic regression between these variables has been identified.

The hydrological forecast is based on this regression using as input the forecast of precipitations of the COSMO-LAMI model, presenting the best available resolution in open data and calibrated on the study area. In order to include the spatial variability of the event, the computation is performed on the Cosmo grid cell containing the prevailing area of the Ravone catchment and on the 8 neighboring cells.

To validate the forecast algorithm, a hindcast analysis using the COSMO-LAMI forecasts for the period 2015–2016 was carried out. The analysis showed that the maximum intensity of precipitation forecast on the area is mainly underestimated, with an average underestimation of approximately a third of the observed value. To compensate for this underestimation, that could be cause missing alarms, the operational dataset used as input for the hydrologic forecast is integrated with a second forecast series where the maximum hourly intensity of precipitation is increased by 33%.

Therefore, an ensemble of forecast scenarios of precipitation is produced and an ensemble of the hydrological forecast is derived. The statistical distribution of this output is computed to provide a boxplot of the hydrological forecast.

In addition to the precipitation, the crucial variable for the hydrological forecasts is the soil moisture of the catchment. We decided to use an estimated value of this variable instead of measured one because

it has the advantage that it is not affected by sensor lacking or failures and local peculiarity. To estimate the soil moisture for catchments of small dimensions as Ravone, it is possible to assess the mean soil moisture of the area by means of a mono-dimensional soil water balance model, as CRITERIA-1D. For the development of the algorithm for the forecasts of exceeding the hydrometric threshold, a new output variable named water holding capacity (WHC) has been added to the CRITERIA-1D model. WHC provides the maximum amount of water the soil can retain before the runoff starts, given the current conditions of soil moisture. For the Ravone study case, CRITERIA-1D is set with the parameters of the prevailing soil on the catchment (silty loam) and the parameters of prevailing crop coverage in the area (fallow); the WHC index is computed on the upper soil layer (30 cm). Weather data (daily temperature and precipitation) used as input are the values of the analysis grid ERG5 on the Emilia-Romagna region.

3. Results and Discussion

The main output of RainBO has been the integration of the data and models described in the Materials and Methods encapsulated in an organic platform [47], as presented in the next paragraph.

3.1. The RainBO Platform

The RainBO platform consists of the following key elements:

- database containing monitoring, territorial, and historical data
- software modules, which are the platform intelligence
- graphic interface, which is the platform output

One of the most important features of the platform is the database containing the monitoring data, whose functionality is to integrate data collected from different monitoring infrastructures, both conventional and unconventional, as well as forecast data, hydrological, and meteorological models, and estimated ones.

In particular, the implementation of an advanced monitoring infrastructure within the RainBO Life project consists of the integration of these types of data:

- real sensors data (e.g., weather stations)
- “virtual sensors” data, not associated with observed measurements from physical sensors, but obtained indirectly through the estimation of correlated data or from simulation models
- forecast data, provided by simulation models

This structure allows us to monitor extreme precipitation events, their evolution, and to generate early warnings. It is worthy to mention that the concept of “virtual sensor” allows us to integrate information from observed and not observed data sources, georeferencing them with the same reference system and synchronizing them over time.

The integration of these new virtual sensors into the RainBO platform has been accomplished in a simple way, using the same data model defined for the physical sensors, without any extension or specialization and providing the platform with an enhanced monitoring infrastructure.

The territorial database hosts both the input data and the output data coming from the processing of the application modules, as well as, obviously, the data necessary to describe the territorial characteristics.

The RainBO platform architecture has been designed according to the following attributes:

- open: each module exposes standard interfaces (web services) to ensure system generality and replicability as well as interoperability and integration with other platforms
- centralized: each DB is centralized and enables data sharing, managed, and updated by different users

- scalable: each module is developed so as to be implemented on different machines
- modular: the platform is formed by individual modules ensuring more flexibility, maintainability over time, as well as platform evolution as each module can evolve or be replaced independently from each other
- configurable: each module is configurable, i.e., the operating parameters must be read from the table and not written in code

RainBO platform has been conceived according to two operational modes:

1. Planning support
2. Event management

Both the modes display a time bar with different time ranges according to the selected operational mode: the menu bar for the planning support mode refers to historical events whereas the menu bar for the event management mode refers to monitoring data (from -24 h to $+72$ h), in addition to menu bars and GIS maps specifically for each mode (Figure 11).

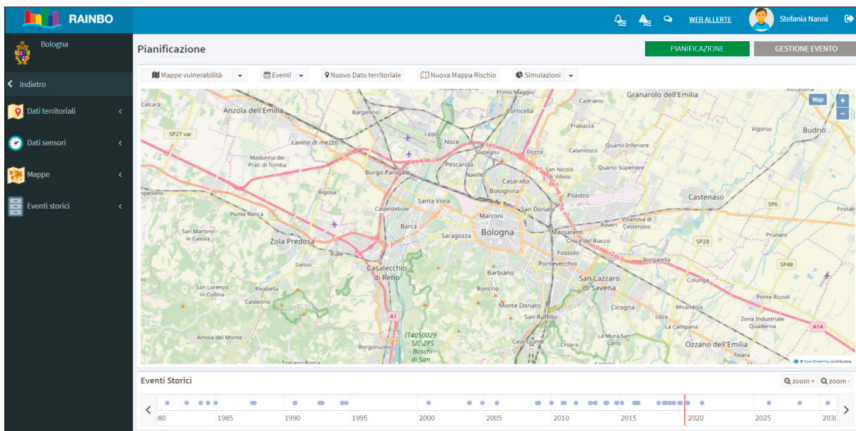


Figure 11. The opening screen of the RainBO platform interface in the planning support mode. On the left bar the thematic maps can be selected and displayed, on the bottom time bar the blue circles, corresponding to historical events, can be clicked and displayed on the map. The two buttons (green and gray) on the upper right corner allows switching from planning support mode to event management mode.

3.2. Territorial Data

To collect territorial data, the data model was defined according to the existing national and regional guidelines for civil protection emergency plans. It requires the mapping of all the critical, sensible, and strategic items, flood maps, river and territory maps (e.g., land use, network infrastructures, buildings, factories, parks).

The territorial database of the RainBO platform contains the existing data listed above: basic regional maps, hazard maps from the Floods Directive, and territorial data at municipality level (e.g., hospitals, schools, emergency areas). The territorial database also contains the maps resulting from the vulnerability module elaborations.

The definition of the spatial data model required an important standardization work to specify its structure, name, and format, to define a standard at the implementation level, both for the RainBO platform and as a reference for data coming from third-party systems.

For instance, the attributes to be provided for schools are the location, the polygon of the area, the number of students, employees and disabled persons, the number of floors of the building, the contacts of the school manager, including the phone numbers. The set of this information, as will be explained below, is necessary both to define the degree of vulnerability of critical sites, but also for the set up of the early warning system.

3.2.1. Hazard, Vulnerability, and Risk Maps

The RainBO platform includes reference hazard maps as:

- hazard maps deriving from the Floods Directive: they represent the potential extent of flooding caused by (natural and artificial) watercourses or by sea, with reference to three scenarios (rare floods (P1—L), infrequent (P2—M) and frequent (P3—H)) represented with three different shades of blue, where the decrease of frequency of flooding corresponds to the decrease in intensity of color. The Floods Directive hazard maps derive from the national hydro-geological management plan (PAI) and they are available for the main basins
- hazards maps from specific hydraulic model/studies for small basins, not included in the Floods Directive maps
- historical events maps that are maps of the flooded areas due to past events. These maps represent an important source of additional information to compare reference maps listed before and real ground effects expected in case of an event.

Concerning these maps, Figure 12a shows the hazard map related to the Parma river in the city of Parma from the Floods Directive. Figure 12b shows the same map integrated with the flooded area during the flood of October 13, 2014. This additional information extends the standard risk area to a secondary one.

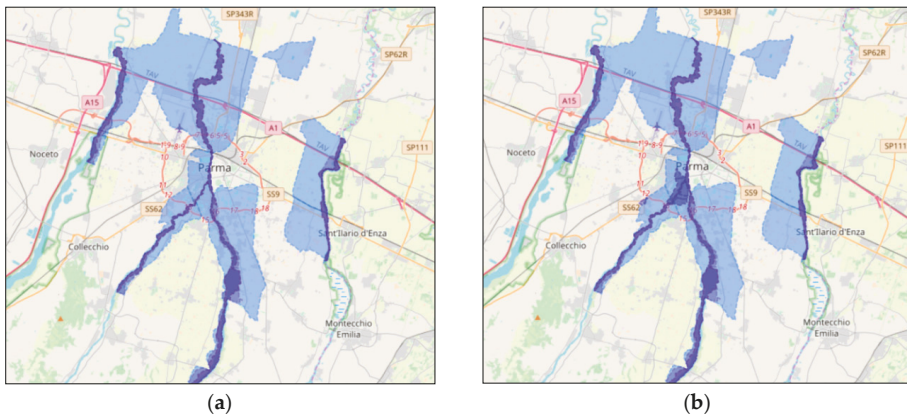


Figure 12. (a) Parma River hazard map from Floods Directive; (b) Parma River hazard map integrated with the flooded area of October 2014. The color from light blue to dark blue shows three different level of hydraulic hazard: P1—L (Low probability of floods or extreme event scenarios), P2—M (infrequent floods: return time between 100 and 200 years—medium probability), P3—H (frequent floods: return time between 20 and 50 years—high probability).

Figure 13 shows the hazard map related to the Reno River in the city of Bologna from the Floods Directive, integrated with the additional hazard map for the Ravone creek.

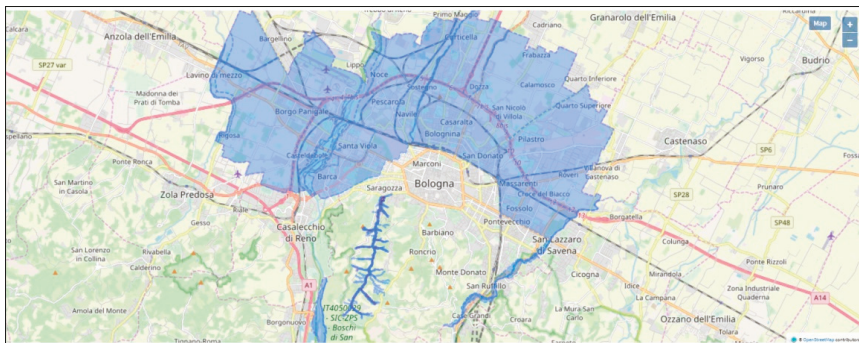


Figure 13. Reno River and Ravone creek hazard map. The color from light blue to dark blue shows three different level of hydraulic hazard: P1—L (low probability of floods or extreme event scenarios), P2—M (infrequent floods: return time between 100 and 200 years—medium probability), P3—H (frequent floods: return time between 20 and 50 years—high probability).

The vulnerability module calculates the degree of vulnerability as described in Section 2.3.3. As a result, 32 vulnerability maps, corresponding to 32 predefined time frames, are produced.

Furthermore, vulnerability maps are a support for territorial planning in prevention and preparedness stages also according to the regional law of December 21, 2017, n.24, which requires the preliminary assessment of the risk, and therefore of the vulnerability, with respect to different types of events, including the hydraulic one, for the purpose of defining the regional urban plan.

In case of an ongoing event, or forecast event, the RainBO platform can select and make available the vulnerability map of the corresponding time frame, providing support for its management.

In more detail, the main difference between the 32 vulnerability maps concerns the distribution of residents, workers, and users of sensible targets during the whole day. By way of example, during the night sensible targets, workplaces, and facilities are usually closed, therefore it is supposed that most of the population are in residential areas. As a consequence, in the vulnerability map referring to this time frame, the urban residential areas are represented in red, whereas during the morning of a working day these areas are green; during the night frame, also sensible targets as schools, gyms, or museums are green areas, whereas during opening hours these areas are red.

Figure 14 shows the vulnerability map of an area of the city of Bologna corresponding to a working day at 4 a.m. The vulnerability level shown in the following pictures is:

- Red for high vulnerability, which means the presence of many people in the grid cell.
- Orange is medium-high vulnerability
- Yellow is medium vulnerability
- Green is low vulnerability, due to the presence of few people in the grid cell

As a result, the RainBO platform provides also the corresponding 32 risk maps. In case other up-to-date or detailed hazard maps (besides the Flood Directive maps) are available, the platform allows us to specify the hazard map on which the risk can be calculated.

As described above, RainBO risk maps based on the vulnerability maps are more detailed and focused on the distribution of sensible and strategic targets and on the time depending presence of citizens in an urban area, with respect to Floods Directive data.

As a result, in case of a forecast event, the risk map, derived from the combination of the hazard map (now from the Floods Directive) and the vulnerability map (selected according to the time frame by the timing of forecast alert between the 32 maps of default) could better support decision-makers to prioritize the warning from the red areas to the green ones.

Moreover, in the planning phase, the capacity of the software to calculate new risk maps from vulnerability maps can support municipal technical and planning offices to evaluate territorial planning choices, as a preventive measure.

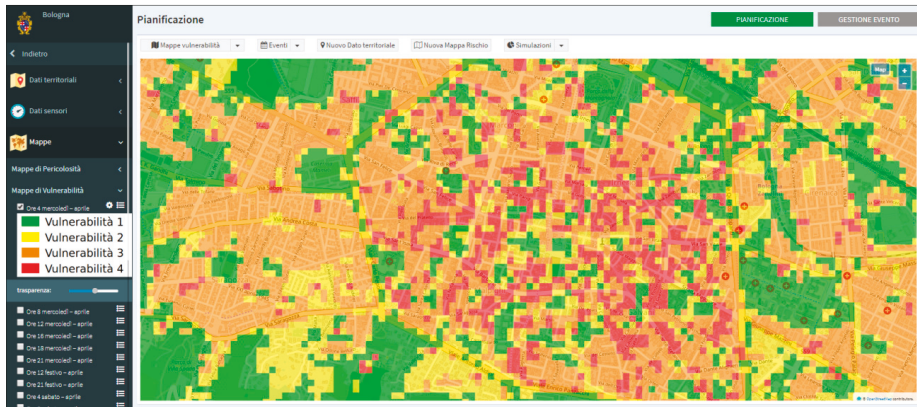


Figure 14. Vulnerability map at 04:00 of a working day. In the color legend, green (“vulnerabilità 1”) is low vulnerability, yellow (“vulnerabilità 2”) is medium vulnerability, orange (“vulnerabilità 3”) is medium-high vulnerability, red (“vulnerabilità 3”) is high vulnerability.

Figure 15 shows the risk map at 4:00 a.m. of a working day related to the Ravone creek, produced by using the hazard map of the catchment integrated within the RainBO platform and not included in the Floods Directive.

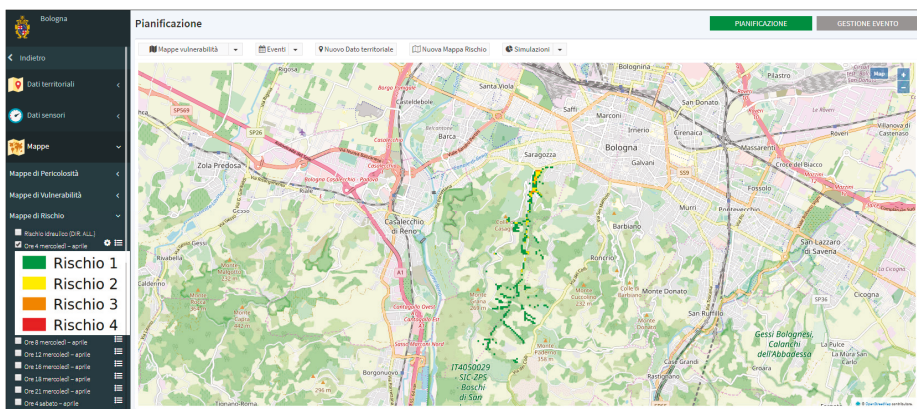


Figure 15. Risk map at 04:00 of a working day referred to the Ravone creek. In the color legend, green (“rischio 1”) is low risk, yellow (“rischio2”) is a medium risk, orange (“rischio3”) is medium-high vulnerability, red (“rischio3”) is high risk.

3.2.2. Historical Events

RainBO platform integrates a database where the most significant past flood events on test catchments provided by Arpaè are stored. This database is aimed at collecting meaningful information for the management of future events. The time bar allows us to identify and explore the flood events in the planning support mode. The most important information linked to the event (e.g., data catchment

of interest, the exceeded threshold of water level gauge, the description of flooded area uploaded on the platform as vectorial data) are highlighted in one view Figures 16 and 17.

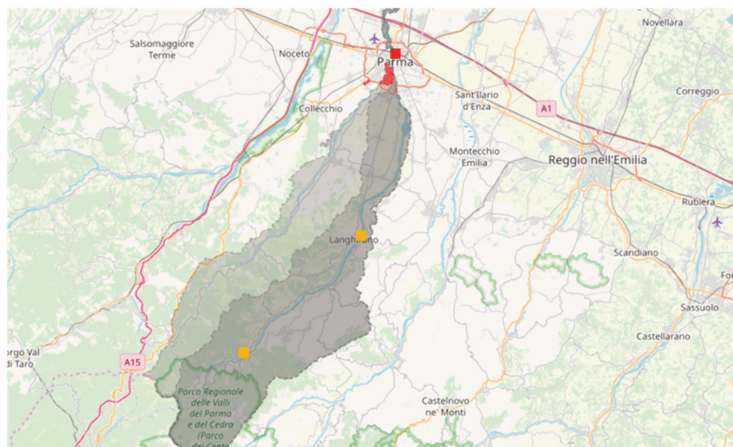


Figure 16. Past flood event on the Parma catchment. The colored squares represent past events where the red (alarm) and orange (pre-alarm) thresholds were exceeded.

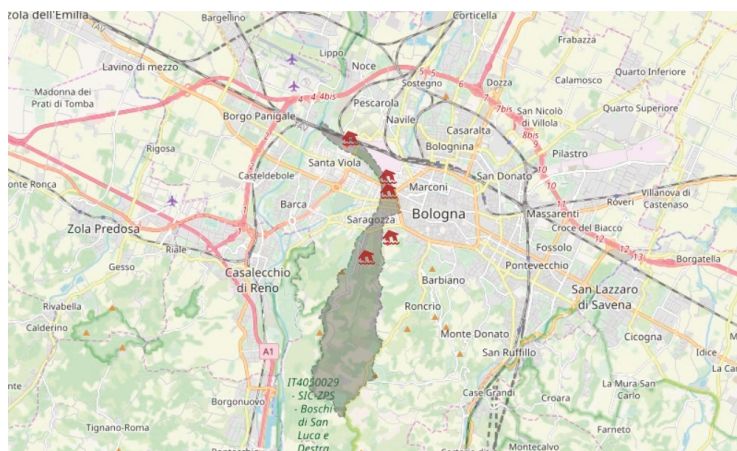


Figure 17. Map of critical points referred to an extreme event occurred on 2015, March 25th in Ravone catchment. The house icons represent the points where damages due to extreme events are recorded.

3.3. Observed, Forecast, and Estimated Data

With regard to the observed data, the RainBO platform collects data from heterogeneous sensors: inclinometers for landslide monitoring, rain gauges, and water level gauges for hydro-pluviometric monitoring of the Arpae network (including the new monitoring stations installed for the RainBO project), inductive-loop detectors for traffic monitoring. The RainBO platform integrates more than 1500 sensors of different types and technologies (Figure 18).

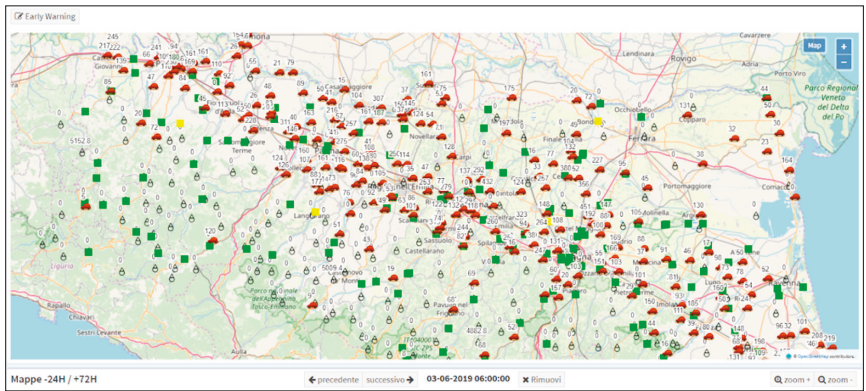


Figure 18. RainBO sensors of observed data: water level gauge (rectangles), rain gauges (drops), and traffic data (cars).

Precipitation forecast maps of the COSMO-LAMI model (Figure 19) are available in a specific section of the platform. Forecasts are summed on 3 h and can be displayed by means of the time bar until the following 72 h.

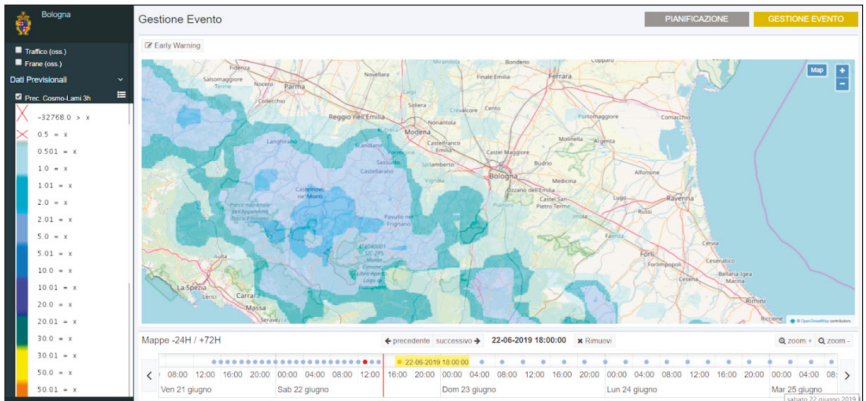


Figure 19. Map of the COSMO-LAMI precipitation forecast. The left-sided color legend represents the quantity of precipitation forecast (unit: mm).

With regard to the estimated data, the system displays maps of radar reflectivity (Figure 20) and radar-estimated precipitation. These two variables are directly related. The hourly maps of these variables can be explored using the time bar for the previous 24 h and it allows the monitoring of ongoing events.

Concerning CMLs, the RainBO platform integrates 73 microwave virtual sensors, corresponding to the midpoint of radio links on the Lepida wireless network (Figure 21).

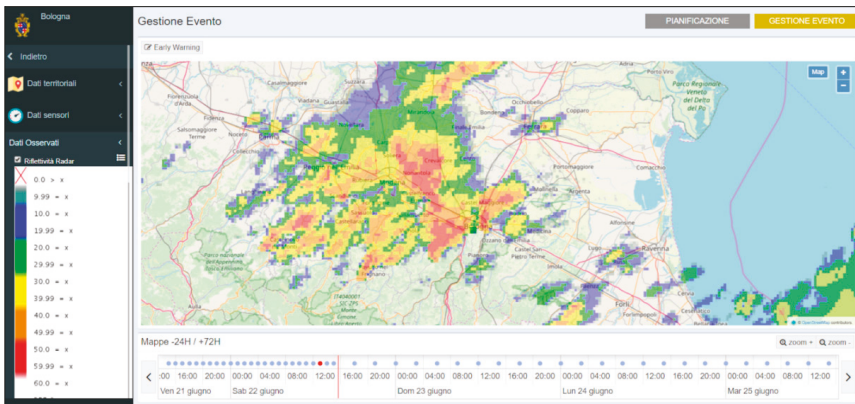


Figure 20. Map of radar reflectivity, a proxy variable to estimate precipitation. The left-sided color legend shows the scale of reflectivity (unit: dBZ).

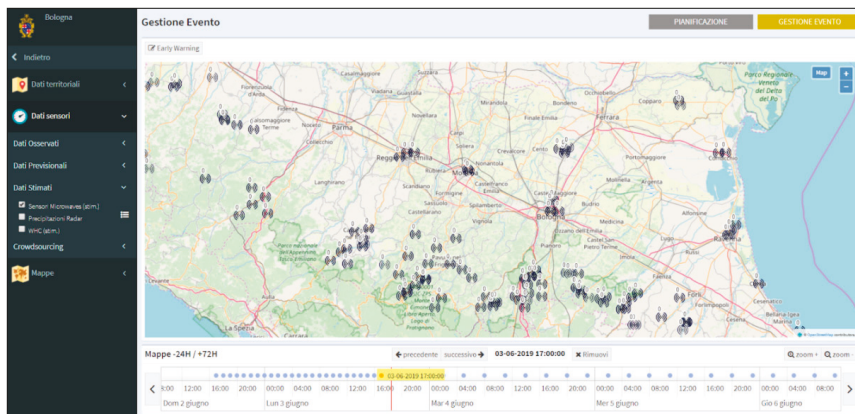


Figure 21. Virtual sensors of precipitation estimated by commercial microwave links (CMLs). The radio wave icons represent the midpoint of radio links on the Lepida wireless network.

3.4. Hydrologic Forecast

RainBO platform provides the forecast of exceeding critical thresholds on the two test catchments, the River Parma for the Parma municipality and the creek Ravone for Bologna municipality. The forecast refers to specific hydraulic sections of the catchments: the culvert entry for Ravone creek, Ponte Verdi, and Ponte Nuovo hydraulic sections for the Parma River.

The forecast covers different time ranges, 6 h for the Parma and 72 h for Ravone, as it is produced by different forecast models, as explained before. In the following, two examples of the RainBO Platform functioning in Event management mode during two extreme events are presented. With regard to the Bologna pilot case, during the afternoon of May 18th, 2019, the Ravone creek exceeded the warning threshold with two water level peaks of 0.82 m at 14 UTC and 0.69 m at 17 UTC.

The water level forecast at the culvert of Ravone issued by the RainBO platform on the morning of May 17th (Figure 22a) matched with the observed values: the exceeding of warning threshold was foreseen with a low probability to exceed the pre-alarm threshold. However, the timing of the event was not correctly forecasted. The hydrological model uses as input the COSMO-LAMI model

that forecasted the precipitation peak during the early morning, whereas it occurred about 8 h later. Therefore the hydraulic forecast shows the same time shift. (Figure 22b).

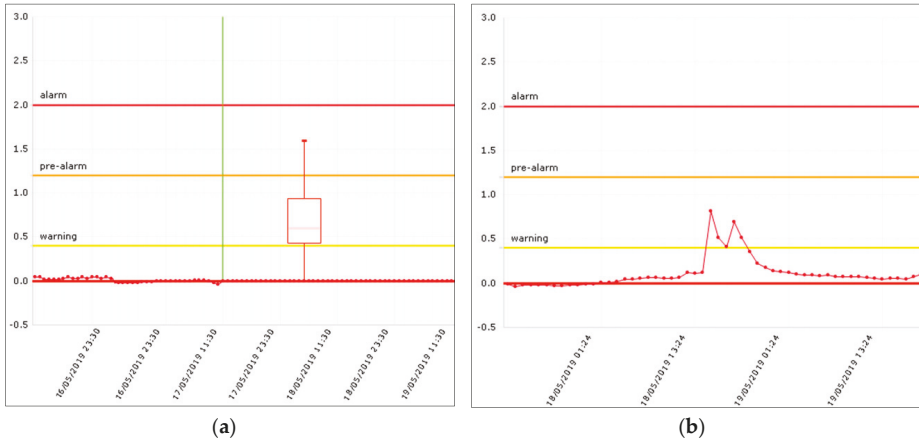


Figure 22. (a) Operational forecast of the maximum water level (m) at the culvert entry of Ravone delivered by the platform on the morning of May 17th, 2019. The green line is the moment of the forecast, on the left, the red dots are the observed data, on the right, the boxplot is the forecast distribution. The box of boxplot represents the interval between the 25° and 75° percentile, the tails are the 5° and 95° percentiles; (b) water level (m) observed at the culvert entry of Ravone, as displayed on the RainBO platform in the event management mode.

Concerning the Parma case study, in 2017, December 12th, the Parma river basin was interested in an intense and prolonged rainfall event, starting from the 14:00 UTC of the 10th of December a weak rainfall interested the basin till the day after when the rainfall started growing in intensity and space. The peak in terms of mean area rainfall was at midnight on December 11th with about 8 mm/hr (Figure 23).

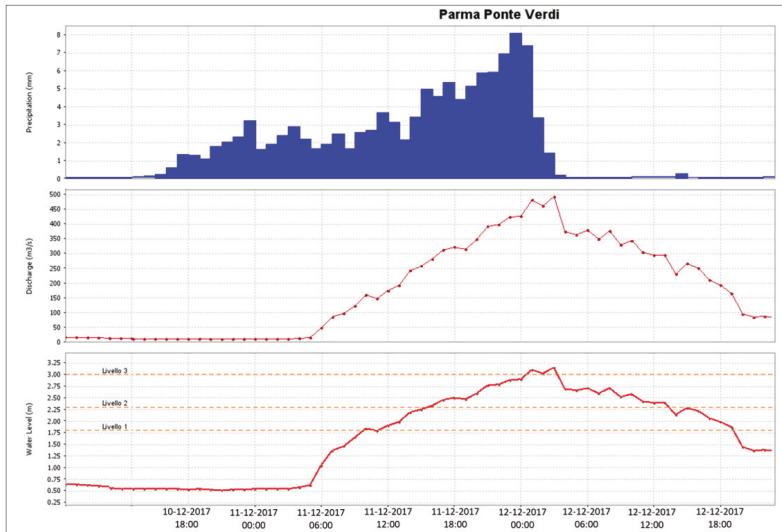


Figure 23. Mean rainfall, discharge, and water level during the December 2017 event.

Looking at the riverside we observed, at 05:00 UTC, the first raise of levels in the river Parma at Ponte Verdi with a level 1 threshold crossing event on the same day at 11:00 UTC. Levels raised continuously in the next hours due to the prolonged rainfall in the basin, reaching the threshold 2 at 16:00 UTC and a peak of 3.14 m (meter above local reference) at 03:00 UTC of the 11th of December, and at the same time, the rainfall in the basin ended with a total amount of mean area rainfall for the entire event of about 116 mm.

The forecast probability generated by the RF model during this event is shown in Figure 24. We can notice that all threshold reached a high probability, between 90–100%, this is obviously related to the high level reached by the river during the event, but we can also consider the forecast lead time provided by the model, in fact, if we look at Table 2, we can find a good consistency between probability and observed effects few hours later, especially for threshold 3 where at 18:00 UTC the probability raise from 12% to 44%, and lately at 20:00 reached a 73%, about 6 h before the effective threshold crossing event, observed at 02:00 UTC (red color).

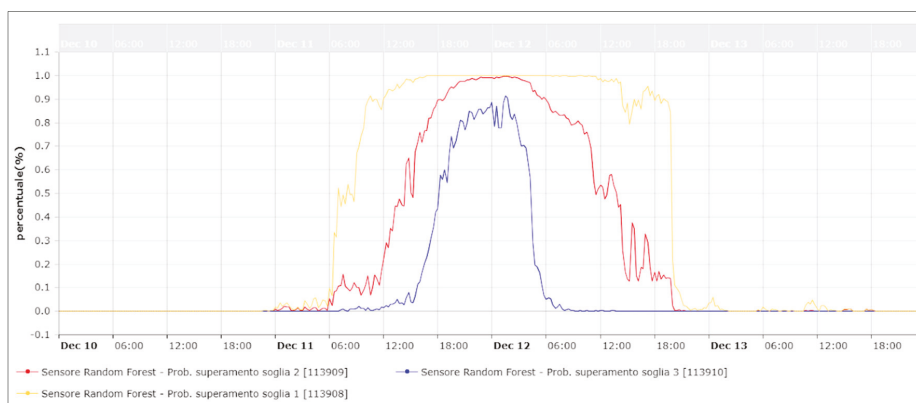


Figure 24. RainBO platform RF results for the Parma River during the event of December 2017.

Table 2. Threshold crossing probability for each level (Green < Threshold 1, Yellow < Threshold 2, Orange < Threshold 3, Red > Threshold 3).

Thr/hrs	07:00 A.M.	08:00 A.M.	09:00 A.M.	10:00 A.M.	12:00 A.M.	02:00 P.M.	04:00 P.M.	06:00 P.M.	08:00 P.M.	10:00 P.M.	00:00 A.M.	02:00 A.M.	03:00 A.M.
1	52	54	67	87	90	96	100	100	100	100	100	100	100
2	11	10	10	11	22	45	76	90	96	99	99	99	99
3	0	0	1	0	1	4	12	44	73	81	89	83	74

3.5. Early Warning Module

An early warning module was developed in the RainBO platform in order to identify the expected scenario as a function of monitoring, forecast and vulnerability maps. A filtering and signaling system allows to select and group essential information useful for the users during extreme events.

In more detail, in the event management mode, two specific icons conceived for early warning are included. The icons are highlighted if a warning occurs. The first icon refers to ongoing events (alert is triggered by observed data of threshold exceeding recorded by water level gauges), whereas the second icon refers to forecasts (alert is triggered by hydrologic models).

In the presence of an alert, a specific dashboard is opened by clicking on the reported event. The dashboard includes only the essential and useful information for the Event management, as the list of catchments where critical thresholds are exceeded (Figure 25), the link to the corresponding charts (Figure 26), the vulnerability map corresponding to the current or forecast scenario.

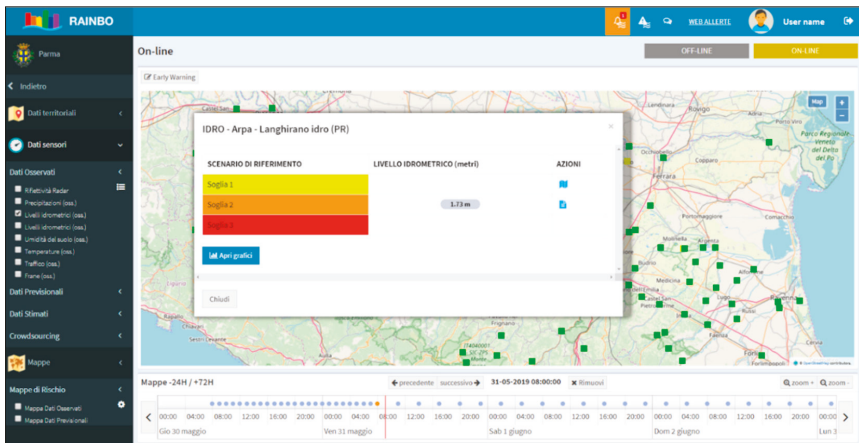


Figure 25. Alert of an ongoing event. The icon on the right side of the platform is highlighted and the dashboard displays the information connected with the event.

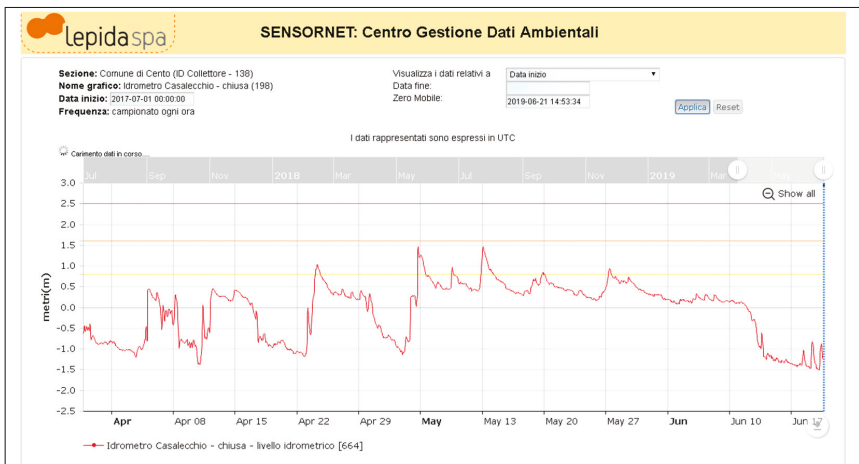


Figure 26. Example of charts of water level gauge and its alarm thresholds.

Furthermore, in the event management mode, a specific tool allows selecting an area of interest where critical targets and sensible targets (with users) are listed, so that reference persons can be identified in order to contact them (Figure 27).

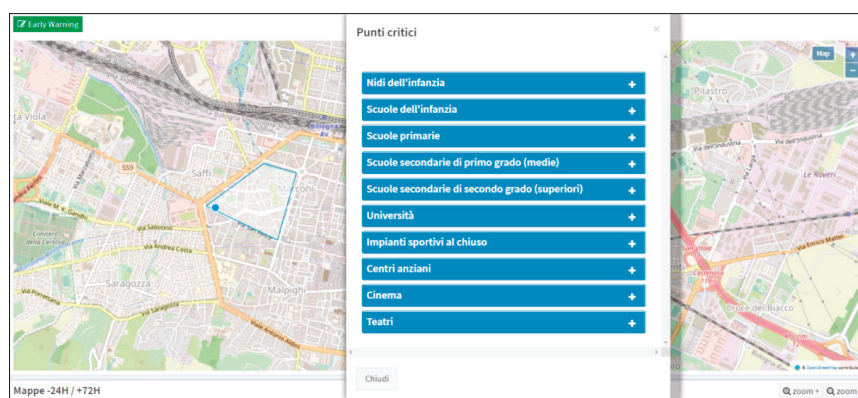


Figure 27. Critical sites list and corresponding information displayed by selecting an area of interest.

3.6. Discussion

In general terms, the flood risk in urban areas can be reduced through the implementation of planning, and monitoring and forecasting phases. These activities are related to different time scales and can be supported through a tool that uses multiple information collected and which can display them easily.

The RainBO platform integrates meteorological and territorial data in time/space and provides a holistic interface for the planning phase and disaster risk reduction, allowing to prevent impacts of flood events and reduce the residual risk during their occurrence.

As flooding in urban areas in Europe is increasing, European projects tackled this issue in urban environments with different features. The EU Interreg project URBAN-PREX aimed at monitoring/forecasting and developing online public EWS for extreme precipitations and pluvial floods in urban areas. URBAN-PREX focused on precipitation monitoring by means of rain gauges located in urban areas and precipitation forecasts.

With respect to this project, the approach of RainBO includes further modules that deal with the planning, monitoring, and forecasting phases. Maps of hazard, vulnerability, and risk are available in the planning phase; data and innovative technology such as CML have been included to monitor precipitation events in the monitoring phase; finally, there is a very clear focus on specific hydrological modeling in the forecasting phase.

Another EU Interreg project named RAINGAIN sought to obtain detailed rainfall data at an urban scale, to predict urban flooding and to implement the use of rainfall and flood data in urban water management practice. In this case, radar technology is used to provide estimates of rainfall in time and space in cities.

RainBO provides estimates of precipitation from different sources such as rain gauges, radar data and CML, and provides a forecast of precipitation from a limited area meteorological model. These data related to precipitation are integrated with other processes (e.g., hydrological modeling) and with territorial data useful before and during the event.

Furthermore, the EU FP7 project STAR-FLOOD aimed to improve the implementation of flood risk strategies in urban areas by building appropriate and resilient flood risk governance. This project stressed the need to have proactive and risk-based systems for forecasting, warning and emergency responses for urban floods that also need to use collaborative approaches. Therefore STAR-FLOOD is more focused on the planning phase, whereas RainBO comprises also a consistent part devoted to forecasting and event management.

Finally, the EU Horizon 2020 project FLOOD-serv aimed to develop a collaborative platform among citizens, public authorities and other stakeholders, which enable alerts in due time to reduce

the adverse effects of the floods. In this regard, it is worthy to mention that the RainBO platform is addressed only to decision-makers; decision-makers of a municipality can support both territorial planning and early warning systems through this platform.

RainBO platform has the added value of combining in only one integrated tool territorial data, historical data, real-time monitoring, a crowdsourcing system, hydraulic models for small creeks and medium rivers and the early warning system.

The strengths of the project both in terms of the development of new products and enhancements of existing ones are:

- Vulnerability map calculation module (for hydraulic risk purposes)
- Integration of observed, estimated, and predicted data
- Hydrological simulation model for small basins

Moreover, a first operational level has been defined for a rainfall monitoring system based on CML and it consists of satisfactory reliability in monitoring convective events, mainly during the summer and spring seasons.

4. Conclusions

The RainBO platform is open, centralized, scalable, modular and configurable; it means that it can include various data and models in a different time and space scale, providing an opportunity of replicability and scalability in other geographical and administrative contexts and also for different purposes.

Furthermore, the effectiveness of the RainBO platform has been confirmed by the other municipalities in the Emilia-Romagna Region (i.e., Cento, Comuni della Val Samoggia, Anzola dell'Emilia) keen to demonstrate this platform.

Some limitations of the RainBO platform are to be mentioned:

- The platform is addressed to decision-makers but not to citizens (the citizens can only send information through crowdsourcing)
- The hydrologic models used within the platform have to be calibrated and validated if applied in different river basins, therefore they are not easily replicable in other contexts
- A very large amount of information can be challenging to manage

From a future perspective, the extension of this platform can be foreseen in other urban areas due to the diffusion of open data. As an increasing number of territorial open data is now available, one of the benefits of the platform is also the convergence on the same hub of these data organized in a functional and rational way.

The specific features of this platform allow the upload of datasets provided from international programs (e.g., Copernicus) to supply the lack of local information or infrastructures.

Another future development could be the re-engineering of the platform with a simplified set of information, conceived for the citizens of specific urban areas.

In the future, an effort should be made to enhance the robustness of this platform, i.e., improving the operational functioning of the monitoring and forecasting phases.

Author Contributions: Conceptualization, S.N. and F.T.; methodology, S.N., F.T., R.M., A.A. and P.L.; software, S.N., S.P. and R.M.; supervision, M.F., G.M., L.B. and S.C.; writing—original draft, G.V., S.N., R.M. and S.C.; writing—review and editing, G.V.

Funding: This project has received funding from the European Union's LIFE programme under project No. LIFE15/CCA/IT/00035.

Acknowledgments: This article results from the RainBO project.

Conflicts of Interest: The authors declare no conflict of interest.

References

1. IPCC. *IPCC Special Report on Managing the Risks of Extreme Events and Disasters to Advance Climate Change Adaptation (SREX)*; Cambridge University Press: Cambridge, UK, 2012.
2. EEA. *Climate Change, Impacts and Vulnerability in Europe—An Indicator-Based Report*; EEA: Copenhagen, Denmark, 2017.
3. Blöschl, G.; Hall, J.; Parajka, J.; Perdigão, R.A.; Merz, B.; Arheimer, B.; Čanjevac, I. Changing climate shifts timing of European floods. *Science* **2017**, *357*, 588–590. [[CrossRef](#)] [[PubMed](#)]
4. Blöschl, G.; Hall, J.; Zivkovic, N. Changing climate both increases and decreases European river floods. *Nature* **2019**, *573*, 108–111. [[CrossRef](#)] [[PubMed](#)]
5. Alfieri, L.; Burek, P.; Feyen, L.; Forzieri, G. Global warming increases the frequency of river floods in Europe. *Hydrol. Earth Syst. Sci.* **2015**, *19*, 2247–2260. [[CrossRef](#)]
6. EU, Directive 2007/60/EC of the European Parliament and of the Council of 23 October 2007 on the Assessment and Management of Flood Risks. 6.11. 2007, pp. 27–34. Available online: <https://eur-lex.europa.eu/legal-content/EN/TXT/?uri=CELEX:32007L0060> (accessed on 26 November 2019).
7. Alfieri, L.; Salamon, P.; Pappenberger, F.; Wetterhall, F.; Thielen, J. Operational early warning systems for water-related hazards in Europe. *Environ. Sci. Policy* **2012**, *21*, 35–49. [[CrossRef](#)]
8. UNEP. *Early Warning Systems: A State of the Art Analysis and Future Directions*; UNEP: Nairobi, Kenya, 2012.
9. UNFCCC. *Adoption of the Paris Agreement*; UN Framework Convention on Climate Change: Bonn, Germany, 2015.
10. UNISDR. *Sendai Framework for Disaster Risk Reduction 2015–2030*; United Nations: Geneva, Switzerland, 2015.
11. UNDRR. *Global Assessment Report on Disaster Risk Reduction*; United Nations: Geneva, Switzerland, 2019.
12. Golnaraghi, M. *Institutional Partnerships in Multi-Hazard Early Warning Systems*; Springer: Berlin/Heidelberg, Germany, 2008; pp. 1–8.
13. Bouwer, L.; Papyrakis, E.; Poussin, J.; Pfuertscheller, C.; Thieken, A. The costing of measures for natural hazard mitigation in Europe. *Nat. Hazards Rev.* **2014**, *15*, 04014010. [[CrossRef](#)]
14. UN. *Transforming Our World: The 2030 Agenda for Sustainable Development*; United Nations: New York, NY, USA, 2015.
15. UNISDR. *Disaster Risk Reduction and Resilience in the 2030 Agenda for Sustainable Development*; United Nations: Geneva, Switzerland, 2015.
16. Hapuarachchi, H.A.P.; Wang, Q.J.; Pagano, T.C. A review of advances in flash flood forecasting. *Hydrol. Process.* **2011**, *25*, 2771–2784. [[CrossRef](#)]
17. Jain, S.K.; Mani, P.; Jain, S.K.; Prakash, P.; Singh, V.P.; Tullos, D.; Kumar, S.; Agarwal, S.P.; Dimri, A.P.A. Brief review of flood forecasting techniques and their applications. *Int. J. River Basin Manag.* **2018**, *16*, 329–344. [[CrossRef](#)]
18. Acosta-Coll, M.; Ballester-Merelo, F.; Martinez-Peiró, M.; De la Hoz-Franco, E. Real-Time Early Warning System Design for Pluvial Flash Floods—A Review. *Sensors* **2018**, *18*, 2255. [[CrossRef](#)] [[PubMed](#)]
19. EU. *Establishing the Urban Agenda for the EU ‘Pact of Amsterdam’*. Agreed at the Informal Meeting of EU Ministers Responsible for Urban Matters on 30 May 2016 in Amsterdam, The Netherlands; EU: Brussels, Belgium, 2016.
20. UN. *New Urban Agenda*; United Nations: Geneva, Switzerland, 2017.
21. URBAN-PREX—Interreg Project. Available online: <http://www.urban-prex.org/> (accessed on 18 November 2019).
22. RAINGAIN—Interreg Project. Available online: <http://www.raingain.eu/en/interreg-ivb-north-west-europe-programme-1> (accessed on 18 November 2019).
23. STAR-FLOOD FP7 Project. Available online: <https://www.starflood.eu/> (accessed on 18 November 2019).
24. FLOOD-SERV Horizon 2020 Project. Available online: <http://www.floodserv-project.eu/> (accessed on 18 November 2019).
25. Climatic Tables of Emilia-Romagna. Available online: https://www.arpae.it/dettaglio_generale.asp?id=4143&idlivello=1591 (accessed on 26 November 2019).
26. Grazzini, F.; Dottori, F.; Di Lorenzo, M.; Spisni, A.; Tomei, F. *Nubifragi e Rischio Idraulico Nella Collina Bolognese: Il Caso Studio del Torrente Ravone*; Public Report of Arpa; Arpa: Bologna, Italy, 2013.
27. Bracaloni, A. *Analisi del Rischio Idraulico in Ambiente Urbano: Il Caso del Torrente Ravone a Bologna*. Master’s Thesis, University of Bologna, Bologna, Italy, 10 March 2016.

28. Dottori, F.; Grazzini, F.; Di Lorenzo, M.; Spisni, A.; Tomei, F. Analysis of flash flood scenarios in an urbanized catchment using a two-dimensional hydraulic model. In Proceedings of the International Association of Hydrological Sciences, Bologna, Italy, 4–6 June 2014.
29. Technical Reports of Hydro-Meteo Events in Emilia-Romagna. Available online: https://www.arpae.it/documenti_find.asp?parolachieve=sim_rapporadar&cerca=si&idlivello=64 (accessed on 18 October 2019).
30. Nanni, S.; Mazzini, G. Advanced Infrastructure for Environmental Monitoring and Early-Warning System Integration, Sensor Networks. In *International Conference on Sensor Networks*; Benavente-Peces, C., Cam-Winget, N., Fleury, E., Ahrens, A., Eds.; Springer Nature: Basel, Switzerland, 2019.
31. Numerical Weather Forecasts of Emilia-Romagna. Open Data of ARPAE. Available online: https://dati.arpae.it/fa_IR/dataset/previsioni-meteorologiche-numeriche-emilia-romagna (accessed on 18 October 2019).
32. Lanza, L.; Stagi, L. Certified accuracy of rainfall data as a standard requirement in scientific investigations. *Adv. Geosci.* **2008**, *16*, 43–48. [[CrossRef](#)]
33. Porcù, F.; Milani, L.; Petracca, M. On the uncertainties in validating satellite instantaneous rainfall estimates with raingauge operational network. *Atmos. Res.* **2014**, *144*, 73–81. [[CrossRef](#)]
34. Casicci, L.; Ioiò, C.; Pecora, S. An operational system for the Po flood forecasting in Italy. In Proceedings of the 7th International Conference on Hydroinformatics, Nice, France, 4–8 September 2006.
35. Zinevich, A.; Messer, H.; Alpert, P. Frontal Rainfall Observation by a Commercial Microwave Communication Network. *J. Appl. Meteorol. Climatol.* **2009**, *48*, 1317–1334. [[CrossRef](#)]
36. Doumounia, A.; Gosset, M. Rainfall monitoring based on microwave links from cellular telecommunication networks: First results from a West African test bed. *Geophys. Res. Lett.* **2014**, *41*, 6016–6022. [[CrossRef](#)]
37. Overeem, A.; Leijnse, H.; Uijlenhoet, R. Country-wide rainfall maps from cellular communication networks. *Proc. Natl. Acad. Sci. USA* **2013**, *110*, 2741–2745. [[CrossRef](#)] [[PubMed](#)]
38. Radar Meteo. Open Data of ARPAE. Available online: <https://dati.arpae.it/dataset/radar-meteo> (accessed on 18 October 2019).
39. Rmap Participatory Monitoring and Exchange System. Available online: <http://rmap.cc/> (accessed on 18 October 2019).
40. Marletto, V.; Ventura, F.; Fontana, G.; Tomei, F. Wheat growth simulation and yield prediction with seasonal forecasts and a numerical model. *Agric. For. Meteorol.* **2007**, *147*, 71–79. [[CrossRef](#)]
41. Tomei, F.; Antolini, G.; Bittelli, M.; Marletto, V.; Pasquali, A.; Van Soetendael, M. Validazione del modello di bilancio idrico CRITERIA. *Ital. J. Agrometeorol.* **2007**, *1*, 66–67.
42. Bittelli, M.; Tomei, F.; Pistocchi, A.; Flury, M.; Boll, J.; Brooks, E.S.; Antolini, G. Development and testing of a physically based, three-dimensional model of surface and subsurface hydrology. *Adv. Water Resour.* **2010**, *33*, 106–122. [[CrossRef](#)]
43. CRITERIA-3D. Open Source Code of ARPAE. Available online: <https://github.com/ARPA-SIMC/CRITERIA3D/wiki/CRITERIA3D> (accessed on 18 October 2019).
44. Breiman, L. Random Forests. *Mach. Learn.* **2001**, *45*, 5. [[CrossRef](#)]
45. RAINLINK Retrieval Algorithm Open Source Code. Available online: <https://github.com/overeem11/RAINLINK> (accessed on 30 October 2019).
46. Crowdsourcing App Rmap4RainBO. Available online: <https://partecipa.RainBOlife.eu> (accessed on 30 October 2019).
47. RainBO Platform. Available online: <http://webgis.rainbolife.eu/prototipo/01-tempo-di-pace.html> (accessed on 18 October 2019).



© 2019 by the authors. Licensee MDPI, Basel, Switzerland. This article is an open access article distributed under the terms and conditions of the Creative Commons Attribution (CC BY) license (<http://creativecommons.org/licenses/by/4.0/>).

Article

Land Use Changes in a Peri-Urban Area and Consequences on the Urban Heat Island

Marianna Nardino ^{1,*} and Nicola Laruccia ²

¹ National Research Council-Institute for Bioeconomy (CNR-IBE), Via Gobetti 101, 40129 Bologna, Italy

² Emilia Romagna Region-Servizio Programmazione e Sviluppo locale Integrato, Viale della Fiera 8, 40127 Bologna, Italy; nicola.laruccia@regione.emilia-romagna.it

* Correspondence: Marianna.Nardino@ibe.cnr.it; Tel.: +39-051-639-9001

Received: 17 October 2019; Accepted: 12 November 2019; Published: 13 November 2019

Abstract: The effect of urbanization on microclimatic conditions is known as “urban heat islands”. In comparison with surrounding rural areas, urban climate is characterized by higher mean temperature, especially during heat waves and during nights. This results in a higher energy requirement for air conditioning in buildings and in a greater bioclimatic discomfort for urban populations. The reasons of this phenomena are ascribable principally to the increase of solar radiation storage and to the decrease of dissipation of water by evapotranspiration in urban environment respect to rural ones. The aim of this paper is to give a quantification of the air temperature increase due to an urbanization process. This quantification is conducted by comparing surface energy balance (incoming and outgoing radiation and turbulent fluxes) in urbanized area versus rural areas. This quantitative approach will be validated using a fluidodynamic model (Envi-Met) in a case study area representative of one among the various regional models of urban area growth. In particular, the model of expansion of small towns around big cities (2003–2008 land use changes) of a plain near-urban area in the Po Valley region (Italy) was used.

Keywords: urban heat island; urbanization; urban surface energy balance; fluidodynamic modeling; Envi-Met

1. Introduction

The urbanization effect refers to a general increase in population and in the amount of industrialization of a settlement, due principally to the increase, in number and extent, of cities and the movement of people from rural to urban areas. The “urban sprawl” is used to define the increase in spatial scale or in the peripheral area of the cities. At the present, more than half of the global population lives in cities and cities themselves are growing to unprecedented sizes [1].

The high density of population and the consequent use of primary resources by urban residents, especially in the North Hemisphere, make cities and their inhabitants key drivers of global environmental changes [2,3].

Land-use and land-cover changes are recognized as causes of local, regional and global warming: The urban areas are the major sources of anthropogenic carbon dioxide emissions from the burning of fossil fuels for heating, from industrial processes, from transportation of people, etc. [4,5]. The main effects of land use changes (from rural to urban) can be found on the surface energy and water balances changes. The partitioning of sensible and latent heat fluxes is a function of varying soil water content and vegetation cover [6,7]. Water balance is strongly influenced by the soil sealing: Urbanization makes the surface permanently covered by impermeable artificial material (e.g. asphalt and concrete), for example through buildings and roads.

An increase of settlement areas over time is defined as land take, also referred to as land consumption. This process includes the development of scattered settlements in rural areas,

the expansion of urban areas around an urban nucleus (including urban sprawl), and the conversion of land within an urban area (densification) [8,9]. Depending on local circumstances, a greater or smaller part of the land take will result in actual soil sealing. Urban sprawl can be defined as the unplanned incremental urban development, characterised by a low-density mix of land uses on the urban fringe. It is important to underline that even planned urban development may result in land take and soil sealing.

Soil sealing and realization of buildings on it alter the surface energy balance with two different main mechanisms:

- (1) Soil sealing reduces the vegetation cover and prevents the storage of rainwater and consequently the amount of water stored into the soil. Consequently, water available for evapotranspiration processes is much lower than in a natural surface. It follows that the latent heat dissipated from urban surfaces is close to zero and the amount of advanced energy will be available for other processes usually related to an increase of the thermal field [10].
- (2) Materials used for the buildings may, according to their specific thermal and optical properties, store energy and radiation in form of heat when the radiation budget (R_n) is positive and release energy when R_n is negative.

The combination of these two different mechanisms results in a different thermal trend that is observed in the built environment compared to the surrounding rural areas.

One of the most prominent feature of the urban climate is the urban heat island (UHI) effect, which is strongly tied to the geometry and dimensions of building, land use patterns, vegetation cover and the intensity of the anthropogenic heat release [11,12]. The UHI makes the city warmer than its rural surroundings and it is stronger at night than during the day. This effect also decreases with increasing wind speed and cloud cover and it's less pronounced in summer and winter [11].

On average, urban temperatures may be 1–3 °C warmer than surrounding urban environment [6].

The aim of this work is to quantify the change in temperature range that can be expected on the basis of different energy balances resulting from the transformation of rural areas in urban residential or productive areas. The changes in the soil use (from natural surface to no permeable surface) returns an environment where the storage of heat during the day by building materials is released during the night, increasing the urban heat island. This effect is the main subject of the present work.

2. Materials and Methods

2.1. Energy Balance Method

The Earth surface radiation balance is described by the following equation:

$$R_n = (Sw_{in} - Sw_{out}) + (Lw_{in} - Lw_{out}) \quad (1)$$

where R_n is the net radiation, Sw_{in} is the incoming shortwave (visible) radiation, Sw_{out} is the outgoing shortwave radiation, Lw_{in} is the incoming longwave (infrared) radiation and Lw_{out} is the outgoing longwave radiation.

The term $(Sw_{in} - Sw_{out})$ is the net shortwave radiation and it can be also described as $(1 - \alpha)Sw_{in}$, where α is the surface albedo used to quantify the solar radiation reflected by a surface. Albedo is a characteristic of the specific surface and depends on the optical characteristics of the reflecting surface.

Lw_{in} and Lw_{out} depend on the atmosphere and surface temperature following the black body equation:

$$LW = \epsilon \sigma T^4 \quad (2)$$

where ϵ is the body infrared emissivity, σ is the Stefan–Boltzmann constant ($5.67 \cdot 10^{-8} \text{ W m}^{-2} \text{ K}^{-4}$) and T is the body temperature expressed in K.

The net radiation given by (1) is then utilized to the partitioning processes at the surface, following the surface energy balance equation [12]:

$$R_n = H + LE + G \quad (3)$$

where H is the sensible heat flux, LE is the latent heat flux and G is the ground heat flux.

Usually the greatest part of the net radiation is used for sensible and evapotranspiration processes while the G term represent only the 10% of the total available energy (R_n).

To estimate the lower dissipation of latent heat flux due to the transformation of cultivated land in urbanized area, it is necessary to quantify the evapotranspiration (ET) before and after the transformation. The ET of a cultivated area depends on climatic characteristics of the site and on eventual water contributions from irrigation, on vegetable cover and on soil type. As vegetable cover, for this study, it was assumed the cultivation of winter wheat, not irrigated and growing in optimal pedological and climatic conditions to ensure a good water supply during vegetation season (November to June). Wheat is one of the more widespread dry crops in the Emilia-Romagna Region plain.

From a sealed surface, the evaporation of rain water can be considered negligible. On the other hand, from a winter wheat crop, in the case of optimal soil and climatic conditions, about 700 lm^{-2} of water per year changes from liquid into vapor phase.

A very simplified, but amply adopted method to calculate potential evapotranspiration (ETc) of a crop consists on multiplying reference evapotranspiration (ET_0) per crop cultural coefficient (Kc):

$$ETc = Kc ET_0 \quad (4)$$

In this study ET_0 was calculated according to Hargreaves method [13] using the data of a meteorological station relatively close to the case study area, San Pietro Capofiume (44.648993°N , 11.650055°E , 11 m a.s.l.). The values of the cultural coefficient Kc for wheat were adopted following the [14] suggestions and reasonable Kc's for spontaneous grasses, growing after crop harvesting, were chosen.

If a land use change occurs, such as a significant urbanization, the terms of this budget equation change significantly and other terms, depending on different processes, must be taken into account. The Equation (3) of the surface energy balance can therefore be rewritten in this way:

$$R_n = H + LE + G + Q_s \quad (5)$$

where Q_s is the storage heat flux, which is strongly dependent on the ratio between green and sealed areas and on the building geometrical, optical and thermal characteristics.

Oke [6] proposed these equations for Q_s :

$$\text{day } Q_s = (0.20\lambda_v + 0.33\lambda_p) R_n + 3\lambda_v + 24\lambda_p \quad (6)$$

$$\text{night } Q_s = (0.54\lambda_v + 0.90\lambda_p) R_n \quad (7)$$

where λ_v is the green area fraction and λ_p is the building area fraction.

The reconstruction of the thermal change given by the lower amount of evapotranspiration of a sealed surface was performed following the Fick law [12]:

$$\Delta T = Q Dz k^{-1} \quad (8)$$

where

Q = Latent Heat Flux + Storage Heat Flux (W m^{-2})

Dz = reference height (2 m)

k = air thermal conductivity ($0.026 \text{ W m}^{-1} \text{ K}^{-1}$)

2.2. Fluidodynamic Simulation (Envi-Met): The Case Study

ENVI-met [15] is a three-dimensional non-hydrostatic microclimate model designed to simulate the surface–plant–air interactions within daily cycle in urban environment with a typical resolution of 0.5 to 10 m in space and 10 s in time.

The model has been widely used in many previous studies to simulated flow around and between buildings, exchange processes of heat and vapor at the ground surface and at the walls, turbulence exchange of vegetation and vegetation parameters, bioclimatology, and particle dispersion [16]. The model was validated as reported in [17].

In order to run the model, the detailed data on soil characteristics, buildings, vegetation, and initial atmospheric conditions for the area of interest were inserted.

After this input phase, the model is ready to run and the desired variables have been selected and saved into the output files [16].

ENVI-met can be used for several studies to test various urban canyon aspects as well as ratios and orientation effects on outdoor thermal comfort, the role of vegetation in the mitigation of the urban heat island effect, and other factors.

3. Results and Discussion

Hourly measurements of the surface radiation balance components (Sw_{in} , Sw_{out} , Lw_{in} , Lw_{out}) are available in stations relatively close to the case study area. San Pietro Capofiume was used as the representative station for rural open space. In this site CNR-IBE performed radiation components measurements for the period 1 January 2002–31 December 2003.

Bologna urban ARPAe (HydroMeteorological Service of the Emilia-Romagna Regional Agency for Environmental Protection) station (44.500754 °N, 11.328789 °E, 78 m a.s.l.) has been considered as the representative station for sealed conditions (measurements period 1 January 2006–31 December 2009). Although this data represents only few years, furthermore non-coincident, from Table 1 it can be inferred that the values of the two stations are substantially super imposable with regard to the Sw_{in} and the Sw_{out} values, while the differences between the values of Lw_{in} and Lw_{out} are attributable to the different surface types (rural and urban), principal aim of this paper.

Table 1. Annual mean values of the surface radiation balance components for rural (San Pietro Capofiume) and urban (Bologna urban) sites.

Station	Sw_{in} ($W m^{-2}$)	Sw_{out} ($W m^{-2}$)	Lw_{in} ($W m^{-2}$)	Lw_{out} ($W m^{-2}$)
Bologna urban	148	26	325	396
San Pietro Capofiume	156	27	305	361

Throughout the hourly measurements, in Table 2 are reported the diurnal and nocturnal R_n values obtained for the two stations and for each month of the year.

Table 2. Annual mean of net radiation values in nocturnal and diurnal hours for rural (San Pietro Capofiume) and urban (Bologna urban) sites.

Month	Nocturnal R_n ($W m^{-2}$)		Diurnal R_n ($W m^{-2}$)	
	San P. Capof.	Bologna Urban	San P. Capof.	Bologna Urban
January	−17	−39	78	52
February	−31	−57	138	124
March	−34	−63	253	201
April	−28	−62	246	278
May	−24	−52	288	280
June	−36	−60	287	285
July	−51	−71	279	293
August	−39	−67	255	239
September	−28	−62	198	189
October	−26	−55	157	141
November	−18	−44	77	71
December	−19	−47	68	48

Table 3 shows the values of mean monthly latent heat flux which would be missed in case of transformation of a wheat field into a sealed surface.

Table 3. Monthly mean values of reference evapotranspiration (ET_0), crop coefficient (K_c), crop potential evapotranspiration (ET_c) and corresponding latent heat flux.

Month	ET_0 (mm)	K_c (Wheat and Spon. Grass)	ET_c (mm)	Latent Heat Flux ($W m^{-2}$)
January	19.8	0.4	7.9	6.9
February	36.3	0.5	18.2	17.4
March	66.9	0.7	46.8	40.8
April	109.1	0.9	98.2	88.4
May	153.1	1.1	168.4	146.7
June	178.4	1.0	178.4	160.7
July	204.0	0.2	40.8	35.6
August	166.1	0.3	49.8	43.4
September	110.8	0.5	55.4	49.9
October	64.3	0.4	25.7	22.4
November	31.0	0.4	12.4	11.2
December	19.1	0.4	7.7	6.7

The area chosen as a case study is located in San Giovanni Persiceto (44.6283 °N, 11.1992 °E, 21 m a.s.l.), a small town close to Bologna city. The urbanization occurred in this area from 2003 to 2008 was estimated comparing aerial images (orthophoto by AGEA for 2008 and QuickBird satellite orthoimages by Digital Globe™–Telespazio for 2003) (Figure 1). The built-up surface varied from 5.5% in the 2003 to 30% in 2008 and the natural cover varied from 94.5% in 2003 to 70% in 2008. Inserting these values as λ_v and λ_p in (6) and (7), the difference of the storage heat flux Q_s between 2003 and 2008 was obtained, separately for night and daytime hours. The annual difference in the cumulated storage heat flux is quite similar between night and day (+80 $W m^{-2}$ for the diurnal hours and −84 $W m^{-2}$ for nocturnal ones) which means that all the heat stored during the day by urban materials is re-emitted into the atmosphere during the night. On a monthly basis, this effect is visible in the winter months and during months with high energy availability (May, June, and July) the day energy accumulation is greater than the night emission (Table 4).



Figure 1. QuickBird satellite orthoimages (@Digital Globe™–Telespazio, 2003) (left) and aerial orthophotographs (AGEA) for 2008 (right).

Table 4. Monthly mean values of storage heat flux during diurnal and nocturnal hours for 2003 and 2008 and relative differences for each year.

Month	Diurnal Qs (W m ⁻²)			Nocturnal Qs (W m ⁻²)		
	2003	2008	Difference	2003	2008	Difference
January	23.4	23.1	-0.3	-10.1	-15.2	-5.1
February	37.9	42.4	4.4	-18.1	-25.1	-7.0
March	66.0	62.9	-3.2	-20.0	-27.8	-7.8
April	64.5	83.6	19.2	-16.6	-24.6	-8.0
May	74.7	84.0	9.3	-14.5	-21.1	-6.6
June	74.3	85.4	11.1	-20.6	-27.8	-7.1
July	72.6	87.5	14.9	-29.4	-37.1	-7.7
August	66.7	73.0	6.3	-22.5	-30.6	-8.1
September	52.7	59.9	7.2	-16.6	-24.6	-8.0
October	42.5	46.9	4.4	-15.3	-22.3	-7.0
November	22.9	28.3	5.4	-10.9	-16.6	-5.8
December	20.8	22.1	1.3	-11.7	-17.8	-6.2

Since the evapotranspiration processes occur only during diurnal hours, the difference between the two reference years in terms of latent heat flux is assigned entirely to daylight hours. The greater energy availability for 2008 for heat transfer processes was obtained summing the diurnal latent heat flux differences (proportioned according to the fractions of cultivated and urban areas in 2003 and 2008) with the differences in diurnal storage heat flux. Nocturnal thermal variation depends only on variations in storage heat flux reported in Table 4.

Table 5 illustrates the total monthly differences (2008 vs 2003) in energy budget for diurnal hours and the corresponding diurnal, nocturnal and mean temperature variations calculated according to (8).

The largest increases in temperature due to an urbanization process occur during the summer months, when the energy available for exchange processes is greater.

This approach is an estimate of changes in energy balance and this leads at uncertainties, but in general the results show an annual mean increment in air temperature of 0.36 °C due to this urbanization process. Again, the single months show the differences due to energy availability, giving greater values of air temperature increment during summer months.

Table 5. Total difference (2008 vs 2003) in energy budget for diurnal hours and corresponding diurnal thermal variation (ΔT day), nocturnal thermal variation (ΔT night) and mean thermal variation (ΔT mean).

Month	$\Delta LE + \text{Diurnal } \Delta Q_s \text{ (W m}^{-2}\text{)}$	$\Delta T \text{ day (}^\circ\text{C)}$	$\Delta T \text{ night (}^\circ\text{C)}$	$\Delta T \text{ mean (}^\circ\text{C)}$
January	2.1	0.11	0.27	0.19
February	0.1	0.00	0.37	0.19
March	13.7	0.71	0.41	0.56
April	3.8	0.20	0.42	0.31
May	28.7	1.49	0.34	0.92
June	30.6	1.59	0.37	0.98
July	−5.7	−0.29	0.40	0.05
August	5.0	0.26	0.42	0.34
September	5.7	0.30	0.42	0.36
October	1.4	0.07	0.36	0.22
November	−2.5	−0.13	0.30	0.09
December	0.4	0.02	0.32	0.17

The same area was studied with the Envi-Met fluidodynamic model in order to have a modeling feedback of estimation method based on the surface energy balance.

The two input areas (2003 and 2008), shown in Figure 2, were inserted through the program ENVI-met Eddie, taking into account the geographical location, building dimensions, land use patterns. The vegetation was assumed to be winter wheat. The domain model consisted of a $140 \times 140 \times 20$ grid with a spatial resolution of $5 \text{ m} \times 5 \text{ m} \times 2 \text{ m}$, resulting in a horizontal area of $700 \times 700 \text{ m}^2$ with a 40 m vertical extent.

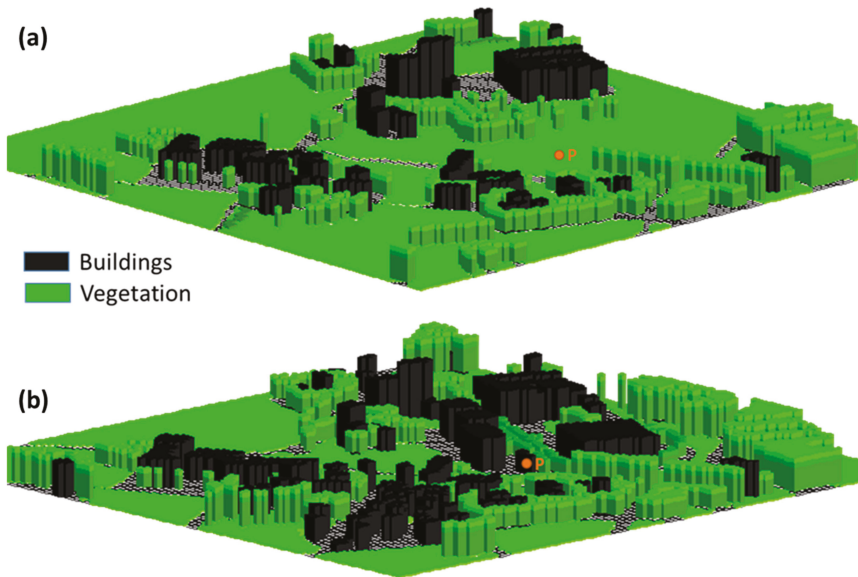


Figure 2. Input maps inserted into Envi-met model for 2003 (a) and 2008 (b).

The case study reported here focused on the simulation of a typical hot day whose values of meteorological variables were obtained considering the data of the nearest ARPae weather station (San Pietro Capofiume).

The simulation started at 9:00 a.m. and lasted for 24 hours. The configuration file contained the atmospheric values:

- Speed and wind direction at 10 m: 1.4 m s^{-1} , 90° ;
- Surface roughness length (z_0): 0.1 m;
- Air temperature: 301.7 K
- Specific humidity at 2500 m: 7 g water/kg air
- Relative humidity at 2 m: 50%

As first results the potential temperature (the temperature that a sample of air attains if reduced to a pressure of 1000 millibars without receiving or losing heat) to the environment difference between the two simulation years (2003 and 2008) were plotted (Figure 3) at 14:00 p.m. The urbanization process carried out from 2003 to 2008 led to a warming of some areas especially those in which it has had a greater overbuilding. In these areas the 2008 potential temperature at 1.6 m height is about $0.4\text{--}0.6^\circ\text{C}$ higher than 2003.

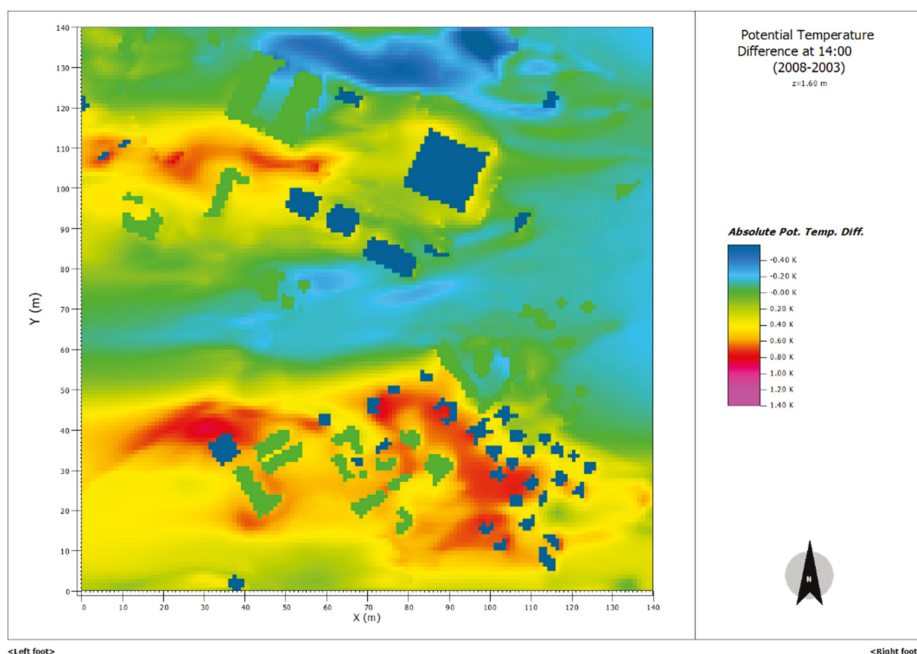


Figure 3. Potential temperature difference (2008–2003) at 14:00 pm at 1.60 m height for the considered case study.

During the night (Figure 4 at 2:00 a.m.) the potential temperature difference between the two years reaches 1°C . This is typical of the urban heat islands, where the greatest effect is recorded during the night, so substantial increase occurs in daily minimum temperatures [18]. In addition, the total area tends to be warmer in 2008 than in 2003, and this effect is more evident during the night hours than daytime.

As a matter of fact, if the air temperature trends is plotted for a strategic point of the considered area (a point which was completely rural in 2003 and that became urban in 2008, marked as P in Figure 2) it can be seen that during the day air temperature tends to be the same for the two years and during the night the change turns out to be even 1°C (Figure 5). The daily mean of air temperature differences is 0.35°C that, looking at Table 5 for June month, is comparable with the night values, but not with the daytime ones. Probably the high available energy during this month means that further exchange processes come into play, that the balance method, used in this work, does not

account for. A better diurnal values estimate is surely necessary, even if during August and September (months similar to June as far as concerns air temperature values) the obtained delta temperature (0.34 °C and 0.36 °C) is very close to the model result.

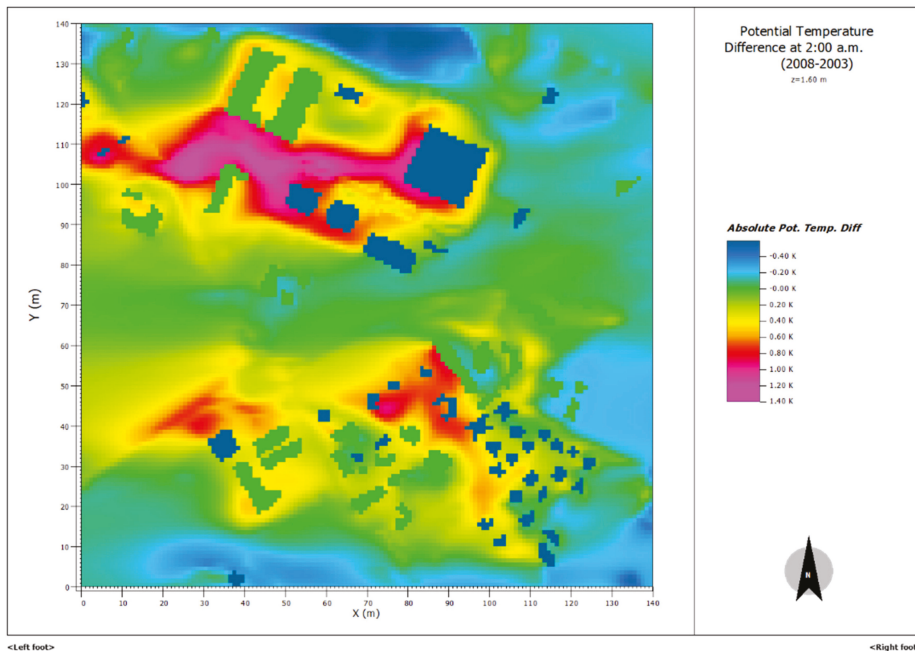


Figure 4. Potential temperature difference (2008–2003) at 2:00 a.m. at 1.60 m height for the considered case study.

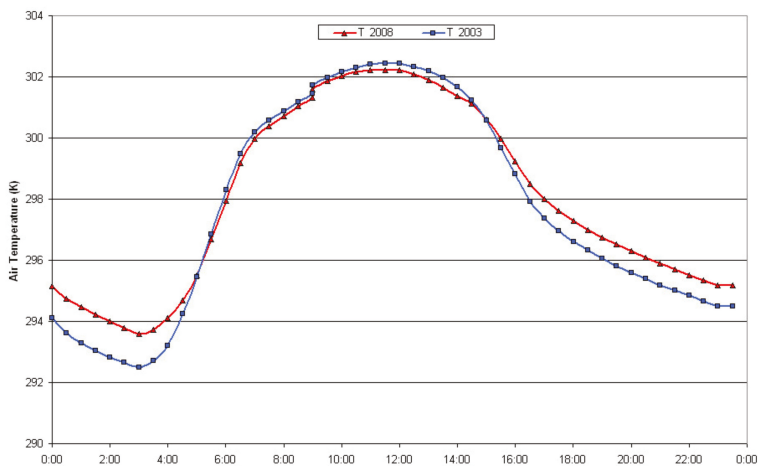


Figure 5. Air temperature for 2003 and 2008 in the P point marked in Figure 2.

June is the month in which the budget method assigned greater evapotranspiration values, but the fluidodynamic model does not consider specifically crop type and evapotranspiration needs. For this reason, the strongest disagreement results especially in this month.

On the other hand, the model results are in strong agreement with the annual average increase obtained with the method of the energy budget (0.36 °C).

This suggests a profitable use of this methodology to estimate the increase in air temperature due to urbanization processes on a regional scale.

4. Conclusions

The effect of an urbanization in a small town shows the consequences of the well-defined and studied “urban heat island”: The impact of such kind of urbanization leads an increment in the air temperature, and therefore a strengthening of the urban heat island, close to 1 °C.

The energy balance method is verified and supported by a fluidodynamic model to have the right data interpretation. The idea is to develop a simple methodology to consider the urbanization effects in terms of temperature increase, economic cost that goes with it and biometeorological uncomfortable for the people.

This methodology could be applied at regional scale to improve and develop spatial planning but taking into considerations the mitigating effects strategies (i.e. urban green, special building materials, study of the orientation of buildings, and shadows).

The radiation and energy budget method utilized to calculate the air temperature differences due to an urbanization process showed some limits and some uncertainties.

Surely, the different approaches to compute evapotranspiration used in the budget method and in the fluidodynamic model and some hypothesis adopted (absence of water deficit in budget method), strongly influenced the results.

Anyway, the fluidodynamic model confirms an air temperature increment of the same magnitude order of the energy budget method, suggesting this last methodology can be considered a sufficiently reliable method to estimate and predict the variation in the thermal field due to changes in land-use. Its application to a regional scale should take into account the different climatic zones and the different models of urban growth (existing residential or production areas densification, expansion of urban area with new buildings, etc.). The storage heat flux computation can be improved considering further variables: volumetric ratio between sealed and unsealed surfaces and optical and thermal properties of building materials.

Land use change, and in particular urbanization process, results in air temperature increase. The methodology developed in this work can be improved to furnish greater information during a regional territory planning. Air temperature increment give a surplus of energy needs of air conditioning systems: throughout thermotechnical computations it is possible to obtain the economic cost to reinstate indoor air temperature after urbanization process.

Moreover, the bioclimatic discomfort for the population caused by urban land use increment can be computed and successively taken into account during the initial design of an urban area.

Author Contributions: The authors contribute at all in this study thanks to different thanks to the different skills: fluid dynamics and agronomics. The manuscript was written together.

Funding: This research received no external funding.

Acknowledgments: The authors would like to thank IdroMeteorological Service (ARPAe) of Emilia-Romagna Region for furnishing meteorological data through DEXTER service, AGEA for orthophotographs and Digital Globe™–Telespazio for QuickBird orthoimages, acquired through internal Map Service of Emilia-Romagna Region.

Conflicts of Interest: The authors declare no conflict of interest.

References

1. World Urbanization Prospects: The 2018 Revision. Available online: <https://population.un.org/wup/Publications/Files/WUP2018-KeyFacts.pdf> (accessed on 13 November 2019).
2. Grimmond, S. Urbanization and global environmental change: Local effects of urban warming. *Geogr. J.* **2007**, *173*, 83–88. [CrossRef]

3. Chapman, A.; Watson, J.E.M.; Salazar, A.; Thatcher, M.; McAlpine, C.A. The impact of urbanization and climate change on urban temperature: A systematic review. *Landsc. Ecol.* **2017**, *32*, 1921–1935. [CrossRef]
4. Lim, Y.K.; Cai, M.; Kalnay, E.; Zhou, L. Observational evidence of sensitivity of surface climate changes to land types and urbanization. *Geophys. Res. Lett.* **2006**, *32*, L22712. [CrossRef]
5. Li, Y.; Zhao, M.; Motesharrei, S.; Mu, Q.; Kalnay, E.; Li, S. Local cooling and warming effects of forest based on satellite data. *Nat. Commun.* **2015**, *6*, 6603. [CrossRef] [PubMed]
6. Oke, T.R. The surface energy budgets of urban area. In *Modelling the Urban Boundary Layer*; AMS: Boston, MA, USA, 1981.
7. Fischer, E.M.; Seneviratne, S.I.; Vidale, P.L.; Lüthi, D.; Schär, C. Soil moisture-atmosphere interactions during the 2003 European summer heat wave. *J. Clim.* **2007**, *20*, 5081–5099. [CrossRef]
8. Liu, Y. Introduction to land use and rural sustainability in China. *Land Use Policy* **2018**, *74*, 1–4. [CrossRef]
9. Liu, Z.; Liu, Y.; Baig, M.H.A. Biophysical effect of conversion from croplands to grasslands in water-limited temperate regions of China. *Sci. Total Environ.* **2019**, *648*, 315–324. [CrossRef] [PubMed]
10. Moulai, M.; Khavari, F.; Shahhosseini, G.; Zanjani, N.E. A study of the urban heat island mitigation strategies: The case of two cities. *Int. J. Urban Manag. Energy Sustain.* **2017**, *1*, 1–7.
11. Memon, R.A.; Leung, D.Y.C.; Chunho, L. A review on the generation, determination and mitigation of Urban Heat Island. *J. Environ. Sci.* **2008**, *20*, 120–127.
12. Stull, R.B. *An Introduction to Boundary Layer Meteorology*; Kluwer Academic Publishers: Dordrecht, The Netherlands, 1988; p. 666.
13. Hargreaves, G.H.; Samani, Z.A. Estimating potential evapotranspiration. *Tech. Note J. Irrig. Drain. Eng.* **1982**, *18*, 980–984.
14. Allen, R.G.; Pereira, L.S.; Raes, D.; Smith, M. Crop Evapotranspiration (Guidelines for Computing Crop Water Requirements). In *FAO Irrigation and Drainage Paper No. 56*; FAO: Rome, Italy, 1998.
15. Bruse, M.; Fleer, H. Simulating surface-plant-air interactions inside urban environments with a three dimensional numerical model. *Environ. Model. Softw.* **1998**, *13*, 372–384. [CrossRef]
16. ENVI-Met Software Home Page. Available online: <http://www.envi-met.com/> (accessed on 13 November 2019).
17. Yang, X.; Zhao, L.; Bruse, M.; Meng, Q. Evaluation of a microclimate model for predicting the thermal behaviour of different ground surfaces. *Build. Environ.* **2013**, *60*, 93–104. [CrossRef]
18. Giridharan, R.; Lau, S.S.Y.; Ganesan, S. Nocturnal heat island effect in urban residential developments of Hong Kong. *Energy Build.* **2005**, *37*, 964–971. [CrossRef]



© 2019 by the authors. Licensee MDPI, Basel, Switzerland. This article is an open access article distributed under the terms and conditions of the Creative Commons Attribution (CC BY) license (<http://creativecommons.org/licenses/by/4.0/>).

Air Pollution Flow Patterns in the Mexico City Region

Alejandro Salcido *, Susana Carreón-Sierra and Ana-Teresa Celada-Murillo

Instituto Nacional de Electricidad y Energías Limpias, Reforma 113, Palmira, Cuernavaca 62490, Morelos, Mexico; susana.carreon@ineel.mx (S.C.-S.); atcelada@ineel.mx (A.-T.C.-M.)

* Correspondence: salcido@ineel.mx; Tel.: +52-777-362-3811 (ext. 7087)

Received: 18 September 2019; Accepted: 31 October 2019; Published: 5 November 2019

Abstract: According to the Mexico City Emissions Inventory, mobile sources are responsible for approximately 86% of nitrogen oxide emissions in this region, and correspond to a NO_x emission of 51 and 58 kilotons per year in Mexico City and the State of Mexico, respectively. Ozone levels in this region are often high and persist as one of the main problems of air pollution. Identifying the main scenarios for the transport and dispersion of air pollutants requires the knowledge of their flow patterns. This work examines the surface flow patterns of air pollutants (NO₂, O₃, SO₂, and PM₁₀) in the area of Mexico City (a region with strong orographic influences) over the period 2001–2010. The flow condition of a pollutant depends on the spatial distribution of its concentration and the mode of wind circulation in the region. We achieved the identification and characterization of the pollutant flow patterns through the exploitation of the 1-hour average values of the pollutant concentrations and wind data provided by the atmospheric monitoring network of Mexico City and the application of the k-means method of cluster analysis. The data objects for the cluster analysis were obtained by modeling Mexico City as a 4-cell spatial domain and describing, for each pollutant, the flow state in a cell by the spatial averages of the horizontal pollutant flow vector and its gradients (the divergence and curl of the flow vector). We identified seven patterns for wind circulation and nine patterns for each of NO₂, O₃, PM₁₀, and SO₂ pollutant flows. Their seasonal and annual average intensities and probabilities of occurrence were estimated.

Keywords: pollution flow patterns; wind circulation patterns; emission inventory; criteria pollutants; Mexico City

1. Introduction

In cities and large urban settlements, tropospheric ozone and particulate matter (PM₁₀ and PM_{2.5}) are the most dangerous air pollutants for human health [1]. Air pollution is a major environmental issue in urban areas, which can affect the well-being and quality of life of citizens. More and more frequently, there are detected chronic diseases of great importance that are associated with continuous exposures to high concentrations of air pollutants. Epidemiological studies have reported that exposure to air pollutants such as particulate matter, nitrogen oxides (NO_x), sulfur dioxide (SO₂), and surface ozone (O₃) associates with an increase in mortality and hospital admissions predominantly related to respiratory and cardiovascular diseases [1,2]. This critical issue concerns the 20 million people (including 9 million children) living in the Mexico City Metropolitan Area (MCMA). Despite the reductions in the emissions of common air pollutants in MCMA since the early 1990s, millions of people remain exposed to concentrations above the critical levels associated with increased risks for cardiovascular and respiratory diseases. The anthropogenic sources still produce and release to the atmosphere every year large amounts of carbon monoxide (CO), nitrogen oxides (NO_x), sulfur dioxide (SO₂), particulate matter (PM₁₀ and PM_{2.5}), and volatile organic compounds (VOC) [3]. However, because of the frequency of occurrence of high levels, persistence, and spatial distribution, the most critical air pollutants in MCMA are by far ozone and PM₁₀ [4–6].

At the MCMA, the complexity of the air pollution problem is also strongly related to other essential factors such as the geographical setting, meteorology, and topography. MCMA lies inside a subtropical basin with latitudes between 19.2 and 19.6 °N and longitudes between 98.9 and 99.4 °W, and an average altitude of 2240 m, surrounded by high mountains (Figure 1). In the north direction, the basin extends into the Mexican plateau and the arid interior of the country, with the Sierra de Guadalupe creating a small 800 m barrier above the basin floor. Its climate classification comprises two seasons: the rainy season from May to October and the dry season from November to April. This classification stems from the two main meteorological patterns on the synoptic-scale: dry westerly winds with anticyclone conditions from November until April, and moist flows from the east due to the weaker trade winds along the other six months [7]. The MCMA meteorology, however, is by far more complicated than this simple classification expresses it. The basin interacts with the Mexican plateau and the lower coastal areas. Moreover, due to the MCMA location, large-scale pressure gradients are generally weak, and intense solar radiation is registered here throughout the year [7–11]. These conditions and the presence of high mountains in the surroundings are ideal for the development of thermally driven winds.

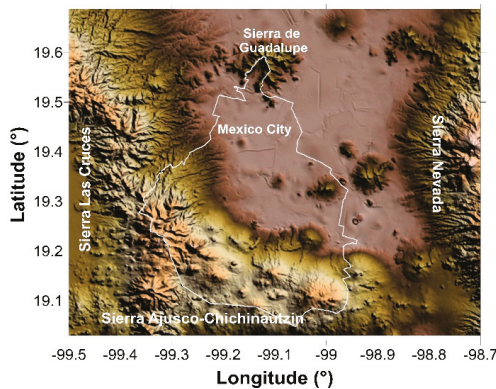


Figure 1. Complex topography in the Mexico City region.

The knowledge of wind circulation and air pollutant spatial distributions constitutes a relevant element to understand the flow dynamics of urban air pollution. It allows knowing how the air pollutant emissions produced in an urban settlement may disperse in the atmosphere, how these air pollutants may be distributed spatially in the city, and how the winds may transport them towards neighboring sites [12,13]. From the standpoint of fluid dynamics, the pollutant-flow vector, defined as the product of the fields of the pollutant concentration and wind velocity,

$$\mathbf{J}(\mathbf{x}, t) = \mu(\mathbf{x}, t)\mathbf{v}(\mathbf{x}, t), \tag{1}$$

describes the transport of a given pollutant in the atmosphere. Then, the surface flow condition of a pollutant depends on both factors: the surface distribution of its concentration and the local wind circulation.

Local wind circulation in Mexico City and its relation to driving forces and air pollution have been studied extensively for almost three decades. However, most of the studies have been performed on an episode-by-episode basis and using small data sets obtained from short-term experimental campaigns with different approaches [14–21]. Some of the main exceptions are the first long-term micrometeorological campaign carried out by Salcido et al. [11] in this region during 2001, and the studies of Klaus et al. [22], de Foy et al. [23], Salcido et al. [24], and Carreón-Sierra et al. [25], which were carried out using data provided by the atmospheric monitoring network of Mexico City (SIMAT:

Sistema de Monitoreo Atmosférico de la Ciudad de México [26]). Klaus et al. [22] reported a principal component analysis of air quality and meteorological data for the period February–December 1995. The study of de Foy et al. [23] reported an examination of wind transport during the experimental campaign of the Megacity Initiative: Local and Global Research Observations (MILAGRO) project; they used cluster analysis for making a comparison to climatology between the period of March 2006 and the period 1998–2006 using hourly wind data of the warm, dry season. In their work, Salcido et al. [24] used a lattice wind model at a meso- β scale to carry out a description and characterization of Mexico City local wind events of the period 2001–2006. Furthermore, Carreón-Sierra et al. [25] proposed an extension of the local wind state using a non-local description based on the wind velocity and its gradients and applied hierarchical cluster analysis to recognize and characterize the Mexico City wind circulation patterns in the period 2001–2006. As far as we know, the last paper reported the first work where a non-local approach is used to characterize the wind condition for identifying patterns with more detail than the simple results produced by the wind rose method.

In this paper, extending our previous work [25], we examine the main surface patterns of wind circulation and pollutant-flow of NO_2 , O_3 , SO_2 , and PM_{10} in the Mexico City region over the period 2001–2010. We achieved the identification and characterization of the pollutant-flow patterns through the exploitation of the 1-hour average values of the pollutant concentrations and wind data provided by the atmospheric monitoring network of Mexico City (SIMAT [26]) and the application of cluster analysis as a data mining procedure. First, we considered Mexico City as a 2D lattice domain and defined the flow condition (or flow state) of a given pollutant in each lattice cell in terms of a flow vector field and its gradients (precisely, the divergence and curl of this flow vector). Second, we used the 1-h average values of the pollutant concentrations and wind data provided by SIMAT to estimate, using Kriging interpolation, discrete representations of the pollutant-flow vector field and its gradients over the lattice domain. Finally, we used the k-means method of cluster analysis [27–29] to identify and characterize the pollution-flow patterns from the clustering modes of the flow states. We identified seven patterns for wind circulation and nine patterns for each of NO_2 , O_3 , PM_{10} , and SO_2 pollutant-flows. Their seasonal and annual average intensities and probabilities of occurrence were also estimated.

2. Materials and Methods

In this section, we detail the study domain, data, and procedure that we used to identify and characterize the wind and pollution-flow patterns.

2.1. Study Domain

We considered the part of Mexico City located at 19.3° – 19.6°N and 99.0° – 99.3°W as the study domain. In Figure 2, we showed this region as enclosed by a solid line square. This region contains 75% of the stations of the wind-monitoring network (REDMET) of SIMAT, 95% of the NO_2 stations, 83% of the O_3 stations, 93% of the PM_{10} stations, and 86% of the SO_2 stations of the air quality monitoring network (RAMA) of SIMAT (Figure 3). Because of the topographic complexity of the mountains surrounding Mexico City, we examined the pollutant flows in this region, assuming it divided into quadrants (NE, NW, SW, and SE). We defined these quadrants using a reference frame with origin at (19.43°N , 99.13°W) and the axes along the west to east (W–E) and south to north (S–N) directions (dotted lines in Figure 2). The origin of the reference frame is the geometric centroid of the REDMET stations. The positions of the geometric centers of the city quadrants are: (19.5°N , 99.1°W), (19.5°N , 99.2°W), (19.4°N , 99.2°W), and (19.4°N , 99.1°W) for the NE, NW, SW, and SE quadrants. The dimensions of each quadrant were 15.66 km length in the west–east direction and 16.56 km length in the south–north direction (each quadrant is a square of 540×540 arcsec). In principle, we expect to detect the ventilation effects due to the openings located at the west and east sides of the Sierra de Guadalupe (north of the city) at NW and NE quadrants, respectively, and to observe in the SE quadrant the effect of the gap situated in the southeast of the Mexico basin. Also, in the SE and NE quadrants, we expect to recognize the effects of the winds blowing along the ventilation channel determined by

the volcanos (Sierra Nevada) on the east side of the city. Moreover, we expect to recognize the wind effects due to the Mexico City mountain-valley system in all quadrants, but mainly in the NW and SW quadrants.

2.2. Data

Figures 2 and 3 illustrate the study domain and the spatial distributions of the stations of the monitoring networks of SIMAT for wind, nitrogen dioxide, ozone, PM₁₀, and sulfur dioxide. These monitoring networks provided the 1-hour average values of the meteorological and air quality variables systematically and made them publicly available through its web site [26]. For the present work, we collected the wind data (wind speed and wind direction) and the air quality data (NO₂, O₃, PM₁₀, and SO₂ surface concentrations) for the period 2001–2010, which constitute a database with 87,600 records, approximately, for each hourly averaged variable.

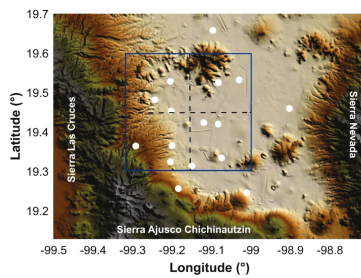


Figure 2. Study domain for Mexico City and spatial distribution of the stations (white dots) of the wind-monitoring network (REDMET) of the atmospheric monitoring network of Mexico City (SIMAT). The REDMET provides 1-hour average values of wind speed and wind direction, and other properties such as temperature and relative humidity.

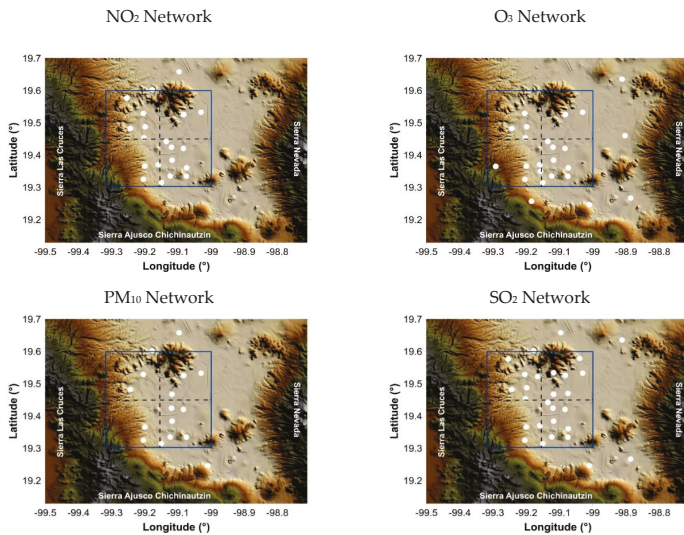


Figure 3. Spatial distribution of the stations (white dots) of the NO₂, O₃, PM₁₀, and SO₂ monitoring networks (RAMA) of SIMAT. The RAMA provides 1-hour average values of the surface concentrations of NO₂, O₃, PM₁₀, and SO₂, among other chemical compounds.

2.3. Study Database

In a first step, we represented the study domain (D) as a square grid G with 289 nodes G_{rs} , where the subscripts $r = 1, 2, \dots, 17$ and $s = 1, 2, \dots, 17$ vary along with the West–East (WE) and South–North (SN) directions, respectively. Using the wind speed and wind direction data supplied by the REDMET stations, and the NO_2 , O_3 , PM_{10} , and SO_2 concentration data supplied by the RAMA stations, we estimated (using Kriging interpolation) the horizontal components of the flow vector field at each grid node G_{rs} and time t ,

$$J_{WE}(r, s, t) = \mu(r, s, t)v_{WE}(r, s, t), \quad J_{SN}(r, s, t) = \mu(r, s, t)v_{SN}(r, s, t) \quad (2)$$

For a given pollutant, at the node G_{rs} and time t , $\mu(r, s, t)$ is the pollutant concentration, and $v_{WE}(r, s, t)$ and $v_{SN}(r, s, t)$ are the wind velocity components. Here, time t is an integer running from 1 to the number H of hours (87,600, approximately) in the period 2001–2010.

Then, we defined a 2D lattice L composed by 64 regular non-overlapping cells C_{ij} covering D , with $i = 1, 2, 3, \dots, 8$ and $j = 1, 2, 3, \dots, 8$, such that each cell C_{ij} is surrounded by nine grid nodes of G , as Figure 4 illustrates it.

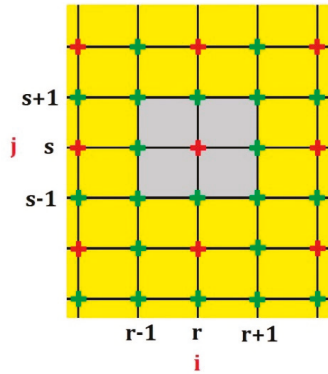


Figure 4. Arrangement of the calculation grid nodes G_{rs} and the lattice cells C_{ij} . The green crosses represent the grid nodes, and the red crosses indicate the centers of the lattice cells. In gray, we show the cell C_{ij} .

The estimations, for each pollutant, of the flow vector components at the grid nodes G_{rs} , allow calculating (numerically) the spatial averages of the components of the pollutant-flow vector and its gradients at the cells C_{ij} of the lattice L using their 2D discrete definitions in terms of centered finite differences [24,30]. For a given pollutant, we will denote the flow vector components at C_{ij} by $j_x(i, j, t)$ and $j_y(i, j, t)$, and the associated divergence and curl of the flow vector will be denoted by $\Gamma(i, j, t)$ and $\Omega(i, j, t)$. Here, x and y denote the WE and SN directions, respectively. At this level, we will be referring to this non-local discrete representation of the flow condition of the study domain as the 64-cell model. It involves 256 ($= 4 \times 64$) parameters to define an *event* of the system (i.e., to describe the flow condition over the complete spatial domain). In this work, for simplicity in the handling and interpretation of the results, we considered the reduction of the 64-cell model to the cases of the 4-cell and 1-cell models, which we obtained using a spatial averaging procedure. In any case, the four parameters (j_x, j_y, Γ, Ω) define the flow state at a lattice cell; therefore, the 4-cell and 1-cell models respectively entail 16 and 4 parameters to describe an *event* of the system. It is convenient to note that the introduction of the additional variables (Γ, Ω) in the flow state definition, allows recovering some of the information lost during the spatial averaging of the flow vector components. This assumption gives a slight non-local character to this description [31].

For each cell C_{ij} , we calculated, hour by hour, the average of the four state-variables over the 2001–2010 period, defining a one generic year database for each pollutant and cell model considered. The results were normalized and then organized in seasonal groups: January–March (winter), April–June (spring), July–September (summer), and October–December (autumn).

We performed data normalization as follows. We determined the maximum absolute values of the magnitude of the pollutant-flow vector $|j|_{\max}$, and the divergence $|\Gamma|_{\max}$, and curl $|\Omega|_{\max}$ of the flow vector, in the generic year database. Then the normalized and dimensionless state variables (all of them now ranging in the interval $[-1, +1]$) were calculated using the following expressions:

$$\hat{j}_x(i, j, t) = \frac{j_x(i, j, t)}{|j|_{\max}}, \tag{3}$$

$$\hat{j}_y(i, j, t) = \frac{j_y(i, j, t)}{|j|_{\max}}, \tag{4}$$

$$\hat{\Gamma}(i, j, t) = \frac{\Gamma(i, j, t)}{|\Gamma|_{\max}}, \tag{5}$$

$$\hat{\Omega}(i, j, t) = \frac{\Omega(i, j, t)}{|\Omega|_{\max}}. \tag{6}$$

2.4. Clustering Method

We used the k-means method of cluster analysis as a procedure of data mining to identify and characterize the main patterns of wind and flow of pollutants in the Mexico City region.

Cluster analysis comprises a broad set of techniques for finding non-overlapping subgroups of data objects in a dataset. When clustering the data objects of a dataset, we seek to organize them into a given number of distinct subsets (groups, or clusters), so that they constitute a partition of the initial dataset; this way, the data objects within each subset are quite similar to each other, while data objects in different groups are quite different from each other [29]. Clustering is an unsupervised problem because we are trying to discover structure (distinct clusters) based on a dataset, without being trained by a response variable.

The k-means clustering method is the simplest and the most frequently used technique of cluster analysis for partitioning a dataset into a set of k groups. In k-means clustering, we seek to partition the set of data objects into a pre-specified number of clusters, so that the total within-cluster variation (TWCV) is as small as possible.

Suppose we have a dataset $X = \{x_1, x_2, \dots, x_N\}$, $x_i \in \mathbf{R}^d$, and we try to partition X into M disjoint clusters C_1, C_2, C_M . Then, the k-means algorithm detects local optimal solutions concerning the TWCV defined as the sum of squared Euclidean distances between each data object x_i and the centroid m_k of the cluster C_k that contains x_i . Analytically, the TWCV is given by

$$\varepsilon(m_1, m_2, \dots, m_M) = \sum_{i=1}^N \sum_{k=1}^M \lambda_{ik} \|x_i - m_k\|^2 \tag{7}$$

where $\lambda_{ik} = 1$ if $x_i \in C_k$, and 0 otherwise. The TWCV measures the clustering goodness, and the optimization problem that defines the k-means clustering resides in minimizing TWCV. In practice, we used the software *DataLab* developed by Hans Lohninger [32] to perform the cluster analysis with the k-means algorithm.

For each air pollutant considered, we define its set of data objects as

$$H = \{Q(t) | t = 1, 2, \dots, T\}. \tag{8}$$

where $T = 8760$ is the number of hours of the generic year, and

$$Q(t) = \left\{ Q_{ijt} \equiv (\hat{j}_x, \hat{j}_y, \hat{\Gamma}, \hat{\Omega})_{ijt} \mid i = 1, 2, \dots, N_x; j = 1, 2, \dots, N_y \right\}, \tag{9}$$

with $N_x = 2$ ($N_x = 1$) and $N_y = 2$ ($N_y = 1$) in the case of the 4-cell (1-cell) model. We organized the dataset H in the seasonal subsets H_{winter} , H_{spring} , H_{summer} , and H_{autumn} comprising, respectively, the data objects of the periods January–March (winter), April–June (spring), July–September (summer), and October–December (autumn). We identified each data object of these subsets with a label of the form MMDDHH that specifies the date (relative to the generic year) and hour of occurrence.

To carry out the cluster analysis for each seasonal period, we build a data matrix structured as described in Table 1.

Table 1. Structure of the data matrix for the cluster analysis.

Columns	Variables
1	DateTime (MMDDHH)
2–5	The four values of the 1-cell model parameters: $(\hat{j}_x, \hat{j}_y, \hat{\Gamma}, \hat{\Omega})_{1C}$
6–21	The 16 values of the 4-cell model parameters: $(\hat{j}_x, \hat{j}_y, \hat{\Gamma}, \hat{\Omega})_{C0}, (\hat{j}_x, \hat{j}_y, \hat{\Gamma}, \hat{\Omega})_{C1}, (\hat{j}_x, \hat{j}_y, \hat{\Gamma}, \hat{\Omega})_{C2}, (\hat{j}_x, \hat{j}_y, \hat{\Gamma}, \hat{\Omega})_{C3}$

For each pollutant, using the respective data matrixes of the seasonal subsets, we can apply the k-means algorithm for clustering the associated data objects considering the parameters of the 1-cell or 4-cell model as the clustering variables. Although we can expect that the 4-cell model variables will produce a physically more detailed clustering of the wind and pollutant-flow events, in this work, for easiness in handling the results, we used only the 1-cell model parameters as clustering variables. The application of the clustering procedure to the 1-cell model data objects will organize them, assigning the cluster number to the date-time labels that identify the events. Consequently, the 4-cell model data objects also receive cluster numbers correspondingly. It means that the data objects of the 4-cell model were also organized into clusters by the same clustering procedure. Therefore, for each pollutant and seasonal period, we have clusters of events characterized by the sixteen parameters of the 4-cell model:

$$(\hat{j}_x, \hat{j}_y, \hat{\Gamma}, \hat{\Omega})_{C0}, (\hat{j}_x, \hat{j}_y, \hat{\Gamma}, \hat{\Omega})_{C1}, (\hat{j}_x, \hat{j}_y, \hat{\Gamma}, \hat{\Omega})_{C2}, (\hat{j}_x, \hat{j}_y, \hat{\Gamma}, \hat{\Omega})_{C3} \tag{10}$$

where C0, C1, C2, and C3 are the cells of the model.

2.5. The Number of Clusters

The k-means clustering is a simple and fast algorithm that can efficiently deal with large datasets. However, the k-means approach requires pre-specifying the number of clusters; and preferably, we would like to use an optimal number of clusters that we defined according to some given criterion. In this work, because of the motivation expressed in the following two paragraphs, we applied the k-means clustering method to organize each seasonal period in six clusters of data objects (events).

2.5.1. Physical Motivation

In Figure 5, we presented the mean diurnal behavior of solar radiation, temperature, and wind speed observed during 2001. We obtained these results from data we measured at an urban site southeast Mexico City (Xochimilco) [11,25]. The plots evidence that the meteorological events comprised in the six time-periods 0–4, 4–8, 8–12, 12–16, 16–20, and 20–24 h, are quite different from each other. The periods 0–4 and 20–24 h show the cooling phase of the atmosphere during the night. In the period 4–8 h, we observe the sunrise occurrence, and that temperature and wind speed reach their minimum values. The period 8–12 h shows the growing phases of solar radiation, temperature, and wind speed, with solar

radiation reaching its maximum. The period 12–16 h depicts the temperature reaching its maximum, while wind speed keeps growing, and solar radiation starts to decrease. Finally, the period 16–20 h shows the sunset occurrence, the wind speed reaching its maximum, and temperature decreasing. Appreciation of these different behaviors suggests searching for six groups during the application of the k-means algorithm for clustering the data objects defined by the events of wind circulation and pollutant-flow in Mexico City.

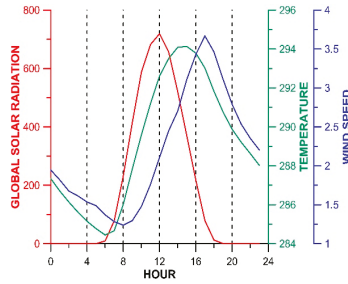


Figure 5. Average diurnal behavior of solar radiation (red line), temperature (green line), and wind speed (blue line) in an urban site (Xochimilco) of Mexico City during 2001 [11,25]. We observe that the meteorological events comprised in the six intervals of 0–4, 4–8, 8–12, 12–16, 16–20, and 20–24 h are different from one period to another. This appraisal suggests searching for six clusters during the cluster analysis of the wind and pollutant-flow events.

2.5.2. The Elbow Method

From the standpoint of cluster analysis, one of the most popular methods for determining the optimal clusters is the *elbow method*. It provides a simple solution. The basic idea is to compute the k-means clustering algorithm using different numbers, k , of clusters. The next step is drawing the total within-cluster variation (or total within-cluster sum of squares) versus the number of clusters. Commonly, the analysts consider the location of a bend in the plot as an indicator of the appropriate number of clusters. However, it is not always clear where the bend point position is. We preferred to calculate the percentage reduction (δ) of the total within-cluster sum of squares of a given k , relative to its value for the previous number of clusters $k - 1$, and then to plot δ as a function of k . As our optimal number of clusters, we selected the value of k from which on the reduction δ is less than 10% each unit step in increasing k . For example, according to this procedure, Figure 6 shows that we must select $k = 6$ when clustering the winter wind data objects of the present work.

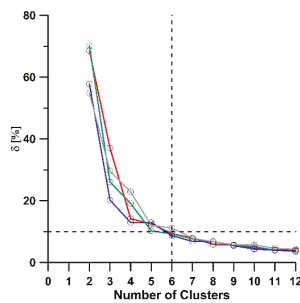


Figure 6. Percentage reduction (δ) of the total within-cluster sum of squares, relative to its previous value, as a function of the number of clusters. Here, for the clustering of the winter wind data objects, we observe that from 6 clusters on, the reduction δ is less than 10% each unit step in the increase of the number of clusters: $0\% \leq \delta \leq 10\%$.

3. Results and Discussion

Figure 7 summarizes the application of the k-means clustering method (with $k = 6$) to the seasonal subsets, H_{winter} , H_{spring} , H_{summer} , and H_{autumn} , of the data objects (events) of wind circulation and pollutant-flows. This figure shows an arrangement with four columns (one per seasonal period) and five rows (one for wind circulation, and four for the pollutant-flows of NO_2 , O_3 , PM_{10} , and SO_2). Each graph shows six plots (one per cluster) differentiated by the line color. The algorithm enumerates the clusters according to their sizes, from the larger to the smaller, so colors mean no more. Each plot presents the *hourly population* of one cluster, that is to say, the number of data objects belonging to the cluster as a function of the hour of the day (Mexico City local time, UTC-6 h).

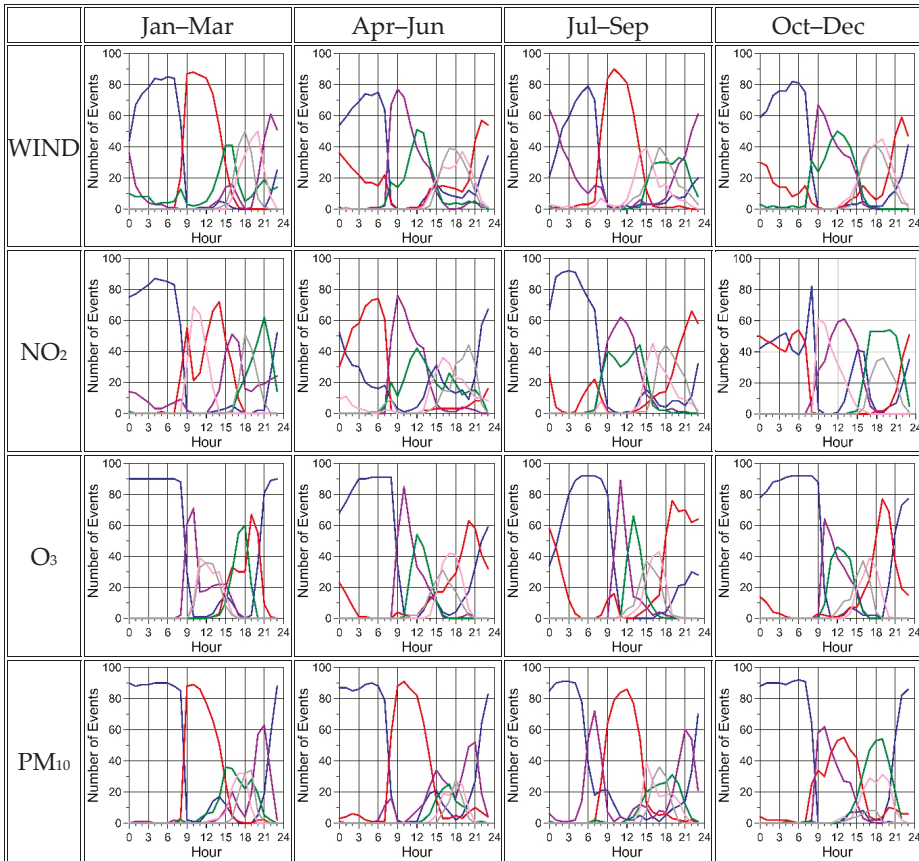


Figure 7. Cont.

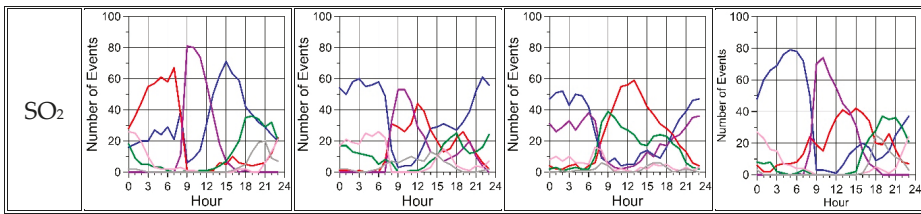


Figure 7. Application of the k-means algorithm (with $k = 6$) to the seasonal subsets of the data objects of the wind circulation (first row) and pollutant-flows (next four rows) events. Each graph shows six plots, one per cluster, individualized by the color. Each plot expresses the *hourly population of the cluster*, i.e., the number of data objects (or events) of the cluster as a function of the hour of the day.

For wind circulation or any given pollutant-flow, a qualitative comparison of graphs in the respective row allowed recognizing some seasonal similarities and differences between the clusters. For example, for the wind circulation (first row), if we pay attention to the clusters represented by a blue-line plot in the four seasons, we can observe an evident regularity: the hourly populations have similar trends and indicate that the majority of their events occurred during the night, mainly from midnight until dawn. We interpreted this regularity as the possible existence of a wind pattern. The plots of the pollutant-flows also show a similar regularity.

The trends of the hourly populations of the clusters provide useful but insufficient information for discovering patterns in sets of events of wind circulation or pollutant-flows. In [25], the authors detected two wind clusters with similar trends in the hourly populations (both in the number of events and in the times of occurrence), but in one case the winds were blowing from the north and in another one from the south, indicating different patterns of wind circulation. However, we can use the information provided by the values of the 16 parameters of the 4-cell model to complement the pattern identification process.

Eight of the sixteen parameters of the 4-cell model are the components of the flow vectors in the quadrants (NW, NE, SW, and SE) of the MCMA. This complementary information and the hourly population plots allowed recognizing the wind circulation patterns shown in Figure 8, and the pollution-flow patterns shown in Figures 9–12. We found seven patterns for wind circulation and nine patterns for each of the pollutant-flows (NO_2 , O_3 , PM_{10} , and SO_2). In Figure 8, we show the hourly population of each wind pattern and a graphic representation of the wind velocity at the quadrants. Figures 9–12 show the hourly population of each pattern, a graphic representation of the flow vector at the quadrants, the surface distribution of the pollutant concentration, and the mean spatial pollutant concentration (expressed in ppb for NO_2 , O_3 , and SO_2 , and in μgm^{-3} for PM_{10}). In these figures, the hourly population of a pattern is an average over the seasons the pattern occurred; the vectors (the wind velocity and the pollutant-flow vectors) are averages over the elements of the pattern and the seasons; the spatial distribution of the pollutant concentrations is the average over the pattern elements and seasons; and the mean spatial concentration of a pollutant is the average over the positions of the average pollutant distribution. The lengths of the arrows that represent the wind and flow vectors were scaled to get the larger one fitted in the square that represents the quadrant, allowing a qualitative comparison of the vector magnitudes among the patterns of wind circulation or the patterns of any of the pollutant flows.

3.1. Wind Circulation Patterns

The proposed methodology for examining the database of the wind events that occurred in Mexico City from 2001 to 2010 allowed discovering there the presence of seven wind circulation patterns and the estimation of their seasonal and annual occurrence frequencies, which we summarized in Table 2. We denoted these patterns as WIND-P $_n$, with $n = 1, 2, \dots, 7$, and enumerated them trying to follow

the order of their appearance during the day. In Figure 8, we presented the hourly population of each wind pattern, including a sketch out of the corresponding wind velocity in the city quadrants.

Table 2. Seasonal and annual frequencies of the wind circulation patterns (%).

Pattern	Jan–Mar (Winter)	Apr–Jun (Spring)	Jul–Sep (Summer)	Oct–Dec (Autumn)	Annual
WIND-P1	33	31	25	32	30
WIND-P2	25	18	24	16	21
WIND-P3	0	12	9	14	9
WIND-P4	20	0	0	0	5
WIND-P5	9	9	20	11	12
WIND-P6	14	21	22	17	18
WIND-P7	0	9	0	10	5

In the following paragraphs, we provide brief descriptions of the wind circulation patterns. We used the Mexico City local time (UTC-6 h) in all figures and descriptions.

WIND-P1: early morning downslope winds. WIND-P1 was the wind pattern with the highest annual frequency (30%). It was observed systematically throughout the year during the night, showing a large peak around hour 6 (Figure 8) and a small peak around hour 15. The mean wind velocities at the quadrants suggest downslope winds from the surrounding mountains, converging towards Mexico City basin. The converging winds represented by the small peak reflect the presence of convective upwards winds due to the urban heat island (UHI) in the Mexico City region. Jauregui [7] and Klaus et al. [33] pointed out that the Mexico City downslope winds are reinforced by UHI.

WIND-P2: northeasterly and easterly winds. The annual average frequency of this wind pattern was 21%. It is observed systematically throughout the year, especially during winter (25%) and summer (24%). The mean velocities correspond to winds blowing from NE in almost all the quadrants of the city (trade winds). The wind events of this pattern occurred from the sunrise (hour 7) up to the hour 17. Its hourly population presents a high peak between hours 10 and 11.

WIND-P3: midday northerly winds. This pattern had an annual frequency of 9%. It was observed during spring (12%), summer (9%), and autumn (14%) from hour 7 to hour 21, with a peak around hour 13. The mean wind velocities in the quadrants indicate winds blowing from the north and northeast sectors.

WIND-P4: westerly and southerly winds. This wind pattern was observed only winter season with a seasonal frequency of 20%; its events occurred throughout the day, but mainly from noon to midnight, reaching its maximum population around hour 17. The mean wind velocities represent winds with a westerly component in the west quadrants and southerly winds in the east quadrants. These velocities correspond to winds blowing from the south and southeast city sectors through a gap between the mountains of the Sierra Ajusco-Chichinautzin and the Sierra Nevada, following the ventilation channel S–N located at the east side of the city (Figure 1). The local winds of this pattern could be related to the subtropical jet stream of winter [34] or with the westerlies that are permanently occurring in subtropical and middle latitudes, but coupled with the winds driven by the gap between the mountains located at the southeast. Doran and Zhong [35] described the main characteristics of a gap wind system in the southeastern corner of Mexico City that produces low-level jets occurring regularly during the late winter.

WIND-P5: afternoon northerly winds. This pattern was observed throughout the year with an annual frequency of 12%. It occurred from noon to midnight, with its maximum around hour 19. The mean wind velocities at the quadrants indicate winds blowing from the north sectors.

WIND-P6: midnight downslope winds. This pattern was observed systematically throughout the year, mainly during the nighttime hours, from the sunset (hour 18) to the sunrise (hour 6 of the next day), with its maximum around midnight. It got an annual average frequency of 18%. The population plot of this pattern has a small peak close to hour 15, which could be related to the UHI effect of the

city. The wind velocities in the western quadrants of the city represent downslope flows from Sierra de las Cruces (at west) and Sierra del Ajusco-Chichinautzin (located at SW and S) toward the town. In the eastern quadrants, otherwise, late afternoon northerly gap winds are observed guided by the S–N ventilation channel of the city.

WIND-P7: UHI-driven winds. This wind pattern was observed only during the spring (9%) and autumn (10%) seasons, with a low annual occurrence frequency of 5%. The wind events of this pattern occurred from the hour 14 to the hour 22, and its population reached a maximum value close to the hour 17. The mean wind velocities of the city quadrants indicate cyclonic winds converging towards Mexico City downtown, which seems to be related to an upwards flow driven by the UHI.

Summarizing, the wind patterns with the most significant frequencies were WIND-P1 and WIND-P2, with annual values of 30% and 21%, respectively. These two patterns, however, correspond to small velocities in comparison with the other five wind patterns. An outstanding feature of WIND-P1 is that, although its events occurred mainly during the night with converging winds, it also comprises daylight events of winds with the same characteristic of convergence towards the city downtown. We cannot interpret these last events as katabatic winds produced by the mountain-valley system; instead, we must understand them as winds associated with convective upwards flows driven by the urban heat island (UHI) effect. The pattern WIND-P6 also occurred during the night, but it peaked at midnight. This wind pattern comprises the downslope winds of the first hours of the night and also reflects the effect of the late afternoon northerly gap winds. The patterns WIND-P3 and WIND-P5 reflect the well-known prevailing winds from N and NE of the Mexico City region, and WIND-P2 evidence the occurrence of the trade winds.

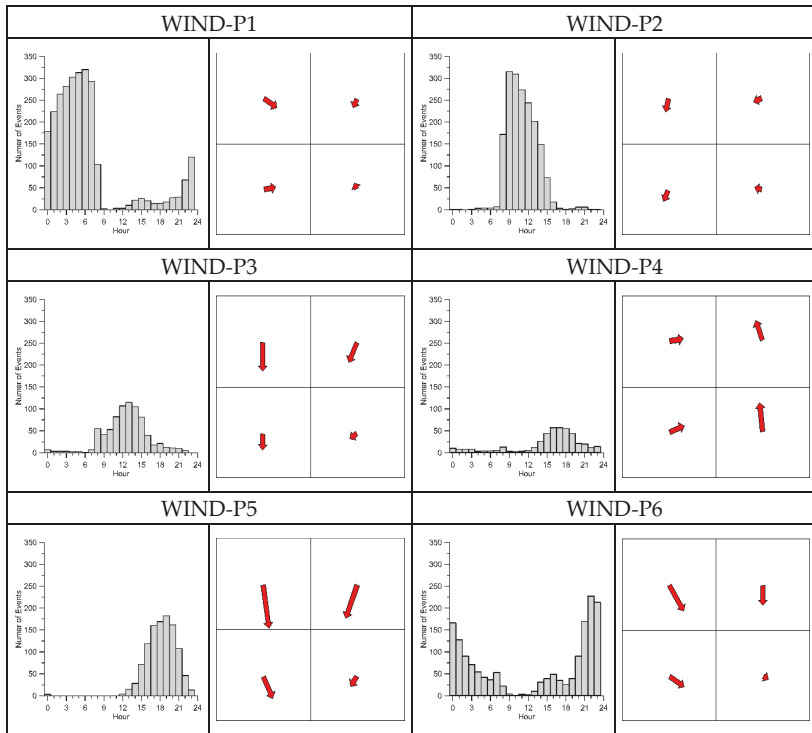


Figure 8. Cont.

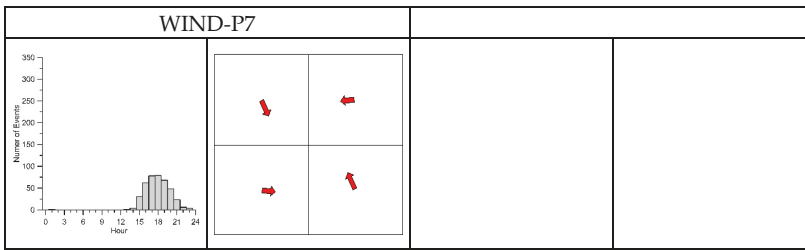


Figure 8. Wind circulation patterns in the Mexico City region during the period 2001–2010. For each pattern, we presented the hourly population (left) and the mean wind velocity (relative to the pattern) at the city quadrants (right). The size of red arrows that stand in for the velocity vectors indicates the velocity magnitude in a scale relative to the edge size of the squares that represent the quadrants.

The wind patterns with the most significant frequencies were WIND-P1 and WIND-P2, with annual values of 30% and 21%, respectively. These two patterns, however, correspond to small velocities in comparison with the other five wind patterns. An outstanding feature of WIND-P1 is that, although its events occurred mainly during the night with converging winds, it also comprises daylight events of winds with the same characteristic of convergence towards the city downtown. We cannot interpret these last events as katabatic winds produced by the mountain–valley system; instead, we must understand them as winds associated with convective upwards flows driven by the urban heat island (UHI) effect. The pattern WIND-P6 also occurred during the night, but it peaked at midnight. This wind pattern comprises the downslope winds of the first hours of the night and also reflects the effect of the late afternoon northerly gap winds. The patterns WIND-P3 and WIND-P5 reflect the well-known prevailing winds from N and NE of the Mexico City region, and WIND-P2 evidence the occurrence of the trade winds.

Our wind patterns agree quite well with the Mexico City wind patterns obtained in [25] for the period 2001–2006 with a slightly different methodology. In Table 3, we described the correspondence between these two sets of patterns. The first column contains the wind patterns WP1–WP7 reported in [25]; the second column presents the wind patterns obtained in the present work; and, the last column provides a brief description of the main characteristics of these patterns.

Table 3. Comparison against the wind patterns reported by Carreón-Sierra et al. [25].

Carreón-Sierra et al.	This Work	Description
WP1	WIND-P1	Early morning downslope winds
WP2	WIND-P2	Northeasterly and easterly winds
WP3	WIND-P3	Midday northerly winds
WP4	WIND-P4	Westerly winds at the western quadrants and
WP5		Southerly winds at the eastern quadrants
WP6	WIND-P5	Afternoon northerly winds
WP7	WIND-P6	Midnight downslope winds
—	WIND-P7	UHI-driven winds

The main differences between both sets of patterns were:

- The pattern WIND-P4 includes the wind patterns WP4 (southerly winds) and WP5 (westerly winds) reported in [25]. However, we detected the pattern WIND-P4 only during the winter season, while the pattern WP4 occurred throughout the year (although with tiny frequencies in spring, summer, and autumn), and the pattern WP5 was only observed during the first semester of the year (winter and spring seasons).

- We recognized a pattern (WIND-P7) associated with cyclonic winds strongly converging towards Mexico City downtown during the daylight hours. The winds in this pattern indicate an upwards flow driven by the UHI. No report exists in [25] about a similar pattern.

3.2. Pollutant Flow Patterns

In Tables 4–7, we enumerated the pollutant-flow patterns (NO₂, O₃, PM₁₀, and SO₂) that we identified for the Mexico City region, their seasonal and annual frequencies and flow intensities (the magnitudes of the flow vectors), and the associated wind circulation patterns. In Figures 9–12, for each pollutant-flow pattern, we presented the average population plot, the mean pollutant-flow vectors at the quadrants NW, NE, SW, and SE of the city, the pollutant surface distribution averaged over the pattern, and its mean spatial value. We denoted the pollution-flow patterns as POL-P_n, where POL indicates the pollutant (POL = NO₂, O₃, PM₁₀, and SO₂), and n is a consecutive integer number from 1 to 9. The cells with the value 0.00 in the tables indicate the seasonal periods where some flow patterns were not detected.

In general, although the pollutant concentrations modulate the magnitudes of the flow vectors, the pollutant-flow patterns reflected the directional characteristics inherited from the wind patterns.

3.2.1. The NO₂ Flow Patterns

We identified nine NO₂ flow patterns for the Mexico City region. Table 4 shows the seasonal and annual average frequencies and average flow intensities of the patterns, expressed in percent (%) and μgm⁻²s⁻¹, respectively. As shown in Figure 9, these flow patterns closely resemble the wind circulation patterns, and Table 4 summarized the relationship between the pollutant-flow and wind circulation patterns.

Table 4. Frequencies (%) and flow intensities (μg/m²s) of Mexico City NO₂ flow patterns (2001–2010).

Pattern	Wind Pattern Inherited	JAN–MAR (Winter)		APR–JUN (Spring)		JUL–SEP (Summer)		OCT–DEC (Autumn)		ANNUAL	
		Freq	Flow	Freq	Flow	Freq	Flow	Freq	Flow	Freq	Flow
NO2-P1	WIND-P1	37.36	10.41	23.81	7.46	35.96	10.31	22.13	13.49	29.79	10.42
NO2-P2	WIND-P2	18.61	15.59	0.00	0.00	12.86	16.83	0.00	0.00	7.83	8.11
NO2-P3	WIND-P4	15.93	18.59	10.85	16.92	0.00	0.00	0.00	0.00	6.63	8.88
NO2-P4	WIND-P6	11.02	32.38	24.08	19.03	17.35	27.07	29.02	7.92	20.41	21.60
NO2-P5	WIND-P2	10.42	46.27	17.03	24.57	0.00	0.00	10.61	30.61	9.49	25.36
NO2-P6	WIND-P7	6.67	21.82	0.00	0.00	0.00	0.00	6.89	5.96	3.38	6.95
NO2-P7	WIND-P3	0.00	0.00	14.93	42.51	15.94	28.30	16.64	30.18	11.93	25.25
NO2-P8	WIND-P5	0.00	0.00	9.29	26.70	8.97	24.39	0.00	0.00	4.58	12.77
NO2-P9	WIND-P5	0.00	0.00	0.00	0.00	8.92	49.99	14.69	48.00	5.95	24.50

The NO₂ flow patterns with the most significant annual frequencies were NO2-P1 (30%), NO2-P4 (20%), and NO2-P7 (12%), but the patterns with the most substantial annual flow intensities were NO2-P5, NO2-P7, and NO2-P9 with 25.4, 25.3, and 24.5 μgm⁻²s⁻¹, respectively.

The flow patterns NO2-P4, NO2-P7, NO2-P8, and NO2-P9 carry nitrogen dioxide from the north to the south quadrants of the city, particularly the pattern NO2-P9, although it occurred only during the second semester of the year. The events of these patterns take the ozone precursor to the SW and SE quadrants, contributing actively to the ozone formation in this area throughout the year.

The patterns NO2-P2 and NO2-P5 carry the pollutant from the eastern to the western quadrants of the city following the trade winds. The events of the NO2-P3 and NO2-P6 patterns, differently, take nitrogen dioxide from west to east on the west side of the city, but from south to north on the eastern side. However, while the pattern NO2-P3 reflects a coupling of the westerly winds and the afternoon southerly gap winds, the pattern NO2-P6 reflects cyclonic transport driven by the UHI.

During the night, the events of the pattern NO2-P1, follow the downslope winds from the surrounding mountains and carry NO₂ to the city downtown. In comparison with the patterns of other

pollutants (O₃, PM₁₀, and SO₂), the NO₂-P1 flow pattern is the only one that revealed considerable nocturnal transport due to the downslope winds. The main reason is that NO₂ accumulates during the night since there are no photochemical reactions that consume it, and some of the mobile sources, which are responsible for approximately 86% of nitrogen oxide emissions in the Mexico City region [3], remain active during the night.

The NO₂ surface distributions, which are averages over the events of the NO₂ flow patterns, reveal a North–South part of the city as the zone with the higher NO₂ concentrations. This zone extends around the N–S axis that separates the west from the east quadrants (although slightly shifted to the eastern quadrants). The highest NO₂ levels occurred, in general, in the south sector, close to the Huizachtepetl (Cerro de la Estrella).

The surface NO₂ distributions with the highest concentrations were in connection with the NO₂-P5 and NO₂-P6 flow patterns, with mean spatial levels of 46 and 41 ppb. These high levels of NO₂ were detected mainly during the winter and autumn. We note that, in these two cases, the high levels of NO₂ extended spatially, covering almost completely the city. In the first case, it was a consequence of blocked transport by the mountains of the Sierra las Cruces, while in the second case, the high levels were a consequence of the cyclonic wind convergence driven by the UHI.

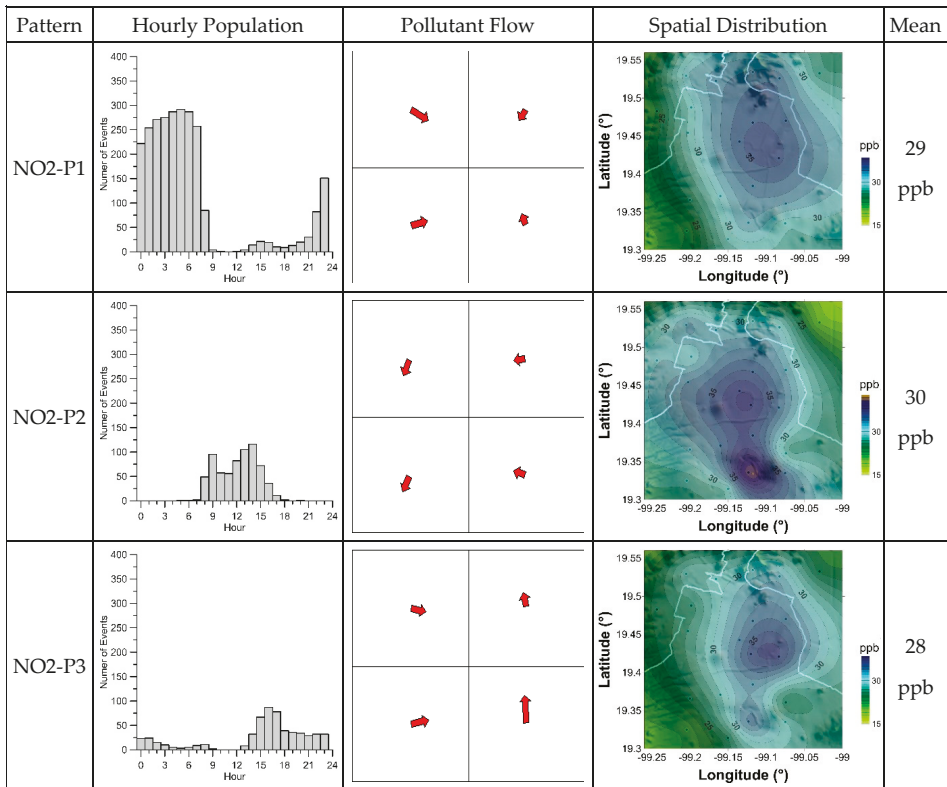


Figure 9. Cont.

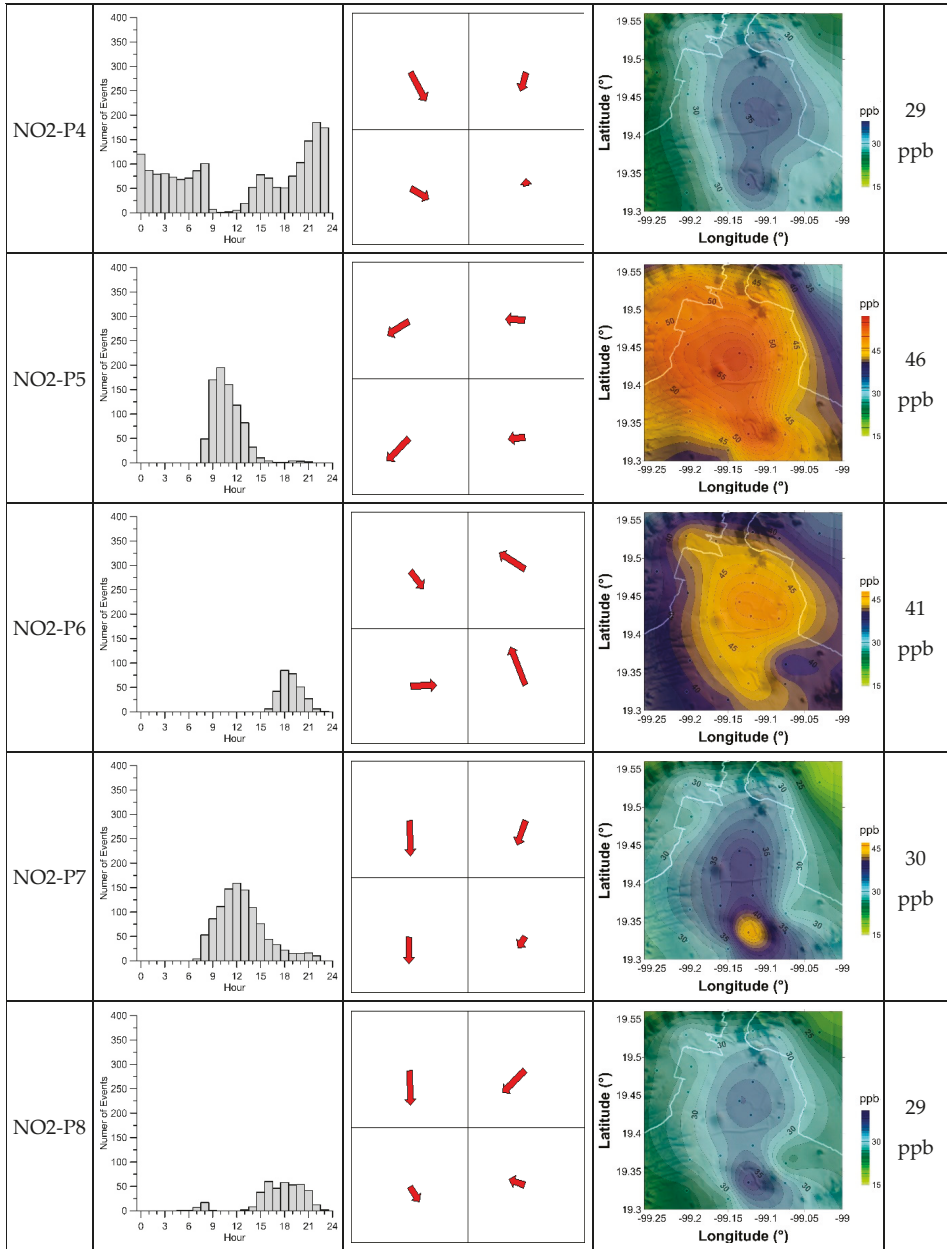


Figure 9. Cont.

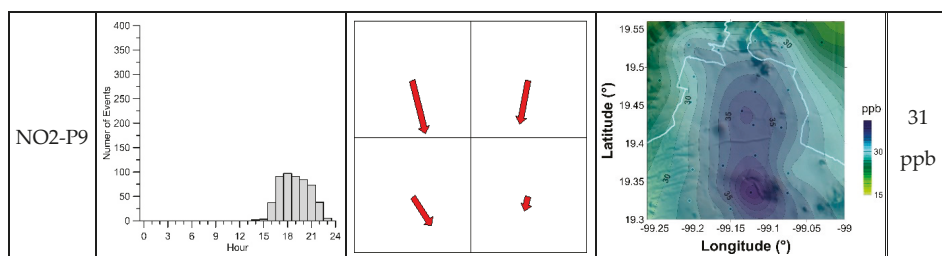


Figure 9. Flow patterns of nitrogen dioxide in the Mexico City region during the period 2001–2010. For each pattern, we included the hourly population (second column), the mean flow vectors (relative to the pattern) at the city quadrants (third column), the surface concentration distributions (fourth column) averaged over the events of the flow pattern, and the mean spatial concentration (last column). The size of red arrows that stand in for the NO₂ flow vectors indicates the flow intensity in a scale relative to the edge size of the squares that represent the quadrants.

3.2.2. The O₃ Flow Patterns

In Table 5 and Figure 10, we summarized the main characteristics of the O₃ flow patterns that we identified. In Table 5, we included the average seasonal and annual occurrence frequencies (%) and flow intensities ($\mu\text{g m}^{-2}\text{s}^{-1}$) of the flow patterns, and the wind patterns from which they inherited their circulation characteristics.

The flow vectors of the diurnal flow patterns O3-P6, O3-P8, and O3-P9 have considerable northerly components and convey ozone from the NW and NE to the SW and SE city quadrants, providing substantial contributions to the high ozone concentrations frequently observed in the south sectors (especially in SW) of the city throughout the year.

Table 5. Frequencies (%) and flow intensities ($\mu\text{g}/\text{m}^2\text{s}$) of the Mexico City O₃ flow patterns (2001–2010).

Pattern	Wind Pattern Inherited	JAN–MAR (Winter)		APR–JUN (Spring)		JUL–SEP (Summer)		OCT–DEC (Autumn)		ANNUAL	
		Freq	Flow	Freq	Flow	Freq	Flow	Freq	Flow	Freq	Flow
O3-P1	WIND-P1	54.54	6.47	46.57	6.66	41.35	7.89	52.20	4.41	48.64	6.36
O3-P2	WIND-P7	11.53	5.00	7.74	4.22	0.00	0.00	6.21	8.92	6.34	4.54
O3-P3	WIND-P2	11.48	13.84	0.00	0.00	0.00	0.00	10.79	29.21	5.55	10.76
O3-P4	WIND-P4	8.29	46.08	0.00	0.00	0.00	0.00	0.00	0.00	2.04	11.52
O3-P5	WIND-P2	7.50	43.99	0.00	0.00	6.52	53.26	0.00	0.00	3.49	24.31
O3-P6	WIND-P2	6.67	61.25	13.19	53.87	9.96	58.24	0.00	0.00	7.45	43.34
O3-P7	WIND-P6	0.00	0.00	18.45	32.28	27.49	20.02	16.51	22.15	15.69	18.62
O3-P8	WIND-P3	0.00	0.00	7.97	139.84	7.88	111.66	8.80	76.76	6.19	82.07
O3-P9	WIND-P5	0.00	0.00	6.09	116.44	6.79	78.33	5.49	99.39	4.61	73.54

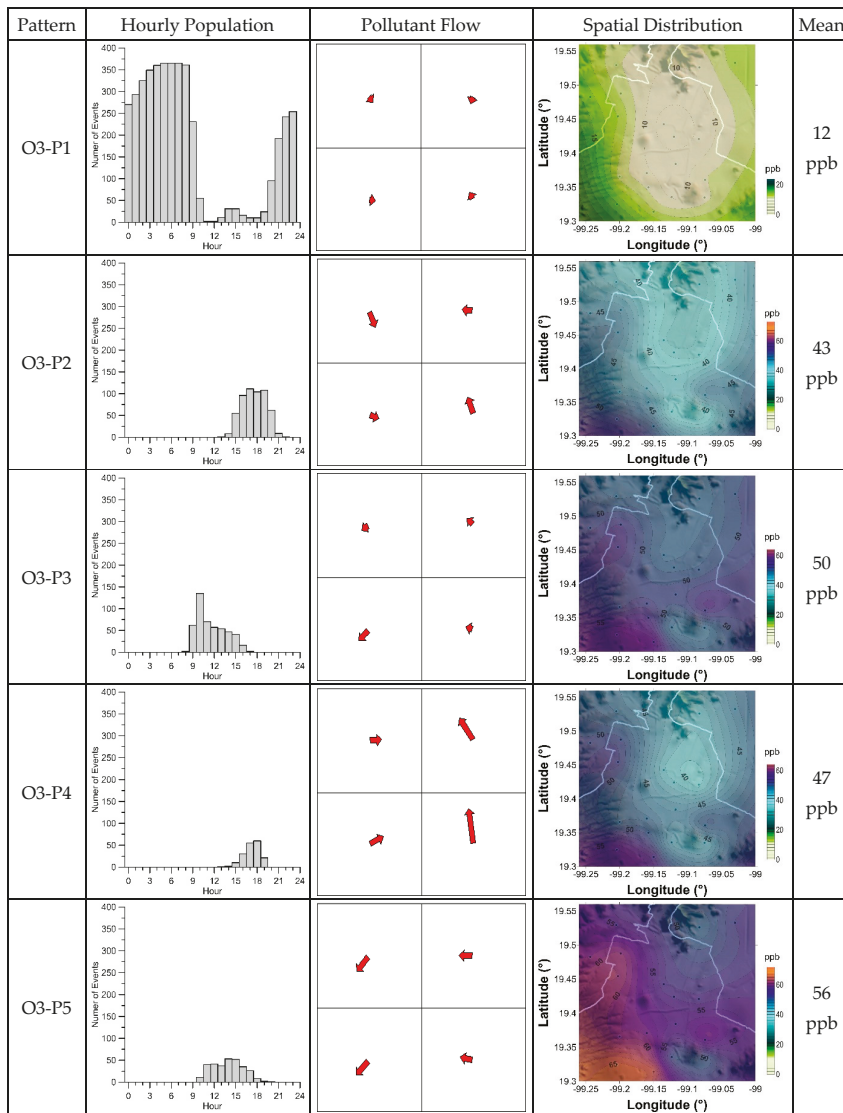


Figure 10. Cont.

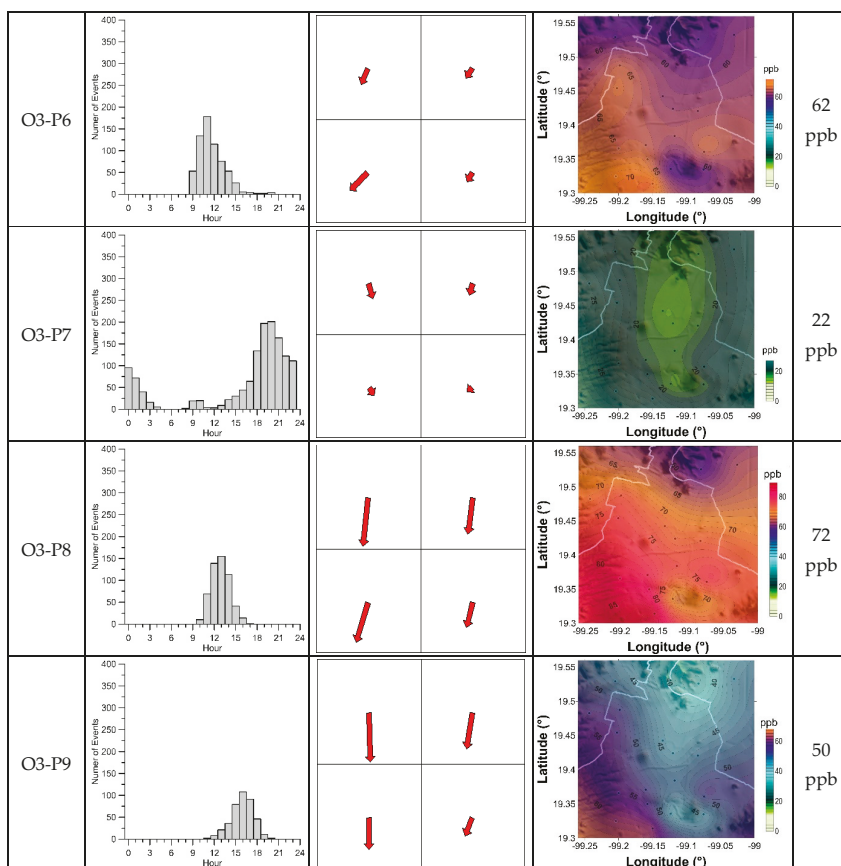


Figure 10. Flow patterns of ozone in the Mexico City region during the period 2001–2010. For each flow pattern, the figures show the hourly population (second column), the mean flow vectors (relative to the pattern) at the city quadrants (third column), the surface concentration distributions (fourth column) averaged over the events of the flow pattern, and the mean spatial concentration (last column). The size of red arrows that stand in for the O₃ flow vectors indicates the flow intensity in a scale relative to the edge size of the squares that represent the quadrants.

The flow patterns O3-P6, O3-P8, and O3-P9 revealed the highest flow intensities (43, 82, and 74 $\mu\text{gm}^{-2}\text{s}^{-1}$, on annual average). Seasonally, we observed the highest O₃ flow intensities during the spring, summer, and autumn.

The flow patterns O3-P3 and O3-P5 bring ozone from East to West in the city following the trade winds (pattern WIND-P2). These patterns reveal flow vectors from NE in the west quadrants of the city, and because of the mountains barrier (Sierra Las Cruces and Sierra Ajusco Chichinautzin), they contribute to the ozone accumulation at SW sector of the Mexico City region. The O₃ surface distributions, averaged over the events of these flow patterns, reveal, in fact, an evident and significant ozone accumulation (ranging from 70 to 100 ppb, approximately) at the SW quadrant.

The flow patterns O3-P1 and O3-P7 comprised nighttime flow events and had the first and second-largest occurrence frequencies. However, their flow intensities are tiny because of the low ozone concentrations (12 ppb and 22 ppb on average, respectively) in the nocturnal atmosphere (ozone production is of photochemical nature). It is interesting to note that the patterns O3-P1 and

O3-P7 and the patterns NO2-P1 and NO2-P4 reveal opposite behaviors (during the night, one observes NO₂ accumulation while O₃ decreases to its lowest levels) due to its relationship through the atmospheric photochemistry.

The O3-P2 is a flow pattern detected during the evening, driven by the UHI winds. It brings ozone from the surrounding parts of the city towards downtown, where an upwards convective flow takes ozone out there again, keeping the ozone levels relatively small in the city.

During winter, the flow events of the O3-P4 pattern bring ozone from west to east in the west side quadrants with small flow intensities, but the same flow pattern carries a considerable amount of ozone from south to north in the east side quadrants of the city, following the ventilation channel located at the west side of Sierra Nevada.

In general, the O₃ surface distributions show relative small concentrations where the NO₂ surface distributions show large emissions and vice versa. It is an evident behavior because of the NO_x-O₃ photochemical interactions.

3.2.3. The PM₁₀ Flow Patterns

We recognized nine PM₁₀ flow patterns, which we enumerated in Table 6 and sketched out in Figure 11. In Table 6, we presented the seasonal and annual averages of the occurrence frequencies and the flow intensities of the PM₁₀ flow patterns, expressed in % and μg/m²s, respectively. The directional characteristics of wind inherited by the PM₁₀ patterns are also briefly indicated in this table.

Table 6. Frequencies (%) and flows (μg/m²s) of the Mexico City PM₁₀ flow patterns (2001–2010).

Pattern	Wind Pattern Inherited	JAN–MAR		APR–JUN		JUL–SEP		OCT–DEC		ANNUAL	
		Freq	Flow	Freq	Flow	Freq	Flow	Freq	Flow	Freq	Flow
PM10-P1	WIND-P1	47.50	7.83	44.78	8.81	36.10	7.18	47.76	5.48	44.01	7.32
PM10-P2	WIND-P3	22.96	21.59	27.01	22.33	23.10	21.95	18.41	26.57	22.86	23.11
PM10-P3	WIND-P6	10.37	35.14	15.43	40.72	20.43	18.59	0.00	0.00	11.56	23.61
PM10-P4	WIND-P7	9.68	28.89	4.90	27.44	0.00	0.00	7.35	9.11	5.46	16.36
PM10-P5	WIND-P4	5.05	67.28	0.00	0.00	0.00	0.00	1.45	71.00	1.61	34.57
PM10-P6	WIND-P5	4.44	70.95	3.11	55.82	6.70	27.05	0.00	0.00	3.56	38.46
PM10-P7	WIND-P5	0.00	0.00	4.76	110.13	5.21	63.14	0.00	0.00	2.50	43.32
PM10-P8	WIND-P5	0.00	0.00	0.00	0.00	8.47	42.87	12.52	55.29	5.29	24.54
PM10-P9	WIND-P2	0.00	0.00	0.00	0.00	0.00	0.00	12.52	19.84	3.15	4.96

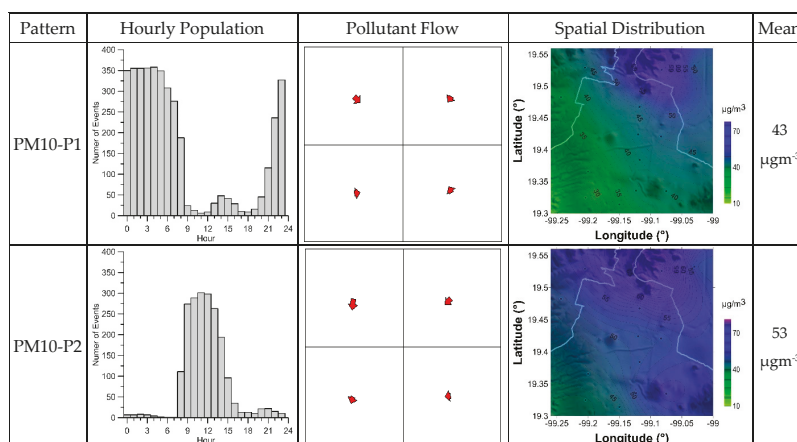


Figure 11. Cont.

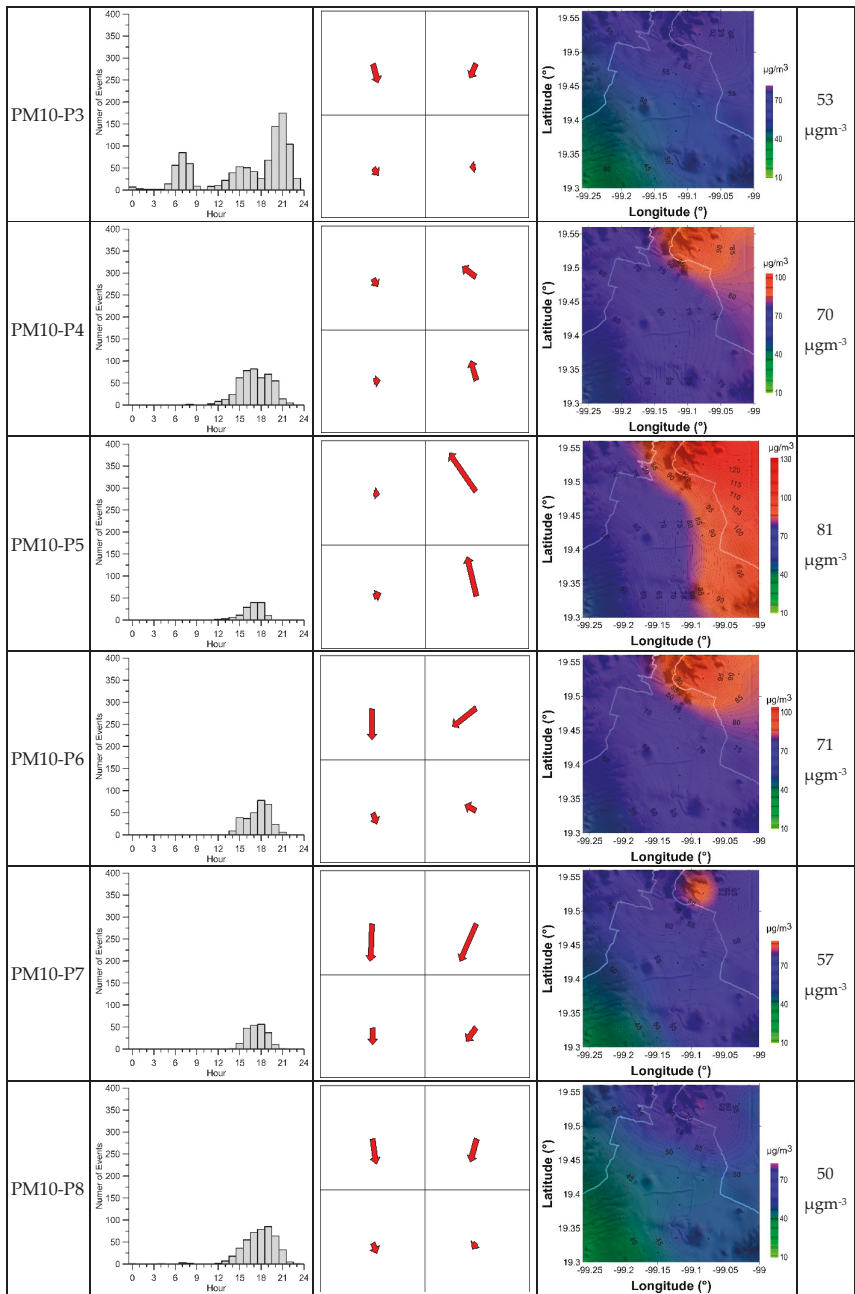


Figure 11. Cont.

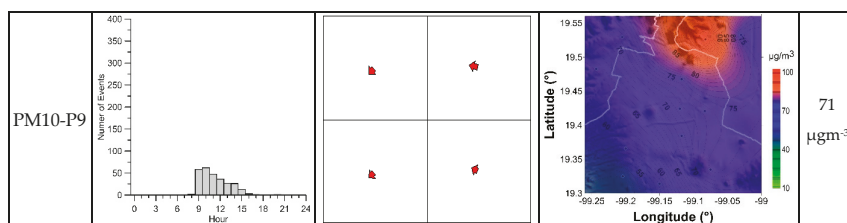


Figure 11. Flow patterns of PM₁₀ in the Mexico City region during the period 2001–2010. For each flow pattern, the figures show the hourly population (second column), the mean flow vectors (relative to the pattern) at the city quadrants (third column), the surface concentration distributions (fourth column) averaged over the events of the flow pattern, and the mean spatial concentration (last column). The size of red arrows that stand in for the PM₁₀ flow vectors indicates the flow intensity in a scale relative to the edge size of the squares that represent the quadrants.

The PM₁₀ flow patterns with the highest annual flow intensities were PM10-P7 ($43 \mu\text{g m}^{-2}\text{s}^{-1}$), PM10-P6 ($39 \mu\text{g m}^{-2}\text{s}^{-1}$), PM10-P5 ($35 \mu\text{g m}^{-2}\text{s}^{-1}$), and PM10-P8 ($26 \mu\text{g m}^{-2}\text{s}^{-1}$); but their annual frequencies were of the smaller (3%, 4%, 2%, and 5%, respectively). All these four patterns reveal a remarkable flow intensity at the NE city quadrant throughout the year, although with different flow directions. The patterns PM10-P6, PM10-P7, and PM10-P8 exhibited also flow vectors with intense northerly components in the NW quadrant, which convey particle PM₁₀ from the north to the south in the west side of the city. The events of these patterns also carried particulate matter from the northeast to the south sectors of the city, particularly in the NE quadrant. The flow intensities of the flow pattern PM10-P6 were 71, 56, and $27 \mu\text{g m}^{-2}\text{s}^{-1}$ during the winter, spring, and summer seasons; for PM10-P7 were 110 and $63 \mu\text{g m}^{-2}\text{s}^{-1}$ during the spring and summer, and for PM10-P8 were 43 and $55 \mu\text{g m}^{-2}\text{s}^{-1}$ during the summer and autumn, respectively.

The events of the PM10-P4 and PM10-P5 flow patterns carried particles from south to northwest in the quadrants of the east side of the city: PM10-P4 with flow intensities of 29 and $27 \mu\text{g m}^{-2}\text{s}^{-1}$ during the winter and spring, and PM10-P5 with flow intensities of 67 and $71 \mu\text{g m}^{-2}\text{s}^{-1}$ during the winter and autumn, respectively.

The events of the flow patterns PM10-P1 and PM10-P2 occurred throughout the year with the highest frequencies of occurrence (44% and 22%, on an annual average). The flow intensity of the PM10-P1 (a nocturnal pattern) was too small all year, but the flow intensity of the PM10-P2 (a diurnal pattern) was similar to those of the other flow patterns. The patterns PM10-P1 and PM10-P3 reflect the influence of the downslope winds driven by the mountain-valley system. These patterns, furthermore, reflect the effect of the urban heat island, which is revealed in the hourly population by the small peak around the hour 15 (daylight winds converging to the downtown).

For all the PM₁₀ flow patterns, the average surface distributions of the pollutant reveal the NE quadrant as the zone of the city with the highest PM₁₀ concentrations, and the SW quadrant as the zone with the lowest levels of PM₁₀. It suggests that, at the NE of the town, in the surrounding area of Xalostoc on the east side of the Sierra de Guadalupe, there exists considerable sources of particulate matter, which release PM₁₀ to the atmosphere all year long.

It is interesting to observe that the events of the pattern PM10-P5 revealed flow vectors at the NE and SE quadrants with intense southerly components, which produced, on average, the highest mean spatial concentration of PM₁₀ ($81 \mu\text{g m}^{-3}$) in the city. This result displays the east side quadrants of the city as the most polluted areas by PM₁₀ during the winter and autumn.

3.2.4. The SO₂ Flow Patterns

Table 7 and Figure 12 enumerate and sketch out the SO₂ flow patterns that we identified. Table 7 presents the average seasonal and annual occurrence frequencies and flow intensities of these patterns,

including their relationship with the wind circulation patterns. Figure 12 shows the hourly population of the patterns, the corresponding flow vectors, and the surface distribution of the SO₂ emissions produced by the events of these flow patterns.

Table 7. Frequencies (%) and flows (µg/m²s) of the Mexico City SO₂ flow patterns (2001–2010).

Pattern	Wind Pattern Inherited	JAN–MAR (Winter)		APR–JUN (Spring)		JUL–SEP (Summer)		OCT–DEC (Autumn)		ANNUAL	
		Freq	Flow	Freq	Flow	Freq	Flow	Freq	Flow	Freq	Flow
SO2-P1	WIND-P1	24.49	8.36	40.11	3.98	29.48	4.21	36.64	3.76	32.71	5.08
SO2-P2	WIND-P2	17.08	17.38	15.38	8.84	24.86	6.85	19.09	8.98	19.13	10.51
SO2-P3	WIND-P6	12.92	20.64	12.23	12.22	0.00	0.00	11.75	24.80	9.19	14.41
SO2-P4	WIND-P6	6.39	32.30	0.00	0.00	5.39	21.32	7.17	19.54	4.74	18.29
SO2-P5	WIND-P5	3.80	47.19	0.00	0.00	0.00	0.00	4.40	44.40	2.04	22.90
SO2-P6	WIND-P4	35.32	1.19	0.00	0.00	0.00	0.00	0.00	0.00	8.71	0.30
SO2-P7	WIND-P3	0.00	0.00	17.08	17.24	16.30	15.11	20.95	16.85	13.65	12.30
SO2-P8	WIND-P3	0.00	0.00	4.58	34.87	1.81	30.81	0.00	0.00	1.60	16.42
SO2-P9	WIND-P6	0.00	0.00	10.62	14.65	22.15	10.08	0.00	0.00	8.23	6.18

We observed, in general, that all the SO₂ flow patterns presented small flow intensities and produced small surface concentrations (we underline that the Mexican air quality standard for SO₂ is 110 ppb on a 24 h average, and 25 ppb on an annual average). Nevertheless, it is particularly interesting to observe that the flow patterns SO2-P3 (winter, spring, and autumn), SO2-P4 (winter, summer, and autumn), SO2-P5 (winter and autumn), and SO2-P9 (spring and summer), which were detected mainly during the night hours, exhibit the flow vector at the NW quadrant with a flow intensity relatively larger than in the other quadrants. However, the corresponding wind patterns show winds of similar magnitudes in all the quadrants.

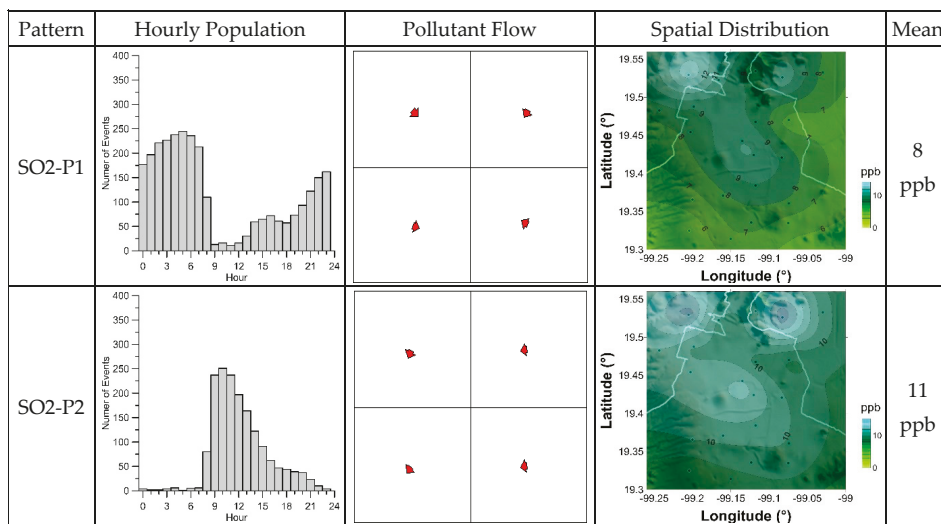


Figure 12. Cont.

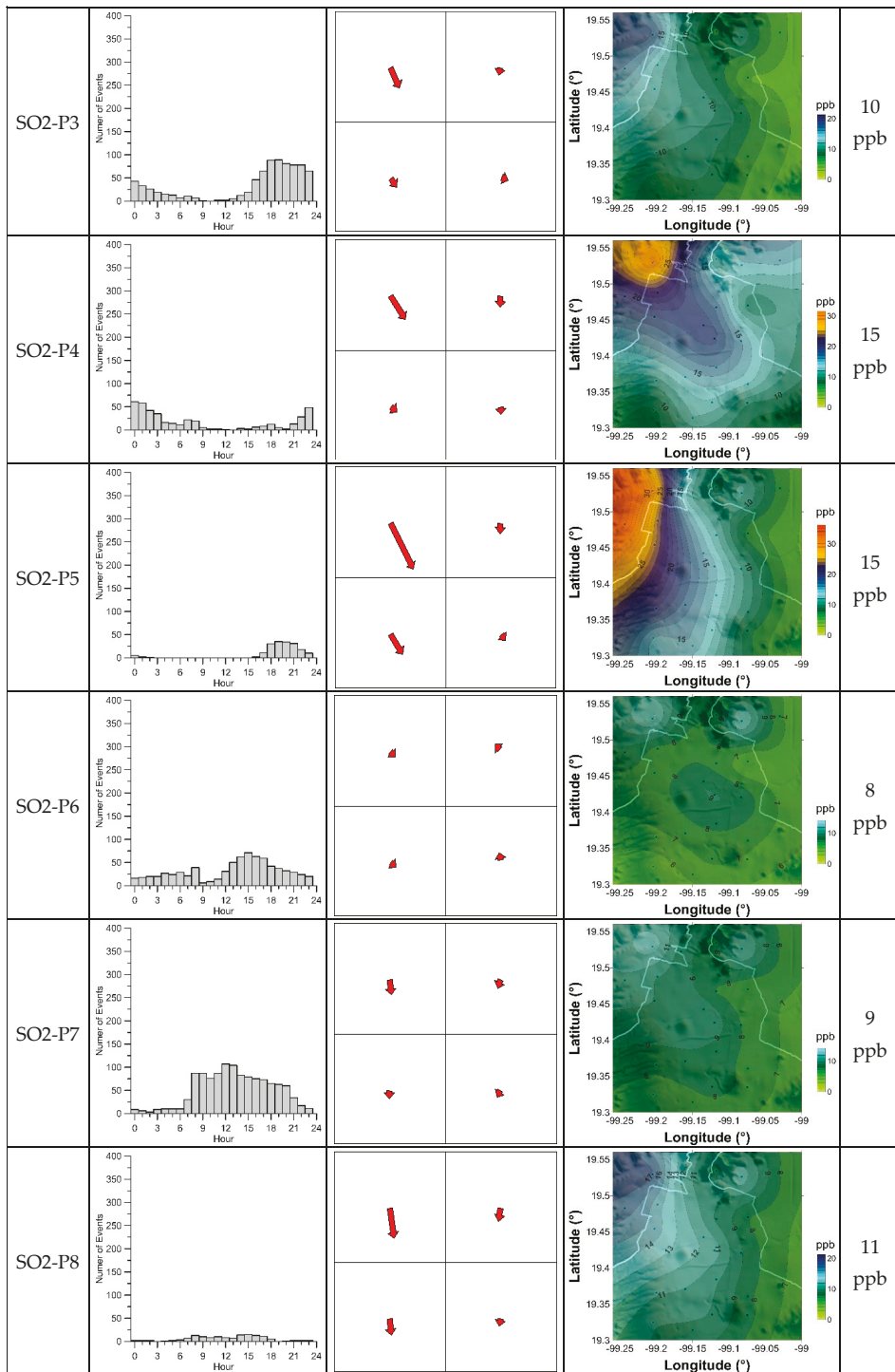


Figure 12. Cont.

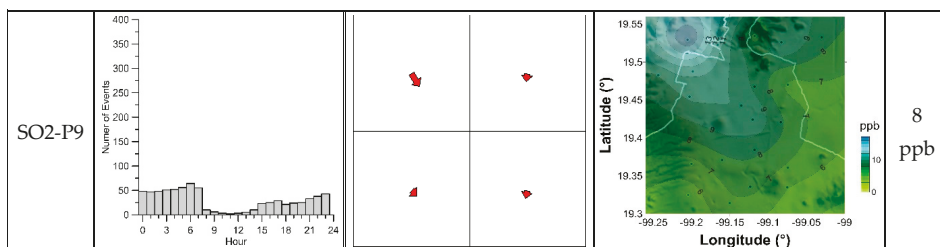


Figure 12. Flow patterns of sulfur dioxide in the Mexico City region during the period 2001–2010. For each flow pattern, the figures show the hourly population (second column), the mean flow vectors (relative to the pattern) at the city quadrants (third column), the surface concentration distributions (fourth column) averaged over the events of the flow pattern, and the mean spatial concentration (last column). The size of red arrows that stand in for the SO_2 flow vectors indicates the flow intensity in a scale relative to the edge size of the squares that represent the quadrants.

The events of the flow patterns SO_2 -P7 (spring, summer, and autumn) and SO_2 -P8 (spring and summer) occurred during daylight hours and show the NW-quadrant flow vector larger than in the other quadrants. Consistently with these observations, the mean spatial SO_2 surface distributions reveal the NW quadrant of the city as the zone with the highest levels of concentration, particularly in the case of the patterns SO_2 -P4 and SO_2 -P5. This situation seems to indicate that in the NW quadrant of the city, there are intense activities that release sulfur dioxide to the atmosphere during the night.

The SO_2 -P1 and SO_2 -P2 flow patterns, as was the case with the other pollutants, were the most frequent patterns (33% and 19%, respectively, on annual average) and the only ones detected all over the year; however, their flow intensities were tiny.

4. Conclusions

We used a simple model to define the pollutant-flow conditions in terms of the horizontal components of the flow vector and its gradients (divergence and curl). We applied this model to the hourly data of wind and pollutant concentration measured during the period 2001–2010 by the atmospheric monitoring network of Mexico City. We obtained the main flow patterns of NO_2 , O_3 , PM_{10} , and SO_2 using a 4-cell model of the city and the k-means algorithm of cluster analysis. Estimations of the seasonal and annual occurrence frequencies and flow intensities of the flow patterns were obtained.

The pollution flow patterns reflect some of the wind circulation conditions of the Mexico City wind patterns; however, since the pollutant-flow conditions also depend on the pollutant concentration, the flow patterns revealed situations of pollutant transport that cannot be inferred simply from the wind circulation modes. Different pollutants under the same wind patterns produced different pollutant-flow patterns. For example, the SO_2 flow patterns (SO_2 -P3, SO_2 -P4, and SO_2 -P5) display large flow intensities at the NW quadrant bringing this pollutant towards the Mexico City region, mainly during winter and autumn seasons; however, the corresponding wind patterns exhibit wind velocities with similar magnitudes in almost all the quadrants. The events of the flow patterns SO_2 -P8 occurred with similar conditions, but during the spring and summer periods. Similarly, the PM_{10} -P4 and PM_{10} -P5, and PM_{10} -P6 and PM_{10} -P7 flow patterns revealed large flow intensities in the NE quadrant, although winds have similar magnitudes in other quadrants.

The pollutant-flow patterns of NO_2 , O_3 , PM_{10} , and SO_2 represent the main scenarios of the pollutant transport in the Mexico City region. They provide information that can guide, enrich, and enlighten the results of Mexico City air quality studies based on modeling techniques.

Author Contributions: Conceptualization, A.S.; Formal analysis, A.S.; Investigation, S.C.-S. and A.-T.C.-M.; Methodology, A.S., S.C.-S. and A.-T.C.-M.; Software, A.S. and S.C.-S.; Supervision, A.S.; Writing—original draft, A.S., S.C.-S. and A.-T.C.-M.; Writing—review & editing, A.S. and A.-T.C.-M.

Funding: This research received no external funding.

Acknowledgments: We thank Ana Laura Colín Aguilar (Instituto Nacional de Electricidad y Energías Limpias) for beneficial comments to make the paper more comprehensible.

Conflicts of Interest: The authors declare no conflict of interest.

References

1. Pascal, M.; Corso, M.; Chanel, O.; Declercq, C.; Badaloni, C.; Cesaroni, G.; Henschel, S.; Meister, K.; Haluza, D.; Martin-Olmedo, P.; et al. Assessing the public health impacts of urban air pollution in 25 European cities: Results of the Aphekom project. *Sci. Total Environ.* **2013**, *449*, 390–400. [[CrossRef](#)] [[PubMed](#)]
2. Sicard, P.; Lesne, O.; Alexandre, N.; Mangin, A.; Collomp, R. Air quality trends and potential health effects—Development of an aggregate risk index. *Atmos. Environ.* **2011**, *45*, 1145–1153. [[CrossRef](#)]
3. Secretaría del Medio Ambiente. *Gobierno del Distrito Federal. Inventario de Emisiones de Contaminantes Criterio de la Zona Metropolitana del Valle de México*, 1st ed.; Secretaría del Medio Ambiente del DF: Mexico City, Mexico, 2008.
4. Bravo, H.A.; Torres, R.J. Air Pollution Levels and Trends in the Mexico City Metropolitan Area. In *Urban Air Pollution and Forests: Resources at Risk in the Mexico City Air Basin*; Springer: New York, NY, USA, 2002; pp. 121–159.
5. Bonner, J.C.; Rice, A.B.; Lindroos, P.M.; O'Brien, P.O.; Dreher, K.L.; Rosas, I.; Alfaro-Moreno, E.; Osornio-Vargas, A.R. Induction of the lung myofibroblast PDGF receptor system by urban ambient particles from Mexico City. *Am. J. Respir. Cell. Mol. Biol.* **1998**, *19*, 672–680. [[CrossRef](#)]
6. Osornio-Vargas, A.R.; Bonner, J.C.; Alfaro-Moreno, E.; Martinez, L.; Garcia-Cuellar, C.; Ponce-de-Leon-Rosales, S.; Miranda, J.; Rosas, I. Proinflammatory and cytotoxic effects of Mexico City air pollution particulate matter in vitro are dependent on particle size and composition. *Environ. Health Perspect.* **2003**, *111*, 1289–1293. [[CrossRef](#)]
7. Jáuregui, E. Local wind and air pollution interaction in the Mexico basin. *Atmósfera* **1988**, *1*, 131–140.
8. De Foy, B.; Caetano, E.; Magaña, V.; Zitácuaro, A.; Cárdenas, B.; Retama, A.; Ramos, R.; Molina, L.T.; Molina, M.J. Mexico City basin wind circulation during the MCMA-2003 field campaign. *Atmos. Chem. Phys.* **2005**, *5*, 2267–2288. [[CrossRef](#)]
9. Oke, T.R.; Zeuner, G.; Jauregui, E. The Surface Energy Balance in Mexico City. *Atmos. Environ. Part B Urban Atmos.* **1992**, *26*, 433–444. [[CrossRef](#)]
10. Jauregui, E.; Luyando, E. Global radiation attenuation by air pollution and its effects on the thermal climate in Mexico City. *Int. J. Clim.* **1999**, *19*, 683–694. [[CrossRef](#)]
11. Salcido, A.; Celada, A.T.; Villegas, R.; Salas, H.; Sozzi, R.; Georgiadis, T. A micrometeorological database for the Mexico City Metropolitan Area. *Nuovo Cim. C Geophys. Space Phys. C* **2003**, *26*, 317–355.
12. Castro, T.; Salcido, A. Influencia de la contaminación atmosférica de la Zona Metropolitana de la Ciudad de México en tres sitios perimetrales. In *Contaminación Atmosférica V*; El Colegio Nacional: Mexico City, Mexico, 2006.
13. Molina, L.T.; Madronich, S.; Gaffney, J.S.; Apel, E.; de Foy, B.; Fast, J.; Ferrare, R.; Herndon, S.; Jimenez, J.L.; Lamb, B.; et al. An overview of the MILAGRO 2006 Campaign: Mexico City emissions and their transport and transformation. *Atmos. Chem. Phys.* **2010**, *10*, 8697–8760. [[CrossRef](#)]
14. Bossert, J.E. An Investigation of Flow Regimes Affecting the Mexico City Region. *J. Appl. Meteorol.* **1997**, *36*, 119–140. [[CrossRef](#)]
15. Fast, J.D.; Zhong, S. Meteorological factors associated with inhomogeneous ozone concentrations within the Mexico City basin. *J. Geophys. Res.* **1998**, *103*, 18927–18946. [[CrossRef](#)]
16. Doran, J.C.; Abbott, S.; Archuleta, J.; Bian, X.; Chow, J.; Coulter, R.L.; de Wekker, S.F.J.; Edgerton, S.; Elliott, S.; Fernandez, A.; et al. The IMADA-AVER Boundary Layer Experiment in the Mexico City Area. *Bull. Am. Meteorol. Soc.* **1998**, *79*, 2497–2508. [[CrossRef](#)]
17. Mora, M.; Braun, R.A.; Shingler, T.; Soroshian, A. Analysis of remotely sensed and surface data of aerosols and meteorology for the Mexico Megalopolis Area between 2003 and 2015. *J. Geophys. Res. Atmos. JGR* **2017**, *122*, 8705–8723. [[CrossRef](#)] [[PubMed](#)]

18. Fast, J.D.; de Foy, B.; Acevedo Rosas, F.; Caetano, E.; Carmichael, G.; Emmons, L.; McKenna, D.; Mena, M.; Skamarock, W.; Tie, X.; et al. A meteorological overview of the MILAGRO field campaigns. *Atmos. Chem. Phys.* **2007**, *7*, 2233–2257. [[CrossRef](#)]
19. Salcido, A.; Celada-Murillo, A.T.; Castro, T. A meso- β Scale Description of Surface Wind Events in Mexico City during the MILAGRO 2006 Campaign. In Proceedings of the IASTED Technology Conferences, Environmental Management and Engineering (EME), Banff, AB, Canada, 15–17 July 2010; Alhaji, R.S., Leung, V.C.M., Petela, R., Saif, M., Thring, R., Eds.; Acta Press: Calgary, AB, Canada, 2010. Track 699-041. [[CrossRef](#)]
20. Celada-Murillo, A.; Carreón-Sierra, S.; Salcido, A.; Castro, T.; Peralta, O.; Georgiadis, T. Main Characteristics of Mexico City Local Wind Events during the MILAGRO 2006 Campaign within a Meso- β Scale Lattice Wind Modeling Approach. *ISRN Meteorol.* **2013**, *2013*, 605210. [[CrossRef](#)]
21. Salcido, A.; Carreón-Sierra, S.; Celada-Murillo, A.T. A Brief Clustering Analysis of the Mexico City Local Wind States Occurred During the MILAGRO Campaign. In Proceedings of the IASTED International Conference on Environmental Management and Engineering (EME), Banff, AB, Canada, 16–17 July 2014. [[CrossRef](#)]
22. Klaus, D.; Poth, A.; Voss, M.; Jauregui, E. Ozone distributions in Mexico City using principal component analysis and its relation to meteorological parameters. *Atmósfera* **2001**, *14*, 171–188.
23. De Foy, B.; Fast, J.D.; Paech, S.J.; Phillips, D.; Walters, J.T.; Coulter, R.L.; Martin, T.J.; Pekour, M.S.; Shaw, W.J.; Kastendeuch, P.P.; et al. Basin-scale wind transport during the MILAGRO field campaign and comparison to climatology using cluster analysis. *Atmos. Chem. Phys.* **2008**, *8*, 1209–1224. [[CrossRef](#)]
24. Salcido, A.; Carreón-Sierra, S.; Georgiadis, T.; Celada-Murillo, A.T.; Castro, T. Lattice Wind Description and Characterization of Mexico City Local Wind Events. Period 2001–2006. *Climate* **2015**, *3*, 542–562. [[CrossRef](#)]
25. Carreón-Sierra, S.; Salcido, A.; Castro, T.; Celada-Murillo, A.T. Cluster Analysis of the Wind Events and Seasonal Wind Circulation Patterns in the Mexico City Region. *Atmosphere* **2015**, *6*, 1006–1031. [[CrossRef](#)]
26. Mexico City Air Quality Monitoring Network (Sistema de Monitoreo Atmosférico de la Ciudad de México). Available online: <http://www.aire.cdmx.gob.mx/default.php> (accessed on 23 July 2019).
27. Everitt, B.S.; Landau, S.; Leese, M. *Cluster Analysis*, 4th ed.; Arnold: London, UK, 2001; ISBN 9780340761199.
28. Hartigan, J.A.; Wong, M.A. Algorithm AS 136: A K-Means Clustering Algorithm. *Appl. Stat.* **1979**, *28*, 100–108. [[CrossRef](#)]
29. James, G.; Witten, D.; Hastie, T.; Tibshirani, R. *An Introduction to Statistical Learning with Applications in R*; Springer: New York, NY, USA; Heidelberg, Germany; Dordrecht, The Netherlands; London, UK, 2013; Corrected at Eighth Printing 2017. [[CrossRef](#)]
30. Shaefer, J.T.; Doswell, C.A. On the interpolation of a vector field. *Mon. Weather Rev.* **1979**, *107*, 458–476. [[CrossRef](#)]
31. Salcido, A. A Phenomenological Gradient Approach to Generalized Constitutive Equations for Isotropic Fluids. *J. Appl. Math. Phys.* **2018**, *6*, 1494–1506. [[CrossRef](#)]
32. Lohninger, H. *DataLab 3.911*; Epina GmbH: Gütersloh, Germany, 2019.
33. Klaus, D.; Jauregui, E.; Poth, A.; Stein, G.; Voss, M. Regular circulation structures in the tropical basin of Mexico City as a consequence of the urban heat island effect. *Erdkunde* **1999**, *53*, 231–243. [[CrossRef](#)]
34. Krishnamurti, T.N. The Subtropical Jet Stream of Winter. *J. Meteorol.* **1960**, *18*, 172–191. [[CrossRef](#)]
35. Doran, J.C.; Zhong, S. Thermally Driven Gap Winds into the Mexico City Basin. *J. Appl. Meteorol.* **2000**, *39*, 1330–1340. [[CrossRef](#)]



Article

The Role of Green Infrastructures in Urban Planning for Climate Change Adaptation

Luisa Sturiale ^{1,*} and Alessandro Scuderi ²

¹ Department of Civil Engineering and Architecture, University of Catania, 95100 Catania, Italy

² Department of Agricultural, Food and Environment, University of Catania, 95100 Catania, Italy; scuderia@unict.it

* Correspondence: luisa.sturiale@unict.it

Received: 31 July 2019; Accepted: 28 September 2019; Published: 4 October 2019

Abstract: The population that lives in cities has surpassed the one that lives in the countryside. Cities are recognized as a priority source of pollution. The degradation of air quality and the phenomenon of Urban Heat Island (UHI) are some of the most well-known consequences of urban development. The adaptation of the cities is emerging as one of the greatest challenges that urban planners will face in this century. Urban Green Infrastructures (GIs) could help cities adapt to climate change, and the strategy of expansion of greening in urban planning could play an important role in enhancing the sustainability and resilience of cities and communities. Many studies have shown the benefits of GIs to climate change mitigation and adaptation in urban areas and their role as an important urban planning tool to satisfy environmental, social, and economic needs of urban areas. The objective of this article is to propose a methodological approach to evaluate the social perception of citizens regarding urban green areas. The proposed methodology, applied to the reality of the “urban green system” of Catania, is based on an integrated approach between participatory planning and the methods social multi criteria evaluation to guiding the city’s government to realize a new urban resilient development.

Keywords: urban green system; ecosystem services; climate change benefits; resilient city; urban resilient development; green urban planning

1. Introduction

The actions against climate change and its effects on society and the environment are oriented in two directions: Mitigation, to progressively reduce the emissions of climate-changing gases responsible for global warming, and adaptation, to reduce the vulnerability of environmental, social, and economic systems and to increase their capacity for climate resilience. “Many adaptation and mitigation options can help address climate change, but no single option is sufficient by itself. Effective implementation depends on policies and cooperation at all scales and can be enhanced through integrated responses that link mitigation and adaptation with other societal objectives” [1].

The evaluation of the integrated effects of planning and planning choices aimed at reducing climate-changing emissions is a priority theme in the document “Transforming our world: The 2030 Agenda for Sustainable Development [2]”. The 2030 agenda establishes 17 sustainable development goals (SDGs) and 169 targets to be achieved within the next 15 years. Goal 11, sustainable cities and communities, is specifically dedicated to urban systems, and its ambitious goal is to “make cities and human settlements inclusive, safe, resilient, and sustainable.”

The percentage of people living in urban areas will increase from 50.0% in 2010 to nearly 70.0% by 2150 [3]. For the first time in history, the population that lives in cities has surpassed the one that lives in the countryside or outside the inhabited centers. The cities are recognized as the priority source of pollution. Most energy consumption is connected to cities, which have to make the greatest

efforts to manage sustainable resources under the social, environmental, and economic aspects and to improve the quality of life of their citizens. Heat waves in cities generate serious inconveniences for the most vulnerable citizens, especially the elderly and children. Urban socio-ecological systems are characterized by a high population density, an extensive change in land use, and the use of natural resources not directly present locally. In Europe, urbanization processes are progressing rapidly, causing soil sealing and the reduction of its functions and quality. One of the major consequences of urbanization, in terms of the impact on human health and environmental quality, is the "urban heat island" (UHI) effect (the phenomenon whereby cities appear to be warmer than the surrounding rural area). It is estimated that climate change will greatly aggravate the extent of the UHI, particularly in hot regions characterized by periods of summer dryness such as the Mediterranean Basin.

Protecting, upgrading, and increasing urban and peri-urban forests and street trees through the enhancement of the green infrastructures (GIs), is therefore fundamental for the sustainable development of urban areas that represent "demand areas for Ecosystem Services, "the goods and services provided to man by nature.

The maintenance of urban green spaces is also one of the approaches suggested by the IPCC (2014) [1]. For the management of climate change risk through adaptation, in particular through the reduction of vulnerability and exposure through development, planning and practices that include "low-regret" measures, i.e. those that produce benefits even in the absence of climate change and with which the adaptation costs are relatively low compared to the benefits of the action. Lastly, the maintenance of urban green spaces is one of the approaches suggested by SDGs 11 (Sustainable Cities and Communities) of the UN Agenda to 2030 [2].

In recent thinking, the GIs have been identified as 'best practices' in local governance when combined with traditional "grey" infrastructure to achieve greater urban sustainability and resilience. Moreover, GIs are recognized for their value for adapting to the emerging and irreversible impacts of climate change. In addition, some local governments have adopted GIs as a climate change adaptation measure, particularly if the strategies result in multiple other benefits. Indeed, adaptation to climate change is also seen as having ecological, economic, and social dimensions [3].

For three out of four European citizens, climate change is a very serious problem. The changes observed in the climate are already having far-reaching repercussions on ecosystems, economic sectors, human health, and welfare in Europe. Overall, the economic losses recorded in Europe in the period 1980–2016 caused by meteorological phenomena and other extreme climate-related events exceeded Euro 436 billion. The biggest losses would be in the industrial, transport, and energy sectors (CE, COM (2018), 738 final).

The cities will have an important role to adopt the law and the provisions that are necessary at the various levels but also to ensure the best quality of life in urban areas. Climate impact requires the use of innovative solutions and the rethinking of urban management and planning [4].

New urban and territorial structures, low energy consumption buildings and infrastructures, green areas and the adoption of advanced technologies mitigate global emissions and local pollution, promote adaptation to climate change, reduce the energy costs of families and businesses, and improve the climate of cities.

GIs and their integration in urban planning appear as one of the most appropriate and effective ways to improve the microclimate and face the impacts of climate change and mainly the UHI effect. GIs forms include green roofs, green walls, urban forest, bioswales, rain gardens, urban agriculture (urban gardens; community gardening; collective green; peri-urban agriculture, agricultural parks), river parks, local products markets, areas of constructed wetlands, alternative energy farms, and nature conservation areas, among the most common (Figure 1).

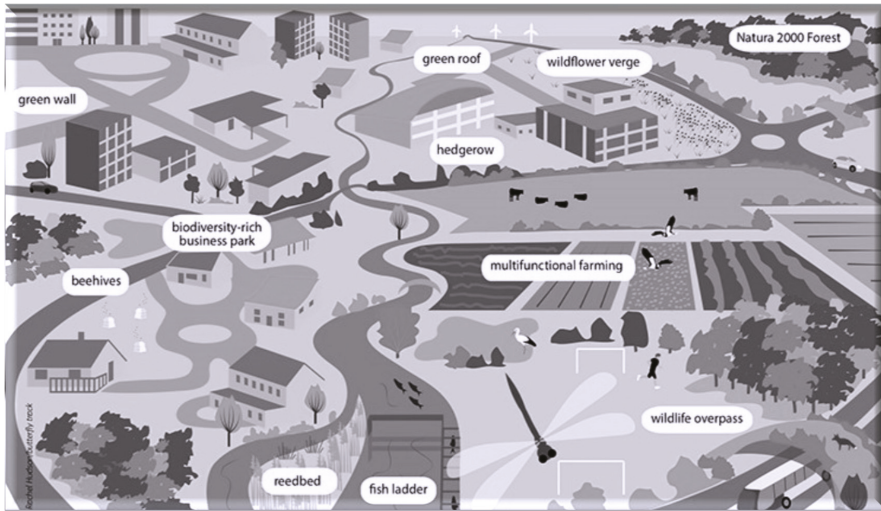


Figure 1. The different forms of Green Infrastructures (adapted from EU 2016) [5].

GIs provide a range of climate change services that can make both a substantial contribution towards adapting to climate change and a limited yet important contribution towards mitigating climate change. Such natural interventions are increasingly being recognized as a desirable ‘win-win’ approach to combating climate change, as they also help to deliver multiple other social, economic, and environmental benefits.

Green Infrastructures, according to the European Union (E.U.) definition, "... are networks of natural and semi-natural areas planned at strategic level with other environmental elements, designed and managed in such a way as to provide a wide spectrum of ecosystem services. This includes green (or blue, in the case of aquatic ecosystems) and other physical elements in areas on land (including coastal areas) and marine areas. On the mainland, green infrastructures are present in a rural and urban context" [6].

In the EU, the term GIs was first introduced in the 2009 commission white paper, "Adapting to Climate Change" [7]. In all the normative acts of the EU, the term "Green Infrastructures" is used in connection with landscape resources, with particular emphasis on ecological connectivity. In contrast, the European Environment Agency (EEA) and other European programs choose to use the term "green spaces," "green systems," or "green structure" when referring to the urban environment or other related issues [8,9].

The objectives of the EU GIs Strategy (2013) [6] are:

- To enhance, conserve, and restore biodiversity by inter alia increasing of spatial and functional connectivity between natural and semi-natural areas and improving landscape permeability and mitigating fragmentation.
- To maintain, strengthen, and, where adequate, to restore the good functioning of ecosystems in order to ensure the delivery of multiple ecosystem and cultural services.
- To acknowledge the economic value of ecosystem services and to increase the value itself, by strengthening their functionality.
- To enhance the social and cultural link with nature and biodiversity, to acknowledge and increase the economic value of ecosystem services and to create incentives for local stakeholders and communities to deliver them.
- To minimize urban sprawl and its negative effects on biodiversity, ecosystem services, and human living conditions.

- To mitigate and adapt to climate change, to increase resilience, and reduce vulnerability to natural disaster risks such as floods, water scarcity and droughts, coastal erosion, forest fires, mudslides, and avalanches as well as urban heat islands.
- To make the best use of limited land resources in Europe.
- To contribute to a healthy living, better places to live, provisioning open spaces and recreation opportunities, increasing urban-rural connections, contributing to sustainable transport systems, and strengthening the sense of community [10].

Many studies show the existence of important links between urban green and impacts on climatic conditions and the reduction of the heat island effects. Parks and trees offer shaded areas and help to cool the air, and they protect from solar radiation. The green surfaces also have a heat absorption effect and lower thermal inertia than when compared to concrete or asphalt surfaces. The integration of vegetation in the facades and on the roofs of buildings helps to balance the interior temperatures.

This article proposes a brief overview of the GIs and their benefits and their role as an important urban planning tool to satisfy different environmental, social, and economic needs of urban areas and to realize a resilient urban development. Urban resilience aims to increase the ability of the whole urban system (including physical, environmental, and socio-economic perspectives) to develop its adaptive capacity, to resist and recover from shocks and stresses, and, at the same time, to reduce its vulnerability. In this context, it becomes interesting to investigate the relationship between GIs and climate comfort within cities and the role of the urban green spaces as an essential component of the policies of mitigation and adaptation to climate change in the planning process. This is followed by the evaluation of green planning policies and adaptation measures in the city of Catania, to acquire useful information in order to guide the city government towards resilient urban planning. The methodology proposed and applied to the green areas of Catania and the planning of investments in GIs, is based on an integrated approach between participatory planning techniques (based on the establishment of focus groups with the various stakeholders) and the NAIADe method (Novel Approach to Imprecise Assessment and Decision Environments) [11] (for the Multi-Critical Social Assessment—SMCE) for the "complex" information collected (quantitative and qualitative data).

2. The Green Infrastructures as Tools for Climate Adaptation of Cities: Experiences and Evaluations

The relationship between city and climate change is now documented internationally by various studies, which highlight the negative effects on the well-being of the population and environmental ecosystems. The phenomena of pollution, heat islands and urban decay are now known, to name a few [12–14]. The E.U. has given a strong impetus to the fight against climate change and environmental protection. To this end, among various measures, it has promoted the European Strategy for Adaptation to Climate Change (2013) [15]. That has the objective of making Europe more resilient to climate change, promoting two types of interventions: Mitigation and adaptation.

The definition of the urban adaptation strategies actively involves citizens and other interested stakeholders to favor "non-regret" interventions that can remedy existing problems and bring immediate benefits and socio-economic benefits to increase adaptive capacity and actions based on an ecosystemic or "green" approach [4]. These actions envisaged are aimed to promote experimental interventions of climatic adaptation of public spaces and encourage the diffusion of different forms of GIs and the increase of public and private urban green areas, adopting the logic of green and blue infrastructures, and safeguarding biodiversity in urban areas.

Climate change requires the use of innovative solutions and new tools for urban management and planning. New urban structures, low energy consumption buildings and infrastructures, green areas, and the adoption of advanced technologies mitigate global emissions and local pollution, which promote adaptation to climate change. In the new vision of a city, sustainable and resilient, the green areas assume ever greater importance and become multifunctional resources for the city and its inhabitants.

The connotation of GIs includes the green space of the complex urban ecosystem, composed of various forms of non-built spaces, including gardens, parks, vertical plants, forestry, urban gardens, agricultural land, greenways, wetlands, and waterways (green and blue infrastructures) [16–18].

The green spaces in urban areas provide indirect and direct benefits to human health and well-being, which are defined as Ecosystem Services (ESs). The ESs “... consist of the flows of matter, energy, and information coming from the stocks of natural capital, which are combined with the services of anthropogenic artifacts to generate well-being and quality of life ...” [19]; they perform the following functions: Environmental-regulator; hydrogeological protection; social, recreational and therapeutic; cultural and educational; aesthetic–architectural.

In particular, the ESs help adapt cities for climate change, through the air purification, global climate regulation, urban temperature regulation, noise reduction, and runoff mitigation. Several studies show the existence of important links between urban greening and impacts on climatic conditions: Parks and trees offer shaded areas and help to cool the air, they are places to find relief during heat waves, they offer plant cover, and they protect from solar radiation; the integration of vegetation in the facades and on the roofs of buildings helps to balance the interior temperatures as well as protect the structures [20–24].

The implementation of GIs promote an integrated approach to land management, determine the positive effects under the aspect: Economic, in the containment of some of the damages resulting from hydrogeological instability; environmental, in the fight against climate change and in restoring the quality of environmental matrices (air, water, soil); in promoting the well-being of citizens and their social relations and promoting social inclusion [4].

The benefits of the GIs are:

- *Health and well-being*: Increasing life expectancy and reducing health inequality; improving levels of physical activity and health; improving psychological health and mental well-being.
- *Climate change*: Heat amelioration; reducing flood risk; improving water quality; sustainable urban drainage; sustainable transport; improving air quality.
- *Land regeneration*: Regeneration of previously developed land; improving quality of the place; increasing environmental quality and aesthetics.
- *Wildlife and habitats*: Increasing habitat area; increasing populations of some protected species; increasing species movement.
- *Economic growth and investments*: Inward investments and job creation, land and property values; local economic regeneration.
- *Stronger communities*: Social interaction, inclusion, and cohesion; community engagement; education and participation; a sense of place; experiencing nature [4].

Worldwide, GIs have been spreading for at least a decade for their social and environmental benefits and as a tool for fighting climate change in urban areas. It is not possible to report the multiple experiences of projects already completed and underway, but some interesting examples will be recalled here.

In the USA, several cities have planned the development of specific GIs plans (New York, Chicago, Washington D.C.) or have foreseen their presence in the climate protection action plans (San Diego); the Greenworks Philadelphia aims to turn Philadelphia into “the greenest city in America” and includes an extensive list of GIs measures (Figure 2) [25,26].



Figure 2. Green waterstorm infrastructure in Philadelphia (USA).

From northern Europe to the Mediterranean area, climate adaptation plans and experimental projects have been adopted or are being drafted for the creation of sustainable eco-neighborhoods and various GIs, in urban areas and also around cities, playing an important role in regulating urban sprawl, regulating urbanization, and the growing senseless land consumption.

Just to name a few, this is the case of the British Green Belts (in urban planning in the UK), the Anella Verda of Barcelona, which includes a network of 12 protected areas around the city connected by increasingly enhanced ecological corridors; the vertical forest in Milan (Figure 3); the Green Belt in Turin; the green ring of the municipality of Mirandola (Modena); urban gardens in Catania [27]. Other projects and studies related to the progressive insertion of the different forms of GIs in the green planning of cities are found from Europe to Asia: In Copenhagen [28], Berlin [29] (Figure 4), Hong Kong [30], Beijing [31], and the Pukou District in Nanjing [32].



Figure 3. Vertical forest in Milan (Italy).



Figure 4. Germany's green roofs.

There is a large literature of specific researches that explore the important role that the GIs in urban areas play in adapting for climate change and as low-cost mitigation strategies [33–35]. Other researches place particular attention on models for evaluating ESs offered by urban GIs [4,27,31,36].

GIs practices such as trees, shrubs, lawns, green roofs, and green walls have been proven efficient in reducing the urban sprawl, the UHI, the harmful air pollutants, and regulating the Green House Gas (GHG) emissions within the cities [36–39].

Based on the urban specificities, on the socio-economic and environmental aspects of the cities considered and on the types of GIs studied, the methodological approaches found in the literature are different. It is possible to identify the application of the i-Tree eco model to present output from energy exchange and hydrological models showing surface temperature and surface runoff in relation to the green infrastructure under current and future climate scenarios (in greater Manchester [40]), or to quantify in biophysical and monetary terms the ecosystem services air purification, global climate regulation, and the ecosystem disservice air pollution associated with biogenic emissions (in Barcelona [36]). Several researches have used integrated approaches recognizing the multi-functionality of GIs, highlighting both the economic aspects and social and environmental aspects (in Nanjing China, morphological spatial pattern analysis MSPA method [29]; in Catania Italy, the *eco-social-green* model using Social Multi Criteria Evaluation SMCE [4]) and for planning and managing urban green infrastructure for urban sustainability and resilient cities [41,42].

Municipalities are called to respond to climate problems with new governance tools to distribute the risk of impacts, which aims to involve citizens to a greater extent in the project proposals for interventions and measures. Indeed, it is important for urban governance to assess the social perception of investments in GI and to estimate the benefits of related ecosystem services. The interactions between stakeholders involved in urban projects have proved useful in different experiences but haven't yet been widely applied to climate change adaptation actions in cities [4].

The good functionality and the correct use of the public green areas require the support of multi-criteria evaluation tools and specific government tools, able to guide the administrators in the choices of planning of the green investments and management as well as to provide citizens with elements of knowledge and respect towards this important common good [43,44]. The success of a particular public green space is not solely in the hands of the architect, urban designer or townplanner; it also relies on people adopting, using, and managing the space. People make places, more than places make people [45,46].

The implementation of GIs promotes an integrated approach to land management, determines positive effects under the economic, social, and environmental aspects. The GIs become an important tool of action for climate adaptation, for the enhancement of ESs and biodiversity, and social cohesion in the model of a sustainable and resilient city of the future.

3. The Perception of the GIs in Urban Green Planning: The Case Study of Catania

In Italy, the GIs are still few, limited to individual local initiatives and in any case, are not included in system logic, which essential for achieving the objectives. The attention to the presence of green in urban areas, in its various forms and functions, has been growing in recent years, so much so that even at the regulatory level several laws have been promulgated on the subject. Among them, the Law on the 14 January 2013, n. 10 rules for the development of urban green spaces, in which the functions of urban green are recognized:

- *Ecosystem services*: Positive effects on the local climate, on air quality, on noise levels, and soil stability are evident, biodiversity conservation
- *Socio-economic aspects*: Meet the needs for recreation, social relations, cultural and healthy growth of its inhabitants.

Despite the multiple benefits associated with green, the Italian situation still shows some critical issues. Urban green is mainly managed on a technical and prescriptive level rather than as a strategic resource to orient local development policies to quality and resilience [4].

The city of Catania is the second city, in terms of importance, surfaces, and inhabitants of the Sicily Region (180,000 square meters, about 350,000 inhabitants, a density of 1.7 inhabitants per square meter). Under the urbanistic aspect, the regulatory plan, drawn up in 1964, was designed for the socio-economic needs of the city of the 60s, where the priorities and the vision were completely different from the current ones, mainly in terms of environmental protection, attention to climate change, and social inclusion. Concerning the socio-economic development of Catania, for the future potential of the urban green areas, the municipal administration has planned a program of interventions in line with climate adaptation measures [47–49]. The known negative impacts of climate change are also recorded in Catania, and some indicators are shown in the following figures (Figures 5 and 6)

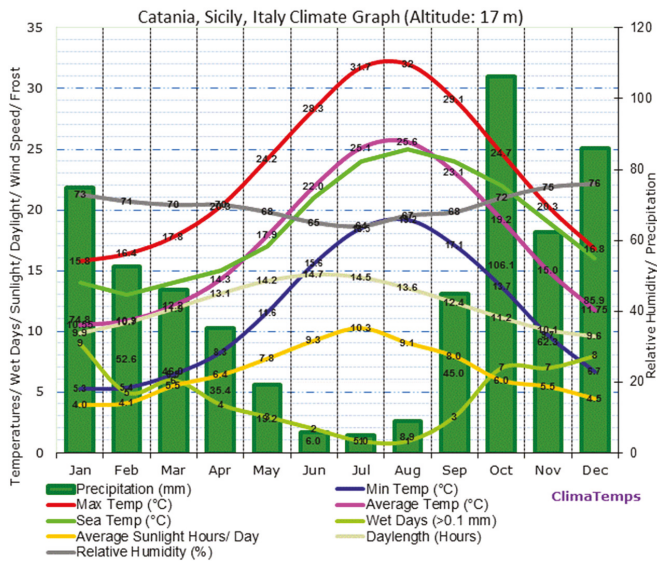


Figure 5. Trend of main climate indicators of the city of Catania (monthly averages).

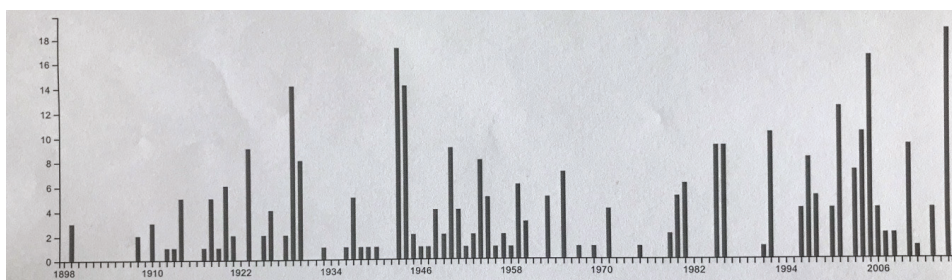


Figure 6. The hottest days in a year in Catania from 1900 to today.

The main climate indicators of Catania are indicated in Figure 5 and the climate trends from 1900 to the present in the area of Catania, analyzing the meteorological data (www.lab.gedidigital.it), it can be summarized as follows:

- The average temperature in the area between 2000 and 2017 was 0.6679 °C above the 20th-century average;
- The number of hot days (above 29 °C during 24 h on average) increased from 2.35 days per year in the 20th-century to 5.222 per year from 2000 onwards (Figure 6); the number of frost days (below −1 °C for 24 h on average 24) remained unchanged at zero days per year.

The municipality of Catania is in the process of defining their adaptation plan. However, the city has already started a series of adaptation measures, including the planning and implementation of GIs and oriented management of public green areas.

In the city of Catania (Kmsq 183), the extension of the urban green is equal to 4,843,660 square meters, and the urban green per inhabitant corresponds to 16.4 square meters.

The scenario of the urban green spaces in Catania is shown in Table 1:

Table 1. The urban green spaces of the city of Catania (*).

Green Typology	Square Metres
Urban Parks (> 8,000 square metres)	513,577
Green equipment (< 8.000 square metres)	431,270
Urban Design Areas	715,500
Urban Forestation	-
School Gardens	350,000
Botanical Gardens and Vivai	20,000
Zoological Gardens	-
Cemetery	50,000
Urban Gardens (mainly managed by families)	2,500
Sports areas/Outdoor play	100,000
Bosch areas (> 500 square metres)	972,769
Uncultivated Green	1,668,044
Total Urban Green	4,843,660

(*) Source: Directorate for Environmental and Green Policies and Energy Management of the Autoparco—Service for the Protection and Management of Public Green, Giardino Bellini and Parchi, 2019.

The green areas play an important and specific role both as an urban component for the conservation and improvement of the landscape and the environment and as a means for aggregative purposes for social and cultural integration.

The GIs should pursue the following objectives among the ones envisaged:

- Improving and preserving the local landscape and environmental restoration;
- Favor urban climate control and reduction of albedo and heat islands;

- Increase the naturalness and biodiversity of the urban territory;
- To stimulate the aggregative, social and therapeutic functions of green areas (e.g., urban gardens, neighborhood parks, healing gardens, spaces for cultural events and shows) (Regulation of the public and private Green of the city of Catania, 2017).

The strategy for the GIs interventions includes the creation of green areas, green avenues, wetlands, and urban gardens according to the classification: Wedges, vortices, margins, strips, islands, hot points, hubs, fences, spurs, and vectors (Figure 7).

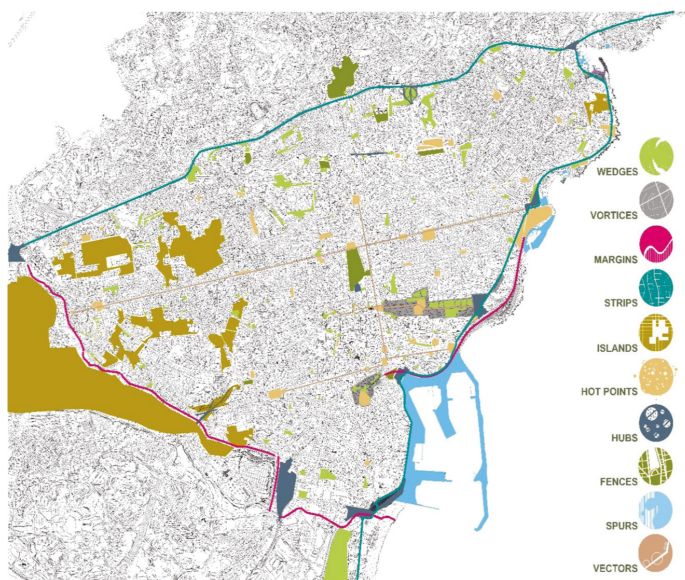


Figure 7. The types of green infrastructures foreseen in the municipality of Catania (2017).

Wedges: Urban areas with the aim of becoming green areas dedicated to developing the relationship between citizen and city. **Vortices:** Model of areas designed to interact with the city with an inaccurate destination (areas that can adapt to the different needs of different groups of society). **Margins:** Represent a bit of a breakthrough, as the boundary criterion of the city is redefined, moving it ever more towards the areas that assume a strategic significance under the aspect of livability (sea, river, park, etc.). In this vision of development, the synergies between the oriented reserve of the Simeto Oasis, Etna Park, and in general with the urban parks (Playa del Bosco, Gioeni Park, etc.) and the city are included. **Strips:** Areas dedicated to the connection between the different areas of Catania, also with the redefinition of the above-mentioned margins. **Island areas** allow the giving back to the territory its centrality, where man has included the buildings over the years. **Hot spots** are red areas, under the cultural, economic, and social aspects in which the interests of a large part of society are concentrated and in which a mitigating action is needed to improve the quality of the environment. This represents the areas where resident population flows, tourists, and populations that gravitates around the city with both structural and infrastructural needs. In these areas, the need for both congestion and pollution generated to create buffer areas to mitigate the effects of the hubs present in the area emerges. **Spurs** are the areas that correspond with the Waterfront project, which start from the port and end up in Ognina, where the city encourages the development of a tourist town on the sea. **Fences:** All the defined and delimited green parks are included. **Vectors** include the areas that represent the main routes of the city's traffic.

The municipality of Catania has realized some GIs and others are in the course of realization, as reported in Figures 8–13 that testify the situation of the interested area before and after the realization of the GI.



Figure 8. Piazza Galatea - Catania (before).



Figure 9. Piazza Galatea—Catania (today).



Figure 10. Tondo Gioeni—Catania (before).



Figure 11. Tondo Gioeni (today, after the realization of the vertical wall).



Figure 12. Corso Martiri della libertà—Catania (before).



Figure 13. Corso Martiri della Libertà (project in progress).

The urban green is a heritage of the complex city, which requires careful assessment that takes into account not only the economic variables but also the social, environmental, and institutional ones. The proposals for investments in GIs, their management, and the evaluation of benefits will have to be shared by the community for an effective pursuit of the objectives set. This is an assessment that considers the dimensions of sustainable development, which will contribute to providing useful elements for the promotion of a model of governance of the city “*eco-social-green*” [4].

Based on the *eco-social-green* model, it will be possible to carry out a social, environmental, and economic assessment of the proposed interventions, through a collaborative process and by sharing

the objectives of valorization, transformation, and redefinition of the green spaces of the city of Catania. The model proposed is called “*eco-social-green*” because we have decided to integrate the aspects that we consider important for the new role attributed to cities. Both at a European level and in the scientific debate, there is increasing attention on the role that cities must have on climate change, biodiversity, conservation, and promotion of social cohesion. A multidimensional approach allows to make decisions in complex conditions, and it gives the possibility to consider economic and non-economic dimensions; the existing synergies and possible conflicts, and the different viewpoints of the subjects involved (public and private).

The attention of the citizens of Catania towards the environment and the presence of greening in the city has recently increased. In fact, the initiatives of “adoption of public green” by private individuals are multiplying (to date, the public green areas of Catania adopted by private individuals, for redevelopment and maintenance, are around 4000 square metres—with savings for municipal management of around 300,000 euros). Citizens are aware that the GIs perform important functions to improve the quality of urban life, both in environmental and social terms and in terms of adaptation to climate change.

4. Methodology

The analysis of the case study evaluated the GIs planning of the metropolitan city of Catania, to experiment with new approaches and opportunities for the definition of green strategies that have found concrete applications in the development of guidelines in politics and local planning tools, as a tool for climate mitigation in an urban environment.

The proposed approach was based on the integration between the participatory planning (based on the establishment of the Focus Groups with the various stakeholders) and the NAIAD method (Novel Approach to Imprecise Assessment and Decision Environments [11], for the Multi-Criteria Social Assessment—SMCE) as possible a methodological structure to acquire and evaluate the “complex” information collected (quantitative and qualitative data) on possible alternative scenarios in relation to the urban green spaces.

The methodology can be considered a social experiment, able to produce collective opinions, to detect communication barriers, to study conflictual behavior, to acquire local information, and to create acceptable options [50–53].

The innovative advantage is the interaction among the participants that highlight the fundamental tools to support a process of evaluation and reciprocal learning. This approach allows us to reveal new visions of the subjects involved in order to have a final participated decision.

The target is that of developing a methodological structure made by suitable tools to acquire first, and process second, qualitative and quantitative information concerning the possible alternative scenarios of the problem under study. Opinions were collected at specific meetings at the local level with stakeholders and sector’s operators involved in the issue from environmental, social, climate, landscape, health safety, and economic points of view.

The opinions were collected through specific Focus Groups with local stakeholders, operators, and citizens interested in the issue in question from different economic, social, and environmental aspects [54]. This was in the presence of 2 researchers, one with the role of moderator and the other with the detector of the responses of the individual subjects involved.

The adoption of this approach was limited to problems of territorial planning referable to SMCE [55–57]. There were numerous articles that employed SMCE for the resolution of problems related to the management of environmental resources, and in general, to valuations of sustainability, climate adaptation, energy policy, etc. [58–61].

The following picture (Figure 14) identifies the steps on which our SMCE was based, with some adaptation concerning the specificity of the context surveyed.

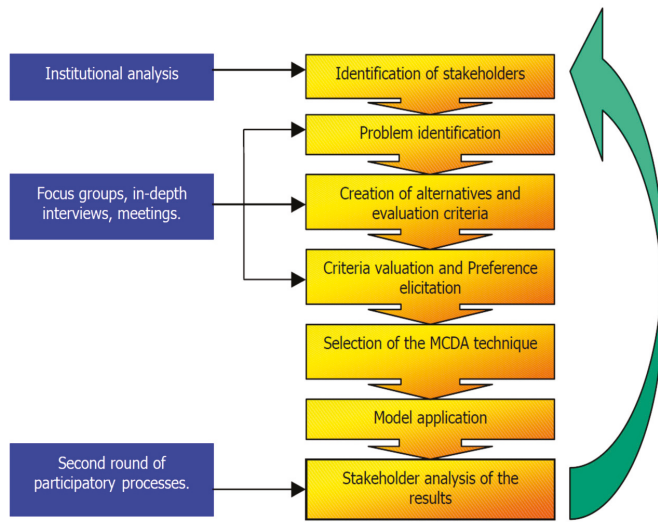


Figure 14. Structure of the model Multi-Critical Social Assessment (SMCE) [4].

In detail, the proposed model was based on:

- The individualization of the citizens and the stakeholders involved (100 questionnaires);
- The definition of the alternative scenarios (definition of the 3hypotheses of the scenario: Inclusive, resilient, and city);
- The definition of the context of evaluation, namely the decisional criteria (urban green spaces of Catania for the shared project);
- The evaluation of the impact of alternative scenarios relative to the criteria in question);
- The final creation of the impact matrix;

The structure used the focus groups as a social research methodology, aimed to acquire information on the opinions of stakeholders regarding a variety of scenarios for future development within the zone examined. The choice of focus groups and, therefore, of the interaction among the actors involved, aimed to support the phase of the choice and evaluation of the different aspects that would be included in the equity matrix. The matrices of impact and equity constituted the basis for the use of the discrete multicriteria evaluation NAIAD model (Novel Approach to Imprecise Assessment and Decision Environments) [62], able to manage qualitative and quantitative data in order to evaluate the measures of intervention. This instrument supported the classification of the alternative scenarios proposed based on the determined decisional criteria and considerations of possible “alliances” and “conflicts” between the groups of stakeholders on the proposed scenarios, thus measuring their acceptability. The NAIAD multicriteria evaluation method applied to this study constituted a discrete method of evaluation capable of managing qualitative and quantitative data. It was an appropriate tool for the planning of problems characterized by great “uncertainty” and “complexity” regarding existing territorial, social, and economic structures and their interrelations [63]. The basic input in the NAIAD method consisted of alternative scenarios to be analyzed, different decisional criteria for their evaluation, and different stakeholders who expressed opinions about the scenarios in question. One of the strengths of this tool in the application to the planning of interventions on green spaces was based on its ability to collect the conflicting perspectives of the stakeholders and to address the compromises among the environmental, social, and economic dimensions.

Concerning the objective of this study, the analysis will be applied to the principal priorities, the methodology used for the definition of the model of management for the green area of Catania, which is the area of investigation for this work.

The evaluation through the Focus Groups was divided into 3 phases, referring in the specific case to the destination of urban areas in a degraded state to be valorized:

Phase 1—consisted of "planning" the meetings. During this phase, the following were established:

- The number of sessions and the time dedicated to each of them (8, as an expression of the individual categories considered: Association of citizens, groups of pensioners, cultural associations, playrooms, trade unions, public institutions, scientific groups, tertiary sector's companies, with time varying from 4 to 8 h);
- The creation of an interview guide to conduct the discussion (scientific and dissemination materials, research papers, photos, maps, relative the problems of urban green areas and on the social, climatic effects deriving from them);
- Selection of participants (stratified selection for homogeneous groups: Age, gender, income).

The questionnaire used for the interviews was designed to explore the perception of environmental issues in the urban context and to evaluate the real needs of the population in terms of environmental quality, perception of climate change, and fruition of public green spaces. It was structured in 10 questions in order to collect information and opinions useful for the research, on the 3 hypotheses proposed: Inclusive, resilient, and city.

Phase 2—consisted of "carrying out" the entire activity, based on the guide to the pre-established interview. It began with the presentation of the topic relating specifically to the action strategy for the management of degraded areas to be recovered, using the support material (articles, results, photographs), prepared specifically to introduce the issue under consideration and stimulate discussion and the interaction of the participants. During this phase, various ideas and opinions were acquired that represented the reactions of the participants involved in the issues raised.

Phase 3—consisted in the elaboration of the "qualitative results" and the production of the final report.

In this regard, various qualitative analysis tools were used, based on intentionally prepared inputs and specific rules. Overall, the Focus Groups can be considered a social experiment, able to produce collective opinions, reveal communication barriers, study conflicting behavior, acquire local information, create acceptable options, synthesize information, etc. The key advantage of the Focus Group dedicated to defining the intervention strategies in green urban areas to be enhanced, when compared to other participatory techniques, lay in the deep interaction between the participants, becoming a "social network." The participants became fundamental tools to support a "mutual learning process" on the questions examined. This participatory comparison technique made it possible to reveal new dimensions of the issue under discussion, thus underlining the possibility for the Focus Group to bring out the opinions in this regard rather than produce generalized results. The analysis phase of the results of the Focus Groups was followed by the multi-criteria analysis where the basic input of the NAIADe method consisted of alternative scenarios to be analyzed, different decision criteria for the relative evaluation, and different stakeholders that expressed opinions on the scenarios in question. Based on this method, 2 types of analysis can be performed:

- A multi-criteria analysis based on the impact matrix, which leads to the definition of the priorities of alternative scenarios regarding certain decision-making criteria;
- An analysis of equity based on the equity matrix, which analyzes possible "alliances" or "conflicts" among different interests in relation to the scenarios in question.

In this regard, the multicriteria analysis, according to the NAIADe methodology, aimed to classify alternative scenarios based on the preferences of individual groups based on certain decision criteria [64–67].

The basic input of the NAIAD method was constituted by the impact matrix (criteria/alternative matrix), including scores that can take the following forms: Crisp numbers, stochastic elements, fuzzy elements, and linguistic elements (such as "very poor", "poor", "good", "very good", "excellent") [18]. When comparing alternative scenarios, the concept of distance was introduced. In the presence of crisp numbers, the distance between the 2 alternative scenarios with respect to the given evaluation criterion was calculated by subtracting the respective crisp numbers.

The classification of alternative scenarios was based on data from the impact matrix, used for:

- Comparison of every single pair of alternatives for all the evaluation criteria considered;
- Calculation of a credibility index for each of the aforementioned comparisons, that measured the credibility of one preference relation "... alternative scenario" a "is better/worse, etc., alternative scenario «b» ... "(preference relationships were used);
- Aggregation of the credibility indices produced during the previous stage leading to a preference intensity index $\mu^*(a, b)$ of an alternative «a» with respect to another «b» for all the evaluation criteria, associated with the concept of entropy $H^*(a, b)$, as an indication of the variation in the credibility indices;
- Classification of alternative scenarios based on previous information.

The final classification of the alternatives was the result (intersection) of 2 different classifications: the classification $\Phi^+(a)$ based on the "best" and "decidedly better" preference relationships; and the classification $\Phi^-(b)$, which was based on the "worst" and "decidedly worse" preference relationships.

In relation to the objective of the present study, the analysis will be applied to the main priorities, for the evaluation of the optimal management model for the enhancement of the green areas of Catania.

5. Results and Discussion

The results of the present work provide a further multidisciplinary contribution to research on the management and planning of green areas in cities. Specifically, the analysis was conducted on the basis of the following question:

What are the strategies for the enhancement of urban green spaces of the City of Catania for climate change adaptation?

Three hypotheses of green recreate strategies were envisaged (Table 1):

Hypothesis 1. INCLUSIVE: *Creation of green areas with inclusive and social functions (equipped parks, urban gardens, etc.).*

Hypothesis 2. RESILIENT: *Creation of urban green areas with non-usable landscape function but as a climate change adaptation measure.*

Hypothesis 3. CITY: *Conservative recovery, cleaning, and maintenance of the current green.*

In order to evaluate the three hypotheses mentioned above, evaluation criteria have been defined, which represent "... a measurable aspect of the judgment that can characterize a dimension of the various choices that are taken into consideration" [68]. In the present case study, twenty evaluation criteria or variables were used. These criteria were defined based on the purpose and objectives of the evaluation of the analyzed case, which can be considered representative of the reality of the City of Catania but overall very similar to other metropolitan areas.

The objectives of the evaluation activity were environmental, social, climate, economic, landscaping, and health and safety.

Specifically, for each objective, the related evaluation criteria are considered and are indicated in Table 2.

Table 2. The objectives and evaluation criteria adopted in the applied model for the urban green areas of Catania.

Goals	Evaluation Criteria
<i>Environmental</i>	air quality; human settlement
<i>Social</i>	usability, multi-functionality, agricultural production, employment commitment
<i>Climate</i>	reduction of temperatures, creation of accessible shade areas, thermal excursion
<i>Economic</i>	cost of realization, the value of the properties; productive exploitation
<i>Landscape</i>	quality of the landscape, the exaltation of the seasons, biodiversity
<i>Health safety</i>	pollution, pathogenic presence, use of pesticides and fertilizers

Source: Our elaboration, data collected direct survey.

According to the above-reported indicators, impact matrix results, as a whole, are reported in the following Table 3.

Table 3. Evaluation of the results of the impact matrix of the various alternatives.

Criteria of Evaluation	Scenario Inclusive	Scenario Resilient	Scenario City
<i>Environmental</i>			
Air quality	Good	Very good	Poor
Smell emanation	Good	Excellent	Good
Anthropization	Poor	Very good	Very good
Waste of water	Poor	Good	Excellent
<i>Social</i>			
Usability	Excellent	Medium	Poor
Multifunctional	Excellent	Very good	Good
Agricultural production	Very good	Poor	Poor
Occupational commitment	Very good	Good	Poor
<i>Climate</i>			
Temperature reduction	Good	Excellent	Very good
Creation of shaded areas	Good	Very good	Good
Temperature range	Good	Very good	Poor
Humidity	Very good	Good	Poor
<i>Economic</i>			
Cost of realization	Good	Poor	Very good
Value of real estate	Very good	Excellent	Good
Productive exploitation	Very good	Good	Poor
<i>Landscape</i>			
Landscape quality	Good	Excellent	Good
Exaltation of the seasons	Excellent	Very good	Poor
Biodiversity	Excellent	Very good	Poor
<i>Health Safety</i>			
Pollution	Good	Very good	Good
Presence of pathogens	Poor	Good	Very good
Use of pesticides and fertilizers	Poor	Good	Very good

Source: Our elaboration, data collected direct survey.

Hypothesis Inclusive as an option to be shared (highlighting the social, landscape, and economic aspects), followed at a short distance by hypothesis Resilient (highlighting environmental, climate, landscape results) and, then, hypothesis City (with a more negative evaluation).

Then the equity matrix was developed. It provided stakeholders' opinions on the three hypotheses suggested. The selection of stakeholders was based on their potentialities to influence the targets of the project. They represent citizens, socially vulnerable groups, and different interested associations and possible users of the interventions, with different qualifications, both into the private and public. In particular, eight typologies of stakeholders were involved (as listed in Table 4). It is important to underline that stakeholders' opinions in the NAIAD model can only be of a quality kind: Language expressions from very poor, poor, medium, good, very good, and excellent (Table 4). These results show

that a big number of the stakeholders and operator groups selected agreed with the evaluation of the three hypotheses.

Table 4. The equity matrix—Stakeholder opinions on the three hypotheses

Typologies of Stakeholders	Scenario Inclusive	Scenario Resilient	Scenario City
A1. Associations of citizens	Very good	Excellent	Poor
A2. Groups of pensioners	Excellent	Poor	Poor
A3. Cultural associations	Very good	Good	Good
A4. Playroom	Excellent	Very good	Good
A5. Trade unions	Very good	Excellent	Good
A6. Public Institutions	Good	Very good	Poor
A7. Scientific groups	Very good	Excellent	Poor
A8. Tertiary sector's companies	Excellent	Excellent	Good

Source: Our elaboration.

The results of the multi-criteria analysis highlighted that our hypothesis was inclusive and was the predominant hypothesis, followed closely by hypothesis Resilient, while hypothesis City gained a marginal meaning.

The results obtained through the equity analysis were used to examine possible alliances or conflicts among the opinions of stakeholders about the decision of what hypotheses to adopt. Besides agreeing on the classification of the different hypotheses, the results (Table 5) show that a high number of stakeholders were in agreement with hypothesis Inclusive.

Table 5. Classification of the scenarios corresponding to the higher consent (0.8423).

Typologies of Stakeholders	Scenario Inclusive	Scenario Resilient	Scenario City
A1 Associations of citizens	0.89	0.83	0.21
A2 Groups of pensioners	0.83	0.59	0.12
A3 Cultural associations	0.85	0.65	0.38
A4 Playrooms	0.74	0.38	0.11
A5 Trade unions	0.64	0.82	0.23
A6 Public Institutions	0.36	0.29	0.28
A7 Scientific groups	0.57	0.92	0.12
A8 Tertiary sector's companies	0.86	0.85	0.54

Source: Our elaboration, data collected direct survey.

The efficiency of this kind of approach relies on the possibility of establishing a “learning platform” that eases participation, information exchange, and reciprocal comprehension of participants, who stimulate each other towards a sharing of the territory. Results allowed the inclusion of several perspectives of the evaluation problem under study, as demonstrated by the different groups involved, increasing the perception of planners about the acceptability of the alternatives proposed that may lead to the improvement in strategic decisions and, therefore, create innovative ideas and new planning solutions based on the possibilities offered by the participated processes.

On the whole, the results obtained from this model of *collaborative governance, eco-social-green*, developed through the integration of a participative tool and a multi-criteria analysis, became strategic for the choices of urban green investments, in particular, related to climate change adaptation measures shared with the community.

6. Conclusions

In the last decade, literature has been enriched by a complex body of knowledge related to the evaluation of the benefits provided by GIs in an urban area to climate change mitigation and adaptation. Many pieces of research provide empirical evidence that can be used to design GIs to decrease the vulnerability of a city to climate change. In particular, the studies have shown the important role of

GIs in contributing to climate change mitigation and offsetting urban carbon emissions (especially with the employment of green roofs and green facades); the thermal comfort due to the cooling effect of green roofs in different types of buildings and in different seasons and others important positive effects. However, the GIs can offer social and psychological benefits to citizens, especially socially vulnerable ones.

From the experiences mentioned and from the researches cited (only some for brevity and even synthetically) it could highlight that various GIs could provide multiple benefits in urban areas and this should be taken into account in the planning and design of the urban landscape. It is important to consider the multi-functionality of the GIs because the focus on a single advantage could, in turn, be harmful from another point of view (trade-off) [45].

It is necessary to replace the expansive building processes with the virtuous ones of urban regeneration, in which the GIs take on an increasingly important role for their functions of social inclusion, environmental protection, and in the mitigation and adaptation for climate change. Adaptation strategies need to preserve and enhance existing GIs, and increase them where possible, especially taking opportunities in restructuring and new developments to create significant new spaces.

The provision of GIs has been widely recognized as playing an important role in meeting the challenge of climate change adaptation. Integration of GIs into more ecosystem-based spatial planning makes the design of GI assets a crucial planning tool for building more sustainable urban environments, resistant to future challenges and adaptable to future needs [46].

The GIs are well established in climate adaptation strategies, but it is important that these strategic tools are encouraged through specific integrated territorial and urban planning; long-term investments, planning, and sustainability in decision making; models of GIs for climate change adaptation and for optimal multiple benefits; evaluating both the economic and social and environmental benefits; encouraging citizen participation in the planning of GIs for climate adaptation [4,42,43].

Due to the multifunctionality of GIs, there is no single science or reference discipline for its study [43]. They are based on the theories and practices of numerous scientific disciplines, such as conservation biology, landscape ecology, urban and regional planning, geographic analysis, information systems, and economists [69]. The research into GIs also needs to adjust to different spatial scales as its application can range from individual buildings to neighborhoods and cities to entire regions [70].

The expected impacts of climate change in urban settlements are very different: Impacts on health and quality of life (in particular of the weaker sections of the population), impacts on the buildings, on water, energy and transport infrastructures, on cultural heritage (due to landslides, floods and heatwaves), impacts on energy production and supply. Thus, to deal effectively with these impacts, we need the coordination of a very broad institutional network (multilevel governance) [43,71].

To date, however, the prospects for the development of the GIs are strictly dependent on its inclusion in planning policies, which local authorities and urban planning regulations must provide and support financially as well.

The ESs must be integrated into the planning and the choices of urban planning policies, making GIs and eco-innovation the fulcrum of an intelligent and sustainable urban transformation towards a new model of sustainable city enhancing biodiversity, environment and social inclusion [72].

The new guidelines on the protection of natural capital and biodiversity and attention to climate change are laying the foundations for outlining new ways of the government of the territory and the cities, with a proactive and engaging approach. Cities are ecosystems full of human presence, rich in knowledge and innovation, which welcome more than 50% of the world's population and about 70% of the Italian population. In cities, the conflict between artificiality and naturalness is maximum and causes loss of biodiversity, quality of ecosystem services, and resilience [73].

A direct consequence of the variety of expected impacts in urban settlements is the multiplicity of institutional actors who, together with citizens, must be involved in adaptation policies. Actors who will have a responsibility at different territorial scales (state, regions, provinces, municipalities)

or responsibilities of certain sectors (basin authorities, energy service management bodies, water companies, etc.) and citizens, for which multilevel governance is required.

This research allowed us to point out that the methodological approach adopted, that was inspired by a model of city "eco-social-green" and based on the integration between the participated planning technique and the multi-criteria analysis, in the case of problems linked to the urban green spaces, represented a strategic tool.

The efficiency of this model of evaluation relies on the possibility of establishing a learning platform that facilitates the participation, information exchange, and reciprocal comprehension of the participants that support a strategy for the development and the fruition of the GIs of the city and to evaluate the perception of the importance of the GIs for climate change adaptation.

As other studies have already indicated [74–76], our study highlights an interesting potential for the wider use of SMCE in the governance of green spaces, for its ability to integrate ecological, social, and economic values, as well as the different stakeholder preferences among social groups, places, and temporal dynamics. Of course, policymakers have a broad ability to improve human well-being in cities through green space governance approaches that take into account their different components, economic, environmental, and social.

The value generated by the presence of GIs in the urban ecosystem, through the application of a vision of green-urban-planning, seems to be a valid instrument for achieving the objectives of realizing resilient and inclusive cities.

Author Contributions: All authors contributed to this work, in particular their individual contributions are: conceptualization L.S.; methodology L.S. and A.S.; validation and formal analysis A.S.; writing original draft and review and editing L.S. and A.S.

Acknowledgments: This work has been financed by the University of Catania within the project "Piano della Ricerca Dipartimentale 2016-2018 of the Department of Civil Engineering and Architecture".

Conflicts of Interest: The authors declare no conflict of interest.

References

1. Intergovernmental Panel on Climate Change (IPCC). *Climate Change 2014; Contribution of Working Groups I, II and III to the Fifth Assessment Report of the Intergovernmental Panel on Climate Change*; Core Writing Team, Pachauri, R.K., Meyer, L.A., Eds.; IPCC: Geneva, Switzerland, 2014; p. 151.
2. United Nations. *Transforming our World: The 2030 Agenda for Sustainable Development*; United Nations: New York, NY, USA, 2015.
3. United Nations. *Revision of the World Urbanization Prospects*; United Nations: New York, NY, USA, 2018.
4. Sturiale, L.; Scuderi, A. The evaluation of green investments in urban areas: A proposal of an eco-social-green model of the city. *Sustainability* **2018**, *10*, 4541. [[CrossRef](#)]
5. European Commission. *The Forms and the Functions of the Green Infrastructures*; European Commission/Environmental: Brussels, Belgium, 2016.
6. Environment Directorate-General for the Environment. *Communication from the commission to the European Parliament, the Council, the European Economic and Social Committee and the Committee of the Regions Green Infrastructure (GI)—Enhancing Europe's Natural Capital*; Environment Directorate-General for the Environment: Bruxelles, Belgium, 2013.
7. EU. 2009 WHITE PAPER *Adapting to Climate Change: Towards a EUROPEAN Framework for Action*; COM 2009 147/4; EU: Brussels, Belgium, 2009.
8. EEA. *Green Infrastructure and Territorial Cohesion. The Concept of Green Infrastructure and its Integration into Policies Using Monitoring Systems*; Technical Report no. 18/2011; European Environment Agency: Copenhagen, Denmark, 2011.
9. Werguin, A.C.; Duhem, B.; Lindholm, G.; Oppermann, B.; Pauleit, S.; Tjallingi, S. (Eds.) *Green Structure and Urban Planning*; Final Report, COST Action, No. C11; Office for Official Publications of the European Communities: Luxembourg, 2005.
10. DG Environmental New Alerts Services. *The Multifunctionality of the Green Infrastructures*; In-Depth Report; DG Environmental New Alerts Services: Bruxelles, Belgium, 2012.

11. Munda, G. Multicriteria Evaluation in a Fuzzy Environment—Theory and Applications. In *Ecological Economics*; Physica-Verlag: Heidelberg, Germany, 1995.
12. OECD. *Competitive Cities and Climate Change*; OECD: Milan, Italy, 2008.
13. World Bank. *Cities and Climate Change: An Urgent Agenda*; The World Bank: Washington, DC, USA, 2010.
14. UN-HABITAT. *Cities and Climate Change: Global Report on Human Settlements 2011*; United Nations Human Settlements Programme; Earthscan: London, UK; Washington, DC, USA, 2011.
15. COM. *The European Strategy on Adaptation to Climate Change*; European Commission: Brussels, Belgium, 2013; p. 216.
16. Monclús, J. *From Park Systems and Green Belts to Green Infrastructures*; Visions, U., Díez Medina, C., Monclús, J., Eds.; Springer: Cham, Germany, 2018.
17. Anguluri, R.; Narayanan, P. Role of green space in urban planning: Outlook towards smart cities. *Urban. Urban Green*. **2017**, *25*, 58–65. [[CrossRef](#)]
18. Jim, C.Y. Green spaces preservation and allocation for sustainable greening of compact cities. *Cities* **2004**, *21*, 311–320. [[CrossRef](#)]
19. Costanza, R. (Ed.) *Ecological Economics: The Science and Management of Sustainability*; Columbia University Press: New York, NY, USA, 1991.
20. Foster, J.; Lowe, A.; Winkelman, S. *The Value of Green Infrastructures for Urban Climate Adaptation*; Center for Clean Air Policy: Washington, DC, USA, 2011.
21. Brink, E.; Aalders, T.; Ádám, D.; Feller, R.; Henselek, Y.; Hoffmann, A.; Ibe, K.; Matthey-Doret, A.; Meyer, M.; Negrut, N.L.; et al. Cascades of green: A review of ecosystem based adaptation in urban areas. *Glob. Environ. Chang.* **2016**, *36*, 111–123. [[CrossRef](#)]
22. Hunt, A.; Watkiss, P. Climate change impacts and adaptation in cities: A review of the literature. *Clim. Chang.* **2011**, *104*, 13–49. [[CrossRef](#)]
23. Escobedo, F.J.; Kroeger, T.; Wagner, J.E. Urban forests and pollution mitigation: Analyzing ecosystem services and disservices. *Environ. Pollut.* **2011**, *159*, 2078–2087. [[CrossRef](#)] [[PubMed](#)]
24. Gómez-Baggethun, E.; Barton, D.N. Classifying and valuing ecosystem services for urban planning. *Ecol. Econ.* **2013**, *86*, 235–245. [[CrossRef](#)]
25. Economides, C. *Green Infrastructure: Sustainable Solutions in 11 Cities across the United States*; Columbia University Water: New York, NY, USA, 2014.
26. Nowak, D.J.; Crane, D.N.; Stevens, J.C. Air pollution removal by urban trees and shrubs in the United States. *Urban For. Urban Green.* **2006**, *4*, 115–123. [[CrossRef](#)]
27. Sturiale, L.; Timpanaro, G.; Foti, V.T.; Scuderi, A.; Stella, G. *Social and Inclusive “Value” Generation in Metropolitan Area with the “Urban Gardens” Planning*; Green Energy and Technology; Springer: Cham, Switzerland, 2019; in press.
28. Caspersen, O.H.; Olafsson, A.S. Recreational mapping and planning for enlargement of the green structure in greater Copenhagen. *Urban Urban For. Green.* **2010**, *9*, 101–112. [[CrossRef](#)]
29. Kabisch, N. Ecosystem service implementation and governance challenges in “urban green spaces” planning—the case of Berlin, Germany. *Land Use Policy* **2015**, *42*, 557–567. [[CrossRef](#)]
30. Jim, C.Y. Planning strategies to overcome constraints on greenspace provision in urban Hong Kong Town. *Plan. Rev.* **2002**, *73*, 127–152.
31. Yang, J.; McBride, J.; Zhou, J.; Sun, Z. The urban forest in Beijing and its role in air pollution reduction. *Urban For. Urban Green.* **2005**, *3*, 65–78. [[CrossRef](#)]
32. Wei, J.; Qian, J.; Tao, Y.; Hu, F.; Ou, W. Evaluating Spatial Priority of Urban Green Infrastructure for Urban Sustainability in Areas of Rapid Urbanization: A Case Study of Pukou in China. *Sustainability* **2018**, *10*, 327. [[CrossRef](#)]
33. Beckett, K.P.; Freer-Smith, P.; Taylor, G. Urban woodlands: their role in reducing the effects of particulate pollution. *Environ. Pollut.* **1998**, *99*, 347–360. [[CrossRef](#)]
34. Nowak, D.J.; Mchale, P.J.; Ibarra, M.; Crane, D.; Stevens, D.J.; Luley, C.J. Modeling the Effects of Urban Vegetation on Air Pollution. In *Air Pollution Modeling and Its Application XII*; Plenum Press: New York, NY, USA, 1998; pp. 399–407.
35. Saunders, S.; Dade, E.; Van Niel, K. An Urban Forest Effects (UFORE) model study of the integrated effects of vegetation on local air pollution in the Western Suburbs of Perth WA. In Proceedings of the 19th International Congress on Modelling and Simulation, Cambridge, UK, 30 March–1 April 2011; pp. 1824–1830.

36. Baró, F.; Chaparro, L.; Gómez-Baggethun, E.; Langemeyer, J.; Nowak, D.J.; Terradas, J. Contribution of ecosystem services to air quality and climate change mitigation policies: the case of urban forests in Barcelona, Spain. *Ambio* **2014**, *43*, 466–479. [[CrossRef](#)]
37. Akbari, H.; Pomerantz, M.; Taha, H. Cool surfaces and shade trees to reduce energy use and improve air quality in urban areas. *Sol. Energy* **2001**, *70*, 295–310. [[CrossRef](#)]
38. Tzoulas, K.; Korpela, K.; Venn, S.; Yli-Pelkonen, V.; Kaźmierczak, A.; Niemela, J.; James, P. Promoting ecosystem and human health in urban areas using green infrastructure: a literature review. *Landsc. Urban Plann.* **2007**, *81*, 167–178. [[CrossRef](#)]
39. Jayasooriya, V.M.; Muthukumar, A.W.M.N.G.S.; Perera, B.J.C. Green infrastructure practices for improvement of urban air quality. *Urban For. Urban Green.* **2017**, *21*, 34–47. [[CrossRef](#)]
40. Gill, S.E.; Handley, J.F.; Ennos, A.R.; Pauleit, S. Adapting Cities for Climate Change: The Role of the Green Infrastructure. *Built Environ.* **2007**, *1*, 115–133. [[CrossRef](#)]
41. Radovanović, M.; Lior, N. Sustainable economic–environmental planning in Southeast Europe—Beyond-GDP and climate change emphases. *Sustain. Dev.* **2017**, *25*, 580–594. [[CrossRef](#)]
42. Breuste, J.; Artmann, M.; Li, J.X.; Xie, M.M. Special issue on green infrastructure for urban sustainability. *J. Urban Plan. Dev.* **2015**, *141*. [[CrossRef](#)]
43. Scuderi, A.; Sturiale, L. *Evaluations of Social Media Strategy for Green Urban planning in Metropolitan Cities; Smart Innovation, Systems and Technologies*; Springer International Publishing AG, part of Springer Nature: New York, NY, USA, 2019; pp. 76–84.
44. Benedict, M.A.; McMahon, E.T. Green Infrastructure: Smart Conservation for the 21st Century. *Renew. Resour. J.* **2002**, *20*, 12–17.
45. Demuzerea, M.; Orrubc, K.; Heidrichd, O.; Olazabalej, E.; Genelettif, D.; Orrugh, H.; Bhavei, A.G.; Mittali, N.; Feliue, E. Mitigating and adapting to climate change: Multi-functional and multi-scale assessment of green urban infrastructure. *J. Environ. Manag.* **2014**, *146*, 107–115. [[CrossRef](#)] [[PubMed](#)]
46. Simonis, U.E. Greening urban development: on climate change and climate policy. *Int. J. Soc. Econ.* **2011**, *11*, 919–928. [[CrossRef](#)]
47. IPCC. *Fifth Assessment Report: Climate Change 2014: Mitigation of Climate Change*; IPCC: Geneva, Switzerland, 2014.
48. Morancho, A.B. A hedonic valuation of urban green areas. *Landsc. Urban Plan.* **2003**, *66*, 35–41. [[CrossRef](#)]
49. Haaland, C.; van den Bosch, C.K. Challenges and strategies for urban green-space planning in cities undergoing densification: A review. *Urban. Urban For. Green.* **2015**, *14*, 760–771. [[CrossRef](#)]
50. Miccoli, S.; Finucci, F.; Murro, R. Social evaluation approaches in landscape projects. *Sustainability* **2014**, *6*, 7906–7920. [[CrossRef](#)]
51. Lo, A.Y.; Jim, C.Y. Willingness of residents to pay and motives for conservation of urban green spaces in the compact city of Hong Kong. *Urban. Urban Green.* **2010**, *9*, 113–120. [[CrossRef](#)]
52. Maloutas, T.; Pantelidou, M. Debatsanddevelopments: The glassmenagerieofurbangovernanceandsocial cohesion concepts and stake/concepts as stakes. *Int. J. Urban Reg. Res.* **2004**, *28*, 449–465. [[CrossRef](#)]
53. Niemelä, J.; Saarela, S.-R.; Tarja Söderman, T.; Kopperoinen, L.; Yli-Pelkonen, V.; Väre, S.; Kotze, D.J. Using the ecosystem services approach for betterplanning and conservation of urban green spaces: A Finland case study. *Biodivers. Conserv.* **2010**, *19*, 3225–3243. [[CrossRef](#)]
54. Soderberg, H.; Karman, E. *MIKA: Methodologiesfor Integrationof Knowledge Areas—The Caseof Sustainable Urban Water Management*; Department of Built Environment & Sustainable Development, Chalmers Architecture, Chalmers University of Technology: Goeteborg, Sweden, 2003.
55. Panell, D.J.; Glenn, N.A. A framework for the economic evaluation and selection of sustainability indicators in agriculture. *Ecol. Econ.* **2000**, *33*, 135–149. [[CrossRef](#)]
56. Siciliano, G. Social multicriteria evaluation of farming practices in the presence of soil degradation. A case study in Southern Tuscany, Italy. *Environ. Dev. Sustain.* **2009**, *11*, 1107–1133. [[CrossRef](#)]
57. Vargas Isaza, O.L. La evaluación multicriterio social y su aporte a la conservación de los bosques social multicriteria. *Rev. Fac. Nac. De Agron. Medellín* **2005**, *58*, 2665–2683.
58. De Marchi, B.; Funtowicz, S.O.; Lo Cascio, S.; Munda, G. Combining participative and institutional approacheswith multicriteria evaluation. An empirical study for water issues in Troina, Sicily. *Ecol. Econ.* **2000**, *34*, 267–282. [[CrossRef](#)]

59. Greco, S.; Matarazzo, B.; Slowinski, R. Dominance based Rough Set Approach to decision under uncertainty and time preference. *Ann. Oper. Res.* **2010**, *176*, 41–75. [CrossRef]
60. Munaretto, S.; Siciliano, G.; Turvani, M. Integrating adaptive governance and participatory multicriteria methods: A framework for climate adaptation governance. *Ecol. Soc.* **2014**, *19*, 74. [CrossRef]
61. Scuderi, A.; Sturiale, L. Multi-criteria evaluation model to face phytosanitary emergencies: The case of citrus fruits farming in Italy. *Agric. Econ.* **2016**, *62*, 205–214. [CrossRef]
62. Munda, G. *Social Multicriteria Evaluation for a Sustainable Economy*; Springer: Berlin, Germany, 2008.
63. Munda, G. A NAIADe based Approach for Sustainability Benchmarking. *Int. J. Environ. Technol. Manag.* **2006**, *6*, 65–78. [CrossRef]
64. Shmelev, E.S.; Rodriguez-Labajos, B. Dynamic multidimensional assessment of sustainability at the macro level: The case of Austria. *Ecol. Econ.* **2009**, *68*, 2560–2573. [CrossRef]
65. Torrieri, F.; Concilio, G.; Nijkamp, P. Decision support tools for urban contingency policy. A scenario approach to risk management of the Vesuvio area in Naples—Italy. *J. Conting. Crisis Manag.* **2002**, *10*, 95–112. [CrossRef]
66. Tiwari, A.P. Choice and Preference of Water Supply Institutions—An Exploratory Study of Stakeholders’ Preferences of Water Sector Reform in Metro City of Delhi, India. 2007. Available online: http://agua.isf.es/semana%E2%80%A6/Doc7_APTiwari_2pag_xcra_a_dobre%20cara.pdf (accessed on 24 May 2019).
67. Bekessy, S.A.; White, M.; Gordon, A.; Moilanen, A.; Mccarthy, M.A.; Wintle, B.A. Transparent planning for biodiversity and development in the urban fringe. *Landsc. Urban Plan.* **2012**, *108*, 140–149. [CrossRef]
68. Voogd, H. *Multiple Criteria Evaluation for Urban and Regional Planning*; Lion: London, UK, 1983.
69. European Commission. *The Multifunctionality of Green Infrastructures*; Science for Environment Policy/In-depth Reports; European Commission: Bruxelles, Belgium, 2012.
70. Naumann, S.; Davis, M.; Kaphengst, T.; Pieterse, M.; Rayment, M. *Design, Implementation and Cost Elements of Green Infrastructure Projects*; Final report; European Commission: Brussels, Belgium, 2011.
71. Matthews, T.; YLob, A.; AByrnc, J. Reconceptualizing green infrastructure for climate change adaptation: Barriers to adoption and drivers for uptake by spatial planners. *Landsc. Urban Plan.* **2015**, *138*, 155–163. [CrossRef]
72. Foti, V.T.; Scuderi, A.; Stella, G.; Sturiale, L.; Timpanaro, G.; Trovato, M.R. The integration of agriculture in the politics of social regeneration of degraded urban areas. In *Integrated Evaluation for the Management of Contemporary Cities*; Mondini, G., Fattinanzi, E., Oppio, A., Bottero, M., Stanghellini, S., Eds.; Results of SIEV, Green Energy and Technology; Springer: Cham, Switzerland, 2018; pp. 99–111.
73. Forest Research. *Benefits of Green Infrastructures*; Report by Forest Research; Forest Research: Farnham, UK, 2010.
74. Langemeyerab, J.; Gómez-Baggethun, E.; Haasede, D.; Scheuerd, S.; Elmqvist, T. Bridging the gap between ecosystem service assessments and land-use planning through Multi-Criteria Decision Analysis (MCDA). *Environ. Sci. Policy* **2016**, *62*, 45–56. [CrossRef]
75. Srdjevic, Z.; Lakicevic, M.; Srdjevic, B. Approach of decision making based on the analytic hierarchy process for urban landscape management. *Environ. Manag.* **2013**, *51*, 777–785. [CrossRef]
76. Grêt-Regamey, A.; Celio, E.; Klein, T.M.; Wissen Hayek, U. Understanding ESs trade-offs with interactive procedural modeling for sustainable urban planning. *Landsc. Urban Plan.* **2013**, *109*, 107–111. [CrossRef]



© 2019 by the authors. Licensee MDPI, Basel, Switzerland. This article is an open access article distributed under the terms and conditions of the Creative Commons Attribution (CC BY) license (<http://creativecommons.org/licenses/by/4.0/>).

Article

Negotiating Institutional Pathways for Sustaining Climate Change Resilience and Risk Governance in Indonesia

Jonatan A. Lassa

Emergency & Disaster Management, College of Indigenous Futures, Arts & Society, Charles Darwin University, Darwin, NT 0909, Australia; jonatan.lassa@cdu.edu.au; Tel.: +61-8-8946-6756

Received: 8 July 2019; Accepted: 23 July 2019; Published: 30 July 2019

Abstract: Institutions matter because they are instrumental in systematically adapting to global climate change, reducing disaster risks, and building resilience. Without institutionalised action, adapting to climatic change remains ad-hoc. Using exploratory research design and longitudinal observations, this research investigates how urban stakeholders and policy entrepreneurs negotiate institutional architecture and pathways for sustaining climate change adaptation and resilience implementation. This paper introduces hybrid institutionalism as a framework to understand how city administrators, local policy makers, and policy advocates navigate complex institutional landscapes that are characterised by volatility and uncertainties. Grounded in the experience from a recent experiment in Indonesia, this research suggests that institutionalisation of adaptation and resilience agenda involves different forms of institutionalisation and institutionalism through time. Future continuity of adaptation to climate change action depends on the dynamic nature of the institutionalism that leads to uncertainty in mainstreaming risk reduction. However, this research found that pathway-dependency theory emerges as a better predictor for institutionalising climate change adaptation and resilience in Indonesia.

Keywords: ACCCRN; Climate change adaptation; institutionalising adaptation; hybrid institutionalism; mainstreaming resilience; urban resilience and adaptation

1. Introduction

Many transformative adaptation projects have been exogenously driven by international donors with the aim to build and deepen resilience in both developed and developing worlds. They are often piloted in different ways to build institutional capacity and create institutional pathways that enable local actors worldwide to accelerate urban adaptation [1]. Some of the examples include Asian Cities Climate Change Resilience Network (ACCCRN), 100 Resilient Cities (both funded by Rockefeller Foundation), Making Cities Resilient campaign from United Nations International Strategy for Disaster Reduction (UNISDR), and the UN-Habitat's City Resilience Profiling Programme and many others. These initiatives have been serving as platforms to trigger local adaptation outcomes and disaster resilience.

Responding to the rise of climate risks and disaster vulnerabilities in Asian cities and the needs to build adaptive capacity of the city's governments in Asia, the Rockefeller Foundation, through the \$59 million multiyear project, namely ACCCRN, has been supporting 50 secondary cities during 2009–2016 including its two pioneering cities in Indonesia—Semarang City and Bandar Lampung City—to help these cities develop a resilience strategy and build resilience [2].

Three specific adaptation outcomes of ACCCRN in Indonesia include (1) an improved capacity to plan, finance, coordinate, and implement climate change resilience strategies in the selected cities, (2) shared practical adaptation knowledge to address climate change and deepen the quality of awareness,

engagement, demand, and implementation by the selected cities, and finally (3) expansion and/or replication of the ACCCRN models for urban resilience-building in other cities [3,4].

Institutions matter because they are instrumental in systematically adapting to global climate change, reducing disaster risks and building resilience [1]. Without institutionalised action, risk reduction and climatic change adaptation remains ad-hoc in many urban settings. This study investigates the experiments of institutionalising climate adaptation and resilience agendas initiated and implemented by ACCCRN project during 2009–2016 in Semarang City (Figure 1), Indonesia. The key questions include: how urban stakeholders and policy makers negotiate and come to terms with potential forms of institutional scenarios crafted to tackle climate change impacts and disaster risk reduction (DRR) in cities? And how urban stakeholders negotiate institutional pathways for sustaining climate risk governance and achieving resilience? This study contributes to the debate on how to make climate change resilience a local reality by understanding challenges and opportunities faced by local actors in mainstreaming urban adaptation.

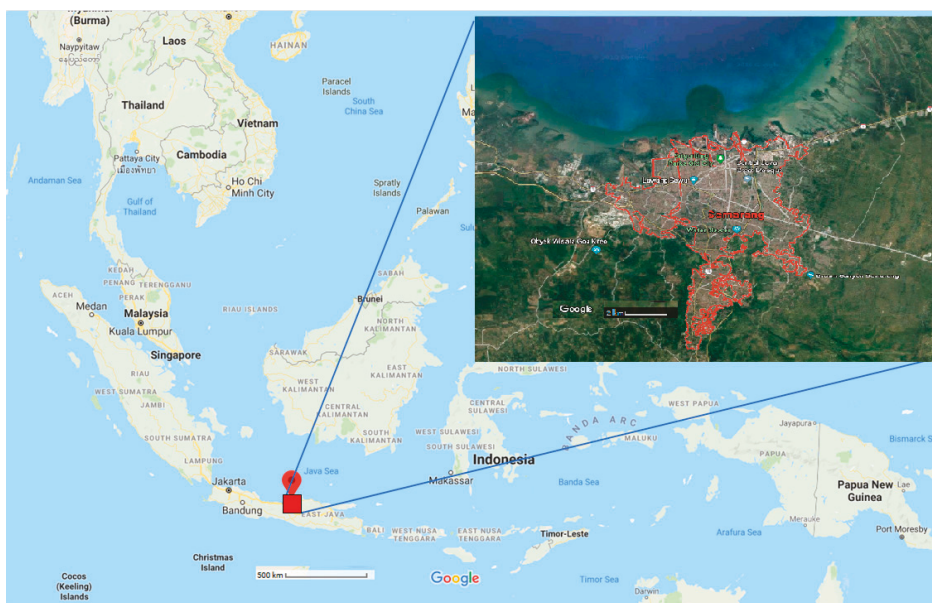


Figure 1. City of Semarang Map.

As an institutionalist scholar, the author is motivated to show how institutionalism is used to institutionalise various agendas into institutionalised anticipatory adaptation and disaster risk reduction. This paper adopts the understanding of institutional change as a result of complex interplay between institutions and agents [4]. Institutions refer to formal and informal constraints while agents refer to actors such as local champions and organisations such as local governmental departments and NGOs.

2. Theoretical frameworks: Institutions, Institutionalism, and Institutionalisation

Institutions matter because they have become instrumental in making life and death decisions [5]. Institutions not only define what and who will be at risk from climate impacts, but also amend the way risks are defined, perceived, and acted upon [6]. Douglas North argued that “Institutions are the humanly devised constraints that structure human interaction, which are made of: formal constraints (i.e., rules, laws, constitutions), informal constraints (i.e., norms of behaviour, conventions, self-imposed

codes of conduct), and their enforcement characteristics" [7]. North's vision of institutions suggests that institutions structure beyond human-to-human interactions as they also shape human-nature interactions. Unlike the view of behaviourists, institutionalists view institutions as the causality of the communities' behaviour and disaster risk outcomes [8]. Unmanageable risks and occurrence of preventable disasters indicates a lack of political commitments or an absence of public institutions [9]. Interestingly, while many have been working on institutionalisations of and/or mainstreaming climate change adaptation (CCA) and/or disaster risk reduction (DRR) [10–12], the author argues that there is still lack of critical discussion concerning institutions, institutionalism, and institutionalisation as both output/outcomes and process of adaptation and resilience experiments and interventions. In this paper, adaptation is understood as the human systems' adjustments and intervention to 'moderate or avoid harm or exploit beneficial opportunities' [1]. Despite not being synonymous, this paper uses the CCA/DRR as interchangeable as both have shared spaced in reducing risk, adapting to climatic extremes, and building resilience.

Institutionalism is a general approach to understanding institutions [13]. They matter because each type of institutionalism provides the lenses through which resilience initiatives and solutions are institutionalised. The author argues that institutions can be seen as outputs or outcomes of a long process of institutionalisations informed by institutionalism. Institutionalism is the rationality behind both institutions and the process of institutionalisation. For example, one legislative product, like a law, an act, or a bill, is a product of the long process of negotiation, debates and cooperation involving a wider range of actors as well as a process. Furthermore, one cannot study institutions and institutionalisation of CCA and DRR without clearly understanding the school of thought behind the change of and the formation of institutions and the institutionalisation processes that occur in the real world.

The theoretical approach to institutionalism is divided into "old" and "new" schools of thought. The old school emphasizes analysis of the formal-legal and administrative arrangements of government and the public sector [13]. Translating North's vision above to the context of DRR and CCA, institutions can be defined as an admixture of formal rules (e.g., climate-related bills, disaster management acts) [12]. However, the real world is too complex to be seen from a particular view of institutionalism. The "new" institutionalism deals with informal norms (including values, traditions, and beliefs). Both approaches deal with enforcement characteristics (e.g., coercive instruments that regulate land-use and building practices) that shape the landscape of adaptation and disaster risk reduction policy and implementation.

Figure 2 offers the general framework of institutionalisation of a development solution. It argues that an institutionalised action starts from the vision of resilience with a new discourse exercise regarding the change of status quo and the need for resilience and risk reduction. The translation of a resilience vision into institutionalised action depends very much on the types of institutionalism (which will be discuss in Sections 2.1 and 2.2) that will inform the process of mainstreaming and/or institutionalising adaptation and resilience.

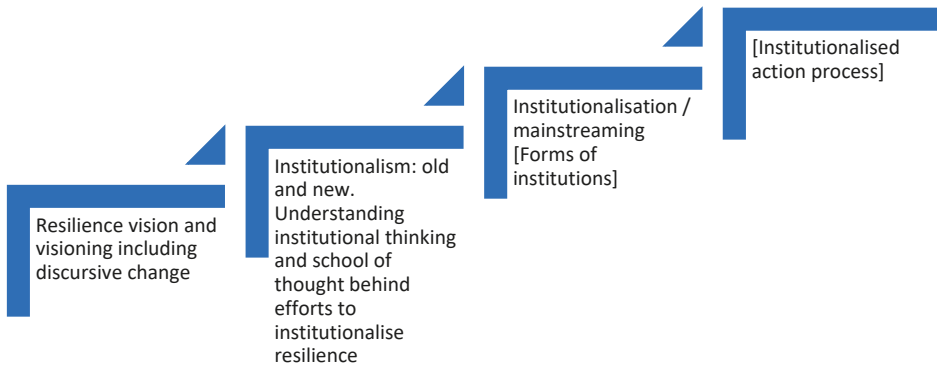


Figure 2. Resilience institutionalisation processes. Source: Author, 2019.

2.1. Old Institutionalism

A formal approach to resilience has been the main research agenda. For example, researchers have argued that the best instrument for addressing CCA and DRR is to work through the existing formal development process and mechanism [12] which can be defined as existing institutional machineries, ranging from formal bureaucratic processes and routines to existing political and social economic institutions and formal/informal processes that deal with the complexity of urban development. Nevertheless, institutionalisation also includes creating new and amending existing regulations, policies, codes, planning documents, and DRR/CCA-related support programmes [12].

DRR/CCA can be a routine development process as they can be embedded or nested inside existing local mechanism and institutions. Integration of risk and vulnerability information into development planning is an example of routinised adaptation and resilience building [14]. Anguelovski and others [15] defined institutionalisations as “linkage to existing urban planning, decision-making, and governance arrangement” [15].

One of the approaches of old institutionalism is often in favour of the roles of international institutions in shaping disaster and climate policy in developing world via the works of the United Nations and international non-governmental organisations (INGOs). Their initiatives can be seen as exogenous adaptation and resilience which can be transformed into endogenous adaptation through time. However, endogenous adaptation does not negate the need for external actors. Their interactions are structured in a way that it is impossible to understand continuity of DRR and CCA unless—as this paper argues—they are understood as an ‘ecosystem of institutionalism’ and/or where the real world of CCA/DRR operates according to complex interaction of institutions, institutionalisms, and institutionalisation. In this paper, the word ‘institutionalisation’ is used interchangeably with ‘mainstreaming’.

The Hyogo Framework for Action (HFA) promoted the norm of institutionalisation that is based on a solid legal formal framework such as a specific legislation which eventually enables governments at different levels to develop comprehensive disaster resilience implementation [16]. UN-Habitat also sees the importance of specific climate-related legislation as a legitimate form of institutionalisation [17]. In the context of CCA, this can mean creating a specific administrative task put under existing environmental agencies [12,18]. HFA and Sendai Framework advocate for ‘strong basis for implementation’ as the institutionalisation process requires a constitutional basis, resource allocation, and the existence of multi-stakeholder platforms to ensure continued commitment and implementation of disaster resilience agenda [19].

2.2. New Institutionalism

The new institutionalism is divided into a few categories including the rational choice approach, the historical pathways approach, and the discursive approach [13,20,21].

2.2.1. Rational Choice and New Economics Institutionalism

Rational choice institutionalism (ROI) views policy response to climate change as an expression of pure rational choice of local actors to maximise their resilience and safety by adopting adaptation and risk reduction [13]. Regardless of the motivation of international donors, ROI also views governmental institutions and local actors in the developing world as rational agents as they approve any adaptation project based on the interest of their local affairs alone. The typical solution to the adaptation problem is therefore education and capacity building. Unfortunately, there has been mounting evidence that suggests human are not fully rational agents as everyone has limited rationality, and often make foolish decisions due to by-default challenges such as such as imperfect information, lack of motivation, limits of cognitive-ability, time-boundedness, and context [20].

North [7] is one of the key sources for new economic institutionalism (NEI) thinking. NEI views that institutional change from risk-ignorant to risk reduction occur because actors are motivated (or not) by incentives and/or disincentives provided by formal/informal institutions. Therefore, institutions incentivise or disincentivise actors' decisions and preferences to reduce CCA and DRR. This can manifest in the form of projects and resources or the lack of it. Future progress of CCA and DRR is heavily dependent on the institutional context that structures the enforcement of and/or the implementation of CCA + DRR agendas. This theory is often called new institutional economics theory [7] and in this paper, incentive is understood as more than monetary value to also include social, cultural, political, and symbolic incentives [20].

2.2.2. Pathway-Dependency Theory

Pathway-dependency often refers to the idea that institutional change occurs not according to rational choice but simply according to historical pathways [20,22]. Local actors' interests in adaptation and resilience is not simply based on knowledge informed by texts books and scientific papers. It is often known as historical regularities in the sense that future pathways (e.g., for urban adaptation and resilience) are simply built on the institutional paths from the past. Institutional pathways also point to the fact that climate disasters and urban crises and their impacts often create complex situations which pose difficulties for local actors to make strategic and rational decisions [22] about CCA and DRR. Consequently, their resilience strategies unfold as they interact with changes in the dynamic relationship between social dynamics and hazardous environments [20,22].

On the contrary, climate change adaptation policy and practice is likely to emerge incrementally in that it involves unpredictable institutional arrangements because ex-ante institutional design might be impossible to be developed by the climate resilience policy entrepreneurs. This implies that resilience strategies at each level of governance are more a result of historical interactions than of anything planned [22]. Such historical interactions include local and international interactions where endogenous climate change policy making can only be made if there is adequate exogenous support that trigger and empower endogenous responses [23].

2.2.3. Discursive Institutionalism

Discursive institutionalism aspires institutional changes through the roles of ideas and ideation. The roles of agents' "discursive abilities" [21] is critical to institutional change. This theory assumes a more dynamic and agent-centred approach to institutional change. The institutionalisation of new alternatives or approaches such as climate resilience within an already established institutional stream can be explained by discursive institutionalism. In the real world, roles of local champions can be seen as institutional solutions to unfamiliar agendas like climate change adaptation [24]. Without new ideas

and new ideation exercise, the status quo remains. New ideas provide the opportunity to depart from the status quo. In trying to drive climate change adaptation agenda, discursive abilities of local actors are instrumental for change. The practical instruments for discursive exercises can manifest in the form of local champions [24], public relations and awareness, transmission of knowledge and ideas, training and capacity building, and so on.

2.3. Hybrid Institutionalism

Mainstreaming or institutionalising CCA/DRR in a modern urban context requires a multiplicity of efforts. Global champions such as Roberts [10] narrate long-term evolution of the process of climate change institutionalisation in the development context of Durban, South Africa. Roberts offers a practical framework namely ‘institutional marker’ where she identifies institutionalisation or mainstreaming of resilience via a multipronged approach including: first, the existence of a local champion that serves as a messenger and climate policy entrepreneur, second, the adoption of certain climate change issues in municipal plans, third, resource allocation (human and financial) for climate related issues, and fourth, climate change becomes an important factor in both political and administrative decision making.

Table 1 offers a summary of mainstreaming adaptation options that are complementary in nature. These strategies are flexibly selected by local stakeholders as they see fit and necessary. This suggests that a mixture of formal and informal approaches is needed. Furthermore, a hybrid approach suggests that local reform occurs in the context of complex interaction of local and international actors, as well as state and non-state actors. This also suggests the reality in formal institutional settings are characterised by informalities. This can mean local champions adopt certain ideas or discourse that can be introduced informally. This kind of policy change tends to assume that actors and new ideas must come first (See Roberts [10]). This is later followed by processes (formal and informal) that lead to change in formal development plans and fiscal allocation that occurs in both political and formal administrative settings. Nevertheless, institutionalisation may also mean small changes such as adding new job descriptions of city administrators, training and guidance for local officials, and tweaking developing monitoring and evaluation tools that are sensitive to climate change [1]. Therefore, the author argues that institutionalisation of adaptation and resilience take place at the discretion of and interests of empowered local actors.

2.4. Climate Risk Governance Concept in Urban Context

Public governance means governing beyond the conventional governmental power to include different actors including all non-governmental organisation (NGOs) including civil society organisations, non-profit service providers, and business groups [13,20]. Therefore, climate risk governance and/or disaster risk governance concept suggests the polycentric nature of decision making in solving urban climate problem [20]. Furthermore, climate risk governance suggests that there is positive power exercised by external actors as they promote urban climate resilience to be endogenised [23]. ACCCRN is therefore treated here as an example of how urban climate risk governance is exercised where each player ranging from local (from government and NGOs) to international actors (international donors, international NGOs, think tanks) negotiate and shape the process of institutionalising resilience and adaptation.

Table 1. Hypothetical options for institutionalisation and mainstreaming adaptation. Source: Author, 2019.

Types of Institutions	Type of Institutionalisation	Type of Institutionalism	Timelines and Remarks
Formal approach	Legislation	Old institutionalism	Long-term implication—Potential stable budget allocation; Required political process and deliberative
	Mayor regulation	Old institutionalism	Mid-term; Required executive commitments
	Mid-term development plan	Old institutionalism	5-year period; Depending on drafting process
	Annual development plan	Old institutionalism	Short-term; Depending on context
Formal approach	Establishment of specific department	Old institutionalism	Mid- to long-term; Depending on legislative mandates
	Fiscal allocation	Hybrid approach	Short-term to long-term: required stable political commitments
	Adding specific tasks and agendas to departmental plan	Hybrid approach	Short-term based on local actors' discretionary power
Informal approach	Compliance to United Nations framework	Path-dependency and New economic institutionalism (NEI)	Timelines depending on the nature of the framework
	Ideation through local network	Discursive	Short- to long-term; Depending on incentives
	Ideation through local champions	Discursive	Short-term; Depending on incentives
	Ideation through international networking	Discursive and NEI	Short- to long-term; Depending on incentives
	NGOs/CSOs driven initiatives	Path-dependency theory	Short- to long-term; Depending on incentives
	NGOnising formal process	Path-dependency theory	Short- to long-term; Depending on incentives
Hybrid approach	International initiatives and projects	New economic institutionalism	Short- to long-term; Depending on incentives
	Education and training	Rational choice theory	Capacity building
	Multi-stakeholder forums or platforms	Discursive	Short- to long-term; Depending on incentives to run the platforms
	Vulnerability analysis documents	Discursive	Short-term; Updating is needed—depending on incentives
	Shared-learning dialogues	Discursive	Project lifetime; Depending on incentives to run the platforms
	Resilience strategy document	Discursive	Short-term; Depending on incentives
Hybrid approach	Systematic documentation	Discursive	Project lifetime; Depending on incentives
	Conference and seminars	Discursive	Project lifetime; Depending on incentives

Noted: NGO is non-governmental organisations; NGO-nising means, the process of institutionalisation of resilience using an NGO-like structure, such as foundations and/or associations.

3. Methods

The author used both exploratory research and longitudinal observations to understand the evolution of institutionalisation processes during the year 2009 to 2016 and post 2016. The participant observations and stakeholder interviews using open-ended interviews with 10 key informants recruited through snowball selection from June–December 2012 (face to face in Semarang). Participant-observation in several meetings including one conference in Surabaya in December 2015. Triangulations were made based on numerous approaches, including desk research, online observations from posted links, ACCCRN websites, published formal planning documents, and City of Semarang websites during 2012–2018. Qualitative analysis was applied to the analysis of the findings.

4. Findings: Mainstreaming Adaptation in Semarang City

Unless otherwise state, Section 4 is mainly informed by the field works during 2012 and personal observations including online observation completed during 2015–2018. To avoid confusion, all the personal interviews will be indicated as ‘personal communication’ when cited in the next sections.

4.1. Vulnerability and Risk Context

Semarang City has been increasingly affected by flood risks and severe coastal inundation. There are currently approximately 1.6 million people living in the city with average density of 4000 people/KM-2 in 2016, where some sub-districts, especially its vulnerable North Coast, host more than 11,000 people/KM-2. The city is also sinking due to the high rate of land subsidence which continues to occur at the rate from 1 mm/year to 10 cm/year. Some parts of the North Coast of the city already experience about 12–18 mm/year [25]. As of today, it is estimated that about 7 percent of the city’s area have been inundated, significantly affecting a large population and many strategic assets such as the seaport infrastructure [26]. The main reason for the rise in risk level and vulnerabilities is the wide spread of urban settlements that has taken place over the last four decades [25]. The situation is likely to exacerbate in the future due to increases in mean sea level.

4.2. Asian Cities Climate Change Resilience Network (ACCCRN) Processes and Semarang City Team Formation

The ACCCRN project seeks to imprint new adaptation pathways within cities through the urban climate governance processes [27] which unfolded in four phases. The first phase (starting 2009—the introductory phase) involved city selection and early shared learning dialogues (SLDs) where city stakeholders were invited to participate and were able to learn and share climate change and other urban development issues [28]. SLDs is critical part of ACCCRN’s urban governance framework as it emphasised on capacity building and shared learning [4].

During the second phase (2009–2011), ACCCRN worked through a multi-stakeholder forum, namely City Team, to complete a vulnerability assessment (VA) on the citywide scale. Following the VA, the City Team, in coordination with ACCCRN Indonesia (Mercy Corps) and the Rockefeller Foundation, conducted pilot projects and sector studies such as rainwater harvesting. The third phase (2011–2013) included the completion of the city resilience strategy (CRS) and the development of concept notes towards prioritised intervention (Figure 3). Physical project implementation occurred in the third phase. The final phase included engaging and influencing process at a national level. This included efforts to expand the approach to fifteen other cities that had shown strong interest in replicating resilience building processes [2].

During the early set-up (during the 2009–2011 period), a Semarang City Team (SCT) was formed, composed of an advisory team and a technical team. The advisory team consists of representatives from the city government, led by the city’s executive secretary under the Mayor, and the technical team consists of representatives from municipal government agencies, local universities, and local NGOs. The role of the SCT was crucial, as the members were to monitor, control, organise, conduct studies,

manage projects, and report on all activities, processes, and methodologies applied under ACCCRN. The City Team was mandated to lead, facilitate, and catalyse the development of the city resilience strategy document and to institutionalise the strategy for long-term development. SCT had been the backbone of the climate resilience initiatives and emerged as a collective decision-making body.

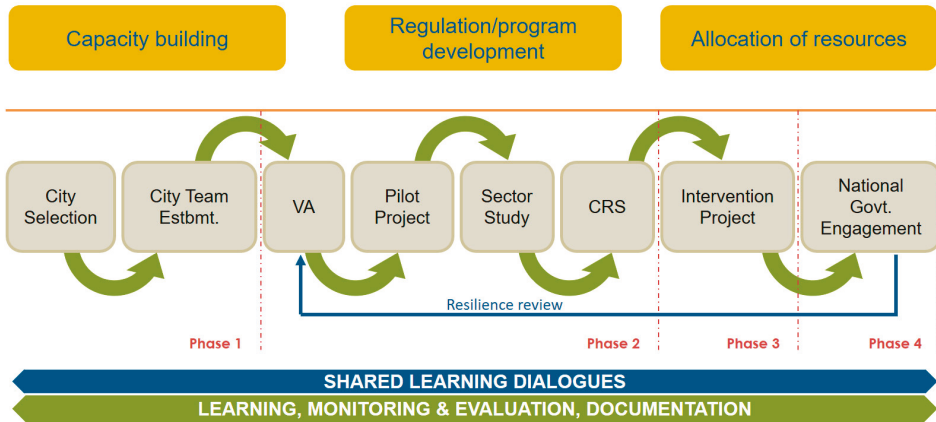


Figure 3. Asian Cities Climate Change Resilience Network (ACCCRN) Typical Process in Semarang City. (Source: Sutarto [29])

The ACCCRN Indonesia country strategy 2010–2013 focused on four key activities to ensure continuation of the interventions after the project. First, to manage the project implementation in the city, targeting the capacity-building of City Team members, transforming the City Team into a city climate change resource centre, and facilitating external support for the city government. Physical project implementation included the establishment of flood warning systems and the capacity development of the local communities to conserve the mangrove ecosystem in the coastal areas of the City [29,30]. Second, to disseminate the ideas and educational materials of urban climate change resilience through multiple means such as social networks, conferences, and workshops. Third, to link up with the national government ministries. Fourth, to scale-up projects through the national associations of cities governments and other national and international networks [29].

4.3. Kickstart of Project as First Level Institutionalisation

Governments are formal institutions. Therefore, driving new innovation with and by governments requires some formal basis. ACCCRN in Semarang City formally began with decision letters from the mayors. City’s leadership was a key variable for this initial stage. The decision letters mandated the formation of the SCT (see Table 2). No other formal regulation was created at the city level to support the initiatives. In Indonesia’s legal hierarchy, a decision letter from a mayor does not have good enough power to generate and mobilise both human resources as well as fiscal allocation to implement any innovative action.

Table 2. Evolution of climate risk governance in Semarang City. Source: Author, 2019.

Governance Variables	Agenda 21	Disaster Management	Urban Climate Change Resilience Arrangement Since 2009
Timeframe	Semarang Agenda 21 2001	Existing structure since 2010	2009–2011 2011–2015 Since 2015 towards Post-ACCCRN
Nature of the organization	Multi-stakeholder forum	Government agency	Multi-stakeholder platform NGO/association
Leadership	Single departmental leader	Single departmental leader	Appointed coordinator— Head of Development Planning Agency Recruited executives
Decision making model	Top down	Command and control—top down	Shared decision making Board member
Chief executive	Head of Environmental Protection Unit	City Secretary	Head of Planning Division of Development Planning Agency Executive director
Executive secretary	Head of Environmental Protection Unit	Head of BFPBD	Secretary of Development Planning Agency NGO Manager
Membership	Loose membership	Single agency	15 members (city government staff, local NGOs and local universities) Individual members of the present city team
Funders	World Bank	APBD	ACCCRN External funders
Quantity of public consultation	One-off workshop	n/a	Regular meeting—monthly Internal arrangement

Note: BFPBD is the local disaster management office.

Therefore, in order to keep adaptation agenda on top of the city development plan, SCT must be able to create some spaces that allow them to work with limited resources. ACCCRN provided basic resources that can help by jump-starting the city to tackle climate change and urban risks. Two years after the launch of ACCCRN in Semarang, a small reform took place in the government of the City of Semarang where the Department of Development Planning (Bappeda) that used to be a less influential department in the past was revitalised to be a stronger planning institution. Bappeda has been mandated to not only coordinating city planning but also monitoring and evaluating city departments and all sectorial development. In reality, Bappeda had just been functioning as a positive advocate for any innovative policy including climate resilience ([31], personal communication)“ Bappeda now is just like a sharp knife’ because the agency has started to re-establish its mandates not only as a gatekeeper and quality controller for city development planning agenda but also as a sharpener of development ideas and proposals” ([32], personal communication).

4.4. City Resilience Strategy

ACCCRN facilitated the drafting of City Resilience Strategy (CRS)—a fundamental framework that aims at guiding the city to develop policy anticipating and addressing future impacts of climate change. The key features of CRS include a document containing broad adaptation agendas and guidance, prepared by local stakeholders and local government, vulnerability and risk context, organised evidence and analysis justifying adaptation interventions, priorities for resilience actions, consistency with existing planning documents and processes that are fit to local institutional settings, guidance for the private sector and civil society groups to design and implement their own adaptation actions, and linkage and coordination with complementary activities for donors and other funding [3,23,29].

The purpose of the CRS document was also to inform other development policy documents in Semarang City such as the Mid-Term Development Plan (RPJMD) documents. One of the reasons for this adoption is because the Chief Executive of the SCT and the Bappeda Head of Planning Unit happened to be the same person. The City Team was managed under the leadership of city development planning department (Bappeda). This coincidence allowed the CRS to inform the mid-term development plan (RPJMD) for the 2010–2015 period and Semarang Spatial Planning 2011–2030 ([31,33], personal communication). Prior to the CRS document, climate change-related discussion via shared learning dialogues (SLDs) have been directly ‘fast tracked’ into policy and practices ([34], personal communication). For example, the adoption of CRS recommendations such as rainwater harvesting, and a flood early warning system have been adopted as both policy and programmes in the city [30] and reference ([31,32], personal communication). The inclusion of adaptation agenda depends on the existence and commitments of local champions in the planning process as well as fiscal capability. One of the current issues is, VA and CRS documents might have been outdated and the question is how the actors allocate resources to update the documents?

4.5. Local Champion and Leadership

Effective progress towards building resilience in Semarang City has been associated with the roles of local champions. But local champions cannot be easily hand-picked and strategically planned. It took two years for the project to ‘recruit’ one of the most notable champions, Mr. Purnomo Dwi Sasongko (hereafter Purnomo), who was later elected as the Executive Secretary of the International Council for Local Environmental Initiatives (ICLEI) of Southeast Asia. He joined the SCT in Semarang in 2011 and was soon after promoted as the Head of the Planning and Infrastructure Unit of Bappeda. “Mr Purnomo was the key climate risk communicator and ‘ACCCRN spokesperson’ to the city’s high officials, such as the head of Bappeda and the mayor” ([34], personal communication). He was aware that climate risk communication and strategic sense-making among the city departments are the necessary conditions to create critical awareness regarding the importance of climate integration into city development. Purnomo believed that Bappeda remains the city coordinating body overseeing

annual development plans from 32 departments (a.k.a. local government units shorted as SKPDs) ([31], personal communication).

“Communication is key to all the cities departments. I have to find a proper message that is suitable for the respective department” ([31], personal communication). Purnomo proactively communicates CRS to cities’ department focal points by making sense of the need to address climate change within the city departments (SKPDs) ([31,32], personal communication). “To the Public Works department, I could clearly articulate the linkage of drainage maintenance with climate adaptation. As a planner who only recently transformed myself from being a relative climate ignorant to be a climate advocate within the city planning departments, I believe that adaptation can be linked to many urban sectors, from public works to marine and fisheries, water resource management, disaster risk management, environmental services and protection, health, etc. Furthermore, Adaptation is not an extra task for city departments if the key staff in the departments understand how to integrate climate change adaptation into existing issues” ([31], personal communication). Both CRS and VA documents are considered ‘academic inputs’ to the local government. ‘The city needs to deepen the climate adaptation details’ ([31], personal communication). Regardless, both CRS and VA were noted as legitimate document that can inform mid- to long-term city planning ([31,34], personal communication).

4.6. Resilience Agendas in Development Planning Documents

There is solid evidence that the CRS document has been adopted into the mid-term development plan (RPJMD) 2010–2015, where it mentioned climate change six times including the fact that it recognised climate change impacts to city infrastructure such as road construction, as the rainfall drops become less unpredictable, road construction quality is compromised [35]. Furthermore, the document explicitly shows that climate change becomes a routine business of the Environmental Protection Department and formally budgeted about US\$ 1 million a year during 2011–2015 with a focus on urban waste management ([35], Appendix 1 p. 13). Furthermore, there is a clear view that spatial planning is key to mitigate and adapt to climate change ([35] p.V-18 and VI-12).

Interestingly, climate change is still mentioned eight times in the RPJMD 2016–2021, mostly in the introduction. The document also briefly contains risk and vulnerability information. There is an earmarked budgeting for CCA (budget line 2.05.28), allocated for mangrove restoration each year about US\$ 275,000 or about a 75 percent decline from previous RPJMD 2010–2015. Unfortunately, it is becoming more realistic than the previous mid-term development plan. Also, the government is aiming at creating 28 climate resilience villages (namely Kampung Proklim) by the end of 2021 ([36], p. VIII-14). The RPJMD 2016–2021 was later revised in 2017, where there is a new budget earmarked as “areas that have the capacity for adaptation and mitigation” with a budget plan from about US\$ 425,000 in 2017 to about 625,000 in 2021 to cover all areas ([37], p. VI-14).

4.7. Fiscal Capability and Allocation

Cities can generate higher (fiscal) capacity and welfare that can assist their urban population to reduce existing risks [38]. In Indonesia, local opportunities for climate adaptation can be created through self-sustaining incentives that directly shape adaptation imperatives. The increase in cities’ capacity to reform their local tax and retribution and curb corruption in tax collection, as demonstrated by Bandar Lampung City [18], is key to boosting fiscal capacity so cities can have greater freedom to invest in the sectors that challenge them most.

The issue is how local actors can sustain the CCA/DRR agenda, commitment, and discourse within the city. One transformative dimension of the ACCCRN initiative is that the Semarang City Planning Agency recently acknowledged the fact that almost all the coastal areas in Semarang are owned by private firms, making it particularly difficult to create mechanisms for coastal protection ([31], personal communication). The city faces serious governance challenges and financial burdens in buying back the coastlines. The SCT influenced the city officials to plan to buy back some of the coastal lands for public access ([31,32], personal communication).

The high visibility of urban risks such as the heavily inundated Northern parts of Semarang City has made it easier for the rest of the city departments to consider climate change adaptation in the annual budget allocation. Transformation is seen at the discursive level. There were adoptions of some proposed activities from the CRS document into annual programme and projects. For instance, at the earmarked budget line, there was no single indication that the Environmental Protection Office (BLHD) had made allocation for addressing the impact of climate change during 2005–2010 budgets. While for the 2011–2015 period, the city started to allocate US\$10,000–12,500 annually to either host regular meetings of the SCT or to allocate annual budgets to scale-up rainwater harvesting and mangrove ecosystem development during 2011–2013. Climate change was budgeted under the 5th programme of BLHD, namely ‘protection and conservation of natural resources’ in 2011–2013. The amount seems trivial, but the discourse behind the allocation is an important first step towards bolder action.

Since the fiscal capacity of many cities in Indonesia has increased in the last 10 years [18], Semarang City has the capacity to fund its own climate adaptation activities in the future. During the 2012 fiscal period, under the flagship of ‘climate adaptation’, the city managed to allocate US\$ 100,000 to buy back some hectares of coastal land ([31–33], personal communication). In the future, the plan to buy back land is expected to continue as long as the land value goes down as a result of nearly permanent inundation in the northern part of the city.

4.8. NGOisation of Formal Platforms?

NGOisation is defined by the author as a form of institutionalisation in that the multi-stakeholder platform comprises of governmental and non-governmental actors (including NGOs, academics, experts, private sectors and others) have been transformed into into an NGO-like structure. Such transformation, at least in theory, allows the actors to use it as a vehicle to carry on the mandate of adaptation and resilience in more flexible ways.

To ensure that adaptation outcomes can be sustained after the exit of ACCCRN in 2016, the SCT members negotiated to establish a working group or a unit outside the government that may be useful only for conducting objective studies to inform city planning ([31], personal communication). At least three scenarios have been discussed by members of the SCT concerning how to endogenously sustain climate change intervention in Semarang City beyond 2016, after ACCCRN.

The first scenario was a voluntary mechanism. This suggests that committed individuals from city departments who could influence from within using their discretionary roles in planning at sub-department and department levels. Their personal network with the higher authorities was vital to promote the idea of urban sustainability and adaptation. This option was limited. It requires committed leaders at all levels, and reality suggests that the city does not have this luxury all the time ([31,33], personal communication). In fact, there is only a small minority of positive deviant bureaucrats that function as climate goal-keepers in their own departments as well as city secretariat levels.

The second scenario involved mandatory mechanisms, which works through formalised processes with clear mandates and responsibilities as in the case of Surat [39]. Therefore, city resilience-building should be translated into formal rules that provide mandates for the relevant city institutions. This suggests that the city institutions will decide focal points (persons) that may (not) be fit for the task of being climate advocates. This requires two approaches that may complement each other. The first was having a strong formal scenario where there should be a regulation translated into annual operation (e.g., protocol or standard operational procedures) for planning and financing the city. This further requires changes at higher levels, e.g., a Ministry of Home Affairs (MoHA) regulation that mandates city governments to consider climate change as a cross-cutting issue. The second approach is a less formal scenario where local governments, at least at the mayor and legislative levels, can co-create climate regulation/legislation informed by the CRS document.

The later scenario can be achieved through three steps. The first is to create a mayoral regulation that could function for five years, suggesting that city departments work according to the mayor’s interests as reflected in the regulation. This can be done at any time as long as the mayor is interested

in and committed to the issue. Second, the mayor's five-year development agenda, reflected in the city's mid-term development plan (RPJMD), must cite or adopt a climate adaptation agenda from the CRS document. This scenario later materialised in the last two planning documents [35–37]. Third, a more long-term approach is that the city can create a local regulation, that can be drafted and endorsed by the mayor with or without the support from the city legislators. The later process involves a lengthy process including political lobbying with some degree of uncertainties.

The third Scenario involves transforming the present SCT into an NGO-like structure ([40], personal communication), where it can maintain its flexibility and interest in promoting climate change adaptation by working through personal contacts among the city's decision-makers. This option, of NGOisation, in theory could work in the short term. It would already have been exercised in many places in Indonesia where strong environmental NGOs have been working over the last decades. However, strong environmental NGOs do not always succeed in the long run especially when the local political and administrative context change and funding mechanism for NGOs is not certain.

What is interesting is the view of the SCT that functions as a hub of knowledge (or rather as a discursive machine) and technology transfer for climate adaptation. Technology transfer is exemplified by the transfer of technology and knowledge of flood early warning system and appropriate breakwater technologies to protect mangroves [30] and reference ([34], personal communication). Interestingly, the successful technological transfer from ACCCRN can be seen as a direct outcome of its unique approach as it provided multiyear projects that guarantee deeper engagement with local administration and allowing climate change discourse to penetrate in the city structure in a rather informal fashion [30,41].

SCT members are aware of the high turnover of knowledgeable officials at middle and high ranks in public administration in many city/district departments have become a challenge in local governance. This will eventually lead to a lack of institutional memory within many local government offices. New mayors might mean new programmes and new ignorance ([31–34], personal communication). This awareness motivates the empowered officials and stakeholders to develop a structure that allow them to be drivers of CCA knowledge sharing beyond the City of Semarang.

Finally, as implied by all the scenarios above, institutional barriers are not easy to tackle. The SCT finally decided to transform itself into a CSO-like structure namely IUCCE (Initiative for Urban Climate Change and Environment) (Table 1). IUCCE [42] aims to “help achieve the objectives and foster urban resilience to climate change and changing environment”. While this problem has been identified, it has become less clear how future climate governance in the city of Semarang will evolve under the UCCE regime.

A closer look at the work of IUCCE indicates that the organisation has been playing roles as a think tank that works beyond the city's jurisdiction. Some of the knowledge products include technical guide on community-based disaster risk reduction, documentation of knowledge concerning mangrove and flood early warning systems etc. While IUCCE can still be functional as an informal “City Team”, it is safe to argue that investment of ACCCRN has been clearly successful in terms of knowledge and technological transfer.

4.9. 100 Resilience Cities Project in Semarang City

Climate change, including climate risk reduction, remains a marginal task under a few departments including environmental protection department where a few climate adaptation activities (especially mangrove planting) are budgeted for RPJMD 2016–2021 ([36], Section 3.6). While the DRR agenda remains at the discretion of local emergency management agency, for CCA however, based on the lessons during 2011–2015, the actual fiscal allocation does not reflect the budget as proposed by the planners.

After the ACCCRN, the formality of STC is not diminished even though incentives for regular activities, pilot projects, as well as adaptation projects such as flood warning systems ([31], personal communication) have literally come to an end, while at the same time, the Semarang City graduated

from ACCCRN into the new initiatives, namely 100 Resilience Cities project funded by the Rockefeller Foundation [43].

5. Discussion

5.1. Institutionalisation: Formal and Informal

Old forms of institutionalisation that emphasise the formal approach for reform in formal policy settings remains the imperative of global framework and initiatives. The Hyogo Framework for Action and Sendai's norm of institutionalising resilience can be exemplified by the process of mainstreaming in Surat with the formation of the Climate Change Trust based on the Public Trust Act at state level [39]. However, context shapes the forms of institutionalisation as it can manifest as a general climate policy or specific DRR plan (case of Quito, Ecuador). Institutionalisation can also mean a shift from a resilience strategy that led to the endorsement of the Climate Change Trust (case of Surat, India) [15,39]. Such legal formal achievement in Surat remains to be seen in the City of Semarang as it requires a long local political process. It is also clear that some of the achievements such as resource allocation have been endogenously provided by the executive government in Semarang City, as also noted in the other study such as, Durban [10], Surat [39], and Bandar Lampung City [18,23].

The findings suggest that institutionalisation process take place in several domains, including formal development planning. In terms of institutionalised practice, CCA has become a key task of the local environmental agency while DRR is seen as the task for the local disaster management agency. Such an achievement is predictable, as informed by previous research in different context [12] as well as in Indonesia context [18,23].

In the context of Indonesia's national disaster risk reduction policy reform, institutional change started from legislation and followed by the creation of new administrative units to deal with broader disaster risk problems. Equivalent processes did not occur for climate change adaptation at a national level. In the absence of national guidelines for cities to be adaptive to climate change, secondary cities in the developing world often create their climate adaptation policies and practices through external influences, as exemplified by different ACCCRN cities in India and Indonesia [39,44].

5.2. Hybrid Approach to Institutionalisation

Local institutional uncertainty has made future adaptation in cities less predictable. Previous studies suggest that the negative outcomes are particularly due to little stability at public administration and bureaucratic levels, because the local government sector has been affected by dynamic political change and decentralisation. This has been quite clear from the other ACCCRN pioneering cities such as Bandar Lampung [23].

The process of adaptation in cities involved the complex process of exogenous and endogenous efforts in building resilience. While it seems almost impossible to fix the institutional mechanism under the project timeline, the local actors used a rather pragmatic approach to institutionalise climate action. The agenda of hybrid institutionalism has led to pragmatic institutionalisation as it goes beyond what was once seen as multi-pronged approach [10].

Local champions exercised their discursive power. Their network and platform serve as guardians and gate-keepers of city planning, as seen in Western Cape, South Africa, where climate policy entrepreneurs have been the key to adaptation mainstreaming [45]. Their impact can help reduce institutional uncertainty temporarily. The challenge is, local champions and good leadership are often 'given' and cannot be easily planned or recruited in advance.

Responding to the challenges at local and national levels where climate adaptation agenda remains unclear and local capacity remains low, Sharma and Tomar [44] suggested pragmatic solutions namely 'entry points' including embedding adaptation and resilience through existing development and disaster management plans. The first ACCCRN process during 2009–2014 (Section 4.2) are the entry points. To gain quick wins, the 'entry points' approach has also been promoted by some researchers,

such as in Reference [46]. The framing of ‘entry points’ indicates the nature of exogenous intervention. However, the challenge is how to win at the ‘exit point’ after the end of international projects remains an important issue for local actors.

The pragmatic approach also requires working with local proponents such as local champions as they can be seen as ‘institutions’ as they not only create their own rules of the game but play the roles as both goal-keepers and climate policy entrepreneurs. The champions have been the key officials from within existing institutions whose strong passion and interest in promoting innovation within the local government level were seen as vital [47–49] and Reference ([50], personal communication). These champions tend to have a balanced self-interest and public interest in promoting climate resilience agenda not only in Semarang but also in other ACCCRN cities such as Hat Yai City, Thailand [51]. This satisfies the rational choice theory approach as they acted based on their best interest. However, their inability to jumpstart adaptation without external aid suggests that their engagement is largely driven by their interests in incentives created by the projects. This justifies that NEI is the mechanism that helps local actors sustain CCA agendas.

The pragmatic approach to institutionalising CCA also includes the strategy of NGOisation of the SCT platform. It has been partly used by the actors as a strategy for institutionalising climate change adaptation and resilience building in Semarang City. NGOisation is an approach where urban stakeholders come to terms with the dynamic nature of complex realities of city development. This mechanism is used to solve institutional uncertainty in the city. While at the same time, the key actors continue to benefit from the existing formal mechanisms, such as continuing to use the platform of STC and others (e.g., 100 Resilient Cities Project funded by the Rockefeller Foundation) and existing departmental commitments related to climatic risks ([50], personal communication). Interestingly, the setup of IUCCE as a think tank in Semarang is favoured by most of the SCT members in Semarang City as they see that this ‘NGO-like’ structure can provide a balanced self-interest and public interest in promoting climate resilience.

5.3. Transforming Urban Adaptation Platforms into Permanent Institution?

Global disaster risk frameworks such as the Hyogo Framework for Action and its predecessor, the Sendai Framework for disaster reduction (SFDRR), have promoted the idea of multi-stakeholder engagement, namely DRR platforms (UNISDR 2005), that are supposed to exist at different levels from global to national to local levels of governance. ACCCRN’s City Team in Semarang City can be seen as a CCA/DRR platform or forum. Forums can be seen as institutions as each forum has its own rules of the game. Small groups in any settings that meet regularly suggests that they are bounded by certain values and interests and their rules of the games function as the institutional avenue for them to continue to repeat their interactions [52] until they breakup and the game does not benefit the members.

Therefore, urban adaptation platforms including disaster management platforms are in themselves part of institutional development. Unfortunately, there are always costs associated with regular run of forums and platforms. Empirically speaking, local and national multi-stakeholder platforms have been established in many parts of the world including Indonesia [53], where some were more functional while others were simply function as institutional decoration.

5.4. Path-Dependency Theory as a Predictor for Urban Adaptation?

The challenge in the City of Semarang today is not entirely new as in the case of the Semarang Agenda 21 way back in 1997/1998. Semarang City was among the first Indonesian cities to adopt the sustainability framework of Local Agenda 21. The agenda was locally branded as ‘Semarang Environmental Agenda: Toward a sustainable city 1998–2003’ (hereinafter SEA21) [54]. Semarang City was selected for the pilot project initiated by the World Bank with the acceptance from the Semarang City government ([55], personal communication). Agenda 21 focused on process and trust building as the project conducted extensive consultation with sectoral experts, government officials, NGOs, academics,

and others, which resulted in the 18 chapters of Agenda 21–Indonesia in 1997 [54]. The document identified high- and medium-priority programmes, to be completed in five years (1998–2003) and 10 years (1998–2008), respectively. These priorities included population management, self-resilient community, public transportation, coastal inundation, domestic waste reduction, treatment of human waste, waste management, clean production, healthy rivers, and clean air programmes.

In retrospect, the present institutional pathways for adaptation follow the historical path of the urban sustainability agendas stipulated by SEA21 developed 20 years ago in the same city. To the stakeholders, the most successful contribution of SEA21 to the city administration is the capacity-building ([55], personal communication). The knowledge transfers from the initiative facilitated new awareness for trained staff concerning environmental and urban sustainability. The programme may have been short-lived, but there was a discursive turn within the city's private sectors regarding environmental quality where Bapedalda (Local Environmental Protection Agency or now BLHD) was able to establish a stick-and-carrot approach [56] and reference ([55], personal communication).

Lessons from SEA21 suggested that the process of institutionalising international initiatives such as ACCCRN and others (through formal planning documentation, policy adoption, etc.) often hit the hard wall of local institutions. The issue is not that there was no innovation but innovation in ideas, policies, and practices are often short-lived because such initiatives relied more on persons than systems ([55,57], personal communication). Interestingly, the reliance on persons can be credited as a good start if the persons can play roles as champions with the capability to create adaptation discourse at different levels of governance in cities. The problem is, champions are also timebound. Champions today might not be champions tomorrow as external and internal incentives change through time.

6. Conclusions

This research investigates how local actors negotiate to ensure continuity of CCA and DRR as routine development agenda. The question is how urban stakeholders and policy entrepreneurs negotiate and come to terms with potential forms of institutional scenarios crafted to promote adaptation and deepen resilience in the City of Semarang. The whole arrangements and interactions of ACCCRN from the beginning have been about using different forms of institutionalisation to sustain adaptation and resilience agenda. The continuity of CCA and resilience-building depend on mechanisms where there is regular reproduction of resilience discourse including their urgency and importance at different levels and domains ranging from policy documents to the existence of CCA advocates or champions within the agencies in cities. This goes beyond the binary framework of endogenous versus exogenous initiatives for adaptation.

Hybrid institutionalism has merits to provide better understanding of the complexity around institutionalising urban adaptation in Semarang City. While projects such as ACCCRN have co-facilitated processes that aimed at promoting a more rational choice approach to establish a more permanent mechanism, it turned out that such adaptation initiatives have been trapped in the past institutional trajectory such as NGOising the City Team structure. Lessons from the case of SA21 and the recent development of IUCCE suggests the model of institutionalisation as explained by the theory of historical institutionalism where the 'adaptation pathways' is skewed towards future institutional uncertainty, which makes it difficult for local actors such as the in the City of Semarang to make strategic decisions from within formal institutions [20]. As a result, the STC has transformed itself into an NGO-like structure and served as a think tank instead of policy makers. On the other hand, the emergence of new international initiatives such as 100 Resilient City provides new avenues for the local stakeholders to either restart again or to move forward to the next stages of a city resilient development strategy.

The Semarang City Team has a vision to drive and facilitate a permanent agenda for adaptation and resilience via formal mechanisms. Unfortunately, local dynamic process led these efforts to push the actors from shifting from formal into a more informal approach. The good news is that new

exogenous initiatives remains available via different trajectories as exemplified by the shifts from Semarang Agenda 21, to ACCCRN and to 100 Resilience City programmes. And in between, there is often international frameworks (e.g., among others, the Hyogo Framework or the Sendai Framework) that can be used to ensure resilience discourse remains in the orbits of urban governance.

The author argues that that the (dis)continuity of urban sustainability initiatives, including climate change adaptation and resilience in Semarang city, do occur in the form of hybrid institutionalism but pathway-dependency theory emerges as the most dominant predictor as exemplified by the boom and burst of local platforms ranging from SEA21 to ACCCRN to 100 Resilience City and more into the future. Rational choice thinking and the effort to localise resilience and adaptation often ended up in path-dependency phenomenon where history repeats itself in the form of NGOising the resilience platforms.

Funding: Initial funding was provided by Rockefeller Foundation via ACCCRN Indonesia project managed by Mercy Corps during 2012/2013. Since 2014 this study is self-funded.

Acknowledgments: Personal thanks to Ratri Sutarto, Aniessa Delima Sari, Paul Jeffery, Ninik Mulyawati, Omar Saracho (Mercy Corps) who have been supporting all the logistics of this research in Semarang in 2012. Thanks also to Purnomo (The Head of Planning Unit in Bappeda Semarang), Feri Prihantoro, Lilin Budiarti, Lutfi Muhamad, Gunawan Wicaksono, Raharjo Tjahyono and all colleagues at City Team of Semarang and Jawoto Sih Setyono (Diponegoro University) for kindly supporting this research. The author would like to thank the Indonesia Project at Australian National University for the opportunity to present this draft in late 2016. An earlier draft of this article was published as a Working Paper at the Resilience Development Institute. The author would like to thank the three anonymous reviewers who gave very valuable inputs to improve the previous draft. All the mistakes interpreting the information for the sources are the authors.

Conflicts of Interest: The author received research funds from ACCCRN Indonesia via Mercy Corps. This study is however independent and critical to satisfy scientific interest alone.

Abbreviations

ACCCRN	Asian Cities Climate Change Network
Bapedalda	Local Environmental Protection Agency (old)
Bappeda	Local development planning agency
BLHD	Local Environmental Protection Agency (new)
CCA	Climate change adaptation
HFA	Hyogo Framework for Action
IUCCE	Initiative for Urban Climate Change and Environment
SFDRR	Sendai Framework for disaster risk reduction
STC	Semarang City Team
UN	United Nations
UNISDR	United Nations International Strategy for Disaster Reduction

References

1. IPCC. *Climate Change 2014: Impacts, Adaptation, and Vulnerability. Part A: Global and Sectoral Aspects. Contribution of Working Group II to the Fifth Assessment Report of the Intergovernmental Panel on Climate Change*; Field, C.B., Barros, V.R., Dokken, D.J., Mach, K.J., Mastrandrea, M.D., Bilir, T.E., Chatterjee, M., Ebi, K.L., Estrada, Y.O., Genova, R.C., et al., Eds.; Cambridge University Press: Cambridge, UK; New York, NY, USA, 2014; 1132p.
2. Sari, A.D.; Prayoga, N.; Syam, D.; Theda, F.; Bielman, J.; Pradityo, D. *Climate Change Adaptation towards Urban Resilience: A Journey and Lesson Learnt from ACCCRN in Indonesia, 2009–2016*; ACCCRN Indonesia Project: Jakarta, Indonesia, 2018.
3. Brown, A.; Dayal, A.; Del Rio, C.R. From practice to theory: Emerging lessons from Asia for building urban climate change resilience. *Environ. Urban.* **2012**, *24*, 531–556. [[CrossRef](#)]
4. Tyler, S.; Moench, M. A framework for urban climate resilience. *Clim. Dev.* **2012**, *4*, 311–326. [[CrossRef](#)]
5. Douglas, M. *How Institutions Think*; Syracuse University Press: Syracuse, NY, USA, 1986.

6. Lebel, L.; Nikitina, E.; Kotov, V.; Manuta, J. Assessing institutionalised capacities and practices to reduce the risks of flood disaster. In *Measuring Vulnerability to Natural Hazards: Towards Disaster Resilient Societies*; Birkmann, J., Ed.; United Nations University Press: Tokyo, Japan; New York, NY, USA; Paris, France, 2006.
7. North, D.C. Economic Performance Through Time. In *The New Institutionalism in Sociology*; Brinton, M.C., Nee, V., Eds.; Stanford University Press: Stanford, CA, USA, 1998; pp. 247–257.
8. Underdal, A. *The Causal Significance of Institution*; The IDGEC Synthesis Conference—IHDP Newsletter #1; IHDP: Bali, Indonesia, 2007.
9. Lassa, J.; Surjan, A.; Caballero-Anthony, M.; Fisher, R. Measuring political will: An index of commitment to disaster risk reduction. *Int. J. Disaster Risk Reduct.* **2019**, *34*, 64–74. [[CrossRef](#)]
10. Roberts, D. Thinking globally, acting locally—Institutionalizing climate change at the local government level in Durban, South Africa. *Environ. Urban.* **2008**, *20*, 521–537. [[CrossRef](#)]
11. Román, M.; Linnér, B.-O.; Mickwitz, P. Development policies as a vehicle for addressing climate change. *Clim. Dev.* **2012**, *4*, 251–260. [[CrossRef](#)]
12. Anguelovski, I.; Carmin, J. Something borrowed, everything new: Innovation and institutionalization in urban climate governance. *Curr. Opin. Environ. Sustain.* **2011**, *3*, 169–175. [[CrossRef](#)]
13. Bevir, M. *Key Concept in Governance*; Sage: London, UK, 2009.
14. Heazle, M.; Tangney, P.; Burton, P.; Howes, M.; Grant-Smith, D.; Reis, K.; Bosomworth, K. Mainstreaming climate change adaptation: An incremental approach to disaster risk management in Australia. *Environ. Sci. Policy* **2013**, *33*, 162–170. [[CrossRef](#)]
15. Anguelovski, I.; Chu, E.; Carmin, J. Variations in approaches to urban climate adaptation: Experiences and experimentation from the global South. *Glob. Environ. Chang.* **2014**, *27*, 156–167. [[CrossRef](#)]
16. UNISDR. *Hyogo Framework for Action—Disaster Risk Reduction*; United Nations: Geneva, Switzerland, 2005.
17. Bulkeley, H.; Tuts, R. Understanding urban vulnerability, adaptation and resilience in the context of climate change. *Local Environ.* **2013**, *18*, 646–662. [[CrossRef](#)]
18. Lassa, J.A.; Nugraha, E. From shared learning to shared action in building resilience in the city of Bandar Lampung, Indonesia. *Environ. Urban.* **2015**, *27*, 161–180. [[CrossRef](#)]
19. UNISDR. *Sendai Framework for Disaster Risk Reduction*; United Nations: Geneva, Switzerland, 2015.
20. Lassa, J.A. Institutional Vulnerability and Governance of Disaster Risk Reduction: Macro, Meso and Micro Scale Assessment. PhD. Thesis, University of Bonn, Bonn, Germany, 2011.
21. Schmidt, V.A. Discursive Institutionalism: The Explanatory Power of Ideas and Discourse. *Annu. Rev. Political Sci.* **2008**, *11*, 303–326. [[CrossRef](#)]
22. Kaag, M.M.A.; Brons, J.; de Bruijn, M.E.; van Dijk, J.W.M.; de Haan, L.J.; Nooteboom, G.; Zoomers, A. *Poverty is Bad. Ways Forward in Livelihood Research*; CERES ‘Pathways of Development’ Seminar Paper; Universiteit Utrecht: Utrecht, The Netherlands, 6 February 2003.
23. Nugraha, E.; Lassa, J.A. Towards endogenous disasters and climate adaptation policy making in Indonesia. *Disaster Prev. Manag.* **2018**, *27*, 228–242. [[CrossRef](#)]
24. Leck, H.; Roberts, D. What lies beneath: Understanding the invisible aspects of municipal climate change governance. *Curr. Opin. Environ. Sustain.* **2015**, *13*, 61–67. [[CrossRef](#)]
25. Yastika, P.E.; Shimizu, N.; Abidin, H.Z. Monitoring of long-term land subsidence from 2003 to 2017 in coastal area of Semarang, Indonesia by SBAS DInSAR analyses using Envisat-ASAR, ALOS-PALSAR, and Sentinel-1A SAR data. *Adv. Space Res.* **2009**, *63*, 1719–1736. [[CrossRef](#)]
26. Husnayaen, A.; Rimba, B.; Osawa, T.; Parwata, I.N.S.; Astarini, I.A. Physical assessment of coastal vulnerability under enhanced land subsidence in Semarang, Indonesia, using multi-sensor satellite data. *Adv. Space Res.* **2018**, *61*, 2159–2179. [[CrossRef](#)]
27. Archer, D.; Dodman, D. Making capacity building critical: Power and justice in building urban climate resilience in Indonesia and Thailand. *Urban Clim.* **2015**, *14*, 68–78. [[CrossRef](#)]
28. Reed, S.O.; Friend, R.; Toan, V.C.; Thinphanga, P.; Sutarto, R.; Singh, D. “Shared learning” for building urban climate resilience—Experiences from Asian cities 393. *Environ. Urban.* **2013**, *25*, 393–412. [[CrossRef](#)]
29. Lindsay, J.; Rogers, B.; Church, E.; Gunn, A.; Hammer, K.; Dean, A.J.; Fielding, K. The role of community champion in long-term sustainable urban water planning. *Water* **2019**, *11*, 476. [[CrossRef](#)]

30. Sari, A.D.; Prayoga, N. Enhancing citizen engagement in the face of climate change risks: A case study of the flood early warning system and health information system in Semarang City, Indonesia. In *Climate Change in Cities Innovations in Multi-Level Governance*; Hughes, S., Chu, E.K., Mason, S.G., Eds.; Springer: New York, NY, USA, 2017; pp. 1121–1137.
31. Purnomo, D.S. (Bappeda, Semarang City, Jawa Tengah). Personal communication, 24–25 June 2012; 2 October 2012; 5 December 2012.
32. Lutfi, M. (Bappeda, Semarang City, Jawa Tengah). Personal communication, 15 December 2012.
33. Gunawan, W. (BLHD, Semarang City, Jawa Tengah). Personal communication, 6 June 2012.
34. Delima, S.A. (Mercy Corps/ACCCRN Indonesia Project, Semarang City, Jawa Tengah). Personal communication. 28 June 2012; 11 December 2012.
35. Semarang City. *Mid-Term Development Plan [Rencana Pembangunan Jangka Menengah] 2011–2015*; Semarang City Government: Semarang, Indonesia, 2011.
36. Semarang City. *Mid-Term Development Plan [Rencana Pembangunan Jangka Menengah] 2016–2021*; Semarang City Government: Semarang, Indonesia, 2016.
37. Semarang City. *Revision of Mid-Term Development Plan [Rencana Pembangunan Jangka Menengah] 2016–2021*; Semarang City Government: Semarang, Indonesia, 2017.
38. Lall, S.V.; Deichmann, U. *Density and Disasters: Economics of Urban Hazard Risk*; Policy Research Working Paper 5161; World Bank: Washington, DC, USA, 2009.
39. Karanth, A.; Archer, D. Institutionalising mechanisms for building urban climate resilience: Experiences from India. *Dev. Pract.* **2014**, *24*, 514–526. [[CrossRef](#)]
40. Jawoto, S. (Diponegoro University, Semarang City, Jawa Tengah). Personal communication, 18 December 2012.
41. Taylor, J.; Lassa, J. *How can Climate Change Vulnerability Assessments Best Impact Policy and Planning? Lessons from Indonesia*; IIED Asian Cities Climate Resilience WP Series, No 22; IIED: London, UK, 2015; pp. 1–33.
42. IUCCE. About Initiative for Urban Climate Change and Environment. 2019. Available online: iucce.org (accessed on 10 January 2019).
43. Semarang City. Resilient Semarang Moving Together Towards a Resilient Semarang. 2016. Available online: www.100resilientcities.org/wp-content/uploads/2016/05/Semarang20Resilience20Strategy20-202016.pdf (accessed on 10 January 2019).
44. Sharma, D.; Tomar, S. Mainstreaming climate change adaptation in Indian cities. *Urban. Dev.* **2010**, *22*, 451–465. [[CrossRef](#)]
45. Pasquini, L.; Ziervogel, G.; Cowling, R.M.; Shearing, C. What enables local governments to mainstream climate change adaptation? Lessons learned from two municipal case studies in the Western Cape, South Africa. *Clim. Dev.* **2015**, *7*, 60–70. [[CrossRef](#)]
46. Bahadur, A.; Tanner, T.; Pichon, F. *Enhancing Urban Climate Change Resilience: Seven Entry Points for Action*; Sustainable Development Working Paper Series 47; Asian Development Bank: Manila, Philippines, 2016.
47. Sutarto, R.; Jarvie, J. *Integrating Climate Resilience Strategy Into City Planning In Semarang, Indonesia*; Urban Climate Resilience Working Paper Series #1; Institute for Social and Environmental Transition ISET: Boulder, CO, USA, 2012.
48. Carmin, J.; Anguelovski, I.; Roberts, D. Urban Climate Adaptation in the Global South: Planning in an Emerging Policy Domain. *J. Plan. Educ. Res.* **2012**, *32*, 18–32. [[CrossRef](#)]
49. Sutarto, R. *Building Resilience in Indonesian Cities Case Study: ACCCRN Program*; Charles Darwin University: Darwin, Australia, 2017.
50. Prihantoro, F. (Bintari Foundation, Semarang City, Jawa Tengah). Personal communication, 13 December 2012.
51. Siriporananon, S.; Visuthismajarn, P. Key success factors of disaster management policy: A case study of the Asian cities climate change resilience network in Hat Yai city, Thailand. *Kasetsart J. Soc. Sci.* **2018**, *39*, 269–276. [[CrossRef](#)]
52. Mehta, L.; Leach, M.; Newell, P.; Scoones, I.; Sivaramakrishnan, K.; Way, S.A. *Exploring Understandings of Institutions and Uncertainty: New Directions in Natural Resource Management*; IDS Discussion Paper 372; University of Sussex: Sussex, UK, 1999.
53. Djalante, R. Adaptive governance and resilience: The role of multi-stakeholder platforms in disaster risk reduction. *Nat. Hazards Earth Syst. Sci.* **2012**, *12*, 2923–2942. [[CrossRef](#)]
54. Tjahjono, R. The Semarang Environmental Agenda: A stimulus to targeted capacity building among the stakeholders. *Habitat Int.* **2000**, *24*, 443–453.

55. Budiarti, L. (Training and Education/DIKLAT Propinsi Jawa Tengah, Semarang, Jawa Tengah Province). Personal communication, 13 December 2012.
56. Aden, J.; Rock, M. *“What Is Driving the Environmental Behavior of Manufacturing Plants in Semarang? Implications for Policy-Makers”*; Research Report for USAEP Richard Sheppard Region: Asia; USAID Natural Resources Management and Development Portal: Washington, DC, USA, 1998.
57. Tjahjono, R. (Soegijapranata University, Semarang City, Jawa Tengah). Personal communication, 6 December 2012.



© 2019 by the author. Licensee MDPI, Basel, Switzerland. This article is an open access article distributed under the terms and conditions of the Creative Commons Attribution (CC BY) license (<http://creativecommons.org/licenses/by/4.0/>).

Review

Meteorological and Ancillary Data Resources for Climate Research in Urban Areas

Sorin Cheval ^{1,2,3,*}, Dana Micu ⁴, Alexandru Dumitrescu ^{2,5}, Anișoara Irimescu ², Maria Frighenciu ⁶, Cristian Ioja ⁷, Nicu Constantin Tudose ³, Șerban Davidescu ³ and Bogdan Antonescu ^{8,9}

¹ Department of Aviation, “Henri Coandă” Air Force Academy, 500187 Brașov, Romania

² National Meteorological Administration, 013686 Bucharest, Romania; dumitrescu@meteoromania.ro (A.D.); anisoara.irimescu@meteoromania.ro (A.I.)

³ Torrential Watershed Management Unit, Brașov Station, National Research and Development Institute in Forestry “Marin Drăcea”, 500040 Brașov, Romania; cntudose@yahoo.com (N.C.T.); s_davidescu@icas.ro (S.D.)

⁴ Department of Physical Geography, Institute of Geography, Romanian Academy, 023993 Bucharest, Romania; micudanamagdalen@gmail.com

⁵ Research Institute of the University of Bucharest, 030018 Bucharest, Romania

⁶ Doctoral School of Sciences, University of Craiova, 200585 Craiova, Romania; maria.frighenciu@gmail.com

⁷ Center for Environmental Research and Impact Studies, University of Bucharest, 1 Bd. Nicolae Balcescu, 010041 Bucharest, Romania; cristian.ioja@geo.unibuc.ro

⁸ Remote Sensing Department, National Institute of Research and Development for Optoelectronics INOE2000, 77125 Măgurele, Romania; bogdan.antonescu@inoe.ro

⁹ Faculty of Physics, University of Bucharest, 77125, Măgurele, Romania

* Correspondence: sorin.cheval@afahc.ro or sorin.cheval@meteoromania.ro

Received: 15 January 2020; Accepted: 20 February 2020; Published: 25 February 2020

Abstract: An increasing plethora of both meteorological and ancillary data are presently available for climate research and applications in urban areas. The data are often held by local or national institutions (i.e., meteorological services, universities or environmental agencies). This paper outlines a total number of 33 datasets, organized into three main categories of meteorological data resources (14 datasets) and four categories of ancillary data resources (19 datasets), selected for their potential to support urban climate studies, but also for their free accessibility. Such a collection cannot be exhaustive, but we aim to draw the attention of the scientific community to relevant datasets, freely available at temporal and spatial resolutions appropriate for urban climatology. Each dataset contains information about its availability, limitations, and examples of research in urban areas.

Keywords: urban climate; open data; data sources; urban climate monitoring

1. Introduction

Fast natural and anthropogenic variations have been observed at global, regional and local scale in the recent decades, triggering complex impacts on environment and society, such as biodiversity loss, land degradation, reduced water resources and migration. The world population has experienced continuous growth, and urbanization has brought the people living in cities to 55.2% of total world population [1]. At the same time, climate change is a high-priority topic for the public agenda, and huge efforts have been devoted to understanding the temporal and spatial variability of our atmosphere in order to enhance the accuracy of climate predictions. Numerous studies documented climate change hotspots from various perspectives, e.g., climate modelling [2], hydrology [3], or ecosystems [4]. As they are particularly vulnerable to both present and future climate impacts, with considerable risks for human security [5], cities are hotspots both for the present climate and climate change.

Cities are territorial structures with the highest heterogeneity among the spatial systems of the Earth. Cities are also a unique combination of more or less prevalent anthropogenic and natural patches, very diverse landscape fragmentation, land use and land cover, dynamic energy and material fluxes. The availability of consistent information represents a key condition for the daily functionality and long-term development of the urban areas. Climate services address data provisions, statistic indicators, overview or products useful for different applications. In situ observations and gridded data are extensively used for climate services, satellite and aerial remote sensing, crowdsourcing, big data and artificial intelligence have produced a true revolution in climate data assimilation, storage and modelling.

The need of meteorological input for the decision making in urban development has been acknowledged for a long time [6]. Meteorological data are primary resources supporting the climate services designed mainly for present necessities, and continuous information from many other fields, such as land cover, demography, economy, are needed for the efficient adaptation of urban communities to future climate. The combined use of meteorological and ancillary data requires comparable quality, continuity and fine temporal and spatial resolution for efficient applications in urban applications.

There is an extensive body of literature of urban climate studies, which employed a wide range of datasets derived through different algorithms or modelling assumptions from primary data resources (e.g., in situ measurements or satellite). However, these data products have never been overviewed to highlight their advantages and disadvantages and applicability for urban climatological studies. It is worth mentioning some examples of systematic reviews with topics related to urban climatology, which tackled the issue of urban climate/meteorological datasets indirectly, within assessments of methodologies for urban heat island (UHI) [7,8] or of development status of urban meteorological networks [9].

This paper aims at providing a review of the meteorological and ancillary data resources available for urban areas, with emphasis on the possible applications which facilitate the current use of climate resources and adaptation to climate change challenges in urban areas. The review presents relevant meteorological and ancillary data resources currently used in urban climatology, derived from ground-based measurements, gridded datasets, crowdsourcing, remote sensing and airborne sensors, and highlights the benefits and specific limitations of the datasets.

2. Methodology

This research relied on authors' experience in the field of climate research related to urban environment, but also on Internet search technique to find semantically important entities, by querying the Web of Science database of academic literature. The search targeted the English-written scientific articles disseminated within the scientific community as journal papers, conference proceedings papers or book chapters, published after 2000. Some examples of searching terms and syntaxes are: "urban climate", "urban climate reviews", "urban climate datasets", "meteorological and climate datasets", and "urban meteorological networks".

Acknowledging the high importance of other datasets and variables (i.e., anthropogenic heat flux or radiation fluxes), the review targeted three main categories of meteorological resources, namely (1) ground-based measurements, (2) gridded datasets, (3) remote sensing, and four categories of ancillary data. This review tackles four categories, namely (1) societal information, (2) land cover, (3) urban morphology and (4) climate change, adaptation and urban resilience. It has to be stressed that the approach is not aimed to be exhaustive and we consider it as a fundament for more comprehensive review reports.

3. Data Resources

3.1. Meteorological Data Resources

Based on the method of retrieval, the meteorological information can be classified in ground observations, model outputs, and remote sensing data, with different characteristics and utility. Ideally, the meteorological data should simultaneously address the following issues:

- (a) Temporal and spatial stability and homogeneity. Ideally, the observations should be performed in constant locations, quasi-continuously over time, with limited and isolated gaps. The shortcomings related to missing data or changes in station locations can be successfully secured by homogenization procedures [10,11]. The period covered by satellite images can be too short and contain too many gaps for developing climatic studies, but the remote sensing products are valuable for meteorological applications as much as they are consistent temporally and spatially. While any meteorological data retrieved from urban sensors may bring valuable information, the data stability and homogeneity are sometimes difficult to address due to inherent spatial heterogeneity and to the intense changes of the urban morphology and land cover-land use categories.
- (b) Reliability. The observations should comply with the WMO standards for the stations monitoring the regional climate or other known standards for monitoring the local climate [12,13]. Many synoptic stations worldwide are placed within the administrative limits of a city, but it is very likely that more sensors will capture more relevant information about the multifaceted urban climate even if they are not placed in standard conditions [14–16].
- (c) Metadata. Geographical coordinates, instrument specifications, information about the working procedures, spatial and temporal resolution and any changes which have eventually occurred along time must be associated to any meteorological observations and remote sensing products. Besides, information about the proximities are particularly important for sensors placed in an urban environment.

In the recent decades, urban areas have faced a rapid population increase and dynamic transformation of infrastructure and functions, generating a high demand for environmental data. The access to meteorological information has been significantly improved by higher instrumental accuracy, larger storage possibilities and faster transfer capabilities.

3.1.1. In Situ Meteorological Data

The in situ or ground-based observations represent the oldest method for monitoring the urban atmosphere. The Medici Network was the first meteorological network in the world, operated between 1654 and 1670, and included 11 stations, from which 9 were placed in European cities [17]. The longest-running meteorological records in Europe are registered in cities, such as Uppsala 1722, Padua 1725, Milan 1763, Stockholm 1754, Basel 1755, or Prague 1775 [18]. At present, the ground-based observations in urban areas are performed by (a) WMO stations, (b) Urban Meteorological Networks or, more recently, by (c) citizen observatories. While the data collected by WMO stations are available from national meteorological services, this paper focusses on data freely available, usually with a transnational coverage. The main benefits of using in situ meteorological data are the potential continuity of records, flexibility of locations and relatively good accessibility in term of cost and maintenance. The main shortcomings derive from the limited spatial coverage and relevance for urban conditions. The integrated use of in situ and remote sensing data results in more complex products for urban climate studies [19].

The **Integrated Surface Database (ISD)** consists of global hourly and synoptic observations compiled from more than 100 sources into a single common ASCII format and common data model. ISD has a global coverage and it contains a variety of hourly meteorological data from more than 20,000 stations worldwide [20], ranging from 1891 to present. Based on the ISD, the HadISD is a global

sub-daily station dataset, homogenized and quality controlled, including extremes of temperature, pressure and humidity from about 7600 stations from 1931 to present [21].

The **Global Summary of the Day (GSOD)** dataset produced by the National Climatic Data Center (NCDC). These data are derived from the Integrated Surface Hourly (ISH) dataset, which includes global data obtained from the USAF Climatology Center (synoptic/hourly data). This dataset comprises daily averages computed from global hourly station data, providing access to daily weather elements including mean values of: temperature, dew point temperature, sea level pressure, station pressure, visibility, and wind speed plus maximum and minimum temperature, maximum sustained wind speed and maximum gust, precipitation amount, snow depth, and weather indicators (e.g., fog, rain, drizzle, snow, hail, thunder). GSOD data are updated on a real-time basis with a lag of 1–2 days relative to the date–time of the observations, based on Greenwich Mean Time, for about 9000 stations worldwide. Historical data are accessible from 1929 to the present, but the records since 1973 are more complete and consistent. This dataset was used to analyze the observed changes in climate extremes (temperature, precipitation and wind) in 217 urban areas and 142 paired non-urban and urban stations across the globe, over the 1972–2012 period [22].

The **European Climate Assessment and Dataset (ECA&D)** is a platform aggregating a daily series of observations provided by the climatological divisions of national meteorological and hydrological services of 63 participating European countries, as well as by station time series of the observatories and research centers throughout Europe and the Mediterranean [23]. The input data are provided by a total number of 69 participants, and they are tested for homogeneity and quality control by the ECA&D team. The platform provides access to a blended series, for which it has applied an automated updating procedure relying on the daily data extracted from SYNOP messages distributed in near real-time through the Global Telecommunication System (GTS) (including a procedure of gap filling based on a daily series of nearby observations located within a 12.5 km distance and at a height difference of less than 25 m), and a non-blended series, accessible for public use as provided by the participants. A predefined set of aggregated indices for climate extremes derived from the ECA&D is also available. Gridded daily temperature, precipitation and pressure fields constructed from the ECA&D create the E-OBS daily gridded database [24], available at 0.1° to 0.25° regular grids, covering the same geographic area from 1950 to present. E-OBS also allows grid box average comparisons with the results of Regional Climate Models for validation purposes [25–27]. These datasets were used in various urban climatology studies relying on observations addressing the challenges of climate change in European cities, e.g., assessment of the impact of climate change on thermal performance of residential buildings [28]; and change in extreme heat/cold stress [29–31].

Urban Meteorological Networks (UMNs) have been implemented in several cities around the world in order to supplement and detail the observations provided by standard WMO stations. It is extremely useful information for assessing the urban heat island (UHI), as it can capture the urban thermal behavior at better resolution than the WMO stations. [9] overview the scientific and logistical issues in a study of 24 UMNs from the USA, Europe and Asia. The urban climate of Bucharest (Romania) is currently monitored by 3 long-term WMO standard meteorological stations, and 6 sensors placed in urban conditions, fully operational since November 2014 [32]. The city of Ghent (Belgium) has implemented since July 2016 the MOCCA network (Monitoring the City’s Climate and Atmosphere) to monitor the canopy layer UHI. [14] demonstrated the MOCCA network importance and its complementarity with two modelling approaches (i.e., the SURFEX land surface model and UrbClim boundary layer model). The Birmingham Urban Climate Laboratory (BUCL) is another high-density urban meteorological network (<https://www.birmingham.ac.uk/schools/gees/centres/bucl/maps-data/index.aspx>), comprising 25 weather stations and more than 100 air temperature low-cost wireless sensors, which provided hourly air temperature records in near real-time for the city of Birmingham (UK) between June 2012 and December 2014 [33,34]. The Berlin city (Germany) monitoring network of the Freie University, Institute for Meteorology (FUMINET) is measuring meteorological data every five minutes for microclimate and human thermal comfort investigations. Novi Sad (Serbia) has

also implemented an automatic microclimatic urban monitoring network [35,36], comprising 25 urban stations and two stations located in non-urbanized environments, collecting air temperature and humidity data every 10 minute. In its turn, the climate of Szeged (Hungary) is monitored by 23 weather stations placed in urban conditions [37] and available at <http://en.urban-path.hu/monitoring-system.html>. UNM data can be accessed by contacting the corresponding authors/organizations.

Air temperature in the Barrow city (Alaska) and its surroundings has been monitored since 2001 through 70 temperature data loggers, for highlighting winter urban heat island [38] and urban-suburban soil temperature contrasts [39]. The winter heat urban effects were also investigated in the arctic city of Norilsk (Russia), using data provided by automatic weather stations, iButton sensors, combined with MODIS remote sensing data [40]. The lack of a dense network of air temperature measurement points across the Eurasian arctic region was the reason for the establishing in 2015 of the Urban Heat Island Arctic Research Campaigns (UHIARC) network, which provides access to accurate, spatially dense and interconnected climate information about temperature anomalies at city scale (<http://urbanreanalysis.ru/uhiarc.html>). This network was deployed in several mid-sized cities of the region and combines data provided by air temperature data loggers (iButton) and automatic weather stations located in each target city. Its importance and applicability were already proven in some studies focusing on the winter urban heat island in the cities of Apatity, Vorkuta, Salekhard, Nadym and NovyUrengoy of Russia [41,42]. In Asia, a Community Weather Information Network (CWIN) was established in Hong Kong in 2007 in order to improve the data coverage of the Hong Kong Observatory (HKO) by extending meteorological measurement in schools and at community levels. Using the data provided by CWIN, HKO provides improved impact-based forecasts at multi-time scales and warnings/advisories for several natural phenomena and processes (tropical cyclones, thunderstorms, heavy rains, landslides, flooding, cold/very hot weather episodes) [43].

There is still an inadequate number of networks providing data with an appropriate high spatial density for high resolution modelling of urban climate. This situation is mostly determined by security, associated high costs, and difficulty in finding appropriate measurements sites [9]. However, under the future changing climate projections with expected increases of weather extremes by the end of the 21st century in most regions of the globe [44], the need for denser measurement networks and high resolution meteorological data is likely to increase, especially in densely populated areas.

The potential of **crowdsourcing** to provide useful data for urban climatology has been carefully considered in the recent years, once the number of sensors held by citizen extensively increased [44–47]. Data collected either by volunteers running personal weather stations, such as Weather Underground or Netatmo networks [48], or by smartphones [49,50] are now publicly accessible and allow individuals to share real-time weather information. Such data are collected in non-standard conditions and quality control is mandatory, but they can be retained as a valuable data resource, with a continuous expansion, which could provide real-time and high temporal and spatial resolution meteorological information over areas with heterogeneous environments lacking in dense traditional meteorological networks such as cities.

Ref [47] provided a systematic review of crowdsourcing for climate and atmospheric research, identifying initiatives, projects and programs based on citizen science and amateur weather stations (e.g., UK Met Office Weather Observation Website in the UK; Meteoclimatic in the Iberian Peninsula; CoCoRaHS in the US; Birmingham snow depth; Air Quality Egg), mobile app (e.g., WeatherSignal; iCelsius), moving platforms (e.g., OpenSense), which have been implemented in many areas of regions around the world. The applicability of these data resources was demonstrated in several studies (e.g., [51–54]). A further example of applicability is offered by [55], who integrated air temperature measurements from the Weather Underground network of Atlanta and Chicago in the analysis of the performance of the National Weather Service Heat Warning System against ground observations and satellite imagery, by assigning them to the pixels of LST Aqua and Terra MODIS satellite retrievals. In this study, the crowdsourced climate information was found to be reliable in the description of the general patterns described by the National Weather Service and weather station measurements. [56]

provide evidence of crowdsource meteorological data from citizen weather stations to improve weather forecasting with the Weather Research and Forecasting (WRF) model for two cities in Russia (Saint Petersburg and Moscow).

3.1.2. Gridded Datasets

Gridded climate datasets represent an alternative to instrumental measurements, especially for areas with spatially scarce distribution of WMO stations or poor quality measurements. While better spatial coverage provided at low cost is an important advantage, the gridded meteorological data are associated with a lower accuracy than the measurements, depending on the quality and density of input data.

The **E-OBS** dataset of the ECA&D provides free access to a long time gridded series of daily climate data for Europe, available at 0.1° spatial resolution, covering the period from 1950 to present [24]. E-OBS was also designed to allow grid box average comparisons with the results of Regional Climate Models for validation purposes [25–27]. Both ECA&D and E-OBS datasets were used in various urban climatology studies relying on observations addressing the challenges of climate change in the European urban areas, e.g., assessment of the impact of climate change on the thermal performance of residential buildings [29]; change in extreme heat/cold and heat/cold stress [29,30].

The **Climatologies at High Resolution for the Earth's Land Surface Areas (CHELSA)** dataset is hosted by the Swiss Federal Institute for Forest, Snow and Landscape Research WSL and is based on a statistical downscaling of the ERA interim global circulation model [57]. CHELSA has a global coverage, and it contains monthly mean temperature and precipitation for the time period 1979–2013 at a 30-arc sec-spatial resolution. Recently, [58] employed the CHELSA dataset, validated with independent station data provided by the Global Historical Climatology Network (<https://www.ncdc.noaa.gov/data-access/land-based-station-data/land-based-datasets/global-historical-climatology-network-ghcn>), to analyze the trend in urban heat island intensity from 1992 to 2012 for eight megacities in Asia. The study revealed the ability of the dataset to capture the characteristics of the urban heat island and a good match between the increase in air temperature and urban sprawl.

Berkeley Earth provides open access to historical temperature data products that allow statistical diagnostics of local urban climatologies and trend magnitudes based on the estimates of the monthly means of average, maximum and minimum surface air temperature anomaly over land areas [59]. The land temperature dataset has an extensive time coverage from 1753 (or 1833 for minimum and maximum temperatures) until present, relying on a large inventory of weather station observations (from over 30,000 weather stations). The dataset provides access to gridded temperatures, regional averages (available for the northern and southern hemisphere, country, state, city and individual station scale) and bias-corrected station data based on 'breakpoint' detection (using a similar method used in the Global Historical Climatology Network dataset—[60]) in station records, which resulted from changes in station location or measurement equipment. With regards to the water impact in metropolitan areas, the Service for Water Indicators in Climate Change Adaptation (SWICCA) offers open source climate impact information necessary for the sustainable management of watersheds, including urban areas, across Europe. The time-series of the future river flow and water-related indicators, bias-corrected data associated with three climate change projections (RCP 2.6; 4.5 and 8.5), socio-economic scenarios (0.1 deg. grid) and land use projections (10 km grid) are available through SWICCA, a service run by the Swedish Meteorological and Hydrological Institute (SMHI).

Other observational platforms may supplement the ground sensors with very useful information for urban climate research (i.e., airborne sensors or different vehicles). Here, we refer only to airborne sensors, which can be used for temperature profiling over the city and rural areas, infra-red imaging or the development of digital surface and elevation models. More than five decades ago, sensors placed in a helicopter were used to retrieve temperature and pressure information for studying the urban heat island effect in New York City [61]. Unmanned Aerial Vehicles (UAVs) or drones are conveying unprecedented advantages for urban climate monitoring, as they can retrieve the variability

of temperatures across urban land surfaces, at high resolution and low cost [62,63]. The Natural Environment Research Council's Data Repository for Atmospheric Science and Earth Observation (CEDA) data collection archive provides access to several datasets of airborne observations by aircraft available from ongoing or ended collaborative projects, for assessing atmospheric composition and air quality in urban areas e.g., urban emissions (QUEFA), urban visibility (VISURB), biomonitoring of urban habitat (BIOHYPE), analysis of atmospheric chemical species and meteorological parameters (GASPOL) and airborne PM10 pollutants (PHYTOX), street-level air circulation and pollutants mix within the urban canopy (URBMET).

3.1.3. Remote Sensing Data

The need for reliable information with good spatial coverage in urban areas is also addressed by **remote sensing applications** aiming to retrieve data relevant for climate studies. Products delivered by satellite (Table 1), radar and airborne sensors represent a powerful tool set for urban climate studies, since the cost at user's desk and technical developments enhanced their availability for scientific research in the last two decades. [64] and [65] document the remote sensing of urban climates and differentiate the UHI, which refers to UHI effects in the canopy or boundary layer, by the surface urban heat island (SUHI), representing the radiative temperature difference between urban and non-urban areas at the level of the subjacent surface. The use of satellite imagery in urban climate studies may be impeded by factors like cloudiness, technical limitation and various time constraints (i.e., short range or temporal discontinuities).

Table 1. Characteristics of satellite remote sensing products delivering Land Surface Temperature data.

<i>Sensor</i>	<i>Satellite</i>	<i>Spatial Resolution</i>	<i>Temporal Resolution</i>	<i>Time Span</i>
SEVIRI	MSG	3 to 5 km	15 min	2004 to date
AVHRR	NOAA	1.1 km	2 images/24 h	1981 to date
MODIS	Terra/Aqua	1 km	4 images/24 h	2000/2002 to date
SLSTR	Copernicus Sentinel-3	1 km	1 image/24 h	2017 to date
TM, ETM+, OLI, TIRS	Landsat 4, 5, 7, 8	60–120 m (30 m resampled)	1 image/8 or 16 days	1982 to date

The World Meteorological Organization acknowledges 105 satellite instruments which have provided LST over time, categorized from primary to marginal relevance [66]. The first LST products were available at fair quality in the 1960s, but the first high-relevance products were delivered by the NASA satellite Nimbus-5 in 1973. However, the operation for urban climate research was prohibited by the 30 to 32 km spatial resolution.

The **Moderate-Resolution Imaging Spectro-Radiometer (MODIS)** instruments aboard NASA Terra/Aqua satellites have become a popular tool for urban climate studies due to a few major advantages: (1) spatial and temporal resolutions (1-km and 4 images daily) appropriate for urban climate applications; (2) significant time span, suitable for climatology, as the monitoring has been regularly performed since 2000 (Terra) and 2002 (Aqua). LST is a key parameter in the estimation of urban heat fluxes and highlighting the presence and magnitude of UHI (Figure 1) and heat health risk [67,68] and has been widely used in climatological studies at urban scale (e.g., [69–75]).

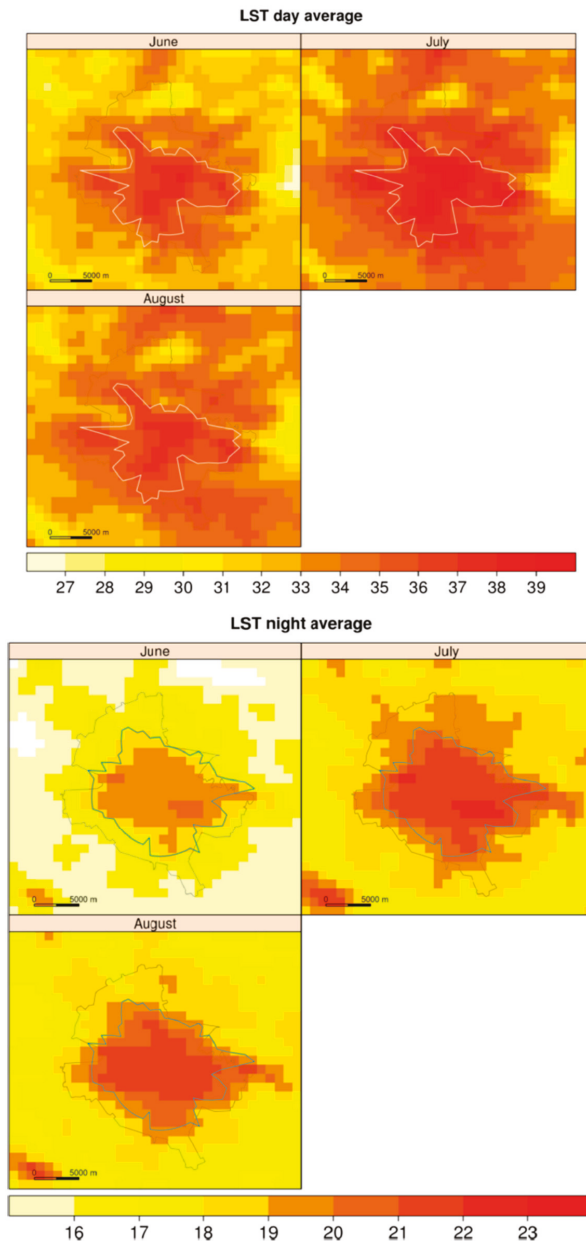


Figure 1. Average LST values and Bucharest’s UHI limit (white contour line for daytime and blue contour line for nighttime), as retrieved from MODIS images (2000–2012). The administrative limit is marked with a light grey line [71] (Material from: ‘Cheval, S.; Dumitrescu, A. The summer surface urban heat island of Bucharest (Romania) retrieved from MODIS images, *Theor. Appl. Climatol.*, published [2015], [Springer]’.)

The **Spinning Enhanced Visible Infra-Red Imager (SEVIRI)** sensors placed on the Meteosat Second Generation (MSG) satellites operated by EUMETSAT provide LST information since 2004. The

spatial resolution (3 to 5 km) is reasonable for investigating the urban environment, especially in cities with large extent covering dozens of kilometres, while the 15-min full disk coverage makes SEVIRI a very robust tool for operational purposes, such as forecast and near-real-time meteorological evaluation.

NOAA's Advanced Very High-Resolution Radiometer (AVHRR) two and three instruments have retrieved LST at 1.1 km resolution since 1981. Early studies of the SUHI were based on AVHRR data [76–78], and the datasets are still used [79].

The Landsat missions jointly operated by NASA and the U.S. Geological Survey have provided a series of Earth Observation satellites since 1972. The spatial resolution of the **Landsat's Thematic Mapper (TM), Enhanced Thematic Mapper Plus (ETM+), Operational Land Imager (OLI) and Thermal Infrared Sensor (TIRS)** reached 30 m and contributed significantly to implementation of urban climate research [80–82]. Landsat is among the most widely used satellite resources in the detection and characterization of SUHI [83], due to its main advantages residing from the free availability (since 2008), long time series (more than 30 years), high spatial resolution (30 to 120 m) and the swath coverage of 185×185 km (Landsat 5, 7 and 8). However, the long revisiting cycle of 16 days, only daytime data availability, the strong dependence of weather conditions (e.g., cloud cover or cloud proximity which could result in missing data) and the lack of an operational Landsat LST product combining data from the Landsat sensors have to be noted as the main drawbacks impeding the detection and monitoring of inter-annual variability of SUHI [84,85]. In response to the need of an operational land surface temperature product for Landsat thermal data, [86] developed an operational algorithm for (emissivity correction and retrieval methodology) Landsat LST for all sensors, which have been successfully validated with in situ observations from four surface radiation budget network sites and two inland water bodies (Salton Sea and Lake Tahoe) in the US. The proposed algorithm will be implemented by the United States Geological Survey/The National Aeronautics and Space Administration and made available through the Land Processes Distributed Active Archive Center portal, which will provide access, for the first time, to consistent LST records dating back to Landsat 4 (1982 to present).

The **Sea and Land Surface Temperature Radiometer (SLSTR)** sensor, on-board on Sentinel-3 satellite, have retrieved LST at 1 km spatial resolution and daily temporal resolution since 2016. UHI research is based on LST retrieved by SLSTR sensors [87].

The **Copernicus Atmosphere Monitoring Service (CAMS)** has been implemented by the European Centre for Medium-Range Weather Forecasts (ECMWF), and it offers reliable information for improving life quality and urban planning. CAMS combines satellite and non-satellite observations with computer-based forecast models to provide near-real-time analysis and forecast of air quality and atmospheric composition related to pollutants and greenhouse gases (e.g., particulate matter, pollen, nitrogen dioxide and sulphur dioxide). The CAMS service data portfolio comprises a broad range of CAMS products available for urban agglomerations, such as (1) solar radiation and UV, (2) air quality and atmospheric composition, (3) emissions and surface fluxes of pollutants and (4) greenhouse gases and radiative climate forcing.

The urban heat island (UHI) is a key challenge for climate change adaptation in urban environments worldwide. Exploiting the benefits of remote sensing resources, the Center for International Earth Science Information Network (CIESIN), University of Columbia released in 2013 the first version of the **Global Urban Heat Island Dataset**, providing access to global data of average summer daytime maximum (1:30 p.m. overpass) and nighttime minimum (1:30 a.m. overpass) land surface temperature (LST) for urban areas, as well as to data referring to LST difference between the urban extents and their rural surroundings within a 10 km buffer. This dataset relies on the urban extents resulting from the SEDAC's Global Rural-Urban Mapping Project, Version 1 (GRUMPv1) and land surface temperatures are from SEDAC's Global Summer Land Surface Temperature (LST) Grids (2013), which are derived from the Aqua Level-3 Moderate Resolution Imaging Spectroradiometer (MODIS) Version 5 global daytime and nighttime LST 8-day composite data (MYD11A2). LST grid data are available for a 40-day window from July to August (Julian dates 185 to 224) for the urban areas located in

the northern hemisphere, and from January to February (Julian dates 001 to 040) for those in the southern hemisphere. This dataset allowed the analysis of surface temperature anomalies in more than 30,000 cities, which have been further used to model the links between population, background climate and UHI intensity [88].

Light detecting and ranging (LIDAR) is an active type of remote sensing technology that ensures collection of accurate elevation-based information about anthropogenic features of urban environments and land cover, with a great potential to assist smart cities and support climate change resilience at city scale [89]. This technology proved a good applicability in urban flood modelling related to storm water flow and accumulation [89,90], solar potential at building roof level and city parcels for identifying optimal solar panel parameters [89,91]; Figure 2 and emergency response planning using building footprints, building heights, travel and congestion times [89]. [92] reviewed the results of climatic and vegetation surveys in urban environments relying on static, mobile or aerial laser scanning. We identified few examples of microclimate urban studies employing the LIDAR technique for showing the vegetation effects on urban climate [93,94]. Such results highlighted the relevance of LIDAR acquired data in urban green space planning under an increasing need for urban climate change adaptation.

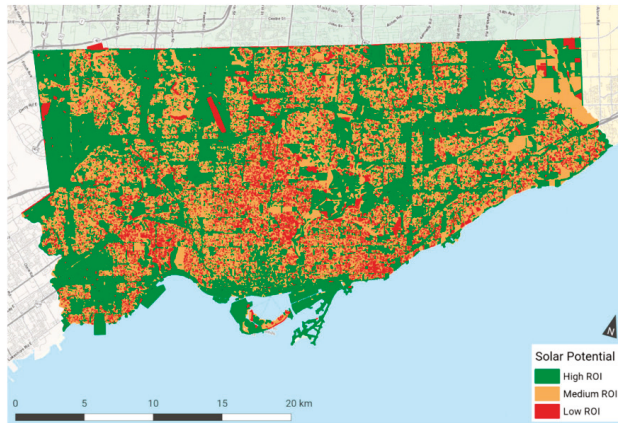


Figure 2. Estimation of solar potential in Toronto City using Lidar-derived DTM [89]

Table 2 summarizes the categories of meteorological data for urban climate studies and applications included in this review.

3.2. Ancillary Data Resources

Climate research always needs to be sustained by non-meteorological information, such as topography, roughness or anthropogenic influence, which can explain the formation and dynamics of certain atmospheric phenomena. Ancillary data are contextual information incorporated in urban climate studies together with meteorological input. [95] classify the input data for both mesoscale and microscale urban modelling in five categories, as follows: (1) land cover, (2) building morphology, (3) building design and architecture, (4) building use, anthropogenic heat and socio-economic data, and (5) urban vegetation data. This paper describes several data sources referring to air quality, land cover / land use, and urban morphology.

Table 2. Meteorological data sources for urban climate studies and applications.

Category	Dataset	Data Format	Spatial Resolution	Temporal Resolution	Temporal Coverage	Source
In situ	Integrated Surface Database (ISD)	ASCII	Data from 35,000 weather stations worldwide	Hourly, daily	1901 to present	https://www.ncdc.noaa.gov/isd
	Global Summary of the Day (GSOD)	ASCII	Data from over 9000 weather stations		1929 to present (since 1973 data are the most complete)	http://www.climate.gov/global-summary-day-gsod
	European Climate Assessment and Dataset (ECA&D)	ASCII	Data from 18,909 weather stations across Europe and the Mediterranean	Daily	1900 to present (blended series) and 1900 to a certain year (depending on the EC&D participant)	https://www.ecad.eu/
	Urban Meteorological Networks (UMNs)	ASCII	Various	Hourly or sub-hourly	Various	http://en.urban-path.hu/monitoring-system.html https://www.birmingham.ac.uk/schools/gees/centres/buc/maps-data/index.aspx
Gridded Datasets	Crowdsourcing	ASCII	Various	Sub-hourly	Various	Data could be accessed by contacting the owners https://dev.netatmo.com/ https://www.w.underground.com/pws/overview
	E-OBS	Grid (NetCDF-4)	0.1 to 0.25° regular grids	Daily	1950-01-01 to 2019-07-31 (2020: the latest version — released on October 2019)	https://www.ecad.eu/download/ensembles/download.php
	Climatologies at High Resolution for the Earth's Land Surface Areas (CHERLSA)	Grid (tif)	30 arcsec, ~1 km	Monthly	1979–2013	http://chelsa-climate.org/
Remote Sensing Data	Berkeley Earth	ASCII graphs	-	Monthly and annual summaries	1750-present (land only) 1850-present (land and ocean)	http://berkeleyearth.org/
	Service for Water Indicators in Climate Change Adaptation (SWICCA)					http://swicca.eu/
	Moderate-resolution Imaging Spectro-radiometer (MODIS)	HDF4	1 km	Daily eight-day mean	2000-present	https://hpaac.usgs.gov/tools/data-pool/ https://hpaac.usgs.gov/tools/earthdata-search/
	Spinning Enhanced Visible Infra-Red Imager (SEVIRI)	HDF5	3 km	15 min Hourly Daily Weekly Monthly Seasonal Yearly	1991–present	https://landsat.ipma.pt/ChangeSystemProdLong.do?system=Landsat+MSC&alg=LST https://wui.cmsaf.eu/safra/action/viewProduktSearch?menuName=PRODUKT_SUCHE , https://land.copernicus.eu/global/products/ls
	NOAA's Advanced Very High Resolution Radiometer (AVHRR)	NetCDF	4 km	Daily	1978-present	https://www.bouc.class.noaa.gov/saf/products/search?sub_id=0&dataType_family=AVHRR&submitx=1&sasubmity=6
Sea and Land Surface Temperature Radiometer (SLSTR)	the Landsat's Thematic Mapper (TM), Enhanced Thematic Mapper Plus (ETM+), Operational Land Imager (OLI) and Thermal Infrared Sensor (TIRS)		30 m		1982-present	http://slab.gr/downloads_LandsatLST.html
	Sea and Land Surface Temperature Radiometer (SLSTR)	NC	1 km	Daily	2016-present	https://slhub.copernicus.eu/dhus/#/home https://search.earthdata.nasa.gov/
	Copernicus Atmosphere Monitoring Service (CAMS)	Grid (NetCDF, Grib Edition2)	-	Daily and hourly	Near real-time data and hourly forecast	http://copernicus-atmosphere.eu

3.2.1. Societal Information

Urban Audit Data Collection of EUROSTAT is a valuable resource of indicators providing relevant information about the quality of life in individual European cities and their commuting zones (Functional Urban Areas). The key topics covered within the database include demography, housing, health, labor market, education, environment, transport and tourism. Data are collected by the National Statistical Institutes, the Directorate-General for Regional and Urban Policy and Eurostat. The statistics have been used in several climate change vulnerability assessments in European urban areas (e.g., [96–98]).

LandScan High Resolution global Population Dataset, created by the Oak Ridge National Laboratory, is a high-resolution population distribution dataset (30 arc seconds or 1km at Equator) available in a GIS raster (ESRI Grid) format. The dataset has a global coverage and comprises sub-national census records provided by the International Program Center Bureau of Census and is a valuable resource allowing assessments, estimations and visualizations of population at risk. This dataset was employed to identify major cities across the globe (administrative capitals or cities that account more than 1,000,000 inhabitants) to investigate the extent to which 520 iconic cities are likely to experience a shift in response to climate change by 2050 (future cities) relative to their current climate conditions (current cities), in relation to the changes in climate variability and seasonality [99].

3.2.2. Land Cover

Ref [100] published a comprehensive inventory of land cover (LC) products available at global and regional level, including high spatial resolution products useful for urban climate applications, used as a basis for this review.

The **Global Land Survey (GLS)** is a 30 m global land cover dataset, based on Landsat images. The U.S. Geological Survey (USGS) and the National Aeronautics and Space Administration (NASA) have collaborated to develop the Global Land Surveys (GLS) datasets. This collection contains images acquired from 1972 to 2012, centered on 1975 (based on images acquired from 1972 to 1983 and from 1982 to 1987), 1990 (based on images acquired from 1987 to 1997), 2000 (based on images acquired from 1999 to 2003), 2005 (based on images acquired from 2003 to 2008) and 2010 (based on images acquired from 2008 to 2012). The GLS datasets were used to estimate the intensity of urbanization [101].

The **Global High-Resolution Urban Data from Landsat** are produced by NASA Goddard Space Flight Center and the Department of Geographical Sciences at the University of Maryland from Landsat data and include:

- (a) The **Global Man-Made Impervious Surface (GMIS)** is one of the first 30m global dataset estimates of fractional impervious cover derived from the Global Land Survey (GLS) for 2010. The GMIS dataset includes: the global percent of impervious cover and the uncertainty for the global impervious cover. The urban studies are related to urban extend [102];
- (b) The **Global Human Built-Up and Settlement Extent (HBASE)** is one of the first 30 m global datasets and estimates the urban extend cover derived from the Global Land Survey (GLS) for 2010. The urban studies are related to urban extend [102].
- (c) The **Urban Landsat: Cities from Space** (1999–2003) is one of the first 30m global datasets providing composite Landsat images and raw data for urban areas that can be used in interdisciplinary studies of remote sensing and the environment.

The GMIS and HBASE datasets are complementary. The built-up and settlement extend mask (in HBASE dataset) was created for the post-processing of the GMIS dataset.

All the datasets can be used for local modelling in order to study the urban impacts on the energy, water, and carbon cycles or to analyse at country level.

The **GlobeLand30 (GLOB)** is a high-resolution dataset (30 m) of global land use/cover, based on TM5 and ETM + of America Land Resources Satellite (Landsat) and the multispectral images of China Environmental Disaster Alleviation Satellite (HJ-1) from 2010) [103]. The LC product includes

information on land cover data, and other information highly relevant for urban climate analysis, such as artificial surfaces (habitation, industrial and mining area, transportation facilities, and interior urban green zones and water bodies, etc.). GlobeLand30 was exploited by [104] for investigating the urban expansion impact on a global scale.

At European level most of the LC products at local level are produced under **ESA CCI LC** and **Copernicus Land Monitoring Service (CLMS)** initiatives. The ESA CCI LC products have global coverage at 300 m spatial resolution. The datasets were derived based on a multi-year and multi-sensor strategy of MERIS and SPOT-Vegetation time series, continued under the Copernicus Climate Change Service (C3S), implemented by the European Centre for Medium-Range Weather Forecasts (ECMWF) on behalf of the European Commission, in order to assure continuity. At C3S Climate Data Store (CDS), 27 land cover datasets (from 1992 to 2018) are available for download, used for climate modelling, urban expansion [105,106] or UHI [73]. Figure 3 illustrates the relationship between LST and land cover based on the CCI-LC dataset.

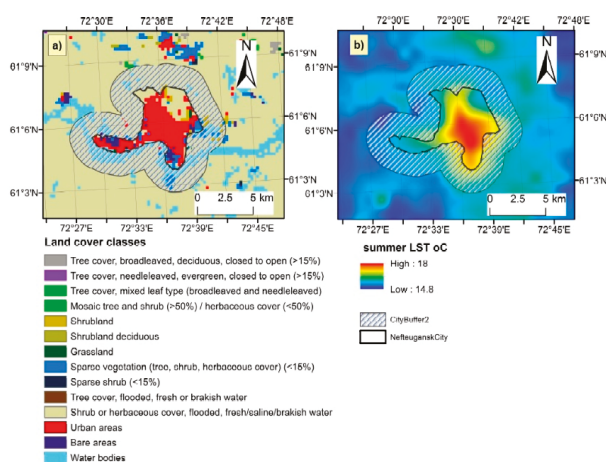


Figure 3. Example of CCI-LC and LST use in the urban study by [73].

The CLMS offers LC products at global, regional (Pan-European) and local level, as follows:

- (a) The **global LC product** is available only for 2015 based on Proba-V at 100 m spatial resolution. It uses the FAO Land Cover Classification System (LCCS), totaling 23 classes [107].
- (b) The Pan-European LC products include:
 - i. **Corine Land Cover (CLC)** is a land cover inventory (in 44 classes) project initiated in 1980s and updated in 1990, 2000, 2006, 2012 and 2018 with 100 m spatial resolution.;
 - ii. **Pan-European High-Resolution Layers (HRL)** provide information on specific land cover characteristics (imperviousness density, forest, grassland, wetland and water bodies and the new small woody features [108], and are complementary to the CLC dataset. The imperviousness data have a spatial resolution of 20 m and 100 m for 2006, 2009, 2012 and 2015.
 - iii. The **European Settlement Map (EMS)** is a very high-resolution dataset with spatial resolutions of 2.5 m, 10 m and 100 m. The first dataset, released in 2014, mapped the settlements in Europe based on 2010–2013 images. During the last year, different improvements have been developed: benchmarking process with population data; increases the number of classes to 13 (buildings, green, streets, water, railways, airports, open space inside the built-up area and same categories outside the built-up area) [109].

- (c) The **Local LC Products** include the **Urban Atlas (UA)** which provide reliable, inter-comparable, high-resolution land use maps with 17 classes for large urban zones and their surroundings (more than 100,000 inhabitants), at 10 m spatial resolution for 2006 and 2012. The UA is also including the Building Height at 10 m spatial resolution for 2012.

The **MODIS Land Cover product** is a 500 m global land cover dataset based on MODIS Terra and Aqua data from 2001 to 2018, extensively used in urban climate research [110].

The **GlobCover Portal** provides access to the results of the GlobCover project, an ESA initiative started in 2005 in partnership with JRC, EEA, FAO, UNEP, GOCF-GOLD and IGBP. The aim of the project was to develop a service capable of delivering global composites and land cover maps (with 22 land cover classes) using as input observations from the 300m MERIS sensor on board the ENVISAT satellite mission. ESA makes the land cover maps available, which cover two periods: December 2004–June 2006 and January–December 2009.

The **Open-ECOCLIMAP** dataset has been available since 30 June 2014 at The ECOCLIMAP program, and is a dual database at 1 km resolution, that includes an ecosystem classification and a coherent set of land surface parameters, that are primarily mandatory in meteorological modelling (notably leaf area index and albedo). Hence, the aim of this innovative physiography is to enhance the quality of initialization and impose some surface attributes within the scope of weather forecasting and climate related studies.

3.2.3. Urban Morphology

The **World Urban Database and Access Portal Tool (WUDAPT)** project is a community-based initiative of the International Association of Urban Climate (IAUC) which supports urban climate research and various forecasting applications on surface energy budget, meso- to urban-scale weather and atmospheric chemical composition and air quality. The tool adopted a common framework for acquisition, storage and dissemination of relevant data about urban form (e.g., surface cover, properties of construction materials, surface geometry) and function (e.g., transportation, energy use), which are relevant for a coherent description of heterogeneous urban landscapes, as a prerequisite for understanding the urban climate characteristics.

WUDAPT rely on the local climate zone (LCZ) typology scheme proposed by [111], which categorizes 17 distinct landscapes (out of which 10 are urban), in relation to a number of surface parameters related to the main built and land cover types. The procedure employs geospatial data (multi-year series of multispectral and SAR satellite observations) as input in the random forest classifier to detect specific features for both urban and natural LCZ types [112].

The WUDAPT portal provides free access to maps (in GeoTIFF and KML format) and metadata of classified local climate zones for more than 150 cities worldwide. Data are structured in a hierarchical format, with increasing details from level zero (local climate zones along with parameter ranges) to level one (more precise parameter values for each LCZs) and level two (detailed description of urban landscape parameters at refined scales suited for boundary-layer modelling).

Alternatively, urban morphology can be obtained from OpenStreetMap [113] or from the building-resolving data provided by the local authorities.

3.2.4. Climate Change, Adaptation and Urban Resilience

Urban Audit dataset through the Geographic Information System of the Commission (GISCO) supplies the users with geographical information concerning the boundaries of cities and the functional urban areas, defined according to the EC-OECD city internationally harmonized definition [114]. The coverage is the EU-28 plus Iceland, Norway and Switzerland, and the dataset is available in ESRI format (shapefile and geostatistical database) at scales ranging from 1:100,000 (2011–2014, 2018) to 1:3,000,000 (2001, 2004). [29] employed the Urban Audit GISCO dataset and the urban morphological zones from the European Environment Agency to analyze future change in heatwaves, droughts and floods in all 571 European cities targeted by Urban Audit, and to elaborate low, medium and high

hazard impact scenarios in relation to climate projections of all ensemble members of CMIP5 for the RCP8.5 emission scenario. The study provides evidence of an increasing exposure to heatwave days in all cities, an intensification of drought in the southern European cities and increasing frequency of river floods in the northern European cities.

Urban Adaptation Map Viewer (UAMV) is a web platform available at <<https://climate-adapt.eea.europa.eu/knowledge/tools/urban-adaptation/Urban-Adaptation-datasets>>, aggregating information from various sources (e.g., Met Office, EURO-CORDEX, E-OBS dataset, C3S, JRC, Urban Audit) and providing free access to five types of datasets and metadata from European cities, as follows: (1) climate and climate related hazards (e.g., hot summer days, cooling degree days, extreme heat waves, winter heavy precipitation, meteorological drought, forest fire danger, sea level rise); (2) exposure of cities to climate-related hazards (e.g., areas and population affected by wildfires, river flooding, coastal flooding); (3) physical characteristics of urban areas (urban morphological zone—UMZ, share of green and impervious areas in city core and UMZs); (4) socio-economic characteristics of cities (e.g., population, share of elderly and children, share of lone-pensioner households, unemployed people); and (5) adaptation activities.

Lobellia Earth is a newly released (2018) web platform for visualizing and exploring the annual and monthly climatologies in user specific locations for the period 1981–2010. The visualization tool (as maps and graphs) of the past climate uses ERA5 data from ECMWF that allow the analysis of spatial distribution of air temperature (average, maximum and minimum air temperature), precipitation, average wind speed, wind gust and cloud cover and several climate extreme indices (e.g., frost days, warm nights, heavy and very heavy precipitation days). In this platform, the user could only visualize the climatological information (maps and graphs) about different target urban areas. The platform supports the UN Habitat's City Resilience Profiling Programme (CRPT) using downscaling and bias correction techniques for providing high-resolution climate projection data of EUROCORDEX project and tailored climate information about future climate change threats and vulnerabilities for five pilots of cities sensitive to climate change (i.e., Asuncion, Yakutsk, Maputo, Dakar and Port Vila). Climate projection data for the target urban areas are available only by request from the Lobelia Earth developers. Exploring the benefits of Earth observation, Lobelia Earth, with the contribution of Royal Netherlands Meteorological Institute, supplies air quality information for three European pilot cities (i.e., NO₂ and PM₁₀ concentrations in Barcelona, Madrid and Amsterdam). Table 3 summarizes the categories of ancillary data for urban climate studies and applications described in this review.

Table 3. Ancillary data sources for urban climate studies and applications.

	Details (e.g., Data Format, Resolution, Year of Compliance)		Source
Societal information	Urban Audit data collection of EUROSTAT	Data format: ASCII Temporal coverage: 2010–2019 (depending on the indicator)	https://ec.europa.eu/eurostat/web/cities/data/database
	LandScan High Resolution global Population Dataset	Data format: ESRI Grid Spatial resolution: 30 arc seconds or ~1 km at equator	https://www.easstview.com/resources/e-collections/landscan/
	Global Land Survey (GLS)	Data format: GeoTIFF Spatial resolution: 30 m Temporal coverage: 2010	http://earthexplore.usgs.gov/ https://sedac.ciesin.columbia.edu/data/set/ulandsat-gmis-v1/ https://sedac.ciesin.columbia.edu/data/set/ulandsat-hbase-v1/ https://sedac.ciesin.columbia.edu/data/set/ulandsat-cities-from-space/
	The Global Man-made Impervious Surface (GMIS) Global Human Built-up And Settlement Extent (HBASE)	Data format: GeoTIFF Spatial resolution: 100 m Temporal coverage: 2010	http://www.globallandcover.com/GLC3D/download/index.aspx
Land cover	Urban Landsat: Cities from Space	Data format: GeoTIFF Spatial resolution: 30 m Temporal coverage: 2010 (2009–2011)	https://viewer.vito.be/download
	GlobeLand30 (GLOB)	Data format: GeoTIFF Spatial resolution: 100 m Temporal coverage: 2015	https://land.copernicus.eu/pan-european/corine-land-cover/clc2018?tab=download
	Copernicus Land Monitoring Service (CLMS)	Data format: GeoTIFF, ESRI Geodatabase, SQLite Database Spatial resolution: 100 m Temporal coverage: 1990 (1986–1998), 2000 (+/- 1 year), 2006 (+/- 1 year), 2012 (2011–2012), 2018 (2017–2018)	https://land.copernicus.eu/pan-european/high-resolution-layers/imperviousness/status-maps/2015?tab=download https://land.copernicus.eu/pan-european/GHSL/european-settlement-map/esm-2012-release-2017-urban-green?tab=download
	Corine Land Cover (CLC)	Data format: GeoTIFF Spatial resolution: 20 m and 100 m Temporal coverage: 2006 (2005–2007), 2009 (2008–2010), 2012 (2011–2013), 2015 (2014–2016)	https://land.copernicus.eu/local/urban-atlas/urban-atlas-2012?tab=download
	Pan-European High-Resolution Layers (HRL)	Data format: GeoTIFF Spatial resolution: 2.5 m, 10 m and 100 m Release: 2014, 2016, 2017	https://pdaac.usgs.gov/tools/earthdata-search/ https://pdaac.usgs.gov/tools/usgs-earthexplorer/ https://pdaac.usgs.gov/tools/data-pool/
	European Settlement Map (EMS)	Data format: vector file ESRI format Spatial resolution: 10 m Temporal coverage: 2006 (2005–2007), 2012 (2011–2013)	http://due.esrin.esa.int/page_globcover.php
	Urban Atlas (UA)	Data format: GeoTIFF Spatial resolution: 10 m	https://openseaource.umr-cnrm.fr/projects/eoclimap/files
	Building Height	Temporal coverage: 2012 (2011–2014)	
	MODIS Land Cover	Data format: HDF4 Spatial resolution: 500 m Temporal coverage: 2001–2018	
	GlobCover Portal	Data format: GeoTIFF Spatial resolution: 300 m Temporal coverage: 2005, 2009	
Open-ECCOCLIMAP	Data format: ASCII Spatial resolution: 1 km Temporal coverage: 2005, 2009		

Table 3. *Cont.*

	Dataset	Details (e.g., Data Format, Resolution, Year of Compliance)	Source
Urban morphology	World Urban Database and Access Portal Tool (WUDAPT)	Data format: ESRI shapefile and geodatabase Scale 1:100000 (UA2018; 2011–2014), Scale 1:3 Million (UA2004; 2001) Temporal availability: 2015–2018 (UA2018), 2011–2014 (UA2011–2014), 2004 (UA2004), 2001 (UA2001)	http://www.wudapt.org/
Climate change, adaptation and urban resilience	Urban Audit dataset	Available only for visualization (e.g., in ArcGIS JavaScript, ArcGIS Online Map Viewer, ArcGis Earth)	https://ec.europa.eu/eurostat/web/gisco/geodata/reference-data/administrative-units-statistical-units/urban-audit
	Urban Adaptation Map Viewer (UAMV)	Dataset comprises 15 indicators of climate and climate-related hazards (e.g., heat waves, heavy precipitation, meteorological drought, fire danger); 7 exposure indicators of cities to climate-related hazards (e.g., wildfires, river flooding, sea level rise); 4 indicators of physical characteristics of urban areas (e.g., urban morphological zone, percentage of impervious area in core city); 10 socio-economic indicators for cities (e.g., population, total use of water); adaptation activities of cities.	https://climate-adapt.teen.europa.eu/knowledge/tools/urban-adaptation/Urban-Adaptation-datasets
	LOBELLA EARTH	Available only for visualization as distribution maps and graphs using Climate Explorer (past climate)	https://www.lobella.earth/

4. Conclusions

The rapid development of urban areas has derived complex challenges for environmental sciences, demanding better data, in terms of accuracy, resolution and easy accessibility. At present, there are several data sources providing valuable meteorological and ancillary information for urban climate research, and this paper presents an outline based on criteria like data availability, geographical coverage and, above all, the demonstrated utility for urban climate. We are confident that, far from being comprehensive, such an outline is a starting point and a useful tool for urban climate researchers and practitioners.

Five categories of meteorological data are identified and presented in this review paper, i.e., ground-based data and remote sensing, while the ancillary data can be classified in air quality, land cover/land use, and urban topography. One can remark the following conclusions: 1) the information sources providing meteorological and ancillary data for urban climate research are numerous; 2) spatial and temporal resolutions support a variety of applications, from weather forecast to climate modelling. It has to be mentioned that the combined use of data from various sources have a significant potential to support the improvement of data and products, as the shortcomings may be addressed with keeping the advantages associated to each dataset.

Author Contributions: Conceptualization, S.C., D.M., A.D., A.I.; methodology, S.C., D.M., A.D., A.I.; software, S.C., D.M., A.I.; validation, M.F., C.I., N.C.T., S.D. and B.A.; formal analysis, S.C., D.M., A.I. All authors have read and agreed to the published version of the manuscript.

Funding: This research was partially funded by Ministry of Research and Innovation, Romania, grant number PN-III-P1-1.1-PD-2016-1579.

Acknowledgments: This work was partially conducted in the framework of the research theme "Climate hazards in the Romanian Plain" of the Institute of Geography, Romanian Academy.

Conflicts of Interest: The authors declare no conflict of interest.

References

1. The World Bank Group. 2019. Available online: <https://data.worldbank.org/indicator/sp.urb.totl.in.zs> (accessed on 10 January 2020).
2. Diffenbaugh, N.S.; Giorgi, F. Climate change hotspots in the CMIP5 global climate model ensemble. *Clim. Chang.* **2012**, *114*, 813–822. [[CrossRef](#)]
3. Prudhomme, C.; Giuntoli, I.; Robinson, E.L.; Clark, D.B.; Arnell, N.W.; Dankers, R.; Fekete, B.; Franssen, W.; Gerten, D.; Gosling, S.; et al. Hydrological Droughts in the 21st Century, Hotspots and Uncertainties from a Global Multimodel Ensemble Experiment. *Proc. Natl. Acad. Sci. USA* **2013**, *111*. [[CrossRef](#)]
4. Turco, M.; Palazzi, E.; von Hardenberg, J.; Provenzale, A. Observed climate change hot-spots. *Geophys. Res. Lett.* **2015**, *42*. [[CrossRef](#)]
5. de Sherbinin, A. Climate Change Hotspots Mapping: What Have We Learned? *Clim. Chang.* **2013**, *123*, 23–37. [[CrossRef](#)]
6. Chandler, T.J. *Urban Climatology and Its Relevance to Urban Design*; WMO No 438, Technical Note No 149; WHO: Geneva, Switzerland, 1976; 80p.
7. Stewart, I.D. A systematic review and scientific critique literature of methodology in modern urban heat island literature. *Int. J. Climatol.* **2011**, *31*. [[CrossRef](#)]
8. Deilami, K.; Kamruzzaman, M.D.; Liu, Y. Urban heat island effect: A systematic review of spatio-temporal factors, data, methods and mitigation measures. *Int. J. Appl. Earth Obs. Geoinf.* **2018**. [[CrossRef](#)]
9. Muller, C.; Chapman, L.; Grimmond, C.; Young, D.; Cai, X. Sensors and the city: A review of urban meteorological networks. *Int. J. Clim.* **2013**, *33*, 1585–1600. [[CrossRef](#)]
10. Savić, S.; Milošević, D.; Marković, V.; Kujundžić-Dačović, R. Homogenisation of mean air temperature time series from Vojvodina (North Serbia). *Geogr. Pannonica* **2012**, *16*, 38–43. [[CrossRef](#)]
11. Dumitrescu, A.; Cheval, S.; Guijarro, J.A. Homogenization of a combined hourly air temperature dataset over Romania. *Int. J. Climatol.* **2019**. [[CrossRef](#)]

12. Oke, T.R. *Initial Guidance to Obtain Representative Meteorological Observations at Urban Sites*; WMO/TD No. 1250; WMO: Geneva, Switzerland, 2006; 51p.
13. WMO. *Guide to Meteorological Instruments and Methods of Observations*; WMO-no.8; WMO: Geneva, Switzerland, 2017; 1177p.
14. Caluwaerts, S.; Hamdi, R.; Top, S.; Lauwaet, D.; Berckmans, J.; Degrauwe, D.; Dejonghe, H.; De Ridder, K.; De Troch, R.; Duchène, F.; et al. The urban climate of Ghent, Belgium: A case study combining a high-accuracy monitoring network with numerical simulations. *Urban Clim.* **2020**, *31*, 100565. [[CrossRef](#)]
15. Bilandžija, D. Spatio-Temporal Climate and Agroclimate Diversities over the Zagreb City Area. *Geogr. Pannonica* **2019**, *23*, 385–397. [[CrossRef](#)]
16. Dian, C.; Pongrácz, R.; Incze, D.; Bartholy, J.; Talamon, A. Analysis of the Urban Heat Island Intensity Based on air Temperature Measurements in a Renovated Part of Budapest (Hungary). *Geogr. Pannonica* **2019**, *23*, 277–288. [[CrossRef](#)]
17. Camuffo, D.; Bertolin, C. The earliest temperature observations in the world: The Medici Network (1654-1670). *Clim. Chang.* **2012**, *111*, 335–363. [[CrossRef](#)]
18. Burt, S. *The Weather Observer's Handbook*; Cambridge University Press: Cambridge, UK, 2012; 458p.
19. Sheng, L.; Tang, X.; You, H.; Gu, Q.; Hu, H. Comparison of the urban heat island intensity quantified by using air temperature and Landsat land surface temperature in Hangzhou, China. *Ecol. Indic.* **2017**, *72*, 738–746. [[CrossRef](#)]
20. Smith, A.; Lott, N.; Vose, R. The integrated surface database: Recent developments and partnerships. *Bull. Am. Meteorol. Soc.* **2011**, *92*, 704–708. [[CrossRef](#)]
21. Dunn, R.; Willett, K.; Parker, E.D.; Mitchell, L. Expanding HadISD: Quality-controlled, sub-daily station data from 1931. *Geosci. Instrum. Methods Data Syst.* **2016**, *5*, 473–491. [[CrossRef](#)]
22. Mishra, V.; Ganguly, A.R.; Nijssen, B.; Lattenmaier, D.P. Changes in observed climate extremes in global urban areas. *Environ. Res. Lett.* **2015**, *10*, 024005. [[CrossRef](#)]
23. Klein Tank, A.M.G.; Wijngaard, J.B.; Können, G.P.; Böhm, R.; Demarée, G.; Gocheva, A.; Heino, R. Daily dataset of 20th-century surface air temperature and precipitation series for the European Climate Assessment. *Int. J. Climatol.* **2002**, *22*, 1441–1453. [[CrossRef](#)]
24. Cornes, R.; van der Schrier, G.; van den Besselaar, E.J.M.; Jones, P.D. An Ensemble Version of the E-OBS Temperature and Precipitation Datasets. *J. Geophys. Res. Atmos.* **2018**, *123*, 9391–9409. [[CrossRef](#)]
25. Haylock, M.R.; Hofstra, N.; Klein Tank, A.M.G.; Klok, E.J.; Jones, P.D.; New, M. A European daily high-resolution gridded dataset of surface temperature and precipitation. *J. Geophys. Res.* **2008**, *113*, D20119. [[CrossRef](#)]
26. Pereira, S.C.; Marta-Almeida, M.; Carvalho, A.C.; Rocha, A. Heat waves and cold spells changes in Iberia for a future climate scenario. *Int. J. Clim.* **2017**, *37*, 5192–5205. [[CrossRef](#)]
27. Fallmann, J.; Wagner, S.; Emeis, S. High resolution climate projections to assess the future vulnerability of European urban areas to climatological extreme events. *Theor. Appl. Climatol.* **2017**, *127*, 667–683. [[CrossRef](#)]
28. Soutullo, S.; Giancola, E.; Jiménez, M.J.; Ferrer, J.A.; Sánchez, M.N. How climate trends impact on the thermal performance of a typical residential building in Madrid. *Energies* **2019**, *13*, 237. [[CrossRef](#)]
29. Guerreiro, S.B.; Dawson, R.J.; Kilsby, C.; Lewis, E.; Ford, A. Future heat-waves, droughts and floods in 571 European cities. *Environ. Res. Lett.* **2018**, *13*, 034009. [[CrossRef](#)]
30. Lorenz, R.; Stalhandske, Z.; Fischer, E.M. Detection of a climate change signal in extreme heat, heat stress and cold in Europe from observations. *Geophys. Res. Lett.* **2019**, *46*, 8363–8374. [[CrossRef](#)]
31. Founda, D.; Oierros, F.; Katavoutas, G.; Keramitsoglou, I. Observed trends in thermal stress at European Cities with different background climates. *Atmosphere* **2019**, *10*, 436. [[CrossRef](#)]
32. Cheval, S.; Dumitrescu, A. Rapid daily and sub-daily temperature variations in an urban environment. *Clim. Res.* **2017**, *73*, 233–246. [[CrossRef](#)]
33. Chapman, L.; Muller, C.L.; Young, D.T.; Cai, X.-M.; Grimmond, C.S.B. An introduction to the Birmingham urban climate laboratory. In Proceedings of the 8th International Conference on Urban Climates, Dublin, Ireland, 6–10 August 2012.
34. Azevedo, J.A.; Chapman, L.; Muller, C.L. Quantifying the daytime and night-time urban heat island in Birmingham, UK: A comparison of satellite derived land surface temperature and high resolution air temperature observations. *Remote Sens.* **2016**, *8*, 153. [[CrossRef](#)]

35. Šećerov, I.; Savić, S.; Milošević, D.; Marković, V.; Bajšanski, I. Development of an automated urban climate monitoring system in Novi Sad (Serbia). *Geogr. Pannonica* **2015**, *19*, 174–183. [[CrossRef](#)]
36. Šećerov, I.; Savić, S.; Milošević, D.; Arsenović, D.M.; Dolinaj, D.M.; Popov, S.B. Progressing urban climate research using a high-density monitoring network system. *Environ. Monit Assess.* **2019**, *191*, 89. [[CrossRef](#)]
37. Skarbit, N.; Stewart, I.D.; Unger, J.; Gál, T. Employing an urban meteorological network to monitor air temperature conditions in the “local climate zones” of Szeged, Hungary. *Int. J. Climatol.* **2017**, *37*, 582–596. [[CrossRef](#)]
38. Hinkel, K.M.; Nelson, F.E. Anthropogenic heat island at Barrow, Alaska, during winter (2001–2005). *J. Geophys. Res. Atmos.* **2007**, *112*, D6. [[CrossRef](#)]
39. Klene, A.E.; Nelson, F.E.; Hinkel, K.M. Urban–rural contrasts in summer soil-surface temperature and active-layer thickness, Barrow, Alaska, USA. *Polar Geogr.* **2013**, *36*, 183–201. [[CrossRef](#)]
40. Varentsov, M.I.; Konstantinov, P.I.; Samsonov, T.E.; Repina, I.A. Investigation of the urban heat island phenomenon during polar night based on experimental measurements and remote sensing of Norilsk city (in Russian). *Sovrem. Probl. Distantsionnogo Zondirovaniya Zemlitz Kosm.* **2014**, *11*, 329–337.
41. Konstantinov, P.I.; Grishchenko, M.Y.; Varentsov, M.I. Mapping urban heat islands of arctic cities using combined data on field measurements and satellite images based on the example of the city of Apatity (Murmansk Oblast) *Izv. Atmos. Ocean Phy.* **2015**, *51*, 992–998. [[CrossRef](#)]
42. Konstantinov, P.; Varentsov, M.; Esau, I. A high density urban temperature network deployed for several cities of Euroasian Arctic. *Environ. Res. Lett.* **2018**, *13*, 075007. [[CrossRef](#)]
43. Lee, T.; Wong, W.; Tam, K. Urban-focused weather and climate services in Hong Kong. *Geosci. Lett.* **2018**, *5*, 18. [[CrossRef](#)]
44. IPCC. 2012: *Managing the Risks of Extreme Events and Disasters to Advance Climate Change Adaptation. A Special Report of Working Groups I and II of the Intergovernmental Panel on Climate Change*; Field, C.B., V. Barros, T.F., Stocker, D., Qin, D.J., Dokken, K.L., Ebi, M.D., Mastrandrea, K.J., Mach, G.-K., Plattner, S.K., Allen, M.T., et al., Eds.; Cambridge University Press: Cambridge, UK; New York, NY, USA, 2012; 582p.
45. Wolters, D.; Brandsma, T. Estimating the urban heat island in residential areas in The Netherlands using observations by weather amateurs. *J. Appl. Meteorol. Climatol.* **2012**, *51*, 711–721. [[CrossRef](#)]
46. Bell, S.; Cornford, D.; Bastin, L. How good are citizen weather stations? Addressing a biased opinion. *Weather* **2015**, *70*, 75–84. [[CrossRef](#)]
47. Muller, C.L.; Chapman, L.; Johnston, S.; Kidd, C.; Illingworth, S.; Foody, G.; Overreem, A.; Leigh, R.R. Crowdsourcing for climate and atmospheric sciences: Current status and future potential. *Int. J. Climatol.* **2015**, *35*, 3185–3203. [[CrossRef](#)]
48. Meier, F.; Fenner, D.; Grassmann, T.; Marco, O.; Scherer, D. Crowdsourcing air temperature from citizen weather stations for urban climate research. *Urban Clim.* **2017**, *19*, 170–191. [[CrossRef](#)]
49. Overeem, A.; Robinson, J.; Leijnse, H.; SteeneveldGert-Jan Horn, B.; Uijlenhoet, R. Crowdsourcing urban air temperatures from smartphone battery temperatures. *Geophys. Res. Lett.* **2013**, *40*, 4081–4085. [[CrossRef](#)]
50. Droste, A.; Pape, J.J.; Overeem, A.; Leijnse, H.; SteeneveldGert-Jan van Delden, A.; Uijlenhoet, R. Crowdsourcing urban air temperatures through smartphone battery temperatures in São Paulo, Brazil. *J. Atmos. Ocean. Technol.* **2017**, *34*, 1853–1866. [[CrossRef](#)]
51. Cifelli, R.; Doesken, N.; Kennedy, P.; Carey, L.D.; Rutledge, S.A.; Gimmestad, C.; Depue, T. The community collaborative rain, hail, and snow network: Informal education for scientists and citizens. *Bull. Am. Meteorol. Soc.* **2005**, *86*, 1069–1077. [[CrossRef](#)]
52. Shan, Q.; Brown, D. Wireless temperature sensor using bluetooth. In Proceedings of the IWAN 2005: International Workshop on Wireless Ad Hoc Networks, London, UK, 23–26 May 2005.
53. Anderson, A.R.S.; Chapman, M.; Drobot, S.D.; Tadesse, A.; Lambi, B.; Wiener, G.; Pisano, P. Quality of mobile air temperature and atmospheric pressure observations from the 2010 development test environment experiment. *J. Appl. Meteorol. Clim.* **2012**, *51*, 691–701. [[CrossRef](#)]
54. Devarakonda, S.; Sevusu, P.; Liu, H.; Liu, R.; Iftode, L.; Nath, B. Real-time Air Quality Monitoring through Mobile Sensing in Metropolitan Areas. In Proceedings of the Conference UrbComp’13, Chicago, IL, USA, 11–14 August 2013.
55. Vargo, J.; Xiao, Q.; Liu, Y. The performance of the National Weather Service Heat Warning System against ground observations and satellite imagery. *Adv. Meteorol.* **2015**. [[CrossRef](#)]

56. Uteov, A.; Kalyuzhnaya, A.; Boukhanovsky, A. The cities weather forecast by crowdsourced atmospheric data. *Procedia Comput. Sci.* **2019**, *156*, 347–356. [CrossRef]
57. Karger, D.N.; Conrad, O.; Böhrer, J.; Kawohl, T.; Kreft, H.; Soria-Auza, R.W.; Zimmermann, N.; Linder, H.P.; Kessler, M. Climatologies at high resolution for the Earth land surface areas. *Sci. Data* **2016**, *4*, 170122. [CrossRef] [PubMed]
58. Lee, K.; Kim, Y.; Chan Sung, H.; Ryu, J.; Woo Jeon, S. Trend analysis of urban island intensity according to urban area change in Asian Mega Cities. *Sustainability* **2020**, *12*, 112. [CrossRef]
59. Rohde, R.; Muller, R.; Jacobsen, R.; Perlmutter, S.; Rosenfeld, A.; Wurtele, J.; Curry, J.; Wickham, C.; Mosher, S. Berkeley earth temperature averaging process. *Geoinfor. Geostat. An Overv.* **2013**, *1*, 2. [CrossRef]
60. Menne, M.J.; Williams, C.N., Jr. Homogenization of Temperature Series via Pairwise Comparisons. *J. Clim.* **2009**, *22*, 1700–1717. [CrossRef]
61. Bornstein, R.D. Observations of the Urban Heat Island Effect in New York City. *J. Appl. Meteorol.* **1968**, *7*, 575–582. [CrossRef]
62. Gaitani, N.; Burud, I.; Thiis, T.; Santamouris, M. High-resolution spectral mapping of urban thermal properties with Unmanned Aerial Vehicles. *Build. Environ.* **2017**, *121*, 215–224. [CrossRef]
63. Naughton, J.; McDonald, W. Evaluating the Variability of Urban Land Surface Temperatures Using Drone Observations. *Remote Sens.* **2019**, *11*, 1722. [CrossRef]
64. Voogt, J.; Oke, T. Thermal remote sensing of urban climates. *Remote Sens. Environ.* **2003**, *86*, 370–384. [CrossRef]
65. Sun, H.; Chen, Y.; Zhan, W. Comparing surface- and canopy-layer urban heat islands over Beijing using MODIS data. *Int. J. Remote Sens.* **2015**, *36*, 5448–5465. [CrossRef]
66. OSCAR. Observing Systems Capability Analysis and Review Tool. 2019. Available online: <https://www.wmo-sat.info/oscar/gapanalyses?variable=96> (accessed on 20 October 2019).
67. Tomlinson, C.J.; Chapman, L.; Thornes, J.E.; Baker, C.J. Remote sensing land surface temperature for meteorology and climatology: A review. *Meteorol. Appl.* **2011**, *18*, 296–306. [CrossRef]
68. Ward, K.; Lauf, S.; Kleinschmit, B.; Endlicher, W. Heat waves and urban heat islands in Europe: A review of relevant drivers. *Sci. Total Environ.* **2016**, *569–570*, 527–539. [CrossRef]
69. Jin, M.; Dickinson, R.E.; Zhang, D.-L. The footprint of urban areas on global climate as characterized by MODIS. *J. Clim.* **2005**, *18*, 1551–1565. [CrossRef]
70. Tomlinson, C.J.; Chapman, L.; Thornes, J.E.; Baker, C.J. Derivation of Birmingham’s summer surface urban heat island from MODIS satellite images. *Int. J. Climatol.* **2012**, *32*, 214–224. [CrossRef]
71. Cheval, S.; Dumitrescu, A. The summer surface urban heat island of Bucharest (Romania) retrieved from MODIS images. *Theor. Appl. Climatol.* **2015**, *121*, 631–640. [CrossRef]
72. Morabito, M.; Crisci, A.; Gioli, B.; Gualtieri, G.; Toscano, P.; Di Stefano, V.; Orlandini, S.; Dalal, K. Urban-hazard risk analysis: Mapping of heat-related risks in the elderly in major Italian cities. *PLoS ONE* **2015**, *10*, e0127277. [CrossRef] [PubMed]
73. Miles, V.; Esau, I. Seasonal and spatial characteristics of urban heat islands (UHIs) in Northern West Siberian cities. *Remote Sens.* **2017**, *9*, 989. [CrossRef]
74. Polydoros, A.; Mavrakou, T.; Cartalis, C. Quantifying the trends in land surface temperature and surface urban heat island intensity in Mediterranean cities in view of smart urbanization. *Urban Sci.* **2018**, *2*, 16. [CrossRef]
75. Chen, Q.; Ding, M.Y.X.; Hu, K.; Qi, J. Spatially explicit assessment of heat health risk using multi-sensor remote sensing images and socioeconomic data in Yangtze River Delta, China. *Int. J. Health Geogr.* **2018**, *17*, 15. [CrossRef]
76. Gutman, G.G. Multi-annual time series of AVHRR-derived land surface temperature. *Adv. Space Res.* **1994**, *14*, 27–30. [CrossRef]
77. Streutker, D.R. Satellite-measured growth of the urban heat island of Houston, Texas. *Remote Sens. Environ.* **2003**, *85*, 282–289. [CrossRef]
78. Weng, Q.; Lu, D.; Schubring, J. Estimation of land surface temperature-vegetation abundance relationship for urban heat island studies. *Remote Sens. Environ.* **2004**, *89*, 467–483. [CrossRef]
79. Che, Y.; Guang, J.; de Leeuw, G.; Xue, Y.; Sun, L.; Che, H. Investigations into the development of a satellite-based aerosol climate data record using ATSR-2, AATSR and AVHRR data over north-eastern China from 1987 to 2012. *Atmos. Meas. Tech.* **2019**, *12*, 4091–4112. [CrossRef]

80. Liu, L.; Zhang, Y. Urban heat island analysis using the landsat TM data and ASTER Data: A case study in Hong Kong. *Remote Sens.* **2011**, *3*, 1535–1552. [[CrossRef](#)]
81. Kaplan, G.; Avdan, U.; Avdan, Z.Y. 2018. Urban heat island analysis using the landsat 8 satellite data: A case study in Skopje, Macedonia. *Multidiscip. Digit. Publ. Inst. Proc.* **2018**, *2*, 358.
82. Parastatidis, D.; Mitraka, Z.; Chrysoulakis, N.; Abrams, M. Online Global Land Surface Temperature Estimation from Landsat. *Remote Sens.* **2019**, *9*, 1208. [[CrossRef](#)]
83. Zhou, D.; Xiao, J.; Bonafoni, S.; Berger, C.; Deilami, K.; Zhou, Y.; Frolicking, S.; Yao, R.; Qiao, Z.; Sobrino, J.A. Satellite remote sensing of surface urban heat islands: Progress, challenges and perspectives. *Remote Sens.* **2019**, *11*, 48. [[CrossRef](#)]
84. Quan, J.; Zhan, W.; Chen, Y.; Wang, M.; Wang, J. Time series decomposition of remotely sensed land surface temperature and investigation of trends and seasonal variations in surface urban heat islands. *J. Geophys. Res. Atmos.* **2016**, *121*, 2638–2657. [[CrossRef](#)]
85. Shen, H.; Huang, L.; Zhang, L.; Wu, P.; Zeng, C. Long-term and fine-scale satellite monitoring of the urban heat island effect by the fusion of multi-temporal and multi-sensor remote sensed data: A 26-year case study of the city of Wuhan in China. *Remote Sens. Environ.* **2016**, *172*, 109–125. [[CrossRef](#)]
86. Malakar, N.K.; Hulley, G.C.; Hook, S.J.; Laraby, K.; Cook, M.; Schott, J.R. An operational land surface temperature product for Landsat thermal data: Methodology and validation. *IEEE Trans. Geosci. Remote Sens.* **2018**, *56*, 5717–5735. [[CrossRef](#)]
87. Shumilo, L.; Kussul, N.; Shelestov, A.; Korsunskaya, Y.; Yailymov, B. Sentinel-3 Urban Heat Island Monitoring and analysis for Kyiv Based on Vector Data. In Proceedings of the 10th International Conference on Dependable Systems, Services and Technologies (DESSERT), Leeds, UK, 5–7 June 2019; pp. 131–135.
88. Manoli, G.; Faticchi, S.; Schläpfer, M.; Yu, K.; Crowther, T.W.; Meili, N.; Burlando, P.; Katul, G.G.; Bou-Zeid, E. Magnitude of urban heat islands largely explained by climate and population. *Nature* **2019**, *573*, 55–60. [[CrossRef](#)] [[PubMed](#)]
89. Garnett, R.; Adams, M.D. LIDAR—A technology to assist with smart cities and climate change resilience: A case study in an urban metropolis. *ISPRS Int. J. Geo-Inf.* **2018**, *7*, 161. [[CrossRef](#)]
90. Haile, A.; Rientjes, T. Effects of LiDAR DEM resolution in flood modelling: A model sensitivity study for the city of Tegucigalpa, Honduras. In Proceedings of the ISPRS Wg Iii/3, Iii/4, Vienna, Austria, 29–30 August 2005; pp. 168–173.
91. Rowlands, I.H.; Kemery, B.P.; Beausoleil-Morrison, I. Optimal solar-PV tilt angle and azimuth: An Ontario (Canada) case-study. *Energy Policy* **2011**, *39*, 1397–1409. [[CrossRef](#)]
92. Szabó, Z.; Schlosser, A.; Túri, Z.; Szabó, S. A Review of Climatic and Vegetation Surveys in Urban Environment with Laser Scanning: A Literature-based Analysis. *Geogr. Panonica* **2019**, *23*, 411–421. [[CrossRef](#)]
93. Kong, F.; Yan, W.; Zheng, G.; Yin, H.; Cavan, G.; Zhan, W.; Zhang, N.; Cheng, L. Retrieval of three-dimensional tree canopy and shade using terrestrial laser scanning (TLS) data to analyze the cooling effect of vegetation. *Agric. For. Meteorol.* **2016**, *217*, 22–34. [[CrossRef](#)]
94. Bournez, E.; Landes, T.; Saudreau, M.; Kastendeuch, P.; Najjar, G. Impact of level of details in the 3D reconstruction of trees for microclimate modeling. *Int. Arch. Photogramm. Remote Sens. Spat. Inf. Sci. ISPRS Arch.* **2016**, *41*, 257–264. [[CrossRef](#)]
95. Masson, V.; Heldens, W.; Bocher, E.; Bonhomme, M.; Bucher, B.; Burmeister, C.; de Munck, C.; Esch, T.; Hidalgo, J.; Kanani-Sühring, F.; et al. City-descriptive input data for urban climate models: Model requirements, data sources and challenges. *Urban Clim.* **2019**, *31*, 100536. [[CrossRef](#)]
96. EEA. *Urban Adaptation to Climate Change in Europe. Challenges and Opportunities for Cities Together with Supportive National and European Policies*; EEA Report 2/2012; EEA: Luxemburg, 2012; 148p.
97. Reckien, D.; Flacke, J.; Olazabal, M.; Heidrich, O. The influence of drivers and barriers in urban adaptation and mitigation plans—Empirical analysis of European cities. *PLoS ONE* **2015**, *10*, e0135597. [[CrossRef](#)] [[PubMed](#)]
98. Tapia, C.; Abajo-Alda, B.; Feliu, E.; Mendizabal, M.; Martínez-Sáenz, J.; Fernández, G.J.; Laburu, T.; Lejarazu, A. Profiling urban vulnerability to climate change: An indicator-based vulnerability assessment for European cities. *Ecol. Indic.* **2017**, *78*, 142–155. [[CrossRef](#)]
99. Bastin, J.-F.; Clark, E.; Elliott, T.; Hart, S.; van den Hoogen, J.; Hordijk, I.; Ma, H.; Majumder, S.; Manoli, G.; Maschler, J.; et al. Understanding climate change from a global analysis of city analogues. *PLoS ONE* **2019**, *14*, e0217592. [[CrossRef](#)]

100. Grekousis, G.; Mountrakis, G.; Kavouras, M. An overview of 21 global and 43 regional land-cover mapping products. *Int. J. Remote Sens.* **2015**, *36*, 5309–5335. [[CrossRef](#)]
101. Wang, P.H. Mapping 2000–2010 Impervious Surface Change in India Using Global Land Survey Landsat Data. *Remote Sens.* **2017**, *9*, 366. [[CrossRef](#)]
102. Liu, X.; Pei, F.; Wen, Y.; Li, X.; Wang, S.; Wu, C.; Cai, Y.; Wu, J.; Chen, J.; Feng, K.; et al. Global urban expansion offsets climate-driven increases in terrestrial net primary productivity. *Nat. Commun.* **2019**, *10*, 5558. [[CrossRef](#)]
103. Chen, J.; Chen, J.; Liao, A.; Cao, X.; Chen, L.; Chen, X.; He, C.; Han, G.; Peng, S.; Lu, M.; et al. Global land cover mapping at 30 m resolution: A POK-based operational approach. *ISPRS J. Photogramm. Remote Sens.* **2015**, *103*, 7–27. [[CrossRef](#)]
104. Liu, X.; de Sherbinin, A.; Zhan, Y. Mapping Urban Extent at Large Spatial Scales Using Machine Learning Methods with VIIRS Nighttime Light and MODIS Daytime NDVI Data. *Remote Sens.* **2019**, *11*, 1247. [[CrossRef](#)]
105. Radwan, T.M.; Blackburn, G.A.; Whyatt, J.D.; Atkinson, P.M. Dramatic Loss of Agricultural Land Due to Urban Expansion Threatens Food Security in the Nile Delta, Egypt. *Remote Sens.* **2019**, *11*, 332. [[CrossRef](#)]
106. van Vliet, J. Direct and indirect loss of natural area from urban expansion. *Nat. Sustain.* **2019**, *2*, 755–763. [[CrossRef](#)]
107. Buchhorn, M.; Smets, B.; Bertels, L.; Lesiv, M.; Tsendbazar, N.-E.; Herold, M.; Fritz, S. Copernicus Global Land Service: Land Cover 100m: Epoch 2015: Globe. *Zenodo* **2019**. [[CrossRef](#)]
108. Congedo, L.; Sallustio, L.; Munafo, M.; Ottaviano, M.; Tonti, D.; Marchetti, M. Copernicus high-resolution layers for land cover classification in Italy. *J. Maps* **2016**, *12*, 1195–1205. [[CrossRef](#)]
109. Ferri, S.; Siragusa, A.; Sabo, F.; Pafi, M.; Halkia, M. *The European settlement map 2017 release. Methodology and output of the European settlement map (ESM2p5m)*; JRC Technical reports; UR 28644 EN; European Commission: Brussels, Belgium, 2017. [[CrossRef](#)]
110. Schneider, A.; Friedl, M.A.; Potere, D. Mapping global urban areas using MODIS 500-m data: New methods and datasets based on 'urban ecoregions'. *Remote Sens. Environ.* **2010**, *114*, 1733–1746. [[CrossRef](#)]
111. Stewart, I.D.; Oke, T. Local Climate Zones for Urban Temperature Studies. *Bull. Amer. Meteor. Soc.* **2012**, *93*, 879–1900. [[CrossRef](#)]
112. Demuzere, M.; Bechtel, B.; Middel, A.; Mills, G. Mapping Europe into local climate zones. *PLoS ONE* **2019**. [[CrossRef](#)]
113. Fan, H.; Zipf, A.; Fu, Q.; Neis, P. Quality assessment for building footprints data on OpenStreetMap. *Int. J. Geogr. Inf. Sci.* **2014**, *28*, 4. [[CrossRef](#)]
114. Dijkstra, L.; Poelman, H. Cities in Europe the New OECD-EC Definition. European Commission. RF 01/2012. Available online: https://ec.europa.eu/regional_policy/sources/docgener/focus/2012_01_city.pdf (accessed on 3 December 2019).



© 2020 by the authors. Licensee MDPI, Basel, Switzerland. This article is an open access article distributed under the terms and conditions of the Creative Commons Attribution (CC BY) license (<http://creativecommons.org/licenses/by/4.0/>).

Review

The Maturing Interdisciplinary Relationship between Human Biometeorological Aspects and Local Adaptation Processes: An Encompassing Overview

Andre Santos Nouri ^{1,2} and Andreas Matzarakis ^{3,4,*}

¹ Faculty of Architecture, University of Lisbon, Rua Sá Nogueira, Pólo Universitário do Alto da Ajuda, 1349-063 Lisbon, Portugal; andrenouri@fa.ulisboa.pt

² Department of Interior Architecture and Environmental Design, Faculty of Art, Design and Architecture, Bilkent University, 06800 Bilkent, Turkey

³ Research Centre Human Biometeorology, German Meteorological Service, D-79104 Freiburg, Germany

⁴ Chair of Environmental Meteorology, Faculty of Environment and Natural Resources, Albert-Ludwigs-University, D-79085 Freiburg, Germany

* Correspondence: andreas.matzarakis@dwd.de; Tel.: +49-69-8062-9610

Received: 10 October 2019; Accepted: 22 November 2019; Published: 25 November 2019

Abstract: To date, top-down approaches have played a fundamental role in expanding the comprehension of both existing, and future, climatological patterns. In liaison, the focus attributed to climatic mitigation has shifted towards the identification of how climatic adaptation can specifically prepare for an era prone to further climatological aggravations. Within this review study, the progress and growing opportunities for the interdisciplinary integration of human biometeorological aspects within existing and future local adaptation efforts are assessed. This encompassing assessment of the existing literature likewise scrutinises existing scientific hurdles in approaching existing/future human thermal wellbeing in local urban contexts. The respective hurdles are subsequently framed into new research opportunities concerning human biometeorology and its increasing interdisciplinary significance in multifaceted urban thermal adaptation processes. It is here where the assembly and solidification of ‘scientific bridges’ are acknowledged within the multifaceted ambition to ensuring a responsive, safe and thermally comfortable urban environment. Amongst other aspects, this review study deliberates upon numerous scientific interferences that must be strengthened, inclusively between the: (i) climatic assessments of both top-down and bottom-up approaches to local human thermal wellbeing; (ii) rooted associations between qualitative and quantitative aspects of thermal comfort in both outdoor and indoor environments; and (iii) efficiency and easy-to-understand communication with non-climatic experts that play an equally fundamental role in consolidating effective adaptation responses in an era of climate change.

Keywords: human biometeorology; thermal comfort; interdisciplinarity; climate change adaptation; thermal sensitive design

1. Introduction

Before the turn of the century, the limited local specificity of global top-down approaches to climatic risk factors within urban environments was already well known by the international scientific community. In particular, such fragility in applicative know-how led to the growing interest in identifying how local bottom-up approaches could be instigated. As a result, and likely associated to the contiguous maturing Climate Change Adaptation (CCA), there has been a rapidly growing interest in how adaptation tools can be locally instigated to improve the climatic responsiveness of the urban public realm, e.g., [1–14].

Moreover, when considering the urban climate condition and human wellbeing within public realm, the scientific community has already recognised the growing importance of bottom-up approaches to climatic risk factors that are already presenting aggravations associated to climate change impacts [15–19]. For this reason, and as exemplified by studies undertaken by [12,20–24] local scales are becoming an arena in which both decision makers and designers are seeking means to address physiological and psychological factors pertaining to human thermal comfort within the public realm in an era of climate change.

Although examinations pertaining to the characteristics of the urban climate date well back to the previous century, e.g., [25–31], the practical application upon contemporary practices of urban design and planning has been limited [3,17,32,33]. Such a desire on behalf of the scientific community to further develop climatic tools can be intertwined with the earlier encompassing perspective of Wilbanks and Kates [34] who suggested that “the bulk of the research relating to local places to global climate change has been top-down, from global toward local, concentrating on methods of impact analysis that use as a starting point climate change scenarios derived from global models, even though these have little regional or local specificity. There is a growing interest, however, in considering a bottom-up approach, asking such questions as (. . .) how efforts at mitigation and adaptation can be locally initiated and adapted” (p. 1).

Such scientific interrogations chronologically coincided with the international recognition that mitigation efforts alone were no longer sufficient to address the potential impacts of climate change. Resultantly, the turn of the century witnessed an exponential leap for CCA efforts. Almost twenty years onwards, the demand for local application orientated approaches and tools are at an all-time high, both at assessment and at design levels. Within local scales, these assessments are predominantly focused upon the concrete symbiotic relationship between that of built form and encircling atmospheric conditions beneath the Urban Canopy Layer (UCL). Subsequently, it is here where the planning and design of the public realm and indoor environments can serve as a niche for interdisciplinary bottom-up approaches that question how efforts at adaptation can be locally initiated and adopted.

2. Review Structure

Within the scientific community, the balance between research articles and review articles discloses the encompassing ambition to develop existing knowledge, and at the same time, continually organise, review and structure the state-of-the-art. The objective of this study falls within the latter category, and aims to present an encompassing overview of the growing interdisciplinary relationships and interrogations concerning human biometeorological aspects associated to the practice of local thermal adaptation efforts. Divided into three predominant sections, the study situates: (i) the investigative prospectus for human biometeorology within the ever consolidating CCA agenda; (ii) the opportunities to further develop existing thermo–physiological approaches to identify both existing and future thermal risk factors that jeopardise urban wellbeing in indoor/outdoor settings; and, (iii) existing approaches and creative means to improve the thermal responsiveness of the urban environment through thermal sensitive urban design and planning efforts within local scales. Aiming to transition from the broader to the more specific facets of disclosed interdisciplinary relationship between human biometeorology and that of thermal adaptation processes, a summary of this division is presented in Figure 1.

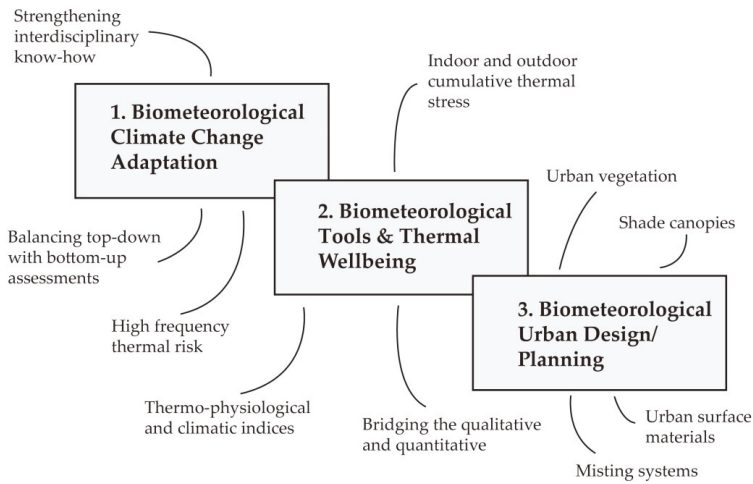


Figure 1. Structure schematic of review throughout the three sequential sections presented in the study.

Within each of the sections, the opportunities presented by human biometeorology to enhance local bottom-up adaptation processes are identified. In Section 2, and within the scope international CCA, based upon the unequivocal and direct thermo-physiological affects climate change shall have upon the human body, current methods, warning systems and impact projection assessments are discussed. Based upon local scales and recognising the increased need to go beyond ‘high-impact but low frequency’ impact projections; biometeorological tools to address the high frequency thermal risk factors are adjacently reviewed. Subsequently, and again with an emphasis on strengthening interdisciplinary bridges, this section moreover discusses the better integration and recognition of qualitative and quantitative aspects of thermal comfort in wholesome thermal comfort evaluations. Interconnected with the previous two points, the review study deliberates upon the fundamental transient associations between comfort thresholds and urban indoor and outdoor contexts. Lastly, and in direct association to local scales and how they can be feasibly modified through creative and flexible thermal sensitive adaptation processes, different existing measures to address local thermo-physiological risk factors in the urban public realm are reviewed. These disclosed measures are considered to be a part of a newly emerging scope for practices such as urban design and planning as a result of the effective bridging with local human biometeorology.

Overall, and throughout this review study, it is argued that the successful approach towards these factors highlights the growing significance of interdisciplinarity between different fields of practice. Ultimately, it is this assembly and fortification of collaborative scientific bridges that will bring different professionals together to tackle the same pressing issues within the urban environment. Naturally, while both scientific existing outcomes and obstacles are identified within the existing state-art-of-the-art, such obstacles are correspondingly framed into scientific opportunities to expanding interdisciplinary mentality/know-how regarding human biometeorology, and moreover, its unequivocally growing prominence in urban adaptation processes.

3. Biometeorological Climate Change Adaptation

Well before the turn of the century, and inclusively prior to the arrival of the CCA, Oke [35] identified that “relatively little of the large body of knowledge concerning urban climate has permeated through to working planners (. . .) the reasons for this state of affairs are many, but amongst those most cited are the inherent complexity of the subject, its interdisciplinary nature and lack of meaningful dialogue between planners and the climatological research community.” (p. 1). Today, and even with

growing consolidation of the CCA, the adjacent enclosure of pertinent biometeorological data and information within municipal and policy documents has been a complicated and a slow process.

3.1. Strengthening Interdisciplinary Know-How

In an earlier study conducted by Alcoforado and Vieira [36] that identified that within the Portuguese context, many cities presented a significant lack of pertinent meteorological data that could otherwise inform such local thermal adaptation efforts. Through the analysis of 15 master plans of urban municipalities, the respective study identified that although climatic information was considered in almost all of them, the information often proved either unreliable, or of little use for local adaptation efforts. Such a discrepancy was later argued by Alcoforado, Andrade, Lopes and Vasconcelos [17] to be attributable to numerous causes, including that the meteorological data from typical stations used in such plans were not applicable for microclimatic studies. Such a conclusion goes back to the prior conclusions of Oke [35], who additionally pointed at the difficulty in translating such information into robust tools for concrete local urban planning. Naturally, such difficulty is further increased at municipal policy and guideline levels.

Nevertheless almost two decades into the twenty-first century, and still within the Portuguese context, although further interdisciplinary strengthening is still considered essential [16], promising interest and integration with municipal entities are starting to be established [37]. This establishment can be inclusively associated to the scientific disseminations of the 'Climate Change and Environmental Systems Research' (CEG/CliMA) group. A group that has thus far conducted research into numerous topics, including overall bioclimatic conditions within Lisbon [38,39], causalities and intensities of Urban Heat Island (UHI) effects [18,40,41], urban wind patterns [42,43] and potential climatic integration within planning policy [15,44].

The exemplified disseminations focused on Lisbon mark a clear progression in addressing Oke's [35] early outlook. Nonetheless, and with CCA serving as a continually growing catalyst for interdisciplinary thermal adaptation efforts, the international growing interaction with non-climatic experts (e.g., urban planners/designers, architects and landscape architects) must be upheld to address local thermo-physiological risk factors, as identified in [2,3,11,33,45–53],

3.2. Balancing Top-Down with Bottom-Up Assessments

As already mentioned, the international scientific community has already recognised the crucial role of bottom-up approaches that focus upon the importance of local scales. Although top-down approaches and disseminations have presented an imperative emerging international co-operative understanding of the existing and future global climatic system, such outcomes are rarely capable (nor so intended) to provide guidance at local scales. Resultantly, the amount of disseminated studies on this topic has increased dramatically since the turn of the century. In accordance, both the limitations and means to improve local scale analysis tools have grown across different disciplines such as urban climatology, and urban planning/design.

So far, and in accordance with Global Circulation Models (GCMs), global temperatures shall continue to rise throughout the 21st century. Yet, it has adjacently been recognised that such top-down climatic assessments are often less useful for local scale analysis tools and adaptation. For instance, within the assessments reports of international entities such as the Intergovernmental Panel on Climate Change (IPCC), the effects of weather are often described with a simple index based upon amalgamations of air temperature (T_a) and Relative Humidity (RH). Although it is indispensable to recognise the value of such descriptions within the maturing CCA agenda, when pondering upon bottom-up approaches to climatic vulnerability, the exclusion of vital non-temperature factors (i.e., radiation fluxes, wind speed (V) and human thermo-physiological factors) have been argued to decrease their usefulness for local thermal decision making and design [2,16,19,54,55].

In the study conducted by Matzarakis and Amelung [54], through the use of synoptic global radiation estimations retrieved from monthly sunshine fractions (extracted from the Hadley Centre's

HadCM3 model—one of the predominant models utilized by the IPCC in its third assessment report in 2001), clear underestimations of global climate change impacts on human thermal comfort thresholds were identified. As an example, Western European areas could witness changes in thermo–physiological indices by up to 15 °C based upon worst case scenarios. The synoptic projections sharply differ from the IPCC projections established upon singular climatic variables such as T_a [56,57]. Retrospectively, the significance of the study was twofold, it: (1) presented how the inclusion of non-temperature variables (i.e., radiation fluxes) could dramatically amplify the gravity of climate change projections; and, (2) showed an initial approach to running climate change scenario variables through a biometeorological model to understand how such variables would interact with the human body, and subsequently, obtain an estimation of thermo–physiological stress levels by the end of the century. Derivative from GCMs, and recognising the analogous limitations of standard climatic variables in weather forecasting activities, a recent study undertaken by Giannaros et al. [58] also emphasised the: (1) significance of human biometeorology in not only assessing present-day meteorological conditions, but warning provisions for both heat waves and cold outbreaks; and, (2) crucial role of effectively and accessibly communicating easy-to-understand to the general public.

Processed from GCMs, both studies conducted by Matzarakis and Amelung [54] and Giannaros, Lagouvardos, Kotroni and Matzarakis [58] marked clear strides in further consolidating the imperative role of human biometeorology in identifying and managing existing/future thermo–physiological risk factors. Subsequently, these strides also validate the continual importance of top-down assessments, even when specific local urban characteristics were not variables considered either study. More specifically, this was accomplished by the on-going robust emphasis upon: (i) frequently overlooked variables such as radiation fluxes; (ii) the symbiotic relationship with the human thermo–physiological system; and lastly, (iii) the critical role of the ease-of-assess, transmission and comprehensibility of the results for non-climatic experts and general public.

3.3. High Frequency Thermal Risk Factors

Contrastingly to the former studies, many top-down climatic disseminations (especially from international bodies), while fundamental, remain frequently “focussed [on] the exposure of cities to hazards that have a huge impact but low frequency. [They] have little to say about the high-frequency and microscale climatic phenomena created within the anthropogenic environment of the city” [59]. Contiguously, and as identified by numerous authors that address human thermal comfort through the elaboration of creative measures through urban planning and design, it is within the anthropogenic environment of the city where human wellbeing becomes crucial [13,60,61].

For this reason, it is here where “landscape architects and urban designers strive to design places that encourage [urban] activities, places where people will want to spend their time (. . .) however unless people are thermally comfortable in the space, they simply won’t use it. Although few people are even aware of the effects that design can have on the sun, wind, humidity and air temperature in a space, a thermally comfortable microclimate is the very foundation of well-loved and well-used outdoor places.” [23]. Analogous inferences were reached by the earlier study conducted by Whyte [29] who advocated that “by asking the right questions in sun and wind studies, by experimentation, we can find better ways to board the sun, to double its light, or to obscure it, or to cut down breezes in winter and induce them in the summer” (p. 45).

Respectively, and based upon the overarching principal that actual adaptation measures take place at finer scales, it is the concrete bond within specific localities which can substantiate such bioclimatic adaptation initiatives and tools in cities [1,13,55,62,63]. It is at this scale where the encircling microclimatic under the UCL that has direct ‘in-situ’ influences upon pedestrian comfort thresholds.

Undoubtedly, such principals enforce the fundamental relationship between resulting local climatic variables beneath the UCL, with that of human biometeorology. Under a more encompassing perspective, this suggests that urban form, layout and design have an enormous capability to enhance

(or reduce) human wellbeing standards in cities. In this way, the interdisciplinary spheres of human biometeorology with that of climatic adaptation measures/tools must continue to be explored further.

4. Biometeorological Tools and Thermal Wellbeing

In accordance with the previously discussed scope of Oke [35], and the ‘climate-comfort’ rational discussed by Olgyay [30], this segment discusses the potentiality of interdisciplinarity in linking human biometeorology tools and assessments with local urban thermal wellbeing. The term ‘locality’ is again approached as the physical niche in which creative interdisciplinary practices such as Public Space Design (PSD) can render relevant, yet direct, thermal modifications of pedestrian thermo-physiological stress thresholds. Specifying this rational a little further in the greater context of local decision making and design, this catalyses two predominant perspectives, as suggested by Nouri, Costa, Santamouris and Matzarakis [3]: (i) the requirement to improve and facilitate the bioclimatic design guidelines within such environmental perspectives for local action and adaptation; and, (ii) given the growth of the CCA agenda, the accompanying cogency for local, thermal and pre-emptive climate-sensitive action and tools.

4.1. Thermo-Physiological and Climatic Indices

To undertake such an exercise, the direct effects of the thermal environment must be evaluated against the human biometeorological system. Such a multifaceted bond can be examined through the use of thermal indices that are centred on the energy balance of the human body [64]. Thus far, within the international community, a vast amount of thermal indices have been developed, and moreover, reviewed against one another. Examples of these studies are presented in Table 1.

Table 1. Example of studies that review and compare the application efficiency of different thermal indices in different settings.

No. of Investigated Indices	Dominant Focused Context	Region Specified	Year	Source
5	Not Stipulated	No	1988	[65]
2	Outdoor	Taiwan	2012	[66]
40	Outdoor	Mediterranean Zones	2014	[67]
162	Indoor/Outdoor	No	2015	[68]
3	Outdoor	Doha, Qatar	2015	[69]
24	Outdoor	Polar, Cold, Temperate, Arid and Tropical	2016	[70]
165	Indoor/Outdoor	No	2016	[71]
4 specific (from 165)	Outdoor	No	2018	[47]
6	Outdoor	No	2018	[72]
6	Outdoor	Mediterranean Zones	2019	[73]
6	Outdoor	Mediterranean Zones	2019	[74]
4	Indoor/Outdoor	No	2019	[75]
1 (MRT *1)	Indoor/Outdoor	No	2019	[76]
- (SVF *2)	Outdoor	No	2019	[77]

*1 MRT—Mean Radiant Temperature, *2 SVF—Sky View Factor.

Since the emergence of thermal indices well before the turn of the century, the international scientific community has since developed hundreds of different indices. Again, such an occurrence naturally leads to review and comparative studies of the indices themselves through different analytical methodologies and within different climatic contexts. Furthermore, and as exemplified by the studies undertaken by Golasi, Salata, Vollaro and Coppi [72], there still remain scientists that pursue the further standardisation of a global outdoor standardisation thermal indices. Although met with some resistance due to the already extensive amount and versatility of existing indices, such studies still salient the continual and important scientific desires to further develop additional approaches to human biometeorology. Adjacently, from the large identified sample of indices, many studies have suggested that only between 6 and 4 thermal indices can provide wholesome local human thermo-physiological evaluations [47,69,73–75]. In addition, and as a distinguished example from many related studies (discussed later in this section), the work undertaken by Lin, Tsai, Hwang and Matzarakis [66] presented important outputs pertaining to crucial relationships with microclimatic variables such as Mean Radiant Temperature (MRT) and Sky View Factor (SVF) ratios. Regarding these two aspects, and although the former two studies in Table 1 do not categorically refer to the comparison of thermal indices, both present noteworthy contemporary reviews regarding the calculation methods of: (i) MRT in indoor and outdoor environments through different applicative algorithms and models [76]; (ii) SVF through a diverse range of reviewed methodologies and software packages, moreover highlighting their respective weaknesses and strengthens within local microclimatic assessments and linkage with urban planning processes and decision making [77].

To illustrate a sample of the inherently different utilised thermal indices within the scientific community, and based upon the typological division suggested by Freitas and Grigorieva [68], of the eight, four typologies were included in Table 2, these being: (i) B–singular parameter model; (ii) C–climatic index based upon algebraic or statistical model; (iii) F–energy balance strain model; (iv) G–energy balance stress model.

Table 2. Illustration of selected thermal indices and their respective index typologies as defined by Freitas and Grigorieva [68].

Index	Acronym	Typology	Source
Perceived Temperature	(PT)	(G)–Energy balance stress model	[78]
Standard Effective Temperature	(SET *)	(G)–Energy balance stress model	[79,80]
Outdoor Standard Effective Temperature	(OUT_SET *)	(G)–Energy balance stress model	[63,81]
Thermal Humidity Index	(THI)	(C)–Algebraic/statistical model	[82]
Predicted Mean Vote	(PMV)	(G)–Energy balance stress model	[28,83]
Predicted Percentage of Dissatisfied	(PPD)	(G)–Energy balance stress model	[28]
Humidex	(HD)	(C)–Algebraic/statistical model	[84]
Index of Thermal Stress	(ITS)	(F)–Energy balance strain model	[31]
Outdoor thermal comfort model	(COMFA)	(G)–Energy balance stress model	[85,86]
Universal Thermal Climate Index	(UTCI)	(G)–Energy balance stress model	[87–89]
Wet Bulb Temperature	(WBGT)	(B)–Single-parameter model	[90,91]
Predicted Heat Strain	(PHS)	(F)–Energy balance strain model	[92]
Physiologically Equivalent Temperature	(PET)	(G)–Energy balance stress model	[26,93,94]
modified Physiologically Equivalent Temperature	(mPET)	(G)–Energy balance stress model *1	[95]

*1 New modified physiologically equivalent temperature (mPET) index included in (G) typology due to its close proximity to the original Munich energy-balance model for Individuals (MEMI).

Based upon the studies disclosed in Table 1, of the four typologies presented in Table 2, the predominantly utilized indices for outdoor studies have been those constructed upon the energy balance stress models, in particular, the Physiologically Equivalent Temperature (PET), Predicted Mean Vote (PMV), Universal Thermal Climate Index (UTCI) and Standard Effective Temperature (SET*) indices [96], especially for the climatic evaluation for urban planning and design [75].

In the case of the latter two examples in Table 2, of all of the thermo–physiological indices, PET has been one of the most commonly used steady-state model in human biometeorological studies [67]. Constructed upon the Munich Energy-balance Model for Individuals (MEMI) [97], it is designated as the T_a at which, in a typical indoor setting, the human energy budget is maintained by the skin temperature (T_{skin}), core temperature (T_{core}) and perspiration rate that are equivalent to those under the conditions to be investigated [93]. Retrospectively, the likely reason for its higher application can be attributable to: (i) its feasibility in being calibrated on easily obtainable microclimatic elements, and (ii) its measuring unit being ($^{\circ}\text{C}$), which in turn, simplifies its comprehension by non-climatic experts, including urban designers/planners and architects. This being said, synonymous to the equally maturing body of knowledge in human biometeorology, numerous studies have already made headway in the development of the PET index as well. Directed specifically towards improving the calibration of the integrated thermoregulation and clothing models utilised by the PET index, Chen and Matzarakis [95] launched the new modified Physiologically Equivalent Temperature (mPET) index. As discussed in the study, the main modifications of the mPET are the integrated thermoregulation model (modified from a single double-node body model to a multiple-segment model) and updated the clothing model, resulting in more accurate evaluations of the human bio-heat transfer mechanism, particularly during periods of higher thermal stimuli. Such increased accuracy of the modified index was subsequently verified by numerous studies in different countries and climatic contexts [5,19,73,98,99].

4.2. Bridging the Qualitative with the Quantitative

As mentioned in the introduction, in addition to physiological aspects, there is also a demand in accompanying the associated call for investigating psychological factors of human thermal comfort. Although located predominantly within the qualitative spectrum, the ‘intangible’ attributes of human psychology have also been recognised to play a crucial role in diurnal human thermal comfort investigations. Such recognition has arisen at both in indoor contexts, e.g., [100–106], and outdoor contexts, e.g., [24,29,32,48,107–114].

Based upon a bottom-up perspective that focuses upon the role of local scales in ensuring human wellbeing during an era of climate change, Figure 2 illustrates the required interactions between that of: (1) Physiological aspects, which consider the direct quantitative influences of encircling microclimates upon the human-biometeorological system; (2) Psychological aspects, which prompts the adjacently important value of qualitative aspects of thermal comfort thresholds, including assessments of human behaviour patterns, and that of thermal adaptability; and lastly, (3) the interaction with further climate change impacts during the unravelling of the twenty-first century, that are already aggravating existing human thermal comfort standards. From the interaction of these three aspects, originates the requirement for further interdisciplinary biometeorological tools that can aid local assessment and design practices, both now, and in the future through informed CCA efforts.

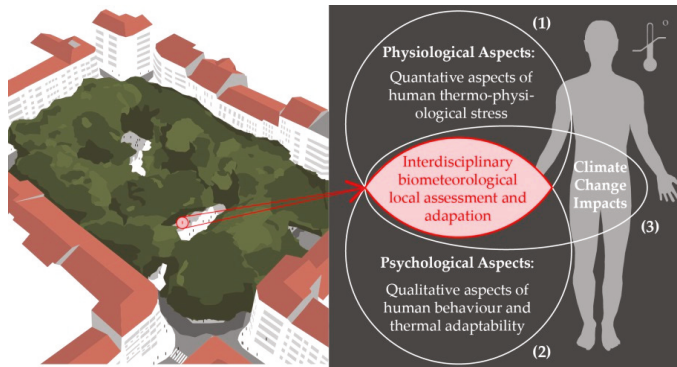


Figure 2. Illustrative division of human biometeorological facets within local scales based upon a bottom-up approach in century prone to climate change impacts.

Although the comparative significance between qualitative and quantitative aspects of thermal comfort is still debated within different studies (i.e., where some authors methodically favour one aspect more than the other), numerous veracities are concomitant to both schools of thought. To start with, it is consensus that there is an unmistakable opportunity to explore how specific qualitative aspects of thermal comfort can build upon quantitative assessments. Such an opportunity can be allied to a few simple premises, that: (i) predominantly in outdoor environments, human beings rarely pursue microclimatic monotony [109,115], reversely, it is the very desire of climatic diversity and stimulation (and even overstimulation beyond stipulated thermal comfort levels [108,111]) that also lures pedestrians outdoors [29]; (ii) human beings are by default peripatetic, meaning that their movement patterns are based upon complex behaviour and decision making processes associated to ‘intangible’ attributes (e.g., expectations, past experience, perceived control and time of exposure) [32,116].

As a result, improving this integration between these two aspects could potentially present means to better predict and account for human psychological attributes for local thermal sensitive design and planning. Of the attributes previously mentioned, it is suggested that these main attributes can open up new interdisciplinary lines of research, which by default, coerce the bridging with quantitative aspects of thermal comfort. In addition, such a bridging can also entice further considerations also interrelated to indoor conditions, as also suggested by past review studies exemplified by the prominent example disseminated by Brager and de-Dear [117]. As part of their review, they inclusively referenced an entire issue from *Energy and Buildings* [118] that focused upon the variation amongst the human psychological ‘perceived need’ or ‘desire’ for indoor mechanical air conditioning.

4.3. Indoor and Outdoor Cumulative Thermal Stress

In accordance with the human biometeorological evaluation study undertaken by Charalampopoulos, Tsiros, Chronopoulou-Sereli and Matzarakis [11] who utilised the PET index, two preliminary factors were adjoined, these being: (1) the PET Load (PETL), i.e., the amount of variation from the optimal physiological stress range (between PET values of 18–23 °C) as defined by [119,120]; and, (2) the cumulative PET Load (cPETL), i.e., the sum of the PETL for an X amount of hours which can be configured to represent a portion, or the full 24 hours of a respective day. Such an approach enables a preliminary understanding of cumulative human thermal stress loads beyond ‘neutral’ (or background) conditions. Although intended for outdoor assessments, principals of cumulative human thermal stress can also be transposed to methodically approach human psychological attributes, particularly during periods and/or events of accentuated thermal stress, and even climate change [19]. Subsequently, such accentuation periods with higher stimuli can be unambiguously associated to

numerous urban events, particularly heatwaves. Alarming, and beyond the early consensus that increases in heatwaves are ‘very likely’ throughout the twenty-first century [121]; the subsequent fifth assessment report moreover stipulated that the influences of climate change upon heatwaves shall be more significant than the impacts upon global average temperatures [122].

Taking the European heatwave of 2003 as an extreme example which explicitly amplified the need for additional measures to warn, cope and prevent the recurrence of such events upon public health and wellbeing [58,123,124]. Within Western Europe, the data provided by Nogueira et al. [125] identified that between the 29 July and 13 August 2003 within the district of Lisbon there was/were: (i) 15 days with a maximum T_a above 32 °C; (ii) a noteworthy consecutive run of 10 days with T_a above 32 °C; and, (iii) a 5 day period consecutively experiencing T_a above 35 °C. This extreme heat event led to severe implications on urban health, resulting in an estimated mortality rate increase of 37.7% in comparison to what would be expected under normal conditions.

Key lessons for human biometeorology can continue to be extracted from this type climatic event that has serious implications for human health and wellbeing in urban contexts. Such teachings, in turn, again call for more sophisticated integration and analytical tools between the quantitative and qualitative aspects of thermal comfort, both for outdoor and indoor environments. More specifically, and considering the early principals of the urban energy balance as defined by Oke [126] the reciprocal dynamics of indoor environments also play an essential role resultant of the: (i) increased heat storage within urban materials and buildings [18,22,40,127–131]; and the cause-and-effect of, (ii) anthropogenic emissions resultant of urban cooling energy loads associated to interior air conditioning [117,132–135], which by the end of the century can potentially increase by 166% (in energy demand) as a result of climate change [136].

In the case of naturally ventilated residential indoor environments during periods of extreme and extended heat stress, the principals of cumulative human thermal stress load can be strongly connected to psychological aspects. Although previously observed by Givoni [137] that “during periods of rising outdoor temperatures, e.g., a heat wave lasting for several days, the rate of rise of the indoor temperature is lower than that of the outdoors (. . .). As a result, the indoor temperatures during the heat-wave period will be somewhat lower” (p. 22), it is important to note that during extreme events, this ‘somewhat’ reduction while significant, is indicative of continued cumulative human thermal stress load during the night period. Such an extension, invariably, results in disruptions in human sleep cycles as a result of higher nocturnal indoor T_a levels [138,139]. These conclusions were also extended by a more recent review study conducted by Lan et al. [140], who also depicted upon the 2003 heatwave in Europe, and moreover, the associated future risk factors associated to human sleep disruptions as a result of climate change.

With regards to specific implications upon the human biometeorological system, the preceding study by Haskell et al. [141] indicated that T_a above the thermo-neutral thresholds increased wakefulness and decreases Slow Wave Sleep (SWS) which takes place in the late stages of non-Rapid Eye Movement ((n)REM). Such a stage is where energy restoration occurs, including the regulation of body glycogen levels, that are subsequently heavily consumed during active brain function [142]. Up until the more crucial and profound REM stage of sleep, the human body continues to thermo-regulate, and perspiration is proportional to the encircling thermal load [143]. During the latter stage of the sleep cycle, perspiration does not take place [144], and the human hypothalamic thermostat (in control of the body’s T_{core}) becomes sedentary as a result of the poikilothermic state during the REM stage [145]. Resultantly, the successfulness in reaching REM sleep strongly depends upon the adequate down-regulation of T_{core} beforehand. If not accomplished, inclusively in circumstances with high thermal loads, both SWS and REM will likely be replaced by wakefulness to maintain bodily homeothermic conditions [146,147]. Such homeothermy can be backtracked to the functioning principals of the previously mentioned MEMI.

This being said, and in addition to heat stress, exposure to elevated nocturnal RH also plays a pivotal role in thermal stress. More specifically, increased RH levels impedes sweat to evaporate,

thus impeding T_{skin} to dissipate heat and remain wet, thereby, suppressing adequate down-regulation of the body's T_{core} , and similarly decreasing the likelihood of REM sleep [147]. This influence of encircling nocturnal RH upon sleep quality has moreover been identified by other comparable studies, e.g., [140,148,149].

While suggested by prominent thermal comfort studies that people living in naturally ventilated buildings become accustomed to, and moreover grow to accept higher T_a and RH, [137], human biometeorological investigations have come to respectfully rebut such acclimatization easement (especially during periods of higher thermo-physiological loads). Respectively, and as identified by the early analysis undertaken by Libert et al. [150], heat-related sleep disruptions do not adapt even after five days of continuous diurnal and nocturnal heat exposure. Likewise, it was also later documented that the cerebral dynamics of SWS does not change after partial sleep deprivation (SD), where 'sleep pressure' would inevitably be augmented [151].

Subsequently, such results were also evidenced by the more recent study conducted by Nastos and Matzarakis [152] who analysed the daily records of SD against the frequency of daily weather conditions (with PET > 35 °C) and nocturnal conditions (with minimum T_a > 23 °C). The recorded events/admissions for SD were obtained from the psychiatric emergency unit of Eginition Hospital of the Athens University Medical School during the years of 1989 and 1994. It is important to note that in this particular study, the SD admissions dataset did not include cases which were associated to specific organic disturbances. Such an inclusion would very likely increase admission data numbers; but invariably, excessively extend the investigation parameters due to the inherent intricacies of specific human organic disturbances in relationship with SDs (e.g., pertinent to the respiratory system [153], and in oncological cases [154]). Irrespectively, the study identified that during continued periods of both diurnal and nocturnal thermal load, there was a substantial increase in SD, which moreover, did not seem to placate, nor adapt, to the respective conditions over time.

Overall, the studies in this section depict upon the significance of the Circadian Rhythm Cycle (CRC) in human wellbeing, which by definition, also extends to the human biometeorological thermoregulation dynamics during the night. Naturally, the circumstances during the CRC influence wellbeing standards, whereby if one part of the cycle inept, there will be a cause-and-effect relationship upon the following stage. In other words, if the cumulative thermal loads do not fluctuate adequately to allow the human-biometeorological system to regulate, replenish and restore attributes of the human physiology (including during different sleep stages), then this shall have direct implications upon human psychology as well. In this way, the physiological and the psychological attributes pertaining to thermal comfort can be directly related to one another. It is here where central intangible aspects as of human psychology as presented by, e.g., [32] can be further explored, including for urban sensitive planning and design.

Inarguably, there still remain other noteworthy impromptu influences upon these intangible characteristics that influence human behaviour. However, it is argued that such qualitative thermal comfort aspects (e.g., expectations, past experience, perceived control and time of exposure) can be rendered less subjective by more efficiently cross-examining human behaviour patterns and decision making against CRC dynamics and cumulative thermal stress.

Evaluating the specific case-by-case peripatetic behaviour of individual human beings is very complex. Yet it is here reasoned that further studies on this interdisciplinary topic can be undertaken based upon the unambiguous certainties that are already held by the scientific community, including the: (1) universal conduct of the human biometeorological system to thermal stimulus (including in cumulative terms); and, (2) impacts that extreme urban events can have upon both indoor and outdoor environments upon urban human wellbeing, including those associated to future climatic aggravation. For this reason, when one considers the urban populace as whole, it feasible to acknowledge that pedestrians shall, in general, show higher psychological predispositions under certain climatic conditions, particularly under prolonged extreme events.

As represented in Figure 3, this shall not only affect the peripatetic transitioning between indoor and outdoor movement patterns/durations, but the individual psychological aspects that catalyse such human behaviour. More precisely, during periods of extended thermo-physiological stress, elicited from ‘past experience’ of thermal discomfort, there shall be a greater pursuit (i.e., ‘expectation’) to address cumulative discomfort. Since this is associated with the CRC, it cannot be assumed that thermal stress simply resets at the end of the day. Naturally, the longer the susceptibility to cumulative load (including throughout the night) the greater the ‘expectation’ and reduced willingness for more ‘time of exposure’. Subsequently, and as developed throughout this section, it is suggested that there are opportunities for future concrete investigations to better link this symbiotic physiological and psychological relationship.

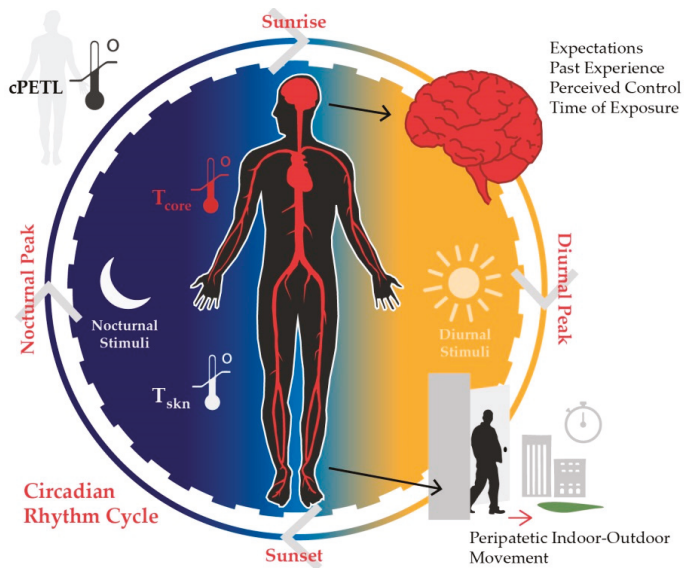







Figure 3. The relationship of the circadian rhythm cycle, cumulative stress and general psychological characteristics.

5. Biometeorological Urban Design/Planning

5.1. Urban Vegetation

So far within the existing literature, numerous review articles have already discussed the state-of-the-art of various aspects pertaining to the influences of vegetation upon urban climates. Of these review articles thus far, e.g., [3,20,128,155–159], the two predominant influences of vegetation pertaining to urban thermal comfort aspects have thus far been the: (i) direct reductions of urban T_a ; and moreover the (ii) associated interrelating reduction of UHI intensities. Other disseminated review studies have moreover deliberated on further positive attributes that vegetation can have upon indoor/outdoor human wellbeing standards in urban contexts. Within Table 3, these review studies are divided into five summarised topics that also play an important role in ensuring urban environmental health and welfare.

Table 3. Selected review studies concerning further positive attributes of vegetation within urban environments.

No.	Predominant Review Topic Summary	Icon	Study Year	Example Review Studies
(i)	Specific effects of green roofs, including indoor thermal behaviour, cooling loads and performance		2014	[160]
			2014	[161]
			2018	[162]
(ii)	Specific quantitative influences and performance of urban green walls/facades		2014	[163]
			2014	[164]
			2017	[165]
(iii)	Air quality and particles dispersion/abatement through the presence of vegetation		2015	[166]
			2015	[167]
			2017	[168]
(iv)	Overall socio-economic benefits, and challenges, of growing urban vegetation in the public realm		2011	[169]
			2015	[170]
(v)	Wider social impacts of street vegetation upon urban ecosystems and communities		2016	[171]

- (i) As suggested by the comprehensive review undertaken by Berardi, GhaffarianHoseini and GhaffarianHoseini [160] there is a very tactile opportunity to continue the exploration into the further quantification and assessments of interdisciplinary approaches regarding urban landscaping, plantations, construction and that of mechanical/environmental engineering. Moreover and in addition to stipulating the different classification of green roofs, the authors also cross-examined the typologies against their ability in mitigating UHI/air pollution, improve stormwater management, reduce urban noise and augment urban diversity. From the same year, and focused at the city scale, Santamouris [161] identified four categories to determine the particular efficiency of green roofs, namely through: (i) climatological variables, including radiation fluctuations; (ii) optical variables, including changes in albedo and absorptivity of the roof's vegetation; (iii) thermal variables, including thermal capacity and heat storage; and lastly, (iv) hydrological variables, including the dynamics of latent heat loss due to evaporation of the water vapour from the vegetative material (or in other words, evapotranspiration). Within the more recent study conducted by Shafique, Kim and Rafiq [162], it was revealed how green roofs can aid simulating urban natural hydrology systems, and also reduce factors such as UHI effects. Still within this recent study, the prominence of further interdisciplinary research was recognised, including in accompanying the demand for such technology through economically sustainable methods.
- (ii) With regards to the application of green walls and facades, the review study conducted by Hunter, Williams, Rayner, Aye, Hes and Livesley [163] reported that their efficiency must be based on multiple microclimatic factors, including G_{rad} , T_a and V (both adjacent to the structure, and


- in-between the gap with the respective wall). In the summary of the study, while the significant potential of green facades were recognised in urban contexts, it was adjacently argued that: (i) they are unlikely mechanisms to modulate internal buildings in all types of construction typologies and climatic contexts; and, (ii) its associated engineering terminology is often too specific to be readily understood across design and planning disciplines. Similarly, and also relating the application of these vegetation structures to different climates, and moreover the influences of different vegetative species, Perez, Coma, Martorell and Cabeza [164] came to similar conclusions. Finally, and within the more recent review study conducted by Medl, Stangl and Florineth [165] (and in addition to the recognised positive attributes mentioned above), the authors argued that there still remains a clear need for further interdisciplinary and standardized measurement approaches to guarantee the better application and erection of effective urban green facades.
- (iii) While the aforementioned studies also discussed issues of urban air quality and pollution dispersion through urban vegetation, Gallagher, Baldauf, Fuller, Kumar, Gill and McNabola [166] and Abhijith, Kumar, Gallagher, McNabola, Baldauf, Pilla, Broderick, Sabatino and Pulvirenti [168] took this analysis a step further. More specifically, it was identified that wind-tunnel and modelling results provide adequate evaluations, yet further real-world studies are still required to validate such findings. Similarly, and still in line with the aforementioned perspective of Oke [35], both studies moreover suggest that to develop clear guidelines for urban planners with regards to air quality and pollution dispersal; better interdisciplinary ‘channels’ must be fortified to enable such knowledge to be translated into practical guidelines to ensure their effective urban implementation. Convergent conclusions pertaining to the associated translation into urban planning and design tools/guidelines were also met by Janhall [167].
 - (iv) Undertaking a more socio-economic approach, the review study launched by Soares, Rego, McPherson, Simpson, Peper and Xiao [169] described the application of the Street Tree Resource Analysis Tool for Urban forest Managers (STRATUM) within Lisbon. The results of the study disclosed a clear quantitative breakdown of economic maintenance/managerial costs of urban vegetation species which was subsequently crossed examined with urban ‘energy savings’, air purification, increased property values, reduced stormwater runoff and CO₂ emissions. Still predominantly within the socio-economic spectrum, the later review study undertaken by Mullaney, Lucke and Trueman [170] also provided an investigation into financial aspects of urban vegetation. More specifically, beyond also disclosing environmental and socio-economic benefits, the costs/management of detailed characteristics such as pavement damage from tree roots were also case-studied.
 - (v) In the last segment, the study conducted by Salmond, Tadaki, Vardoulakis, Arbuthnott, Coutts, Demuzere, Dirks, Heaviside, Lim, Macintyre, McInnes, and Wheeler [171] undertook a more encompassing perspective, which suggested that based upon the existing literature, there needs to be a locally based bottom-up decision making process. Such a process was argued to be innately better associated with local community engagement to better determine ‘what matters to them’, and not just constructed upon the technical scientific aspects of ecological interventions. As a result, a matured interdisciplinary relationship between these cultural and scientific approaches was suggested to be essential to further exploit the disclosed societal and wider benefits provided by urban vegetation.

Parting from review studies, and focussing henceforth on individual investigations regarding the specific relationship of human thermo-physiological thresholds with urban vegetation, two distinct types of studies can be established, those: (1) which focus upon the direct ‘In-Situ’ (IS) influences of vegetation directly upon the encircling area (such as beneath the vegetative crown); and, (2) which investigate the effects of Park Cooling Islands (PCI) resultant of urban vegetation amid different spaces (where normally one is labelled as an urban ‘green space’).

Both within the IS and PCI types of study, the methodical approach towards human thermal comfort thresholds have been different. Most prominently, there is a clear distinction between studies

which have concentrated more upon singular variables (such as T_a), and those which have applied thermo-physiological indices that account for non-temperature variables, including radiation fluxes. Thus far, significant IS effects of urban vegetation specifically upon T_a and its associated connotations upon human thermal comfort have been well documented as exemplified in the studies in Table 4. Adjacently, studies focussing on the effects PCI upon T_a are successively presented in Table 5. Within these tables, the maximum thermal result obtained by the study, year, city and climatic context (through the Köppen Geiger (KG) [172] climatic classification system) are presented.

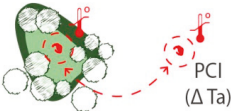
Table 4. Studies concerning in-situ (IS) changes in T_a resultant of urban vegetation.



Thermal Result (T_a Max)	Location	KG	Study Year	Source
-1.5 °C	California	'Csa'	1988	[173]
-0.7 °C	Tokyo	'Cfa'	2008	[174]
-2.2 °C	Athens	'Csa'	2010	[175]
-0.5 °C	Singapore	'Af'	2010	[176]
-1.0 °C	Melbourne	'Cfb'	2013	[177]
-1.0 °C	Manchester	'Cfb'	2014	[178]

Table Result Avg. = -1.2 °C

Table 5. Studies concerning changes in T_a as a result of urban park cooling islands (PCI) effects.



Thermal Result (T_a Max)	Location	KG	Study Year	Source
-4.0 °C	Mexico City	'Cwb'	1990-1	[179]
-2.5 °C	Dehli	'BSh'	1990-1	[180]
-3.0 °C	Kumanoto	'Cfa'	1991	[181]
-2.5 °C	Fukuoka	'Cfa'	1993	[182]
-2.0 °C	Tokyo	'Cfa'	1998	[132]
-4.0 °C	(Scaled model)	-	1999	[183]
-4.0 °C	Tel Aviv	'Csa'	2000	[184]
-4.0 °C	Botswana	'BSh'	2004	[185]
-3.5 °C	Tel Aviv	'Csa'	2006	[186]
-4.4 °C	Taipei	'Cfa'	2007	[187]
-2.5 °C	Taipei	'Cfa'	2010	[188]
-5.0 °C	Athens	'Csa'	2014	[189]
-5.0 °C	Chania	'Csa'	2014	[190]
-7.4 °C	Lisbon	'Csa'	2019	[191]

Table Result Avg. = -3.9 °C

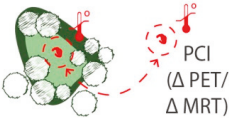
Between Tables 4 and 5, it is possible to identify that the studies have predominantly been undertaken within ‘Temperate’ climates, with variations mostly being discernable within the subcategories pertaining to both annual precipitation levels, and average temperature levels during the summer. Additionally, when considering the thermal effects in both Tables, the summarised averages of ‘maximum thermal effects’ present by the studies show clear thermal differences between IS and PCI typologies. As expected, this divergence can be attributable to the: (i) increased amount of vegetative mass within PCI studies that were able to have a greater impact upon elements such as atmospheric T_a and RH, which in IS studies were easier to dissipate in the atmosphere before allowing the utilised apparatus to record such modifications; and (ii) distances between the study’s measurement locations, which in the case of the some PCI studies could vary up to hundreds of metres, thus entailing other potential microclimatic influences (e.g., sufficiently notable morphological and topographical disparities, rendering urban corridor cooling effects through channelled V acceleration and V gusts).

Adjacently to these T_a studies, aspects of urban vegetation as a tool address and regulate human thermal comfort in urban environments through non-temperature factors have also been discussed extensively. Such factors included the direct role urban tree crowns reducing the amount of radiation reaching pedestrian levels [192–196]. Subsequently, this was followed by studies which focused upon assessments that included non-temperature dynamics through the use of human biometeorological models and indices in both IS studies (Table 6) and PCI studies (Table 7).

Table 6. Studies concerning IS changes in physiologically equivalent temperature (PET)/ mean radiant temperature (MRT) resultant of urban vegetation.

Thermal Result (PET/MRT Max)	Location	KG	Study Year	Source
−11.2 °C (PET)	Szeged	‘Cfb’	2006	[197]
−12.0 °C (PET)	São Paulo	‘Cfa’	2008	[198]
≈ −12.0 °C (MRT)	Huwei	‘Cfa’	2010	[199]
−20.0 °C (PET)	Shanghai	‘Cfa’	2011	[200]
−8.0 °C (PET)	Campinas	‘Cwa’	2012	[201]
−8.3 °C (PET)	Athens	‘Csa’	2012	[33]
−16.6 °C (PET)	Campinas	‘Cwa’	2015	[202]
−27.0 °C (MRT)	Manchester	‘Cfb’	2016	[203]
−4.6 °C (PET)	Toronto	‘Dfb’	2016	[22]
−3.4 °C (PET)	Hong Kong	‘Cwa’	2017	[204]
−9.9 °C (PET)	Lisbon	‘Csa’	2017	[108]
−15.6 °C (PET)	Lisbon	‘Csa’	2018	[99]
Table Result Avg. = −11 °C (PET)/−19.5 °C (MRT)				



Table 7. Studies concerning changes in PET/MRT as a result of urban PCI effects.


Thermal Result (PET/MRT Max)	Location	KG	Study Year	Source
−17.6 °C (PET)	Freiburg	'Cfb'	2003	[205]
−9.0 °C (PET)	Freiburg	'Cfb'	2006	[206]
−33.0 °C (MRT)	Lisbon	'Csa'	2007	[207]
−10.7 °C (PET)	Tel Aviv	'Csa'	2010	[208]
−39.2 °C (MRT)	Lisbon	'Csa'	2011	[209]
−12.0 °C (PET)	Tel Aviv	'Csa'	2012	[210]
−20.0 °C (MRT)	Milan, Genoa, Rome	'Cfa', 'Csa', 'Csa'	2014	[211]
−10.0 °C (PET)	Toulouse	'Cfb'	2016	[212]
−18.0 °C (PET)	Tel Aviv, Beer Sheva, Eilat	'Csa', 'BSh', 'BWh'	2017	[4]

Table Result Avg. = −12.3 °C (PET)/−30.7 °C (MRT)

Both IS and PCI studies that included non-temperature variables revealed very important differences, that can be related back to the outcomes also obtained by Matzarakis and Amelung [54] due to the crucial importance of radiation within thermal comfort studies and projections. In comparison with the former maximum T_a averages from Table 4 (−1.2 °C) and Table 5 (−3.9 °C), PET calculations revealed average maximum reductions of −11.0 °C for IS studies and −12.3 °C for PCI studies. Furthermore, it is worth noting the elevated changes in MRT with a maximum reduction of −39.2 °C obtained by Oliveira, Andrade and Vaz [209]. Such a measurement was undertaken within a small urban park in Lisbon and compared with values presented by the local meteorological station during August 2007. It is worth noting that during the same assessment period/day, the identified difference of T_a was of −3.2 °C.

When considering the differences of obtained PET/MRT measurements between the IS and PCI studies, the changes were more modest. However (and unlike in the case of T_a studies) it is suggested that such difference are less associated to IS/PCI study typology, and more attributable to the type of tree species used in each study. As identified by numerous studies, e.g., [213], the biggest influence upon thermo-physiological impacts from urban trees is associated to tree species, rather than planting layout.

This being said, the type and quantification of the influences on human biometeorology resultant of urban vegetation also greatly depends upon the proposed evaluation methods and assessment scale. Naturally, between the disclosed studies in Table 4 through to Table 7, the applied methodologies on behalf of the authors varied. Yet general trends amongst these studies are clearly identifiable. Such trends in summary demonstrate that PCI effect studies render greater reductions in singular variables due to the larger cluster and/or arrangement of vegetation mass within the designated 'green space'. Although much more modest, the same can be recognised for studies which utilised thermo-physiological variables in PCI assessments. While both types of studies have rendered important outcomes, it is suggested that those which considered reductions in radiation fluxes upon the human biometeorological system are able to present more wholesome evaluations of human thermal wellbeing.

5.2. Shade Canopies

Within the existing literature, numerous studies have also acknowledged the critical role between urban canyons, radiation fluxes and human biometeorological thresholds [5,12,214–218]. Resultantly, when considering the application of shade canopies within local scales, the main microclimatic factor that must be investigated is the structures ability to attenuate solar radiation. In IS terms, while recorded T_a beneath a canopy may be the same as a recording fully exposed to the sun, the amount of solar radiation can vary significantly [16,60,108].

Unlike in the aforementioned studies, the majority of the application of (either ephemeral or permanent) shade canopies in the urban realm has not considered the specific impacts upon the human biometeorological system. Inversely, they more frequently originate from artistic influence (particularly ephemeral solutions) and more-often-than-not thermally impassive urban amenity placement. Resultantly, the current application of shade canopies as an effective thermal attenuation measure typology must be reconsidered, especially in the case of permanent solutions due to risks of over-shading during colder months.

5.3. Urban Surface Materials

Returning again to the principals of the urban energy balance, elements such as local surface materials play a large role in urban heat storage patterns. As a result, and due to the vast amount of paving within the public realm, its heat flux and implications on human biometeorology has been extensively discussed within the existing literature. More specifically, and due to the consensually recognised poor thermal performance of urban materials such as asphalt and concrete, means to augment surface albedos are continually being explored. As suggested by the study undertaken by Gaitani et al. [219] both researchers and manufacturers are already been developing ‘cool’ materials with higher reflectance values compared to the conventionally pigmented materials of the matching colour. In addition, such materials have been considered in local sites where the use of light colours could lead to solar glare issues, thus rendering another type of human discomfort within the public realm. Such efforts fall within a strong growing body of existing literature which consider divergent methods (including the implementation of ‘infrared reflective cool paint’ and ‘photocatalytic compounds’) to increase the thermal behaviour of pavement materials [129,130,220–226].

Retrospectively, considering the existing state-of-the-art, the relationship between human thermal comfort thresholds and surface materials should be approached as a two-step sequential approach. Whereby the assessment and design of pavements through interdisciplinary urban planning/design processes should: (1) be integrated with other measures that can, beforehand, reduce the energy load upon street materials; and subsequently, (2) ensure an effective thermal balance of the material itself by considering factors such as absorbed radiation, emitted infrared radiation, heat storage/convection and the effects of anthropogenic heat caused by urban activities such as vehicular traffic.

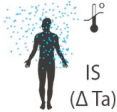
5.4. Misting Systems

The application of water and misting systems within the urban public realm has been a measure typology which was witnessed an increasing change in paradigm. In other words, cooling purposes behind that of pure aesthetics are increasingly becoming more obvious in urban environments. As a result, they are moreover growing in applicative meaning within interdisciplinary CCA efforts to improve local thermal conditions at local scales [227,228].

So far within the state-of-the-art, there is a fairly observable division within existing projects that use water or misting systems to improve thermal comfort levels during the hotter periods of the year. The first cluster, more often orientated towards bioclimatic design approaches [227,229,230], often lack the mechanical background in concretely attaining the correct balance between RH and T_a to cool microclimates without exacerbating acceptable atmospheric moisture levels. On the other hand, the second cluster can be linked back to the rudimentary, yet effective, Japanese cultural cooling

method called ‘Uchimizu’ [231]. Correspondingly, with time, the simple action of scattering of water upon the entrances of residential buildings has evolved, and rendered Japan as one of the frontrunner countries in this cluster. Congruently with the Japanese nocturnal thermal comfort studies previously mentioned in this article, the focus upon diurnal/nocturnal equilibrium between T_a and RH can largely be attributable to Japan having simultaneously elevated humidity levels and temperatures, including during the summer [172]. As a result, the application of ‘dry-mist’ technology both within indoor and outdoor environments has been extensively researched within Japanese cities as demonstrated in Table 8.

Table 8. Exemplification of Japanese misting system studies originating from ancient ‘Uchimizu’ concepts to specifically reduce encircling T_a levels.



Thermal Result (Ta Max)	Location	KG	Study Method.	Study Year	Source
−2.0 °C	Nagoya	‘Cfa’	Field Study	2008	[232]
−1.5 °C	Tokyo	‘Cfa’	Field Study	2008	[233]
−2.5 °C	Tokyo	‘Cfa’	CFD * Study	2008	[234]
−2.0 °C	Yohohama	‘Cfa’	CFDStudy	2009	[231]
−0.8 °C	Osaka	‘Cfa’	Field + CFD Study	2011	[235]
Table Result Avg. = −1.8 °C		* CFD—Computational Fluid Dynamic			

Based upon KG classification climates concomitant with ‘temperate’ yet with hot and wet summers, the outputs from the Japanese studies have marked an important step forwards in addressing how misting systems can be specifically configured to reduce T_a , without exacerbating local atmospheric moisture content in the air. Similar to the average maximum reductions in T_a as presented in Table 4 discussing the IS reductions as a result of urban vegetation, Table 8 presented a comparable result of −1.8 °C. This being said, this second cluster of measures has the problem of being extensively orientated towards engineering approach, with limited or no design connotations. Such a lapse between the engineering spectrum with design applications reinforce the aforementioned conclusions reached by the review study conducted by Hunter, Williams, Rayner, Aye, Hes and Livesley [163] regarding urban green walls and façades.

Subsequently, there needs to be a better interdisciplinary integration of these two clusters, where design and engineering approaches combine to tackle issues of human thermal comfort. Encouragingly, there have already numerous bioclimatic studies which have provided both conceptual, e.g., [108] and constructed, e.g., [115,236] examples of how water can be used to cool the human-biometeorological system without exacerbating encircling atmospheric moisture levels. Nevertheless, there still remains a large opportunity for future studies to continue to dilute the disparity between these two clusters, even if initially based on rudimentary atmospheric principals.

6. Concluding Remarks

Within the contemporary city, the interdisciplinary relationship between biometeorology and local adaptation has already made important progress in addressing urban thermal wellbeing and safety. This being said, and as recognised within the three interconnecting sections of this encompassing review study, there remains the opportunity to further communicate climatic information into urban thermal planning/design tools and assessments. As further advocated by the adjacent review studies

discussed in this study, the interdisciplinary transposal of technical know-how into concrete adaptation tools needs to be enforced. Pertaining specifically to urban human biometeorological aspects with that of urban wellbeing, an encompassing schematic summary is illustrated in Figure 4.

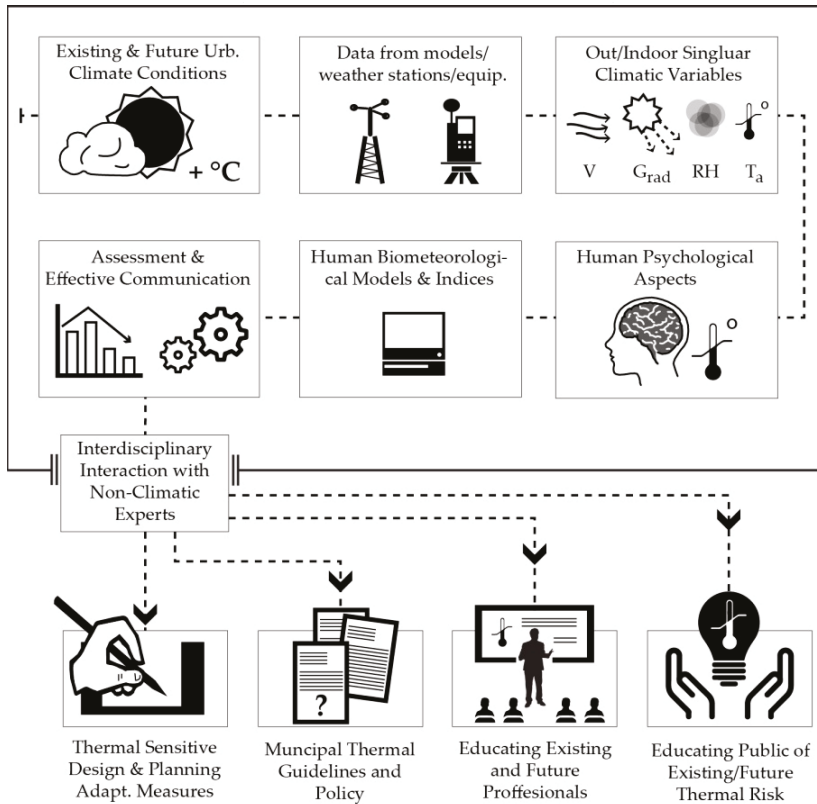


Figure 4. Schematic overview of human biometeorological aspects and augmenting associated interdisciplinary communication with non-climatic experts.

As discussed within the first section of the study, human biometeorology must play an increased role within existing and future thermo–physiological assessments of urban climate conditions. More specifically:

1. Methods of approaching climatic data from climatic models and meteorological stations/equipment should not rely solely upon singular climatic variables to obtain wholesome evaluations of existing or future human thermal comfort conditions as a result of climate change.
2. The information retrieved from such assessments must, unequivocally, be translatable through easy-to-understand guidance for non-climatic experts, and that of the general public. Such interdisciplinary communication channels shall become moreover significant given the expected increase of extreme heat/cold events within urban contexts. Eventually, the sequential multifaceted process of going from identified risk factors, to establishing better thermal response measures and transposing these into municipal climatic policy and guidelines can be strengthened.
3. Due to the inherent nature of thermo–physiological risk factors, undertaken assessments and projections must reach a better equilibrium between ‘huge-impact-but-low-frequency’ with that of ‘high-frequency-yet-continuous’ stimulus within the built environment, particularly during

summer/winter periods. In this way, thermal sensitive urban planning and design can better tackle both of these different, yet, decisive facets of urban climatology.

As discussed within the second segment of the study, further interdisciplinary scientific bridging must be accomplished between:

1. The remarkable and continual evolution of different thermo–physiological indices (including those arising from energy balance stress models, energy balance stain models, statistical/algebraic models and single-parameter models) with that of psychological factors. As mentioned, as this remains a less explored characteristic, this originates the respective opportunity to decrease ‘qualitative subjectivity’ through further research. Such research outlines can be launched through the association between continued physiological cumulative stimulus, circadian rhythm cycles, and anticipated triggers of human psychological behaviour patterns.
2. In association to the previous point, such future lines of research shall also diminish the often over-powering differentiation between evaluation methods between outdoor and indoor environments. Although clear why thermal evaluation methods must be different between these environments, the analytical relationship between the two types of environments must be strengthened. As an example, the effects existing/future extreme heat events shall influence both outdoor and indoor environments; meaning that the daily peripatetic transient relationship between the two environments can be better explored in future thermal comfort research. As result, this shall once again present better means of establishing better thermal response measures, both in indoor and in outdoor contexts.

Within the final section of the study, an overview of existing biometeorological aspects has already been integrated within different typologies of local thermal responsive measures. Such efforts are expected to propagate as the climate change adaptation agenda further matures its approaches and tools to present bottom-up means to attenuate thermo–physiological factors during the twenty-first-century. This being said, the final section of the study also discussed means in which human biometeorological aspects can more concretely aid local bottom-up adaptation processes through thermal sensitive design and planning. Beyond the recurring recognition from the disclosed review and research articles calling for further interdisciplinary communication amongst engineering/technical climatic know-how and urban planning-design tools, it was moreover acknowledged that:

1. While singular-variable evaluations pertaining to the thermal benefits of urban vegetation have been vital for thermal comfort studies (including in both IS and PCI typologies), the exclusion of non-temperature variables limit thermo–physiological interface comprehension with the human biometeorological system.
2. Given that the biggest potential of shade canopies is to limit the amount of global radiation projected upon the human body, the very limited amount of existing studies examining this aspect needs to be addressed by future research. Here, material types, structure size and distribution can all serve as analytical variables for addressing thermal comfort in open spaces that are particularly susceptible to high amounts of radiation. Ironically, the scientific community has produced a very strong body of research concerning the relationship amongst different urban morphological compositions and that of solar radiation. As a result, a rich body of research into which types of street configurations and orientations will serve as an excellent platform to guide such future research.
3. Due to the predominant use of thermally poor preforming materials, (such as urban concrete and asphalt) within cities, while there has been a considerable amount of research into surface materials, there is the opportunity to further explore the application of thermally efficient pavement materials. While existing studies have made clear strides in examining individual material, aggregate and finishing performances, there needs to be further studies that link such materials with other measure typologies within urban fabrics. As an example, there is the prospect

to further examine the affiliation with shading patterns resulting from both tree crowns and shading amenities. Since both of these measures can be utilised to reduce the amount of absorbed solar radiation upon a specific type of investigated pavement, the resulting inferences upon emitted infrared radiation, heat storage and convections can be further explored under specific urban conditions/layouts. Such studies will propagate means to address high surface temperatures and inefficient albedos values in local thermal urban planning/design and decision making.

4. As a result of the remaining disparity between engineering and design approaches to misting systems within the urban realm, similar to the case of shade canopies, there needs to be additional studies that consider wholesome projects which consider actual influences upon the human biometeorological system. Although commonly found within cities, there is a large opportunity for future studies to continue to dilute the segregation between engineering and thermal sensitive design approaches, even if based upon simple atmospheric principals to accomplish their full potential in attenuating thermal comfort stress without exacerbating atmospheric moisture content levels.

Overall, while the scientific community has made large strides in thermal comfort studies which were arguably catalysed by the maturing CCA agenda, there still remains a fertile opportunity for more scientific investigation. Inclusively, this review article suggests that this scientific advancement shall always be synonymously concomitant with interdisciplinarity. In other words, while the deepening of knowledge within a specific field is a quintessential cornerstone to science, the same can be said for the bridging between different disciplines that, are ultimately, set to face similar challenges throughout the twenty-first century. As it stands, the interdisciplinary interaction with non-climatic experts is still not strong enough, or at least, nowhere as strong as the existing thermal assessment capacity of climatological related experts. Again summarised in Figure 4, this fragility arguably risks the weakening of: (i) the concrete know-how of architects, landscape architects, urban designers and planners to more efficiently address human biometeorological constraints, and suggest local bioclimatic measures to address both indoor and outdoor human wellbeing standards; (ii) municipal policy and guidelines that could otherwise aid thermal sensitive design and planning; (iii) the transposition of knowledge to other non-climatic experts such as students to catalyse this interdisciplinary bridging upon upcoming generations of scientists and professionals; and finally, (iv) the production and dissemination of easy-to-use, easy-to-understand information and warning mechanisms for the general public regarding urban climatic risks on wellbeing standards, and just as importantly, the augmentation of such risk factors as a result of climate change.

Author Contributions: The authors declare that each has contributed equally to the production of this document. Whereby, (i) A.S.N. consolidated the overall results obtained within the study; and (ii) A.M. equally provided both general and specific contributions to the scientific content elaborated within this review study.

Funding: This research received no external funding.

Conflicts of Interest: The authors declare no conflict of interest.

References

1. Matzarakis, A. Chapter 14—Climate change and adaptation at regional and local scale. In *Tourism and the Implications of Climate Change: Issues and Actions (Bridging Tourism Theory and Practice)*; Schott, C., Jafari, J., Cai, L., Eds.; Emerald Group Publishing Limited: Bingley, UK, 2010; Volume 3, pp. 237–259.
2. Matzarakis, A.; Endler, C. Climate change and thermal bioclimate in cities: Impacts and options for adaptation in Freiburg, Germany. *Int. J. Biometeorol.* **2010**, *54*, 479–483. [[CrossRef](#)]
3. Nouri, A.S.; Costa, J.P.; Santamouris, M.; Matzarakis, A. Approaches to outdoor thermal comfort thresholds through public space design: A review. *Atmosphere* **2018**, *9*, 108. [[CrossRef](#)]
4. Potchter, O.; Shashua-Bar, L. Urban Greenery as a tool for city cooling: The Israeli experience in a variety of climatic zones. In *Proceedings of the PLEA 2017—Design to Thrive*, Edinburgh, UK, 3–5 July 2017; pp. 2–9.

5. Nouri, A.S.; Costa, J.P.; Matzarakis, A. Examining default urban-aspect-ratios and sky-view-factors to identify priorities for thermal-sensitive public space design in hot-summer Mediterranean climates: The Lisbon case. *Build. Environ.* **2017**, *126*, 442–456. [[CrossRef](#)]
6. Fröhlich, D. Development of a microscale model for the thermal environment in complex areas. In *Fakultät für Umwelt und Natürliche Ressourcen*; der Albert-Ludwigs-Universität: Freiburg im Breisgau, Germany, 2017.
7. Chen, Y.-C.; Fröhlich, D.; Matzarakis, A.; Lin, T.-P. Urban Roughness Estimation Based on Digital Building Models for Urban Wind and Thermal Condition Estimation—Application of the SkyHelios Model. *Atmosphere* **2017**, *8*, 247. [[CrossRef](#)]
8. Santamouris, M.; Kolokotsa, D. *Urban. Climate Mitigation Techniques*; Earthscan, Routledge: London, UK, 2016.
9. Santamouris, M. Cooling the buildings—Past, present and future. *Energy Build.* **2016**, *128*, 617–638. [[CrossRef](#)]
10. Matos Silva, M. *Public Space Design for Flooding: Facing Challenges Presented by Climate Change Adaptation*; Universitat de Barcelona: Barcelona, Spain, 2016.
11. Charalampopoulos, I.; Tsiros, I.; Chronopoulou-Sereli, A.; Matzarakis, A. A methodology for the evaluation of the human-bioclimate performance of open spaces. *Theor. Appl. Climatol.* **2016**, 1–10.
12. Ketterer, C.; Matzarakis, A. Human-biometeorological assessment of heat stress reduction by replanning measures in Stuttgart, Germany. *Landsc. Urban Plan.* **2014**, *122*, 78–88. [[CrossRef](#)]
13. Matzarakis, A.; Fröhlich, D.; Ketterer, C.; Martinelli, L. Urban bioclimate and micro climate—How to construct cities in the era of climate change. In *Climate Change and Sustainable Heritage*; Hofbauer, C., Kandjani, E.M., Meuwissen, J., Eds.; Cambridge Scholars Publishing: Cambridge, UK, 2018; pp. 38–61.
14. Nouri, A.S. A Framework of Thermal Sensitive Urban Design Benchmarks: Potentiating the Longevity of Auckland’s Public Realm. *Buildings* **2015**, *5*, 252–281. [[CrossRef](#)]
15. Alcoforado, M.J.; Matzarakis, A. Planning with urban climate in different climatic zones. *Geographicalia* **2010**, *57*, 5–39.
16. Nouri, A.S.; Lopes, A.; Costa, J.P.; Matzarakis, A. Confronting potential future augmentations of the physiologically equivalent temperature through public space design: The case of Rossio, Lisbon. *Sustain. Cities Soc.* **2018**, *37*, 7–25. [[CrossRef](#)]
17. Alcoforado, M.-J.; Andrade, H.; Lopes, A.; Vasconcelos, J. Application of climatic guidelines to urban planning—The example of Lisbon (Portugal). *Landsc. Urban Plan.* **2009**, *90*, 56–65. [[CrossRef](#)]
18. Lopes, A.; Alves, E.; Alcoforado, M.J.; Machete, R. Lisbon Urban Heat Island Updated: New Highlights about the Relationships between Thermal Patterns and Wind Regimes. *J. Adv. Meteorol.* **2013**, *2013*, 1–11. [[CrossRef](#)]
19. Nouri, A.S.; Charalampopoulos, I.; Matzarakis, A. Beyond Singular Climatic Variables—Identifying the Dynamics of Wholesome Thermo-Physiological Factors for Existing/Future Human Thermal Comfort during Hot Dry Mediterranean Summers. *Int. J. Environ. Res. Public Health* **2018**, *15*, 2362. [[CrossRef](#)] [[PubMed](#)]
20. Santamouris, M.; Ding, L.; Fiorito, F.; Oldfield, P.; Osmond, P.; Paolini, R.; Prasad, D.; Synnefa, A. Passive and active cooling for the built environment—Analysis and assessment of the cooling potential of mitigation technologies using performance data from 220 large scale projects. *Sol. Energy* **2016**, *154*, 14–33. [[CrossRef](#)]
21. Alchapar, N.; Pezzuto, C.; Correa, E.; Labaki, L. The impact of different cooling strategies on urban air temperatures: The cases of Campinas, Brazil and Mendoza, Argentina. *Theor. Appl. Climatol.* **2017**, *130*, 33. [[CrossRef](#)]
22. Wang, Y.; Berardi, U.; Akbari, H. Comparing the effects of urban heat island mitigation strategies for Toronto, Canada. *Energy Build.* **2016**, *114*, 2–19. [[CrossRef](#)]
23. Brown, R. *Design with Microclimate—The Secret to Comfortable Outdoor Space*; Island Press: Washington, DC, USA, 2010.
24. Nouri, A.S.; Costa, J.P. Placemaking and climate change adaptation: New qualitative and quantitative considerations for the “Place Diagram”. *J. Urban Int. Res. Placemaking Urban Sustain.* **2017**, *10*, 1–27. [[CrossRef](#)]
25. Oke, T. The distinction between canopy and boundary layer urban heat islands. *J. Atmos.* **1976**, *14*, 268–277. [[CrossRef](#)]
26. Mayer, H.; Höppe, P. Thermal comfort of man in different urban environments. *Theor. Appl. Climatol.* **1987**, *38*, 43–49. [[CrossRef](#)]
27. Brown, R.; Gillespie, T. *Microclimatic Landscape Design: Creating Thermal Comfort and Energy Efficiency*; John Wiley and Sons: Hoboken, NJ, USA, 1995.

28. Fanger, P. *Thermal Comfort: Analysis and Applications in Environmental Engineering*; McGraw-Hill Book Company: New York, NY, USA, 1972; p. 244.
29. Whyte, W.H. *The Social Life of Small Urban Spaces*; Project for Public Spaces Inc.: New York, NY, USA, 1980.
30. Olgyay, V. *Design with Climate, Bioclimatic Approach to Architectural Regionalism*; Princeton University Press: Princeton, NJ, USA, 1963.
31. Givoni, B. *Man, Climate and Architecture*; Applied Science Publishers: London, UK, 1976.
32. Nikolopoulou, M.; Steemers, K. Thermal comfort and psychological adaptation as a guide for designing urban spaces. *Energy Build.* **2003**, *35*, 95–101. [[CrossRef](#)]
33. Shashua-Bar, L.; Tsiros, I.X.; Hoffman, M. Passive cooling design options to ameliorate thermal comfort in urban streets of a Mediterranean climate (Athens) under hot summer conditions. *Build. Environ.* **2012**, *57*, 110–119. [[CrossRef](#)]
34. Wilbanks, T.J.; Kates, R.W. *Global Change in Local Places: How Scale Matters*; Kluwer Academic Publishers: Dordrecht, The Netherlands, 1999; pp. 601–628.
35. Oke, T. Towards a prescription for the greater use of climatic principles in settlement planning. *Energy Build.* **1984**, *7*, 1–10. [[CrossRef](#)]
36. Alcoforado, M.J.; Vieira, H. Urban climate in Portuguese management plans (in Portuguese with abstract in English). *Soc. E Territ.* **2004**, *37*, 101–116.
37. Alcoforado, M.J.; Lopes, A.; Andrade, H. Urban climatic map studies in Portugal. In *The Urban Climatic Map: A Methodology for Sustainable Urban Planning*; Ng, E., Ren, C., Eds.; Routledge: Abingdon, UK, 2015.
38. Andrade, H. *Bioclima Humano E Temperatura Do Ar Em Lisboa*; Universidade de Lisboa: Lisbon, Portugal, 2003.
39. Oliveira, S.; Andrade, H. An initial assessment of the bioclimatic comfort in an outdoor public space in Lisbon. *Int. J. Biometeorol.* **2007**, 69–84. [[CrossRef](#)]
40. Alcoforado, M.J.; Andrade, H. Nocturnal urban heat island in Lisbon (Portugal): Main features and modelling attempts. *Theor. Appl. Climatol.* **2006**, *84*, 151–159. [[CrossRef](#)]
41. Alcoforado, M.J.; Lopes, A.; Alves, E.; Canário, P. Lisbon Heat Island; Statistical Study. *Finisterra* **2014**, *98*, 61–80.
42. Lopes, A. *Modificações No Clima Da Lisboa Como Consequência Do Crescimento Urbano*; University of Lisbon: Lisbon, Portugal, 2003.
43. Alcoforado, M.J.; Lopes, A.; Andrade, H.; Vasconcelos, J.; Vieira, R. *Observational Studies on Summer Winds in Lisbon (Portugal) and Their Influence on Daytime Regional and Urban Thermal Patterns*; Tel Aviv University Tel Aviv: Merhavim, Israel, 2006; pp. 88–112.
44. Alcoforado, M.J.; Lopes, A.; Andrade, H.; Vasconcelos, J. *Orientações Climáticas Para O Ordenamento Em Lisboa (Relatório 4)*; Centro de Estudos Geográficos da Universidade de Lisboa: Lisboa, Portugal, 2005; p. 83, ISBN 978-972-636-165-7.
45. Matzarakis, A.; Endler, C. Climate change and urban bioclimate: Adaptation possibilities. In Proceedings of the Seventh International Conference on Urban Climate, Yokohama, Japan, 29 June–3 July 2009.
46. Algeciras, J.A.R.; Matzarakis, A. Quantification of thermal bioclimate for the management of urban design in Mediterranean climate of Barcelona, Spain. *Int. J. Biometeorol.* **2015**, *8*, 1261–1270.
47. Potchter, O.; Cohen, P.; Lin, T.; Matzarakis, A. Outdoor human thermal perception in various climates: A comprehensive review of approaches, methods and quantification. *Sci. Total Environ.* **2018**, 631–632, 390–406. [[CrossRef](#)]
48. Lin, T.-P. Thermal perception, adaptation and attendance in a public square in hot and humid regions. *Build. Environ.* **2009**, *44*, 2017–2026. [[CrossRef](#)]
49. Andreou, E. Thermal comfort in outdoor spaces and urban canyon microclimate. *Renew. Energy* **2013**, *55*, 182–188. [[CrossRef](#)]
50. Santamouris, M.; Xirafi, F.; Gaitani, N.; Saliari, M.; Vassilakopoulou, K. Improving the microclimate in a dense urban area using experimental and theoretical techniques—The case of Marousi, Athens. *Int. J. Vent.* **2012**, *11*, 1–16. [[CrossRef](#)]
51. Labaki, L.C.; Fontes, M.S.G.d.C.; Bueno-Bartholomei, C.L.; Dacanal, C. Thermal comfort in public open spaces: Studies in pedestrian streets in São Paulo state, Brazil. *Ambiente Construído* **2012**, *12*, 167–183. [[CrossRef](#)]
52. Fröhlich, D.; Gangwisch, M.; Matzarakis, A. Effect of radiation and wind on thermal comfort in urban environments—Applications of the RayMan and SkyHelios Model. *Urban Clim.* **2019**, *27*, 1–7. [[CrossRef](#)]

53. Katzschner, L. *Microclimatic Thermal Comfort Analysis in Cities for Urban Planning and Open Space Design Network for Comfort and Energy Use in Buildings*; NCUB: London, UK, 2006.
54. Matzarakis, A.; Amelung, B. Physiological Equivalent Temperature as Indicator for Impacts of Climate Change on Thermal Comfort of Humans. In *Seasonal Forecasts, Climatic Change and Human Health. Advances in Global Research 30*; Thomson, M.C., Garcia-Herrera, R., Beniston, M., Eds.; Springer: Berlin, Germany, 2008; pp. 161–172.
55. Matzarakis, A.; Georiadis, T.; Rossi, F. Thermal bioclimate analysis for Europe and Italy. *IL Nuovo Cim.* **2007**, *30*, 623–631.
56. IPCC. *Climate Change 2014: Synthesis Report. Contribution of Working Groups I, II and III to the Fifth Assessment Report of the Intergovernmental Panel on Climate Change*; IPCC: Geneva, Switzerland, 2014; p. 151.
57. IPCC. *IPCC Special Report Emission Scenarios, A Special Report of Working Group III of the Intergovernmental Panel on Climate Change*; IPCC: Cambridge, UK, 2000; p. 27.
58. Giannaros, T.; Lagouvardos, K.; Kotroni, V.; Matzarakis, A. Operational forecasting of human-biometeorological conditions. *Int. J. Biometeorol.* **2018**, *1–5*. [[CrossRef](#)]
59. Hebbert, M.; Webb, B. Towards a Liveable Urban Climate: Lessons from Stuttgart. In *Liveable Cities: Urbanising World: Isocarp 07*; Routledge: Manchester, UK, 2007.
60. Kántor, N.; Chen, L.; Gal, C.V. Human-biometeorological significance of shading in urban public spaces—Summertime measurements in Pécs, Hungary. *Landsc. Urban Plan.* **2018**, *170*, 241–255. [[CrossRef](#)]
61. Nouri, A.S. *Addressing Urban Outdoor Thermal Comfort Thresholds through Public Space Design—A Bottom-Up Interdisciplinary Research Approach for Thermal Sensitive Urban Design in An Era of Climate Change: The Lisbon Case*; University of Lisbon: Lisbon, Portugal, 2018.
62. Nouri, A.S. A bottom-up perspective upon climate change—Approaches towards the local scale and microclimatic assessment. In *Green Design, Materials and Manufacturing Processes*; Bártoło, H., Ed.; Taylor & Francis: Lisbon, Portugal, 2013; pp. 119–124.
63. Spagnolo, J.; de-Dear, R. A field study of thermal comfort in outdoor and semi-outdoor environments in subtropical Sydney, Australia. *Build. Environ.* **2003**, *38*, 721–738. [[CrossRef](#)]
64. VDI. Part I: Environmental meteorology, methods for the human-biometeorological evaluation of climate and air quality for the urban and regional planning at regional level. Part I: Climate. In *VDI/DIN-Handbuch Reinhaltung der Luft*; Verein Deutscher Ingenieure: Düsseldorf, Germany, 1998; p. 29.
65. Beshir, M.; Ramsey, J. Heat Stress Indices: A Review Paper. *Int. J. Ind. Ergon.* **1988**, *3*, 89–102. [[CrossRef](#)]
66. Lin, T.-P.; Tsai, K.-T.; Hwang, R.-L.; Matzarakis, A. Quantification of the effect of thermal indices and sky view factor on park attendance. *Landsc. Urban Plan.* **2012**, *107*, 137–146. [[CrossRef](#)]
67. Pantavou, K.; Santamouris, M.; Asimakopoulos, D.; Theoharatos, G. Empirical calibration of thermal indices in an urban outdoor Mediterranean environment. *Build. Environ.* **2014**, *80*, 283–292. [[CrossRef](#)]
68. Freitas, C.; Grigorieva, E. A comprehensive catalogue and classification of human thermal climate indices. *Int. J. Biometeorol.* **2015**, *59*, 1–12. [[CrossRef](#)] [[PubMed](#)]
69. Fröhlich, D.; Matzarakis, A. A quantitative sensitivity analysis on the behaviour of common thermal indices under hot and windy conditions in Doha, Qatar. *Theor. Appl. Climatol.* **2015**, *124*, 179–187. [[CrossRef](#)]
70. Coccoło, S.; Kämpf, J.; Scartezzini, J.; Pearlmutter, D. Outdoor thermal comfort and thermal stress: A comprehensive review on models and standards. *Urban Clim.* **2016**, *18*, 33–57. [[CrossRef](#)]
71. Freitas, C.; Grigorieva, E. A comparison and appraisal of a comprehensive range of human thermal climate indices. *Int. J. Biometeorol.* **2016**, *61*, 1–26. [[CrossRef](#)] [[PubMed](#)]
72. Golasi, I.; Salata, F.; Vollaro, E.; Coppi, M. Complying with the demand of standarization in outdoor thermal comfort: A first approach to the Global Outdoor Comfort Index (GOCI). *Build. Environ.* **2018**, *130*, 104–119. [[CrossRef](#)]
73. Charalampopoulos, I. A comparative sensitivity analysis of human thermal comfort indices with generalized additive models. *Theor. Appl. Climatol.* **2019**, *1–18*. [[CrossRef](#)]
74. Charalampopoulos, I.; Nouri, A.S. Investigating the behaviour of human thermal indices under divergent atmospheric conditions: A sensitivity analysis approach. *Atmosphere* **2019**, *10*, 580. [[CrossRef](#)]
75. Staiger, H.; Laschewski, G.; Matzarakis, A. Selection of appropriate thermal indices for applications in human biometeorological studies. *Atmosphere* **2019**, *10*, 18. [[CrossRef](#)]

76. Guo, H.; Aviv, D.; Loyola, M.; Teitelbaum, E.; Houchois, N.; Meggers, F. On the understanding of the mean radiant temperature within both the indoor and outdoor environment, a critical review. *Renew. Sustain. Energy Rev.* **2019**, in press. [[CrossRef](#)]
77. Miao, C.; Yu, S.; Hu, Y.; Zhang, H.; He, X.; Chen, W. Review of methods used to estimate the sky view factor in urban street canyons. *Buill. Environ.* **2019**, *168*, 6497. [[CrossRef](#)]
78. Tinz, B.; Jendritzky, G. Europa- und Weltkarten der gefühlten Temperatur. In *Beiträge zur Klima- und Meeresforschung*; Chmielewski, F., Foken, T., Eds.; Deutschland: Berlin/Bayreuth, Germany, 2003; pp. 111–123.
79. Gagge, A.; Fobelets, P.; Bergland, L. A standard predictive index of human response to thermal environment. *Ashrae Trans.* **1986**, *92*, 709–731.
80. Gonzalez, R.; Nishi, Y.; Gagge, A. Experimental evaluation of standard effective temperature: A new biometeorological index of man's thermal discomfort. *Int. J. Biometeorol.* **1974**, *18*, 1–15. [[CrossRef](#)] [[PubMed](#)]
81. de-Dear, R.; Pickup, R. An outdoor thermal comfort index (OUT_SET*)—Part I—The model and its assumptions. In Proceedings of the International Conference on Urban Climatology Macquarie University, Sydney, Australia, 8–12 November 1999.
82. Unger, J. Comparisons of urban and rural bioclimatological conditions in the case of a Central-European city. *Int. J. Biometeorol.* **1999**, *43*, 139–144. [[CrossRef](#)]
83. Alfano, D.A.; Olesen, B.; Palella, B. Polv Ole Fanger's impact ten years later. *Energy Build.* **2017**, *152*, 243–249. [[CrossRef](#)]
84. Masterton, J.; Richardson, F. *Humidex: A Method of Quantifying Human Discomfort Due to Excessive Heat and Humidity*; Environment Canada: Downsview, ON, Canada, 1979.
85. Kenny, A.; Warland, S.; Brown, R. Part A: Assessing the performance of the COMFA outdoor thermal comfort model on subjects performing physical activity. *Int. J. Biometeorol.* **2009**, *53*, 415–428. [[CrossRef](#)] [[PubMed](#)]
86. Brown, R.; Gillespie, T. Estimating outdoor thermal comfort using a cylindrical radiation thermometer and an energy budget model. *Int. J. Biometeorol.* **1986**, *30*, 43–52. [[CrossRef](#)]
87. Jendritzky, G.; Maarouf, A.; Fiala, D.; Staiger, H. An update on the development of a Universal Thermal Climate Index. In Proceedings of the 15th Conference Biometeorology/Aerobiology and 16th International Congress of Biometeorology, Kansas City, KS, USA, 27 October 2002; pp. 129–133.
88. Jendritzky, G.; de-Dear, R.; Havenith, G. UTCI—Why another thermal index? *Int. J. Biometeorol.* **2012**, *56*, 421–428. [[CrossRef](#)]
89. Havenith, G.; Fiala, D.; Blazejczyk, K.; Richards, M.; Bröde, P.; Holmér, I.; Rintamaki, H.; Benschabat, Y.; Jendritzky, G. The UTCI clothing model. *Int. J. Biometeorol.* **2012**, *56*, 461–470. [[CrossRef](#)]
90. Yaglou, C.; Minard, D. Control of heat casualties at military training centers. *AMA Arch. Ind. Health* **1957**, *16*, 302–316.
91. Alfano, F.; Malchaire, J.; Palella, B.; Riccio, G. WBGT index revisited after 60 years of use. *Ann. Occup. Hyg.* **2014**, *58*, 955–970.
92. Malchaire, J.; Piette, A.; Kampmann, B.; Mehnerts, P.; Gebhardt, H.; Havenith, G.; Hartog, E.; Holmer, I.; Parsons, K.; Alfano, G.; et al. Development and Validation of the Predicted Heat Strain Model. *Ann. Occup. Hyg.* **2001**, *45*, 123–135. [[CrossRef](#)]
93. Höpfe, P. The physiological equivalent temperature—A universal index for the biometeorological assessment of the thermal environment. *Int. J. Biometeorol.* **1999**, *43*, 71–75. [[CrossRef](#)] [[PubMed](#)]
94. Matzarakis, A.; Mayer, H.; Iziomon, G.M. Applications of a universal thermal index: Physiological equivalent temperature. *Int. J. Biometeorol.* **1999**, *42*, 76–84. [[CrossRef](#)] [[PubMed](#)]
95. Chen, Y.-C.; Matzarakis, A. Modified physiologically equivalent temperature—Basics and applications for western European climate. *Theor. Appl. Climatol.* **2017**, *132*, 1–15. [[CrossRef](#)]
96. Binarti, F.; Koerniawan, M.; Triyadi, S.; Utami, S.; Matzarakis, A. A review of outdoor thermal comfort indices and neutral ranges for hot-humid regions. *Urban Clim.* **2020**, *31*, 100531. [[CrossRef](#)]
97. Höpfe, P. *The Energy Balance in Humans (Original Title—Die Energiebilanz des Menschen)*; Universität München, Meteorologisches Institut: Munich, Germany, 1984.
98. Lin, T.-P.; Yang, S.-R.; Chen, Y.-C.; Matzarakis, A. The potential of a modified physiologically equivalent temperature (mPET) based on local thermal comfort perception in hot and humid regions. *Theor. Appl. Climatol.* **2018**, *135*, 873–876. [[CrossRef](#)]

99. Nouri, A.S.; Fröhlich, D.; Silva, M.M.; Matzarakis, A. The Impact of Tipuana tipu Species on Local Human Thermal Comfort Thresholds in Different Urban Canyon Cases in Mediterranean Climates: Lisbon, Portugal. *Atmosphere* **2018**, *9*, 2–28.
100. de-Dear, R.; Foldvary, V.; Zhang, H.; Arens, E.; Luo, M.; Parkison, T.; Du, X.; Zhang, W.; Chun, C.; Liu, S. Comfort is in the mind of the beholder: A review of progress in adaptative thermal comfort research over the past two decades. In Proceedings of the 5th International Conference on Human-Environmental System, Nagoya, Japan, 29 October–2 November 2016.
101. Kim, J.; de-Dear, R. Thermal comfort expectations and adaptative behavioural characteristics of primary and secondary school students. *Build. Environ.* **2017**, *127*, 13–22. [[CrossRef](#)]
102. de-Dear, R.; Kim, J.; Candido, C.; Deuble, M. Adaptive thermal comfort in Australian school classrooms. *Build. Res. Inf.* **2015**, *43*, 383–398. [[CrossRef](#)]
103. Humphreys, M.; Nicol, F.; Raja, I. Field studies of indoor thermal comfort and the progress of the adaptive approach. *J. Adv. Build. Energy Res.* **2007**, *1*, 55–88. [[CrossRef](#)]
104. de-Dear, R. Thermal comfort in air-conditioned office buildings in the tropics. In *Standards for Thermal Comfort: Indoor Air Temperature Standards for the 21st Century*; Nicol, F., Humphreys, M., Sykes, O., Roaf, S., Eds.; Chapman and Hall: London, UK, 1995.
105. Heijs, W.; Stringer, P. Research on residential thermal comfort: Some contributions from environmental psychology. *J. Environ. Psychol.* **1988**, *8*, 235–247. [[CrossRef](#)]
106. Song, X.; Yang, L.; Zheng, W.; Ren, Y.; Lin, Y. Analysis on human adaptative levels in different kinds of indoor thermal environment. *Procedia Eng.* **2015**, *121*, 151–157. [[CrossRef](#)]
107. Chen, L.; Ng, E. Outdoor thermal comfort and outdoor activities: A Review of research in the past decade. *Cities* **2012**, 118–125. [[CrossRef](#)]
108. Nouri, A.S.; Costa, J.P. Addressing thermophysiological thresholds and psychological aspects during hot and dry mediterranean summers through public space design: The case of Rossio. *Build. Environ.* **2017**, *118*, 67–90. [[CrossRef](#)]
109. Nikolopoulou, M.; Baker, N.; Steemers, K. Thermal Comfort in Outdoor Urban Spaces: Understanding the Human Parameter. *Sol. Energy* **2001**, *70*, 227–235. [[CrossRef](#)]
110. Thorsson, S.; Lindqvist, M.; Lindqvist, S. Thermal bioclimatic conditions and patterns of behaviour in an urban park in Göteborg, Sweden. *Int. J. Biometeorol.* **2004**, *48*, 149–156. [[CrossRef](#)]
111. Katzschner, L. Behaviour of people in open spaces in dependence of thermal comfort conditions. In Proceedings of the 23rd Conference on Passive and Low Energy Architecture, Geneva, Switzerland, 6–8 September 2006.
112. Nikolopoulou, M.; Steemers, K. Thermal comfort and psychological adaptation as a guide for designing urban spaces. *Energy Build.* **2003**, *35*, 95–101. [[CrossRef](#)]
113. Thorsson, S.; Honjo, T.; Lindberg, F.; Eliasson, I.; Lim, E.-M. Thermal comfort and outdoor activity in Japanese urban public places. *Environ. Behav.* **2007**, *39*, 661–684. [[CrossRef](#)]
114. Zacharias, J.; Stathopoulos, T.; Wu, H. Spatial behavior in San Francisco’s plazas: The effects of microclimate, other people, and environmental design. *Environ. Behav.* **2004**, *36*, 639–658. [[CrossRef](#)]
115. Velazquez, R.; Alvarez, S.; Guerra, J. *Climatic Control. of the Open Spaces in Expo. 1992*; College of Industrial Engineering of Seville: Seville, Spain, 1992.
116. Hirashima, S.; Assis, E.; Nikolopoulou, M. Daytime thermal comfort in urban spaces: A field study in Brazil. *Build. Environ.* **2016**, *107*, 243–253. [[CrossRef](#)]
117. Brager, G.; de-Dear, R. Thermal adaptation in the built environment; A literature review. *Energy Build.* **1998**, *27*, 83–96. [[CrossRef](#)]
118. National Benefits Assessment. *Energy Build.* **1992**, *18*, 171–291.
119. Matzarakis, A.; Mayer, H. Heat Stress in Greece. *Int. J. Biometeorol.* **1997**, *41*, 34–39. [[CrossRef](#)] [[PubMed](#)]
120. Matzarakis, A.; Mayer, H. Another Kind of Environmental Stress: Thermal Stress. WHO Collaborating Centre for Air Quality Management and Air Pollution Control. *News Lett.* **1996**, *18*, 7–10.
121. IPCC. *Synthesis Report—An Assessment of the Intergovernmental Panel on Climate Change—Adopted Section by Section at IPCC Plenary XXVII (Valencia, Spain, 12–17 November 2007)*; IPCC: Geneva, Switzerland, 2007; p. 104.
122. IPCC. *Climate Change 2013: The Physical Science Basis. Working Group Contribution to the IPCC 5th Assessment Report*; IPCC: Cambridge, UK, 2013.

123. Kovats, R.; Ebi, K. Heatwaves and public health in Europe. *J. Public Health* **2006**, *16*, 592–599. [[CrossRef](#)] [[PubMed](#)]
124. Matzarakis, A. The Heat Health Warning System of DWD—Concept and Lessons Learned. In *Perspectives on Atmospheric Sciences*; Karacostas, T., Bais, A., Nastos, P., Eds.; Springer Atmospheric Sciences: Cham, Switzerland, 2016.
125. Nogueira, P.; Falcão, J.; Contreiras, M.; Paixão, E.; Brandão, J.; Batista, I. Mortality in Portugal associated with the heat wave of August 2003: Early estimation of effect, using a rapid method. *Eurosurveillance* **2005**, *10*, 5–6. [[CrossRef](#)]
126. Oke, T. The urban energy balance. *J. Prog. Phys. Geogr.* **1988**, *12*, 38. [[CrossRef](#)]
127. Stathopoulou, M.; Synnefa, A.; Cartalis, C.; Santamouris, M.; Karlessi, T.; Akbari, H. A surface heat island study of Athens using high-resolution satellite imagery and measurements of the optical and thermal properties of commonly used building and paving materials. *J. Sustain. Energy* **2009**, *28*, 59–76. [[CrossRef](#)]
128. Akbari, H.; Cartalis, C.; Kolokotsa, D.; Muscio, A.; Pisello, A.L.; Rossi, F.; Santamouris, M.; Synnefa, A.; Wong, N.H.; Zinzi, M. Local climate change and urban heat island mitigation techniques—The state of the art. *J. Civ. Eng. Manag.* **2016**, *22*, 1–16. [[CrossRef](#)]
129. Yang, J.; Wang, Z.; Kaloush, K. *Unintended Consequences—A Research Synthesis Examining the Use of Reflective Pavements to Mitigate the Urban Heat Island Effect (Revised April 2014)*; Arizona State University National Center for Excellence for SMART Innovations: Phoenix, Arizona, 2013.
130. Santamouris, M. Using cool pavements as a mitigation strategy to fight urban heat islands—A review of the actual developments. *J. Renew. Sustain. Energy Rev.* **2013**, *26*, 224–240. [[CrossRef](#)]
131. Dimoudi, A.; Zoras, S.; Kantzioura, A.; Stogiannou, X.; Kosmopoulos, P.; Pallas, C. Use of cool materials and other bioclimatic interventions in outdoor places in order to mitigate the urban heat island in a medium size city in Greece. *Sustain. Cities Soc.* **2014**, *13*, 89–96. [[CrossRef](#)]
132. Ca, T.; Asaeda, T.; Abu, M. Reductions in air conditioning energy caused by a nearby park. *Energy Build.* **1998**, *29*, 83–92. [[CrossRef](#)]
133. Elhelw, M. Analysis of energy management for heating, ventilating and air-conditioning systems. *Alex. Eng. J.* **2016**, *55*, 811–818. [[CrossRef](#)]
134. Song, L.; Zhou, X.; Zhang, J.; Zheng, S.; Yan, S. Air-conditioning usage pattern and energy consumption for residential space heating in Shanghai China. *Procedia Eng.* **2017**, *205*, 3138–3145. [[CrossRef](#)]
135. Lundgren-Kownacki, K.; Hornyanszky, E.; Chu, T.; Olsson, J.; Becker, P. Challenges of using air conditioning in an increasingly hot climate. *Int. J. Biometeorol.* **2017**, *62*, 401–412. [[CrossRef](#)]
136. Isaac, M.; Vuuren, D.P.V. Modeling global residential sector energy demand for heating and air conditioning in the context of climate change. *Energy Policy* **2009**, *37*, 507–521. [[CrossRef](#)]
137. Givoni, B. Comfort, climate analysis and building design guidelines. *Energy Build.* **1991**, *18*, 11–23. [[CrossRef](#)]
138. Muzet, A.; Libert, J.; Candau, V. Ambient temperature and human sleep. *Experientia* **1984**, *40*, 425–429. [[CrossRef](#)]
139. Glotzbach, S.; Heller, H. Temperature regulation. In *Principles and Practice of Sleep Medicine*; Kryger, M., Roth, T., Dement, W., Eds.; Saunders: New York, NY, USA, 1999; pp. 289–304.
140. Lan, L.; Tsuzuki, K.; Liu, Y.; Lian, Z. Thermal environment and sleep quality: A review. *Energy Build.* **2017**, *149*, 101–113. [[CrossRef](#)]
141. Haskell, E.; Palca, J.; Walker, J.; Berger, R.; Heller, H. The effects of high and low ambient temperatures on human sleep stages. *Electro-Clin. Neurophysiol.* **1981**, *51*, 494–501. [[CrossRef](#)]
142. Sapolsky, R. *Why Zebras Don't Get Ulcers*, 3rd ed.; Holt Paperbacks: New York, NY, USA, 2004.
143. Law, T. *The Future of Thermal Comfort in An Energy-Constrained World*; University of Tasmania Australia: Hobart, Australia, 2013.
144. Gisolfi, C.; Mora, M. *The Hot Brain: Survival, Temperature, and the Human Body*; MIT Press: Cambridge, MA, USA, 2000.
145. Parmeggiani, P. Thermoregulation and sleep. *Front. Biosci.* **2003**, *8*, 557–567. [[CrossRef](#)] [[PubMed](#)]
146. Parmeggiani, P. Interaction between sleep and thermoregulation: An aspect of the control of behavioural states. *Sleep* **1987**, *10*, 426–435. [[CrossRef](#)] [[PubMed](#)]
147. Okamoto-Mizuno, K.; Mizuno, K. Effects of thermal environment on sleep and circadian rhythm. *J. Physiol. Anthropol.* **2012**, *31*, 1–9. [[CrossRef](#)] [[PubMed](#)]

148. Tsuzuki, K.; Okamoto-Mizuno, K.; Mizuno, K. Effects of humid heat exposure on sleep, thermoregulation, melatonin, and microclimate. *J. Therm. Biol.* **2004**, *29*, 31–36. [[CrossRef](#)]
149. Okamoto-Mizuno, K.; Mizuno, K.; Michie, S.; Maeda, A.; Lizuka, S. Effects of humid heat exposure on human sleep stages and body temperature. *Sleep* **1999**, *22*, 767–773.
150. Libert, J.; Di, J.; Fukuda, H.; Muzet, A.; Ehrhart, J.; Amoros, C. Effect of continuous heat exposure on sleep stages in humans. *Sleep* **1988**, *11*, 195–209. [[CrossRef](#)]
151. Bach, V.; Maingourd, Y.; Libert, J.; Oudart, H.; Muzet, A.; Lenzi, P.; Johnson, L. Effect of continuous heat exposure on sleep during partial sleep deprivation. *Sleep* **1994**, *17*, 1–10. [[CrossRef](#)]
152. Nastos, P.; Matzarakis, A. Human-biometeorological effects on sleep in Athens, Greece: A Preliminary Evaluation. *Indoor Built Environ.* **2008**, *17*, 535–542. [[CrossRef](#)]
153. Douglas, J.; Krieger, J.; Peter, J.; Rauscher, H.; Stradling, J. *Sleep Related Breathing Disorders*; Springer-Verlag Wien: New York, NY, USA, 1992.
154. Roscoe, J.; Kaufman, M.; Matteson-Rusby, S.; Palesh, O.; Ryan, J.; Kohli, S.; Perlis, M.; Morrow, G. Cancer-Related Fatigue and Sleep Disorders. *Oncologist* **2007**, *12*, 35–42. [[CrossRef](#)]
155. Givoni, B. Impact of planted areas on urban environmental quality: A review. *J. Atmos. Environ.* **1991**, *25B*, 289–299. [[CrossRef](#)]
156. Santamouris, M. Heat Island Research in Europe: The State of the Art. *Adv. Build. Energy Res.* **2007**, *1*, 123–150. [[CrossRef](#)]
157. Bowler, D.E.; Buyung-Ali, L.; Knight, T.M.; Pullin, A.S. Urban greening to cool towns and cities: A systematic review of the empirical evidence. *Landsc. Urban Plan.* **2010**, *97*, 147–155. [[CrossRef](#)]
158. Gago, E.; Roldan, J.; Pacheco-Torres, R.; Ordóñez, J. The city and urban heat islands: A review of strategies to mitigate adverse effects. *Renew. Sustain. Energy Rev.* **2013**, *25*, 749–758. [[CrossRef](#)]
159. Qiu, G.-Y.; Li, H.-Y.; Zhang, Q.-T.; Chen, W.; Liang, X.-J.; Li, X.-Z. Effects of Evapotranspiration on Mitigation of Urban Temperature by Vegetation and Urban Agriculture. *J. Integr. Agric.* **2013**, *12*, 1307–1315. [[CrossRef](#)]
160. Berardi, U.; GhaffarianHoseini, A.; GhaffarianHoseini, A. State-of-the-art analysis of the environmental benefits of green roofs. *Appl. Energy* **2014**, *115*, 411–428. [[CrossRef](#)]
161. Santamouris, M. Cooling the cities—A review of reflective and green roof mitigation technologies to fight heat island and improve comfort in urban environments. *Sol. Energy* **2014**, *103*, 682–703. [[CrossRef](#)]
162. Shafique, M.; Kim, R.; Rafiq, M. Green roof benefits, opportunities and challenges—A review. *Renew. Sustain. Energy Rev.* **2018**, *90*, 757–773. [[CrossRef](#)]
163. Hunter, A.; Williams, N.; Rayner, J.; Aye, L.; Hes, D.; Livesley, S. Quantifying the thermal performance of green facades: A critical review. *Ecol. Eng.* **2014**, *63*, 102–113. [[CrossRef](#)]
164. Perez, G.; Coma, J.; Martorell, I.; Cabeza, L. Vertical Greenery Systems (VGS) for energy saving in buildings: A review. *Renew. Sustain. Energy Rev.* **2014**, *39*, 139–165. [[CrossRef](#)]
165. Medl, A.; Stangl, R.; Florineth, F. Vertical greening systems—A review on recent technologies and research advancement. *Build. Environ.* **2017**, *125*, 227–239. [[CrossRef](#)]
166. Gallagher, J.; Baldauf, R.; Fuller, C.; Kumar, P.; Gill, L.; McNabola, A. Passive methods for improving air quality in the built environment; A review of porous and solid barriers. *Atmos. Environ.* **2015**, *120*, 61–70. [[CrossRef](#)]
167. Janhall, S. Review on urban vegetation and particle air pollution—Deposition and dispersion. *J. Atmos. Environ.* **2005**, *105*, 130–137. [[CrossRef](#)]
168. Abhijith, K.; Kumar, P.; Gallagher, J.; McNabola, A.; Baldauf, R.; Pilla, F.; Broderick, B.; Sabatino, S.; Pulvirenti, B. Air pollution abatement performances of green infrastructure in open road and built-up street canyon environments—A review. *Atmos. Environ.* **2017**, *162*, 71–86. [[CrossRef](#)]
169. Soares, A.; Rego, F.; McPherson, E.; Simpson, J.; Peper, P.; Xiao, Q. Benefits and costs of street tree in Lisbon, Portugal. *Urban. For. Urban Green.* **2011**, *10*, 69–78. [[CrossRef](#)]
170. Mullaney, J.; Lucke, T.; Trueman, S. A review of benefits and challenges in growing street trees in paved urban environments. *Landsc. Urban Plan.* **2015**, *134*, 157–166. [[CrossRef](#)]
171. Salmond, J.; Tadaki, M.; Vardoulakis, S.; Arbuthnott, K.; Coutts, A.; Demuzere, M.; Dirks, K.; Heaviside, C.; Lim, S.; Macintyre, H.; et al. Health and climate related ecosystem services provided by street trees in the urban environment. *Environ. Health* **2016**, *15*, 96–171. [[CrossRef](#)]
172. Peel, M.; Finlayson, B.; McMahon, T. Updated world map of the Koppen-Geiger climate classification. *J. Hydrol. Earth Syst. Sci.* **2007**, *11*, 1633–1644. [[CrossRef](#)]

173. Taha, H.; Akbari, H.; Rosenfeld, A. *Vegetation Canopy Micro-Climature: A Field Project in Davis, California*; Lawrence Berkeley Laboratory, University of California: Berkley, CA, USA, 1988.
174. Narita, K.; Sugawara, H.; Honjo, T. Effects of roadside trees on the thermal environment within a street canyon. *Geogr. Rep. Tokyo Metrop. Univ.* **2008**, *43*, 41–48.
175. Tsiros, I. Assessment and energy implications of street air temperature cooling by shade trees in Athens (Greece) under extremely hot weather conditions. *J. Renew. Energy* **2010**, *35*, 1866–1869. [[CrossRef](#)]
176. Wong, N.; Jusuf, S. Study on the microclimatic condition along a green pedestrian canyon in Singapore. *Archit. Sci. Rev.* **2010**, *53*, 196–212. [[CrossRef](#)]
177. Berry, R.; Livesley, S.; Aye, L. Tree canopy shade impacts on solar irradiance received by building walls and their surface temperature. *Build. Environ.* **2013**, *69*, 91–100. [[CrossRef](#)]
178. Skelhorn, C.; Lindley, S.; Levenson, G. The impact of vegetation types on air and surface temperatures in a temperate city: A fine scale assessment in Manchester, UK. *Landsc. Urban Plan.* **2014**, *121*, 129–140. [[CrossRef](#)]
179. Jauregui, E. Influence of a large urban park on temperature and convective precipitation in a tropical city. *Energy Build.* **1990**, *15–16*, 457–463. [[CrossRef](#)]
180. Padmanabhamurty, B. Microclimates in Tropical Urban Complexes. *Energy Build.* **1990**, *15*, 83–92. [[CrossRef](#)]
181. Saito, I.; Ishihara, O.; Katayama, T. Study of the effect of green areas on the thermal environment in an urban area. *Energy Build.* **1991**, *15*, 2624–2631. [[CrossRef](#)]
182. Katayama, T.; Ishii, A.; Hayashi, T.; Tsutsumi, J. Field surveys on cooling effects of vegetation in an urban area. *J. Therm. Biol.* **1993**, *18*, 571–576. [[CrossRef](#)]
183. Spronken-Smith, R.; Oke, T. Scale modelling of nocturnal cooling in urban parks. *Bound. Layer Meteorol.* **1999**, *93*, 287–312. [[CrossRef](#)]
184. Shashua-Bar, L.; Hoffman, M. Vegetation as a climatic component in the design of an urban street; An empirical model for predicting the cooling effect of urban green areas with trees. *Energy Build.* **2000**, *31*, 221–235. [[CrossRef](#)]
185. Jonsson, P. Vegetation as an urban climate control in the subtropical city of Gaborone, Botswana. *Int. J. Climatol.* **2004**, *24*, 1307–1322. [[CrossRef](#)]
186. Potchter, O.; Cohen, P.; Bitan, A. Climatic behaviour of various urban parks during hot and humid summer in the Mediterranean city of Tel Aviv, Israel. *Int. J. Climatol.* **2006**, *26*, 1695–1711. [[CrossRef](#)]
187. Chang, C.; Li, M.; Chang, S. A preliminary study on the local cool-island intensity of Taipei city parks. *Landsc. Urban Plan.* **2007**, *80*, 386–395. [[CrossRef](#)]
188. Lin, B.; Lin, Y. Cooling effect of shade trees with different characteristics in a subtropical urban park. *HortScience* **2010**, *45*, 83–86. [[CrossRef](#)]
189. Skoulika, F.; Santamouris, M.; Kolokotsa, D.; Boemi, N. On the thermal characteristics and the mitigation potential of a medium size urban park in Athens, Greece. *Landsc. Urban Plan.* **2014**, *123*, 73–86. [[CrossRef](#)]
190. Tsilini, V.; Papantoniou, S.; Kolokotsa, D.; Maria, E. Urban gardens as a solution to energy poverty and urban heat island. *Sustain. Cities Soc.* **2014**, *14*, 323–333. [[CrossRef](#)]
191. Reis, C.; Lopes, A. Evaluating the cooling potential of urban green spaces to tackle urban climate change in Lisbon. *Sustainability* **2019**, *11*, 2480. [[CrossRef](#)]
192. Viñas, F.; Solanich, J.; Vilardeaga, X.; Montilo, L. *El Árbol En Jardinería Y Paisajismo—Guía de Aplicación Para ESPAÑA Y Países de Clima Mediterráneo Y Templado*, 2nd ed.; Ediciones Omega: Barcelona, Spain, 1995.
193. McPherson, E. Planting design for solar control. In *Energy-Conserving Site Design*; McPherson, E., Ed.; American Society of Landscape Architects: Washington, DC, USA, 1984; pp. 141–164.
194. Brown, R.; Gillespie, T. Estimating radiation received by a person under different species of shade trees. *J. Arboric.* **1990**, *16*, 158–161.
195. Brown, R.; Cherkezoff, L. Of what comfort value, a tree? *J. Arboric.* **1989**, *15*, 158–162.
196. Takács, Á.; Kiss, M.; Gulyás, Á.; Tanács, E.; Kántor, N. Solar Permeability of Different Tree Species in Szeged, Hungary. *Geogr. Pannonica* **2016**, *20*, 32–41. [[CrossRef](#)]
197. Gulyas, A.; Unger, J.; Matzarakis, A. Assessment of the microclimatic and human comfort conditions in a complex urban environment: Modelling and measurements. *Build. Environ.* **2006**, *41*, 1713–1722. [[CrossRef](#)]
198. Spangenberg, J.; Shinzato, P.; Johansson, E.; Duarte, D. Simulation of the influence of vegetation on microclimate and thermal comfort in the city of São Paulo. *Revista da Sociedade Brasileira de Arborização Urbana* **2008**, *3*, 1–19. [[CrossRef](#)]

199. Lin, T.-P.; Matzarakis, A.; Hwang, R.-L. Shading effect on long-term outdoor thermal comfort. *Build. Environ.* **2010**, *45*, 213–221. [[CrossRef](#)]
200. Yang, F.; Lau, S.; Qian, F. Thermal comfort effects of urban design strategies in high-rise urban environments in a sub-tropical climate. *Archit. Sci. Rev.* **2011**, *54*, 285–304. [[CrossRef](#)]
201. Abreu-Harbach, L.V.d.; Labaki, L.; Matzarakis, A. Reduction of mean radiant temperature by cluster of trees in urban and architectural planning in tropical climate. In Proceedings of the PLEA2012—28th Conference: Opportunities, Limits & Needs Towards an Environmentally Responsible Architecture, Lima, Perú, 7–9 November 2012.
202. Abreu-Harbach, L.V.d.; Labaki, L.; Matzarakis, A. Effect of tree planting design and tree species on human thermal comfort in the tropics. *Landsc. Urban Plan.* **2015**, *138*, 99–109. [[CrossRef](#)]
203. Tan, Z.; Lau, K.K.-L.; Ng, E. Urban tree design approaches for mitigating daytime urban heat island effects in a high-density urban environment. *Energy Build.* **2016**, *114*, 265–274. [[CrossRef](#)]
204. Kong, L.; Lau, K.; Yuan, C.; Chen, Y.; Xu, Y.; Ren, C.; Ng, E. Regulation of outdoor thermal comfort by trees in Hong Kong. *Sustain. Cities Soc.* **2017**, *31*, 12–25. [[CrossRef](#)]
205. Streiling, S.; Matzarakis, A. Influence of single and small clusters of trees on the bioclimate of a city: A case study. *J. Arboric.* **2003**, *29*, 309–317.
206. Mayer, H.; Matzarakis, A. Impact of street trees on the thermal comfort of people in summer: A case study in Freiburg (Germany). *Merchavim* **2006**, *6*, 285–300.
207. Andrade, H.; Vieira, R. A climatic study of an urban green space: The Gulbenkian Park in Lisbon (Portugal). *Finisterra* **2007**, *XLII*, 27–46. [[CrossRef](#)]
208. Cohen, P.; Potchter, O. Daily and Seasonal Air Quality Characteristics of Urban Parks in the Mediterranean City of Tel Aviv. In Proceedings of the CLIMAQS Workshop ‘Local Air Quality and its Interactions with Vegetation’, Antwerp, Belgium, 21–22 January 2010.
209. Oliveira, S.; Andrade, H.; Vaz, T. The cooling effect of green spaces as a contribution to the mitigation of urban heat: A case study in Lisbon. *Build. Environ.* **2011**, *46*, 2186–2194. [[CrossRef](#)]
210. Cohen, P.; Potchter, O.; Matzarakis, A. Daily and seasonal climatic conditions of green urban open spaces in the Mediterranean climate and their impact on human comfort. *Build. Environ.* **2012**, *51*, 285–295. [[CrossRef](#)]
211. Perini, K.; Magliocco, A. Effects of vegetation, urban density, building height, and atmospheric conditions on local temperatures and thermal comfort. *Urban For. Urban Green.* **2014**, *13*, 495–506. [[CrossRef](#)]
212. Martins, T.; Adolphe, L.; Bonhomme, M.; Faraut, S.; Ginestet, S.; Michel, C.; Guyard, W. Impact of Urban Cool Island measures on outdoor climate and pedestrian comfort: Solutions for a new district of Toulouse, France. *Sustain. Cities Soc.* **2016**, *26*, 2–26. [[CrossRef](#)]
213. Abreu-Harbach, L.V.d.; Labaki, L.C.; Bueno-Bartholomei, C.L. How much does the shade provided by different trees collaborate to control the urban heat island in tropical climates?—A study in Campinas, Brazil. In Proceedings of the Conference: IC2UHI—Third International Conference on Countermeasures to Urban Heat Islands, Venice, Italy, 13–15 October 2014; pp. 838–849.
214. Ali-Toudert, F.; Mayer, H. Numerical study on the effects of aspect ratio and orientation of an urban street canyon on outdoor thermal comfort in hot and dry climate. *Build. Environ.* **2006**, *41*, 94–108. [[CrossRef](#)]
215. Herrmann, J.; Matzarakis, A. Mean radiant temperature in idealised urban canyons—Examples from Freiburg, Germany. *Int. J. Biometeorol.* **2012**, *56*, 199–203. [[CrossRef](#)]
216. Qaid, A.; Ossen, D. Effect of asymmetrical street aspect ratios on microclimates in hot, humid regions. *Int. J. Biometeorol.* **2015**, 1–21. [[CrossRef](#)]
217. Algeciras, J.A.R.; Consuegra, L.G.; Matzarakis, A. Spatial-temporal study on the effect of urban street configurations on human thermal comfort in the world heritage city of Camagüey-Cuba. *Build. Environ.* **2016**, *101*, 85–101. [[CrossRef](#)]
218. Algeciras, J.A.R.; Tablada, A.; Matzarakis, A. Effect of asymmetrical street canyons on pedestrian thermal comfort in warm-humid climate of Cuba. *Theor. Appl. Climatol.* **2017**, 1–17.
219. Gaitani, N.; Spanou, A.; Saliari, M.; Vassilakopoulou, K.; Papadopoulou, K.; Pavlou, K.; Santamouris, M.; Lagoudaki, A. Improving the microclimate in urban areas: A case study in the centre of Athens. *Build. Serv. Eng. Res. Technol.* **2011**, *32*, 53–71. [[CrossRef](#)]
220. Santamouris, M.; Gaitani, N.; Spanou, A.; Salirai, M.; Giannopoulou, K.; Vasilakopoulou, K.; Kardomateas, T. Using cool paving materials to improve microclimate of urban areas—Design realization and results of the flisvos project. *J. Build. Environ.* **2012**, *53*, 128–136. [[CrossRef](#)]

221. Fintikakis, N.; Gaitani, N.; Santamouris, M.; Assimakopoulos, M.; Assimakopoulos, D.; Fintikaki, M.; Albanis, G.; Papadimitriou, K.; Chrysochoides, E.; Katopodi, K.; et al. Bioclimatic design of open public spaces in the historic centre of Tirana, Albania. *Sustain. Cities Soc.* **2011**, *1*, 54–62. [[CrossRef](#)]
222. Erell, E.; Pearlmutter, D.; Boneh, D.; Kutiel, P. Effect of high-albedo materials on pedestrian heat stress in urban street canyons. *Urban Clim.* **2014**, *10*, 367–386. [[CrossRef](#)]
223. Boriboonsomsin, K.; Reza, F. Mix Design and Benefit Evaluation of High Solar Reflectance Concrete for Pavements. *Transp. Res. Rec. J.* **2011**, *361*, 11–20. [[CrossRef](#)]
224. NCAT. *Strategies for Design and Construction of High-Reflectance Asphalt Pavements*; National Centre for Asphalt Technology: Auburn, AL, USA, 2009; p. 28.
225. Gui, J.; Phelan, P.; Kaloush, K.; Golden, J. Impact of Pavement Thermophysical Properties on Surface Temperatures. *J. Mater. Civ. Eng.* **2007**, *19*, 683–688. [[CrossRef](#)]
226. Synnefa, A.; Karlessi, T.; Gaitani, N.; Santamouris, M.; Assimakopoulos, D.; Papakatsikas, C. Experimental testing of cool colored thin layer asphalt and estimation of its potential to improve the urban microclimate. *Build. Environ.* **2011**, *46*, 38–48. [[CrossRef](#)]
227. Nunes, J.; Zolio, I.; Jacinto, N.; Nunes, A.; Campos, T.; Pacheco, M.; Fonseca, D. *Misting-Cooling Systems for Microclimatic Control in Public Space*; PROAP Landscape Architects: Lisbon, Portugal, 2013; pp. 1–16.
228. Nouri, A.S. A Framework of Thermal Sensitive Urban Design Benchmarks: Potentiating the Longevity of Auckland’s Public Realm. In Proceedings of the Building A Better New Zealand, Auckland, New Zealand, 12 March 2015.
229. TVK. *Place de la Republique*; Trevelo & Viger-Kohler Architectes Urbanistes: Paris, France, 2013; p. 21.
230. Knuijt, M. One Step Beyond. *Open Space* **2013**, *85*, 60–67.
231. Ishii, T.; Tsujimoto, M.; Yoon, G.; Okumiya, M. Cooling system with water mist sprayers for mitigation of heat-island. In Proceedings of the Seventh International Conference on Urban Climate, Yokohama, Japan, 1 July 2009.
232. Ishii, T.; Tsujimoto, M.; Yamanishi, A. The experiment at the platform of dry-mist atomization. In Proceedings of the Summaries of Technical Papers of the Annual Meeting of the Architectural Institute of Japan, Yamagata, Japan, 6 September 2018.
233. Yamada, H.; Yoon, G.; Okumiya, M.; Okuyama, H. Study of cooling system with water mist sprayers: Fundamental examination of particle size distribution and cooling effects. *J. Build. Simul.* **2008**, *1*, 214–222. [[CrossRef](#)]
234. Yoon, G.; Yamada, H.; Okumiya, M. Study on a cooling system using water mist sprayers; System control considering outdoor environment. In Proceedings of the Korea-Japan Joint Symposium on Human-Environment Systems, Cheju, Korea, 30 November 2008.
235. Farnham, C.; Nakao, M.; Nishioka, M.; Nabeshima, M.; Mizuno, T. Study of mist-cooling for semi-enclosed spaces in Osaka, Japan. *Urban Environ. Pollut.* **2011**, *4*, 228–238. [[CrossRef](#)]
236. Alvarez, S.; Rodriguez, E.; Martin, R. Direct air cooling from water drop evaporation. In Proceedings of the PLEA 91—Passive and Low Energy Architecture, Seville, Spain, 24–27 September 1991.



© 2019 by the authors. Licensee MDPI, Basel, Switzerland. This article is an open access article distributed under the terms and conditions of the Creative Commons Attribution (CC BY) license (<http://creativecommons.org/licenses/by/4.0/>).

Perspective

Urban Transformation: From Single-Point Solutions to Systems Innovation

Eleanor Tonks ^{1,*} and Sean Lockie ²

¹ EIT Climate-KIC, 1018 JA Amsterdam, The Netherlands

² EIT Climate-KIC, Fellow RICS, 40129 Bologna, Italy; sean.lockie@climate-kic.org

* Correspondence: ellie.tonks@climate-kic.org

Received: 20 December 2019; Accepted: 15 January 2020; Published: 20 January 2020

Abstract: Adapting our cities to the new climate regime is critical to ensure that human development is not jeopardized and that the world's citizens can thrive where they live. Faced as we are with the imperative to act, we now need to accept that the challenges we face are not technical in nature—they are systemic. Traditionally, investments in low-carbon city solutions have suffered from being small and disaggregated, with a focus on single-point solutions. To truly enable city transformation at scale, we need to completely rewire our approach to urban innovation and implementation. To face our new reality, EIT Climate-KIC works on catalysing systems change through innovation in areas of human activity that have a critical impact on greenhouse gas emissions—cities, land use, materials, and finance—and to create climate-resilient communities. In this paper, EIT Climate-KIC reflects on its key learnings, as an innovation community, on how to apply innovation in service of urban transformation through the application of nature-based solutions.

Keywords: systems change; innovation; nature-based solutions; cities

1. Introduction

Adapting our cities to the new climate regime is critical to ensure that human development is not jeopardized and that the world's citizens can thrive where they live. The number of weather- and climate-related loss events has been increasing rapidly since 1980, causing a similar increase in the economic damages from these events. Today, the annual number of events approximate 700 as compared to 200–300 in the 1980s [1]. There is no doubt that climate change is exacerbating the vulnerability of cities. Despite increasing awareness of short-term climate hazards, the medium- and long-term hazards of climate change are currently being under-reported and actioned on by cities [2]. By 2050, eight times as many city dwellers will be exposed to high temperatures (amounting to 1.6 billion citizens), and over 800 million people will be at risk from the impacts of rising seas and storm surges [3]. Cities cannot afford inaction.

Global targets for emissions reductions set forth in the Paris Climate Agreement have put low-carbon climate-resilient cities high on the political, financial, and social agenda. They are an essential response to climate change and fundamental to achieving the goals of the Paris Agreement. However, urban transformations into low-carbon societies are not only about saving our climate. Multiple benefits arise from this change, including improved health and well-being, cleaner air, employment creation, an opportunity for community renewal, and positively refreshed state–society relationships.

However, so far, the vast majority of action toward sustainable change in cities has arguably been in words—through the creation of policies, strategies, and targets for the slightly too-distant future, established through too many meetings, workshops, conferences, and talking shops, with Climate Action Plans often missing the detail or the financial backing to attract the investment needed to result in change on the ground. Many cities have made ambitious 2050 targets, but the reality is that these will come too late. With the acknowledgement that the EU should “concentrate on immediate and urgent” [4] climate policies for 2030, we argue that 2050 is moving too slowly.

Faced as we are with the imperative to act, we now need to accept that the challenges we face are not technical in nature—they are systemic. For too long, investments in low-carbon city solutions have suffered from being small and disaggregated, with a focus on single-point solutions. Understandably, most cities around the world are interested in similar, well-tested, and well-proven projects in climate adaptation and mitigation. However, the cities and projects themselves are regularly too small to justify the involvement of financiers, and often lack the technical knowledge and network to develop and implement their projects at scale.

To truly enable city transformation at scale, we need to completely rewire our approach to urban innovation and implementation, working toward 2030 rather than 2050 and implementing system-orientated approaches in preference to point solutions. According to the IPCC's 1.5 Degree Special Report [5], the world requires rapid and unprecedented transformations not just in energy supply and consumption, but in land-use, urban, infrastructure, and industrial systems, in order to avoid the most perilous effects of global warming. To face this new reality, EIT Climate-KIC works on catalysing systems change through innovation in areas of human activity that have a critical impact on greenhouse gas emissions—cities, land use, materials, and finance—and to create climate-resilient communities.

In the context of systems innovation for urban adaptation, we view nature-based solutions (NBS) as an opportunity to progress toward a low-carbon and more resilient city: one that puts citizens' health and well-being at the centre of urban development and design. NBS are actions which use or are supported by nature and its restorative system processes to address societal challenges, while enhancing citizen well-being and socially inclusive green growth [6]. Furthermore, NBS can play a crucial role in increasing the resilience of urban environments in the new climate regime. Despite the opportunities presented by NBS for citizen health, urban liveability, and climate adaptation and mitigation efforts, the deployment of solutions within our cities remains limited. Integrating long-term considerations into planning requires thinking beyond infrastructure solutions and focusing on systemic changes.

In this paper, we reflect on the key learnings from EIT Climate-KIC, as an innovation community, on how to apply innovation in service of urban transformation. First, we present the origins and initial purpose of EIT Climate-KIC when it was established nine years ago. Then, we discuss four key learnings on the need for a systems approach. Finally, we present three NBS case studies in which we see elements of these learnings being implemented in a real-world context.

2. An Innovation Community, Nine Years On

EIT Climate-KIC is a knowledge and innovation community established and funded by the European Institute of Innovation and Technology (EIT) in 2010. Our purpose is to tackle climate change through innovation. We draw our purpose from a context in which climate change is advancing fast and its damaging effects are beginning to take hold. We are Europe's largest public-private partnership with this purpose—a growing pan-European community of diverse organisations united by a commitment to direct the power of creativity and human ingenuity at the climate crisis. We bring together large and small companies, scientific institutions, and universities, city authorities, and other public bodies, start-ups, and students. With nearly 400 formal organisational partners from across 25 countries, we work on innovation to mitigate climate change and to adapt to its unavoidable impacts.

To understand our systems innovation approach, it is first vital to reflect on our nine years of experience in tackling climate change through innovation.

In 2009, the context in which we worked was that research leadership in Europe was not being translated into business growth and job creation, and that such leadership could be orientated to focus on tackling some of Europe's most pressing challenges (of which climate change was one). This research leadership was then targeted toward three key areas:

- I. Tackling climate change through innovation;
- II. Developing impactful start-ups and new generations of environmental entrepreneurs;
- III. Working with universities to educate future decision makers.

We have been reasonably successful in this, as we have achieved the following: supported over 1400 innovative start-ups, attracted plus €900 million to those start-ups, leveraged €3.4 billion climate funding, created over 2000 jobs, launched 367 new products and services, and empowered 17,000 participants through our education activities. Furthermore, the innovations we have supported and nurtured are now starting to support climate action. However, a large question remains, did we tackle climate change at the speed and scale that we need? We acknowledge that the answer is probably not. Europe is not on track to its 2050 targets.

3. A Systems Innovation Approach

We understand that most systems we need to transform behave in complex adaptive ways. This means that there are no *right solutions* and that deterministic interventions are bound to fail [7]. Instead, we believe that the best way to shift these systems is through exploration and experimentation, testing ourselves forward through real-world experiences [8]. Now, in 2020, the context in which we work is set out in the IPCC Summary for Policy Makers: “Limiting the risks from global warming of 1.5 °C in the context of sustainable development and poverty eradication implies **system transitions** that can be enabled by an increase of adaptation and mitigation investments, policy instruments, the acceleration of technological innovation and behaviour changes” [5].

Our new strategy (Transformation, in time [9]) is underpinned by four core lessons from our past experiences, which can also be contextualised further through the lens of urban-resilience.

3.1. We Cannot Treat Innovation as Techno-Centric

Over the past nine years, we have realised that a supply-driven innovation approach leads to a techno-centric pipeline characterised by incremental improvements of single-point solutions—and rarely to systemic solutions. EIT Climate-KIC is not alone in treating climate change as a complicated problem [7]. Ever since climate change entered the political stage [10] in the 1970s efforts to stem global warming have mostly focused on developing technical solutions through research and engineering. Furthermore, adaptation has often been framed as a purely technical issue that can be addressed through climate-proofing interventions rather than something integral to how city systems function. This means that we continue to see escalating risk and exposure within urban developments, for example, new developments in high risk locations, insurance priced in ways that does not account for positive adaptation actions, or mortgages that are not systematically pricing in future climate risk. This techno-centric approach has produced many important building blocks of a sustainable future (such as renewable-energy technologies or advanced batteries); however, what we must learn now is how to weave these technological advances into our societal systems, along with other cultural, institutional, social, and economic innovations. At EIT Climate-KIC, we define systems innovation as integrated and coordinated interventions in economic, political, technological, and social systems, and along whole value chains.

3.2. We Cannot Work on a Project-by-Project Level

Instead we must orchestrate the development and deployment of interventions in portfolios. Portfolios are collections of deliberately chosen innovation experiments. These experiments—representing the supply side of innovation—come in the form of diverse and coordinated innovation projects, education programs, start-ups, ecosystem building activities, citizen engagement strategies, and communication initiatives. They focus on different parts of the same problem, on different opportunities to leverage change. On considering a city’s adaptive capacity, we need to shift the locus of interest from individual interventions to the aggregate level, to consider, for example, density and risk exposure, infrastructure vulnerability and resilience, governance, and institutional capacity. One of the distinguishing features of portfolio-based innovation is that, rather than focusing on individual experiments, we seek to understand the aggregate impact of the portfolio.

3.3. *We Need to Demonstrate What Is Possible*

To both inspire and legitimise climate action, we must work with the demand side: governments, corporations, and other challenge owners that share our ambition for transformative action. Ambitious demand-side actors have a strong appetite for change and appreciate the full complexity of the problem, trade-offs or synergies, and the necessary scale for intervention. They are also well-positioned to identify a broad and diverse set of points in the systems they aim to transform, whilst holding the networks to pull through the connected, system-wide solutions we need. EIT Climate-KIC is working at the whole city, region, and supply-chain scale through our Deep Demonstrations programme on systems transformation [11].

3.4. *We Need to Broaden the Innovation Tent*

No single individual, organisation, or government can address the climate crisis alone. Furthermore, the climate risks urban populations face are not only environmental; they raise equity, social justice, and sustainable development issues. To ensure the transition is socially just, diverse communities need to be engaged in decisions made about the future direction of resilience in their towns and cities. For example, involving trade unions, using tools of citizen monitoring and science, and engaging social movements, youth or community organisations, on specific issues, can embed adaptation activities in a socially just resilient transition and contribute to building a politics for transformation. EIT Climate-KIC orchestrates close to 400 innovation partners—from the private, public, and academic sectors—operating as a diverse community that understands the specific needs of different places and contexts. As a community, they bring their own expertise and experience to the systems in which we intervene.

4. Discussion

In the case of the built environment, we see nothing but opportunity, but the scale of change is not happening fast enough, nor is it being framed correctly. With political will and the right policies and incentives in place, NBS can be integrated in new developments from the outset (seen through the Sponge City initiatives in China). Retrospectively including them in existing, densely built-up city districts on public and private land and connecting them on the level of the whole city, however, requires working at scale in a long-term mindset (seen in the City of Copenhagen Cloudburst Plan, launched in 2012 and Philadelphia's Green City, Clean Waters programme, launched in 2011). Below, we explore three cities where nature is helping to catalyse change at the scale needed.

The Wild West End Project [12] in London (UK), a collaboration between public authorities, property owners, NGOs, and the private sector, seeks to create a network of green corridors that can sustain biodiversity and improve ecological connectivity. Taking an aggregate view, this diverse consortium is implementing a portfolio of solutions, including green and biodiversity roofs, living walls, sustainable drainage systems, pocket parks, street trees, terrace planters, and pop-up green spaces, to not only address biodiversity, climate, and micro-climate challenges, but also societal well-being. Between 2016 and 2018, the project saw a 17.5% increase in documented multi-functional green infrastructure measures (54 interventions) across the West End. The project builds on a previous Ecology Masterplan, adopted by The Crown Estate, developed to connect two major parks (Regent's Park and St James's Park) in London's West End, by adopting a long-term, estate-wide approach of installing NBS.

Building on the success of the "My tree—My city" public donation campaign [13] (launched as part of the European Green Capital program in 2011), Hamburg has developed a Green Power Strategic Plan to implement a citywide network of green spaces by 2030 [14]. The plan will connect the city's outer ring with its dynamic centre through a series of green axes (walking- and cycling-friendly regenerated or rewilded habitats along parks and rivers). The green network will enhance urban resilience (by providing flood mitigation for vulnerable spaces around Hamburg's vital ports, and by reducing urban heat island effects), improve air quality, and provide numerous health benefits for citizens.

A third project working at scale toward transformation is the Green City, Clean Waters programme [15] (launched 2011) led by the Philadelphia Water Department, on integrating Philadelphia's water systems to safeguard the ecological and economic future of the city. By implementing a range of measures, such as building green storm water infrastructure on public and private land, creating recreational spaces, and restoring biodiversity along water bodies, the programme aims to enhance the region's waterways by managing stormwater runoff and reducing dependence on additional underground grey infrastructure. The city is investing \$2.4 billion over 25 years to manage more than one-third of the impervious cover within areas of the city served by combined sewers, a decision supported by a triple bottom-line analysis, comparing the green infrastructure approach with traditional alternatives. Through the Green City, Clean Waters programme, the aim is to generate new employment opportunities; increase \$390 million in property value of homes over 45 years; avoid 140 fatalities due to heat reduction over the next 45 years; avoid 250 missed days of work or school per year; and eliminate 1.5 billion lbs of carbon dioxide emissions.

Each of these external case studies can be used to frame, in the context of NBS, the learnings from EIT Climate-KIC in real-world settings. All three view the need for increased application of NBS as not only a climate adaptation measure (a point solution), but rather adopt systems approaches when considering the magnitude of benefits from their interventions (as seen in the indicators of the Green City, Clean Waters programme). Each programme has the ambition to work at scale with a number of different intervention types (as seen by the Wild West End portfolio of solutions), with the support of the demand side (ranging from private land owners to local councils to municipalities to water departments), providing legitimacy and long-term direction for the programmes. Both the Wild West End and "My tree—My city" purposefully seek to engage with a range of stakeholders (from urban planners to local citizens to conservations to children and students). To differing degrees, these cases present practical examples of neighbourhood and city-scale transformation ambitions in the context of urban adaptation. They are not, however, presented as exemplar urban transformations but are instead given as examples through which the learnings from EIT Climate-KIC can be contextualised within an urban context.

5. Conclusions

Decision makers working toward urban resilience should consider these lessons learned from EIT Climate-KIC and the external case studies when seeking to address the risks they are exposed to. First, do not approach adaptation as a purely technical issue that can be solved through techno-centric innovation. Second, rather than focusing on the project-by-project or hazard-by-hazard scale, hold space at the aggregate to look across interventions or developments (taking a portfolio approach at scale). Third, to inspire and legitimise climate action work with the demand side and problem-owners that want to take on the mandate for change. Finally, to ensure the transition is socially just diverse communities need to be meaningfully engaged in decisions made about the future direction of resilience in their towns and cities.

Author Contributions: Conceptualization, S.L. and E.T.; methodology, S.L. and E.T.; investigation, E.T.; resources, E.T.; writing—original draft preparation, S.L. and E.T.; writing—review and editing, E.T.; project administration, E.T. All authors have read and agreed to the published version of the manuscript.

Funding: This research received no external funding.

Conflicts of Interest: The authors declare no conflict of interest.

References

1. NatCatSERVICE Analysis Tool, Download Center for Statistics on Natural Catastrophes. Available online: <http://natcatservice.munichre.com/> (accessed on 16 August 2019).
2. Carbon Disclosure Project. Cities at Risk: Dealing with the Pressures of Climate Change. Available online: <https://www.cdp.net/en/research/global-reports/cities-at-risk> (accessed on 7 December 2019).
3. C40, 2018. The Future We Don't Want. Available online: https://c-production-images.s.amazonaws.com/other_uploads/images/_Future_We_Don't_Want_Report_1.4_hi-res_1.original.pdf (accessed on 7 December 2019).

4. EURACTIV, Juncker Insists 2030 Climate Target Is EU's Top Priority, Not 2050 Plan. Available online: <https://www.euractiv.com/section/climate-strategy-/news/juncker-insists--climate-target-is-eus-top-priority-not--plan/> (accessed on 15 August 2019).
5. Masson-Delmotte, V.; Zhai, P.; Pörtner, H.-O.; Roberts, D.; Skea, J.; Shukla, P.R.; Pirani, A.; Moufouma-Okia, W.; Péan, C.; Pidcock, R.; et al. (Eds.) 2018: Summary for Policymakers. Global Warming of 1.5 °C. An IPCC Special Report on the impacts of global warming of 1.5 °C above pre-industrial levels and related global greenhouse gas emission pathways, in the context of strengthening the global response to the threat of climate change. In *Sustainable Development, and Efforts to Eradicate Poverty*; Intergovernmental Panel on Climate Change: Geneva, Switzerland, 2018; In Press.
6. European Commission, Nature-Based Solutions. Available online: <https://ec.europa.eu/research/environment/index.cfm?pg=nbs> (accessed on 8 December 2019).
7. Innovating in Complexity: From Single-Point Solutions to Directional Systems Innovation. Available online: <https://www.climate-kic.org/opinion/innovating-in-complexity/> (accessed on 16 August 2019).
8. AXILO. Available online: <https://axilo.space> (accessed on 4 August 2019).
9. EIT Climate-KIC. Transformation, in Time. 2019. Available online: <https://www.climate-kic.org/wp-content/uploads///Transformation-in-time.pdf> (accessed on 4 August 2019).
10. The New York Times, Climate Change Losing Earth. Available online: <https://www.nytimes.com/interactive///magazine/climate-change-losing-earth.html> (accessed on 16 August 2019).
11. EIT Climate-KIC, Deep Demonstrations of a Net-Zero Emissions, Resilient Future. Available online: <https://www.climate-kic.org/wp-content/uploads///EIT-Climate-KIC-Deep-Demonstrations.pdf> (accessed on 6 September 2019).
12. Wild West End. Available online: <http://www.wildwestend.london/> (accessed on 15 August 2019).
13. Hamburg European Green Capital 2011, "My Tree—My City" Campaign. Available online: <https://www.hamburg.de/projects/mytree-mycity/> (accessed on 6 September 2019).
14. Green Network Hamburg, on Green Paths through the City. Available online: <https://www.hamburg.de/gruenes-netz//auf-gruenen-wegen-artikel/> (accessed on 6 September 2019).
15. Green City, Clean Waters. Available online: <https://www.phila.gov/water/sustainability/greencitycleanwaters/Pages/default.aspx> (accessed on 16 August 2019).



© 2020 by the authors. Licensee MDPI, Basel, Switzerland. This article is an open access article distributed under the terms and conditions of the Creative Commons Attribution (CC BY) license (<http://creativecommons.org/licenses/by/4.0/>).

MDPI
St. Alban-Anlage 66
4052 Basel
Switzerland
Tel. +41 61 683 77 34
Fax +41 61 302 89 18
www.mdpi.com

Climate Editorial Office
E-mail: climate@mdpi.com
www.mdpi.com/journal/climate



MDPI
St. Alban-Anlage 66
4052 Basel
Switzerland

Tel: +41 61 683 77 34
Fax: +41 61 302 89 18

www.mdpi.com



ISBN 978-3-0365-0145-1